COMPARATIVE TRANSCRIPTOMICS AND CO-EXPRESSION NETWORKS REVEAL TISSUE- AND GENOTYPE-SPECIFIC RESPONSES OF *QDTYs* TO REPRODUCTIVE-STAGE DROUGHT STRESS IN RICE (*ORYZA SATIVA L.*)

BY

JESHURUN ASHER M. TARUN

DISSERTATION

Submitted in partial fulfillment of the requirements
for the degree of Doctor of Philosophy in Crop Sciences
in the Graduate College of the
University of Illinois Urbana-Champaign, 2021

Urbana, Illinois

Doctoral Committee:

Professor Jack Juvik, Chair
Associate Professor Tobias Kretzschmar, Director of Research, Southern Cross University
Associate Professor Patrick Brown, University of California Davis
Associate Professor Erik Sacks
Associate Professor Nathan Schroeder

ABSTRACT

Rice (*Oryza sativa L.*) is more sensitive to drought stress than other cereals. Particularly during reproductive stages, drought causes yield reductions of 50-80%. With at least 25 million hectares of drought-prone rainfed rice, drought remains a major environmental constraint to rice production. While a few gene-expression profiling studies in rice in response to drought at the reproductive-stage have been conducted, our knowledge of biological mechanisms in this respect is limited. Analysis tends to be restricted relative to the drought susceptible Nipponbare-reference genome, potentially missing genes unique to tolerant donor genomes. The objectives of this Ph.D. research were i) understand the genome-wide transcriptional changes at the reproductive-stage using above-ground tissues, ii) identify drought-responsive modules and pathways and assess their potential role and contribution for reproductive-stage drought tolerance, and iii) evaluate the similarities and dissimilarities of drought quantitative trait loci, across three representative genomes and discuss the potential involvement of the identified candidate genes for drought tolerance. The research objectives were addressed through RNA-Sequencing the flag-leaf and panicle tissues using a Drought-Tolerant Yield introgression line, DTY-IL, and the recurrent parent Swarna, under moderate reproductive-stage drought stress. Also, RNA-Sequencing analysis was done using the Nipponbare-reference approach and analyzed using the representative genome from *indica* and *aus* subpopulation.

We employed RNA-Seq to independently analyzed transcriptomes of flag-leaf and panicle tissues of DTY-IL and Swarna under the well-watered condition and after two weeks of moderate reproductive-stage drought stress. Differential expression analysis showed a distinct gene expression profile between the two genotypes and tissues. In flag-leaf, Differentially Expressed Genes (DEGs) downregulated in Swarna under drought were related to post-translational modifications and photosynthesis. At the same time, upregulated DEGs in DTY-IL were enriched for antioxidant enzymes. In panicle, DEGs downregulated in Swarna under drought were involved in DNA damage repair pathways and photosynthesis. Simultaneously, DEGs upregulated in DTY-IL under drought were enriched for post-translational modification, especially 'phosphorylation.'

A co-expression network approach across flag-leaf and panicle tissues in drought-stressed and control plants identified drought-responsive modules of putatively co-regulated genes within

each network. In flag leaf, M14 showed distinct upregulation of cell-wall biogenesis and cytoskeleton-related genes in DTY-IL under drought. This lack of cell wall remodeling in Swarna was suggested to contribute to the leaf-rolling phenotype observed under drought. M16, on the other hand, was associated with the downregulation of photosynthesis-related genes in Swarna under drought. In the panicle, modules M10 and M15 showed upregulation of several secondary metabolic pathway genes in DTY-IL. M10 further showed significant upregulation of several receptor kinases in DTY-IL. Hub genes of importance in differential drought responses included an expansin in the flag leaf and two peroxidases in the panicle.

Overlaying differential expression data with allelic variation in DTY-IL quantitative trait loci allowed for the prioritization of candidate genes. They included a differentially regulated auxin-responsive protein, with DTY-IL-specific amino acid changes in conserved domains, as well as a protein kinase with a DTY-IL-specific frameshift in the C-terminal region. An additional candidate gene was identified in MH63 in the *indica* genome to be a potential negative regulator of drought. The approach highlights how the integration of differential expression and allelic variation can help discover mechanisms and putative causal contributions underlying quantitative trait loci for drought-tolerant yield.

ACKNOWLEDGEMENTS

Firstly, I would like to express my sincere gratitude to my research advisor Dr. Tobias Kretzschmar for giving me the chance to go back to school and supporting my Ph.D. program. During these five years, Dr. Kretzschmar has guided me and taught me that my success in science would depend on my career passion, enthusiasm, and hard work. In addition to my advisor, I would like to thank my thesis committee: Dr. Jack Juvik, Dr. Patrick Brown, Dr. Erik Sacks, and Dr. Nathan Schroeder, for their technical support and inspiration. Special thanks to Sheryl Catausan for her assistance in setting up the Greenhouse and qPCR works. I am also grateful to Dr. Ramil Mauleon for his guidance and contributions and to Dr. Ajay Kohli for his technical contributions to the manuscript. I also would like to express my sincere gratitude to the Lee Foundation Rice Research for the fellowship provided throughout this study.

I also would like to thank the previous Graduate Program Coordinator of the Department of Crop Sciences, Dianne Carson, and the new Graduate Program Coordinator, Christina Pierce-Tomlin, for all their unwavering assistance throughout my time here at Urbana-Champaign.

I want to thank Dr. Jae Hoon and Menghao Yu, Sandeep Sakhale and Emran, for their great friendship. The Filipino Community on campus, especially kuya Edward Chainani, ate Carleen Sacris for their kindness and generosity. During these past few years, they have been my second family in Illinois.

This thesis is dedicated to my loving family: my mom, dad, brother, and sisters for their love and support. My most profound gratefulness to them for supporting all my decisions and for celebrating with me my every achievement.

TABLE OF CONTENTS

CHAPTER 1. COMPARATIVE TRANSCRIPTOMICS ANALYSIS OF FLAG-LEAF AND PANICLE TISSUES UNDER MODERATE REPRODUCTIVE-STAGE DROUGHT STRESS IN RICE .……..1

CHAPTER 2. GENE CO-EXPRESSION NETWORK ANALYSIS OF FLAG-LEAF AND PANICLE TISSUES UNDER MODERATE REPRODUCTIVE-STAGE DROUGHT STRESS IN RICE .……71

CHAPTER 3. COMPARATIVE SEQUENCE ANALYSIS, INTROGRESSION ANALYSIS, AND *qDTYs* CONTRIBUTION TO REPRODUCTIVE-STAGE DROUGHT TOLERANCE IN RICE **.....**……...139

CHAPTER 4. CONCLUSIONS ……....234

CHAPTER 1

COMPARATIVE TRANSCRIPTOMICS ANALYSIS OF FLAG-LEAF AND PANICLE TISSUES UNDER MODERATE REPRODUCTIVE-STAGE DROUGHT STRESS IN RICE

ABSTRACT

Rice (*Oryza sativa L.*) is more sensitive to drought stress than other cereals, particularly during the reproductive stage. This research aimed to identify genes and pathways related to drought-tolerance in rice and differentiate the drought tolerance mechanisms in the flag-leaf and panicle tissues during the reproductive-stage. In rice, we applied differential expression analysis to transcriptomes of flag-leaf and emerging panicle tissues of a Drought-Tolerant Yield to dissect the molecular mechanisms underlying drought-tolerant yield introgression line, DTY-IL, and the recurrent parent Swarna, under moderate reproductive-stage drought stress. The DTY-IL and the drought-susceptible parent Swarna showed distinct gene expression profiles in the flag-leaf and panicle tissue. Drought tolerance in the DTY-IL could be attributed to the upregulation of genes with oxidoreductase activity in the flag-leaf, whereas genes with protein kinase/threonine kinase activity, phosphotransferase activity, and hydrolase activity in the panicle. Drought susceptibility of Swarna could be attributed to downregulation of genes with protein kinase/threonine kinase activity, adenyl and nucleoside binding in the flag-leaf, while genes with different binding activities like tetrapyrrole, monooxygenase, and heme in the panicle. The induced and repressed genes in the DTY-IL and Swarna were characterized by regulatory motifs in their promoters primarily related to the MYB transcription factor. The induced genes with drought-responsive regulatory motifs may play critical roles in regulating drought tolerance in the DTY-IL under reproductive-stage drought stress.

INTRODUCTION

Agriculture in the 21st-century faces an extraordinary challenge: producing sufficient food and fiber to meet the increasing demands of a growing population, despite reductions in the quality and quantity of arable land, limited freshwater, rapid urbanization, and increasingly variable

weather patterns that are associated with climate change (FAO, 2009; Ehrlich and Harte, 2015). The global food requirement proliferates that overall food production needs to increase by an estimated 70% to feed the projected 9 billion people by 2050 (FAO, 2009; Ronald, 2014). Much of the world's major crops have yields below their potential, and genetic gains for four key global crops – maize, rice, wheat, and soybean - are stagnating at around 1% per year, less than the 2.4% rate per year required to double global crop production by 2050 (Ray et al., 2013). Integrated climate change and crop yield prediction models project a decline in the yield of major crops with a potentially increased flood occurrence, droughts, and extreme temperatures (Iizumi et al., 2013). Importantly, this remarkable increase in food production must be achieved with finite or even depleting land resources and water systems while meeting the demand for ecosystem preservation (Ronald, 2014).

Rice feeds more than half of the world's population (FAO, 2017). Most of these people live in Asia, where at least 90% of the world's rice is produced and consumed (Li et al., 2007). Among the different rice ecosystems, approximately 34% of rice is grown in the rainfed lowland, 9 % in the rainfed upland, and 7% in flood-prone areas, while irrigated rice ecosystems occupy 50% of the total rice area (Sandhu and Kumar, 2017).

Among the abiotic stresses, drought is considered the most critical limitation to rice production in rainfed lowlands and is estimated to affect at least 23 million hectares of rice (20% of total rice area) in Asia (Pandey, 2009). Nevertheless, a large proportion of Asia's smallholder farmers still rely on rainfed rice for subsistence and livelihood. Together with poor soil conditions, drought limits upland rice yield in over 19 million hectares, representing 15% of the rice-growing area worldwide (IRRI, 1995). The harvested areas that experienced yield losses by droughts corresponds to 102 million hectares (62% of the global harvested area) for rice from 1983 to 2009, and the global averages of drought-induced yield losses in rice correspond to 0.13 tons per hectare (Kim et al., 2009; Lesk et al., 2016). Annual rice production losses globally due to drought average about 18 million tons (Bernier et al., 2008). Rainfed rice is dependent on the wet season, and shortening and shifting monsoonal rains have made the occurrence of drought during the reproductive-stage more frequent across many parts of South and South-East Asia (Moumeni et al., 2015).

Rice tends to be more sensitive to drought stress than other crops (Lafitte et al., 2004), particularly during the reproductive stage, drought will cause a yield reduction of more than 50% (Venuprasad et al., 2007; Liu and Bennett, 2011; Jin et al., 2013; Vikram et al., 2011; Guo et al., 2013; Shankar et al., 2016). The semi-aquatic nature and high-water rice requirements make it more prone to yield losses from the drought than other cereals like wheat and maize, better adapted to grow with less water (Kumar et al., 2014; Fukao and Xiong, 2013). Intermittent stress during early vegetative stages slows growth but may not significantly reduce the yield of seed crops, whereas stress during reproductive development can considerably diminish productivity (Mickelbart et al., 2015). When drought stress coincides with the irreversible reproductive processes, it causes the most significant reduction in grain yield (Cruz et al., 1984) and more severe yield loss than during the vegetative phase (Xing and Zhang, 2010). Late season drought coinciding with the rice booting to the heading stage affects plant height, panicle exsertion, and flag leaf size (Yue et al., 2008). Drought during rice reproductive development reduces male fertility by affecting male meiosis, microspore development, and anther dehiscence resulting in partial to complete loss of pollen fertility, higher spikelet sterility, and abortion of newly developed seeds resulting in significant yield loss (Cruz et al., 1984; Jin et al., 2013; Guo et al., 2016; He and Serraj, 2012). Pollen fertility is a critical factor for rice yield, with spikelet fertility being the most sensitive yield component. The most delicate stage is immediately before heading in rice (Liu and Bennett, 2011).

Previous work has focused on drought-induced responses at vegetative rice and Arabidopsis stages (Xiong et al., 2011). Most of the efforts to improve grain yield under drought stress were focused on secondary traits such as osmotic potential, leaf temperature, leaf rolling, leaf death, relative water content, and root architecture at the vegetative stage, though they exhibited low heritability and were often not highly correlated with and/or had a negligible effect on grain yield (Pantuwan et al., 2002; Bernier et al., 2008; Basu et al., 2016). However, ultimately grain yield under drought is the most important factor for evaluating drought-tolerance. Studying yield-associated developmental processes and responses specifically under the reproductive-stage will directly determine crop productivity. Thus, in recent years, the focus has shifted to identifying cultivars that demonstrate increased yield under drought stress conditions (Borah et al., 2017). **Information on the responses of rice reproductive tissues and photosynthetic machinery**

under reproductive-stage drought stress is limited, and knowledge of detailed physiological and molecular level responses is lacking (Jin et al., 2013, Moumeni et al., 2015). The panicle's growth and morphology are vital factors in determining the yield. A reduction of photosynthetic activities during the reproductive stage suggests that the grain yield may be affected due to drought (Li et al., 2010). Several studies on the comparative phenotypic screening of breeding materials for grain yield under reproductive-stage drought stress and a normal condition revealed moderate to high heritability of grain yield under drought stress and irrigated condition, indicating the suitability of grain yield as an appropriate selection criterion under drought (Venuprasad et al., 2007; Kumar et al., 2008; Sandhu and Kumar, 2017).

Successful strategies to identify factors contributing to drought tolerance involved mapping of quantitative trait loci (QTLs) for grain yield under drought conditions, so-called DTY (drought tolerant yield) QTLs (Kumar et al., 2014). By crossing the drought-tolerant donor N22 with Swarna, several major-effect DTY QTL, among them *qDTY1.1*, and *qDTY3.2* were identified as having consistent effects on grain yield under reproductive-stage drought stress (RDS) and no apparent yield or performance penalty under non-stress conditions (Vikram et al., 2011). These were subsequently introgressed into drought susceptible elite parents through backcrossing (Kumar et al., 2018), resulting in the release of several drought-tolerant rice varieties. For example, "Bahuguni dhan-1" a sister line of DTY-IL (a complex introgression line from N22 x Swarna cross) used in this study, was recently released in Nepal (Kumar et al., 2018). Also, several other large-effect DTY QTLs were identified from other populations and utilized for their potential to confer drought tolerance (Bernier et al., 2007; Venuprasad et al., 2011; Ghimere et al., 2012; Yadaw et al., 2013). Gene discovery work in *qDTY12.1* resulted in identifying a NAM transcription factor as an intra-QTL hub gene (Dixit *et al*., 2015, Raorane *et al*., 2015).

With the advent of Next-Generation Sequencing (NGS) technology, RNA sequencing (RNA-Seq) has revolutionized how eukaryotic transcriptomes are analyzed. NGS made the direct count of transcripts possible based on the number of sequencing reads. Before, only relative expression levels were obtained in microarray experiments by converting the level of fluorescence on chips (Marguerat and Bahler, 2010). High-throughput expression profiling can be used to map and quantify gene expression, identify novel transcripts and splice variants, and determine allele-specific expression (Wang et al., 2009; Wang et al., 2014). RNA-Seq has been shown to detect a

higher percentage of differentially expressed genes (DEGs) than expression arrays, significantly improving low-abundance genes' accuracy (Wang et al., 2009; Wang et al., 2014). One primary application of transcriptomic technologies is to reveal genes differentially expressed, potentially responsible for a phenotype change between mutant and wild-type samples (Liseron-Monfils and Ware, 2015). To elucidate the photosynthetic system's roles in drought stress adaptation in upland rice, Zhang et al. (2016) conducted a comparative transcriptome analysis between drought susceptible rice cultivar Zhenshan97 and tolerant cultivar IRAT109 at the seedling stage. Only 436 genes showed differential expression between the two genotypes. Strong positive selection during rice cultivars' domestication to upland water deficit conditions highlights the photosynthetic system's crucial role during these two cultivars' domestication. Shankar et al. (2016) performed RNA-Seq analysis to explore the transcriptional difference at the seedling stage among three rice cultivars, including IR64 (S), N22 (T), and salinity-tolerant Pokkali under control and stress conditions. Many transcripts encoding members of NAC and DBP TF families in N22 exhibited differential regulation under drought stress. Up-regulation of transcripts encoding for thioredoxin and genes involved in phenylpropanoid metabolism were also detected in N22. Taking advantage of the combination of DNA re-sequencing and RNA-Seq, Huang et al. (2014) analyzed the drought-tolerant IL and its parental line at tillering stage on their transcriptomic changes under time series drought stress. Most of the observed DEGs in the IL relative to the drought-sensitive recurrent parent under drought were beyond the identified introgressed regions, implying that introgression resulted in novel changes in expressions. The observed drought-induced transcriptome reprogramming in the drought-tolerant IL could arise from the donor line's introgressed chromosome segment. The DEGs in the IL relative to the susceptible recurrent parent under drought might contribute to the enhanced tolerance, finally improving yield performance under drought stress (Huang et al., 2014).

Transcriptome analysis of rice in response to drought stress has been carried out in the past that led to the identification of hundreds of genes that are differentially expressed in an organ- and time-specific fashion concerning onset and severity of the drought conditions (Borah et al., 2017; Zhang et al., 2016; Shankar et al., 2016; Baldoni et al., 2016; Hu and Xiong, 2014; Huang et al., 2014; Wang et al., 2011; Lenka et al., 2011; Ray et al., 2011; Degenkolbe et al., 2009). **To date, only a few gene-expression profiling studies in rice in response to drought at the**

reproductive-stage has been conducted (Wei et al., 2017; Moumeni et al., 2015; Weng et al., 2014; Jin et al., 2013; Ding et al., 2013; Wang et al., 2011a). Such studies have identified many transcription factors, genes encoding for osmolyte production, reactive oxygen species (ROS) scavenging, other metabolic pathways, and signaling pathways (Shankar et al., 2016). These genes can be broadly divided into viz, signaling, and functional components (Tokada et al., 2015).

Understanding the molecular mechanisms underlying drought tolerance at the reproductive stage is needed to be a part of a holistic and successful, knowledge-based crop improvement strategy. At the molecular level, the response to drought stress results in several metabolic pathways' differential expression. For this reason, exploring the subtle differences in gene expression of drought-sensitive and drought-tolerant genotypes enables the identification of drought-related genes that could be used for the selection of drought tolerance traits (Fracasso et al., 2016). To minimize losses caused by drought and stabilize annual crop yield, it is indispensable to find and study genes that can increase drought tolerance in rice. While several major QTL for DTY have been discovered, knowledge regarding the underlying physiological mechanisms is largely lacking.

On the other hand, while several transcriptome studies provided some general insights into rice's drought responses, they did not take the presence of specific DTY QTL into account. In the 2014 and 2015 drought field trials at the International Rice Research Institute (IRRI), a DTY introgression line (DTY-IL) performed well under drought without showing a penalty under irrigated conditions. We decided to investigate this line further in a comparative transcriptomic approach against its drought susceptible recurrent parent Swarna. This research was conducted under reproductive-stage drought stress because i) rice is very susceptible to drought stress, especially at the reproductive-stage, which has more drastic and severe yield loss compared to the vegetative stage, ii) floral fertility is extremely sensitive to water deficit stress, and iii) rainfed drought-prone areas have more frequent droughts at the reproductive-stage. Currently, little information is available on the flag leaf and panicle gene expression profiles of rainfed rice under reproductive-stage drought stress. Our approach is to study differential responses of DTY-IL and Swarna, moderate water-deficit stress at the reproductive stage, and identify putative genes and pathways that are responsive to drought and are potentially involved in drought-tolerance

mechanisms. This will advance our understanding of drought tolerance's genetic mechanisms in rice source and sink tissues under reproductive-stage drought stress.

MATERIALS AND METHODS

Plant Materials and Stress Treatments

Two rice genotypes were used in this study. Swarna is a widely grown *indica* inbred rice in South Asia, with high yield and good quality, but very susceptible to drought stress. IR96321-1447-165-B-3-1-2 is an F_7 drought-tolerant introgression line (DTY-IL) derived from the three-way cross of IR91659:54-35//IR81896-B-B-195/2*IR05F102. IR91659:54-35 is a BC_4F_4 drought-tolerant IL harboring *qDTY1.1* with chromosomal segments introduced from the drought-tolerant donor parent N22 into the background of the recurrent parent Swarna. DTY-IL is also a sister line of I.R. 96321-1447-651-B1-1-2, recently released as a drought-tolerant variety in Nepal (Kumar *et al*., 2018).

To re-evaluate the drought tolerance performance of the two genotypes, a 2x2 factorial experiment was arranged in a randomized complete block design with two treatments (well-watered and 2-weeks drought-stressed), two genotypes, and six replications per treatment under controlled greenhouse conditions at the International Rice Research Institute (IRRI, Los Baños, Philippines) from July to November 2015. Three pre-germinated seeds of the two genotypes were initially seeded on white porcelain pots (individually weighed beforehand) filled with 15 kgs of dry puddled field soil (cleaned but not sterilized). Upon seedling establishment, a healthy seedling was retained in each pot, adequately fertilized, and grown under a well-watered condition in the greenhouse until the booting stage. All pots were irrigated twice daily to maintain the soil saturation. The temperature inside the greenhouse during drought stress induction was at a maximum of 30–34 °C and a minimum of 23–26 °C, and a day-time relative humidity of 69%–95% (Figure 1.1). A day before imposing stress, all the pots were saturated with water and allowed to drain excess water overnight by loosening the base stoppers to maintain the field capacity so that the soil moisture amount in each pot was uniform. Then each pot was weighed to get the saturated weight. During the drought stress period, the pots were weighed daily, and the difference in weight on subsequent days was corrected by adding water to maintain the required field capacity

(Krishnan *et al*., 2017). Pots under reproductive-stage drought stress were covered with white plastic to prevent evapotranspiration. For reproductive-stage drought stress, water was withheld at the reproductive R2 stage, on discrete morphological criteria described by Counce *et al*. (2000), until the soil moisture level dropped to 75% field capacity and was maintained for nine days, whereas control plants were well-watered. On day 10, field capacity was reduced to 50% for three more days (Figure S1B). Two to three flag-leaf from each plant's tiller were sampled for each genotype x treatment combination. Two to three whole panicles from individual tiller (not the one collected with flag-leaf) were sampled for each genotype x treatment combination without the flag leaf sheath. Only those panicles at maximum booting (without any panicle/spikelet exserting from the boot), were considered for sampling. Flag-leaf and whole panicle samples of well-watered and drought-stressed treatments were collected at the R3 stage (Counce *et al*. 2000) on the 13th day of drought and immediately flash-frozen in liquid nitrogen. Six independent biological replicates for each tissue and each genotype x treatment combination were harvested. Re-watering was resumed continuously after sampling until grain maturity.

RNA extraction, library construction, and sequencing

Total RNA was extracted from tissues grounded in liquid N_2 of all the flag leaf and whole panicle tissue samples for each genotype and both treatments. The TRizol reagent (Invitrogen, USA) was used to extract total RNA and isolated using the Qiagen RNeasy Plant Mini Kit (Qiagen, Limburg, Netherlands). The total RNA was treated with DNase I recombinant, RNase-free (Roche, Basel, Switzerland) to remove DNA contamination. The total RNA concentration was quantified using a Nanodrop spectrophotometer (ND-1000; Nanodrop Technologies, Wilmington, DE), with absorbance at 260 nm. An Agilent 2100 BioAnalyzer RNA 6000 Kit (Agilent Technologies) was used to examined RNA quantity and integrity as per the manufacturer's instructions. A 20ul total RNA was sent for sequencing. Illumina library preparation and sequencing of 16 samples per tissue (2 genotypes x 2 treatments x 4 biological replicates) was completed following standard protocols Macrogen INC (Seoul, Korea). Libraries were prepared using the Illumina TruSeq RNA library method according to TruSeq RNA Sample Preparation Guide. Macrogen INC subjected the produced libraries to cluster generation through bridge amplification and paired-end sequencing

on HiSeq 2000 and HiSeq 4000 platforms for the whole panicle and flag leaf tissues to obtain reads of 101 bp paired-end reads. Fastq files were generated using the Illumina pipeline.

The adapters and other Illumina-specific sequences were trimmed away from the raw fasta reads and were filtered using Trimmomatic (version 0.33) (Bolger et al., 2014). Parameter settings were as follows ((ILLUMINACLIP:./Tru-Seq3-PE-2.fa:2:30:15 LEADING:28 TRAILING:28 MINLEN:30). The per base sequence quality was checked after trimming using FastQC (version 0.11.5).

Transcriptome Analysis

The high-quality paired-end reads after quality filtering were used for downstream analysis. Salmon (version 0.7.2) software was used for transcript abundance estimation (Patro et al., 2017). Salmon employs a new dual-phase statistical inference procedure, and its rich model accounts for the effects of sample-specific parameters and biases that are typical of RNA-Seq data, including positional biases in coverage, sequence-specific biases at the 5' and 3' ends of sequenced fragments, fragment G.C. bias, strand-specific protocols, and fragment length distribution. It provides accurate expression estimates quickly while using little memory and disk usage compared to the alignment-based method. Some advantages of using the Salmon for transcript abundance estimation are: 1) this approach corrects for potential changes in gene length across samples (e.g., from differential isoform usage) (Trapnell et al., 2013), and 2) it is also possible to avoid discarding those fragments that can align with multiple genes with homologous sequences, thus increasing sensitivity (Robert and Watson, 2015). To estimate transcript abundance, the rice genome fasta file, and gff3 annotations were downloaded from Rice Genome annotation release 7 (RGAP 7, http://rice.plantbiology.msu.edu/) (Kawahara et al., 2013). The gffread function under Cufflinks (version 2.2.1) (http://cufflinks.cbcb.umd.edu/) software was used to make a transcriptome fasta file. A Salmon index for the transcriptome was built using the converted transcriptome fasta file. This built the quassi-mapping-based index, using an auxiliary k-mer hash over k-mers of length 31, which act as the minimum acceptable length for a good match. Quassi-mapping accurately quantifies transcripts through mapping of reads to transcript position that are computed without performing a base-to-base alignment of the read to the transcript (Srivastava et al., 2016). Salmon used the indexed transcriptome and the trimmed high-quality sequencing reads to quantify in

quassi-mapping mode directly. To allow Salmon to infer the library type automatically, the parameter –l A was provided to Salmon. To assess technical variance in the main abundance estimates produced, parameter –numBootstraps=30 was used, useful for downstream analysis like differential expression. To enable Salmon to learn and correct sequence-specific and fragment-level G.C. content biases, parameters –seqBias and –gcBias were included in quantification.

Importing and summarizing transcript-level estimates for gene-level analysis

The estimated transcript abundance from Salmon was imported and aggregated to the gene level using the Bioconductor package *tximport* (version 1.2.0) (Soneson et al., 2016) complemented with the *readr* package (version 1.1.1) through R (version 3.3.3) software. The package demonstrates that gene-level estimation and inferences are more robust than those at the transcript level. The aggregation of these abundances to the gene level leads to an improved estimation of differential gene expression. The *tximport*-to-*DESeq2* approach uses *estimated* gene counts from the transcript abundance quantifiers but not *normalized* counts.

Gene-level exploratory analysis and visualization

Data quality assessment and quality control are essential steps of any data analysis, and these steps should typically be performed very early in the analysis. The purpose is to detect differentially expressed genes. We are looking for samples whose experimental treatment suffered from an abnormality that renders the data points obtained from these particular samples detrimental to our purpose. To visually explore sample relationships, the shrinkage approach of *DESeq2* implement a variance stabilizing transformation (*vst*) for quality assessment, and clustering of overdispersed count data was used. The *pheatmap* package (version 1.0.8) with the *RColorBrewer* package (version 1.1.2) was used to check the overall similarities and dissimilarities between samples. To visualize the overall effect of experimental covariates and batch effects, we used a 2D PCA and plotted it using *ggplot2* (version 2.2.1) and *gplots* package (version 3.0.1). While the *vst* function builds upon the log2-fold-change shrinkage approach, it is distinct from and not part of the statistical inference procedure for differential expression analysis.

Differential Expression (D.E.) Analysis

A fundamental task in the analysis of count data from RNA-Seq is the detection of differentially expressed genes. Differential expression analysis at the gene-level was done using a Bioconductor package *DESeq2* (version 1.14.1) (Love et al., 2014). The DESeq2 package provides testing methods for differential expression using negative binomial generalized linear models; the shrinkage estimates of dispersion and logarithmic fold changes incorporate data-driven prior distributions. The imported and summarized transcript-level abundance estimates using the *tximport* function were used to construct a gene-level count matrices DESeqDataSet object from Salmon quant.sf with a design formula to inform many of the DESeq2 function how to treat(model) the samples in the analysis. The *DESeqDataSetFromTximport* was created using the counts (Numreads) and average transcript lengths from *tximport*. The design formula was used to estimate the dispersions and to estimate the $\log_2$-fold-changes of the model. An additional design was used to model multiple condition effects, which can be easily extracted with results(). This essentially allows for combining the factors of interest into a single factor with all combinations of the original factors and changing the design to include just this factor (e.g., ~group). Minimal pre-filtering was done to keep only rows that have at least ten reads total. This reduces the duct data object's memory size of the dds data object and increases the speed of the transformation and testing functions within *DESeq2*.

When running the differential testing pipeline, it is important to use the un-normalized estimated counts of sequencing reads as input because the *DESeq2*'s statistical testing methods rely on original count data for calculating the precision of measurement. The *DESeq2* model internally corrects for library size, so transformed or normalized values such as counts scaled by library size will not be used as input. The standard differential expression analysis steps are wrapped into a single function, *DESeq*, which by default produces moderated, or shrunken log2 fold changes using the betaPrior argument wherein a zero-centered Normal prior distribution is assumed for the coefficients other than the intercept. The function *DESeq* performs various steps. Briefly, these estimate size factors (using the average transcript length from dds assay and correcting for library size), the estimation of dispersion values for each gene, and fitting and testing a generalized linear model. In high-throughput biology, we are careful not to use the *p* values

directly as evidence against the null but correct for *multiple testing. DESeq2* uses the Benjamini-Hochberg (B.H.) adjustment (Benjamini and Hochberg, 1995) as implemented in the base R *p.adjust* function. The *results* function automatically performs independent filtering based on the mean of normalized counts for each gene, optimizing the number of genes with an adjusted *p*-value below a given FDR cut-off, alpha. By default, the argument alpha is set to 0.1. We set the adjusted *p-value* cut-off to 0.05 as the final criterion. That is, we considered all genes with an adjusted *p-value* (FDR) below 5% = 0.05 as significant. Since we do not know the mechanisms of drought tolerance of the introgression line yet, we used the contrast argument. Contrast is a linear combination of estimated $\log_2$ fold changes, which can be used to test if differences between groups are equal to zero. We had four groups: groupILControl, groupILDrought, groupSwarnaControl, and groupSwarnaDrought wherein we designed contrast arguments to extract results of $\log_2$ fold changes of interest. The condition effect for each genotype was extracted using the following contrasts: (res.05_NILD_NILC <- results(dds, contrast=c("group","ILDrought", "ILControl"), alpha=.05, parallel = TRUE)) and (res.05_SWAD_SWAC <- results(dds, contrast=c("group","SwarnaDrought", "SwarnaControl"), alpha=.05, parallel = TRUE)). The genotypic effect for each condition was extracted using the following contrasts: (res.05_NILC_SWAC <- results(dds, contrast=c("group","ILControl", "SwarnaControl"), alpha=.05, parallel = TRUE)) and (res.05_NILD_SWAD <- results(dds, contrast=c("group","ILDrought", "SwarnaDrought"), alpha=.05, parallel = TRUE)).

Identification of DEG's with a unique response to drought

To extract the list of genes that showed unique responses to drought from the two genotypes, we composed a four-way Venn Diagram (version 1.6.17) combining the upregulated and downregulated genes of all the pairwise comparisons generated through the contrast argument. We focused on the common responses of the two contrasting genotypes to drought and the DTY-IL and Swarna's unique responses to drought, respectively. Differentially expressed genes (DEGs) were defined as those presenting an absolute fold change (F.C.) ≥ 2 or ≤ 0.5 and an FDR adjusted *P-value* ≤ 0.05 in any pairwise comparison.

Gene Ontology and Functional Enrichment Analysis

Gene ontology enrichment for uniquely identified DEGs was performed using the singular enrichment analysis (SEA) method using agriGO (version 2.0) (Tian et al., 2017), a G.O. analysis tool for the agricultural community. We performed a hypergeometric test and incorporated a false discovery rate correction using the Hochberg (FDR) method of multiple hypothesis testing to reduce false positives with five minimum number of mapping entries against MSU7.0 gene I.D. A cut-off value for the FDR adjusted P-value ≤0.05 was used to screen for G.O. term enrichment.

The STRING database (http://string-db.org) aims to provide a critical assessment and integration of known and predicted protein-protein interactions, including direct (physical) as well as indirect (functional) associations (Szklarczyk, 2017). STRING shows evidence for statistical enrichment of any known biological function or pathway, making full use of the latest protein network information. This is achieved through an included functionality to detect enrichment of functional systems in each currently displayed network in STRING, testing some functional annotation spaces including Gene Ontology, KEGG pathways, Pfam, and InterPro domains (Franceschini et al., 2013). Further functional enrichment was performed using the STRING database (version 10.5) through a Fisher's exact test. The P-values were corrected for multiple testing using the method of Benjamin and Hochberg. A cut-off value for the FDR adjusted P-value of < 0.05 was used to screen for more enriched terms in the set of proteins in the network than the whole genome background (Oryza sativa japonica, NCBI:txid39947).

Promoter analysis

In silico analysis of 2-kb regions of promoters of the unique groups of DEGs in DTY-IL and Swarna under RDS was performed using ELEMENT (version 2.0) against the RGAP 7 genome with a Benjamini-Hochberg cut-off at 0.05. ELEMENT is a web-based tool that identifies statistically over-represented motifs across groups of promoters.

Quantitative PCR Analysis

Primers were designed using QuantPrime (https://quantprime.mpimp-golm.mpg.de). According to the manufacturer's protocol, cDNA was synthesized from 2 µg total RNA using the ImProm-II Reverse Transcription System (Promega, WI, USA). qRT-PCR was performed using

two independent biological replicates and three technical replicates. qRT-PCR was set up in 386-well PCR plates with 0.2 μM primers using SYBR Green PCR Master Mix kit (Applied Biosystems, CA, USA), following the manufacturer's protocol in a reaction volume of 10 μL via a Roche LightCycler 480 Real-Time system (Rotkreuz, Switzerland). Reaction conditions were as follows: denaturation at 95 °C for 5 min, 45 cycles of 95 °C for 10 s, 60 °C for 15 s and 72 °C for 8 s, heating from 65 to 95 °C. Two internal reference genes ELF and ATU, were designed to normalize the relative gene expression levels for flag-leaf and panicle tissue, respectively, using the $2^{\Delta\Delta}$C.T. method with $\Delta CT = CT_{gene} - CT_{reference\ gene}$ (Livak and Schmittgen, 2001). For comparison of fold change, scatterplots were generated using the $\log_2$ fold change determined between RNA-Seq and qRT-PCR, which is defined as ΔΔCT (for comparative threshold cycle).

RESULTS AND DISCUSSION

Generating a transcriptional map of the moderate RDS response in rice

To obtain insight into the transcriptome changes in rice flag-leaf and panicle whole-genome expression profiles under moderate water-deficit treatments and therefore to provide a global overview of the mechanisms underlying drought tolerance in the flag-leaf and panicle, we examined the effects of moderate water deficit treatment on the gene-expression profile of a drought-tolerant drought-introgression line (DTY-IL) and the drought-susceptible parent Swarna at the reproductive-stage, using the Illumina HiSeq platform. The water deficit treatment started at the beginning of the booting stage. The plants were dried until the soil moisture content reached 50%, until which Swarna exhibited almost complete leaf rolling. The water deficit regime was imposed through available soil moisture content, approximating the field conditions at the reproductive phase, a critical stage at which rice is susceptible to water deficit stress, and after which grain yield was drastically decreased.

In our RNA-Sequencing analysis, we focused on three functional categories of genes: 1) differentially expressed common genes, which reflect drought-responsive genes in the DTY-IL and the recurrent parent Swarna, 2) putative genes and pathways for both tissues in Swarna, and 3) putative drought-tolerant genes and pathways for both tissues in DTY-IL.

Mapping rates of paired-end (P.E.) reads against the rice genome (RGAP 7, http://rice.plantbiology.msu.edu/) were in the range of 77.7-92.9% for flag-leaf and 87.9-92.8% for panicle tissue (Table 1.1). There were 28,283 and 33,698 genes with nonzero total read count for flag-leaf and panicle, respectively, that was used for quality assessment and differential expression analysis.

Log_2 transformed and normalized count data were used for quality assessment and quality control of the samples. Sample clustering and heatmap visualization demonstrated a clear separation between genotypes and treatments for flag leaf and panicle samples (Figure 1.2; Figure 1.3). Principal component analysis (PCA) showed that the percentage of total variation accounted for by the first and second principal components were 93% and 81% for flag-leaf and panicle tissue, respectively (Figure 1.4). Biological replicates of each genotype-treatment combination clustered together and the treatment effect were more significant than the genotype effect for both tissues (Figure 1.4). An exception was a single Swarna panicle sample removed from all further analyses as an outlier (Figure 1.5).

Differential expression (D.E.) analysis was done using the raw counts. We further performed statistical tests between gene expression values profiled from each of the four pairwise comparisons using *DESeq2*. The sum of the nonredundant/unique log_2 normalized genes whose expression levels showed significant changes across four different contrasts at FDR adjusted *P-value* ≤ 0.05 were 17,616 and 18,614 for flag-leaf and panicle tissue, respectively. Pairwise DE analysis for all genotype-treatment combinations identified DEGs of significance (log_2 fold changes > 1 or < -1 at FDR-adjusted *P-value* < 0.05) for flag leaf and panicle (Figure 1.6), and a four-way Venn diagram was used to visualize three categories of unique and common responses in flag leaf and panicle tissues (Figure 1.7; Figure 1.8).

Flag-leaf transcriptome under moderate RDS

An analysis of the gene-expression profiles of the differentially expressed common genes indicated that a variety of G.O. terms related to G.O. categories such as biological processes, cellular components, and molecular functions, with the lowest FDR-adjusted *p*-values, were up- and down-regulated in the two genotypes in this study under moderate water deficit treatment. Tables 1.3 to 1.4 summarizes the major GO classifications of the differentially expressed common

genes in the DTY-IL and Swarna. A total of 4180 genes were drought-responsive in flag leaves of both Swarna and DTY-IL (Figure 1.7 (A); Table 1.2). The most general GO terms of 2155 upregulated differentially expressed common genes in DTY-IL and Swarna in the flag-leaf tissue were 2) biological processes: (1) 'regulation of transcription,' (2) 'regulation of nitrogen compound metabolic process,' and (3) 'regulation of biosynthetic process'; and b) molecular functions, which reflect essential aspects of molecular activities, including 'hydrolase activity,' oxidoreductase activity,' and 'transcription factor activity' (Table 1.3). As for 2025 downregulated differentially expressed common genes, we observed that the G.O. categories were related mainly to 'transmembrane transport,' 'localization,' 'oxidation-reduction,' and 'post-translational protein modification' (PTM) (Table 1.4).

In Swarna flag-leaves, a total of 515 (188 up- and 327 downregulated) genes were found to be uniquely drought-responsive (Table 1.2). While no significant G.O. terms were detected for upregulated DEGs (Table 1.2), significant G.O. terms for downregulated DEGs were primarily related to 'post-translational protein modification,' 'photosynthesis,' 'defense response,' and 'programmed cell death' (Figure 1.9). Genes involved in the PTM were different kinds of kinases (particularly receptor kinases, serine/threonine-protein kinases, wall-associated kinases, lectin-like kinases, and DUF26 kinases). PTMs are chemical modifications that play a crucial role in functional proteomic because they regulate activity, localization, and interaction with other cellular molecules such as proteins, nucleic acids, lipids, and cofactors. The downregulation of the different protein kinases in Swarna flag-leaf under reproductive-stage drought stress signifies that these genes might not form a mature protein product. Pathway enrichment suggested photosynthesis, ubiquinone, and other terpenoid-quinone biosynthesis, as well as glutathione-mediated detoxification II and tyrosine biosynthesis (Table 1.5) to be significantly downregulated.

Notable downregulated differentially expressed genes in Swarna were noted through the KEGG Orthology, a database of molecular functions defined in KEGG molecular networks. LOC_Os08g35210 is the respiratory burst oxidase gene, which is one source of reactive oxygen species. Downregulation of this gene would affect the maintenance of homeostasis of reactive oxygen species. A few genes involved in plant hormone signal transduction were also noted. A downregulated gene in Swarna is LOC_Os0320650, an ABA-responsive element binding factor which could contribute to the regulation of stomatal closure. Also, LOC_Os01g59350, a

Transcription Factor TGA, is downregulated in Swarna, and this gene is involved in disease resistance. Thus, downregulation of this gene could contribute to the susceptibility of Swarna to disease. This potentially implies a crosstalk between biotic and abiotic stress response in Swarna flag-leaf.

To evaluate the effect of introgression on the transcriptome of the DTY-IL under drought stress, the genome-wide gene expressions in the DTY-IL and Swarna under RDS were compared. The results indicated that in DTY-IL flag leaves, 108 (74 up- and 34 downregulated) DEGs were uniquely drought-responsive. While no significant G.O. terms could be associated with downregulated DEGs, 'oxidation-reduction,' 'response to stress,' and 'response to stimulus' were among the significant G.O. terms in upregulated DEGs (Figure 1.10). Upregulated DEGs in DTY-IL flag-leaf involved in 'response to stress' were explicitly involved in response to oxidative stress (catalase, zinc knuckle domain-containing protein, and two peroxidase precursors) and plant-pathogen interaction (resistance protein and NBS-LRR disease resistance protein), signifying potential crosstalk between the biotic and drought stress tolerance. To sustain standard morphological structure and physiological function, plant cells must complete normal homeostasis, including electron transfer and oxidation-reduction, and activate oxygen-scavenging to resist stress (Yuan et al., 2017). Cytochrome P450, oxidoreductase, dehydrogenase are some of the upregulated genes with oxidoreductase and electron-carrier activity involved in 'oxidation-reduction' in the flag-leaf of DTY-IL under reproductive-stage drought stress in our study. Pathway enrichment suggested phenylpropanoid biosynthesis, dhurrin, xylan, and scopoletin biosynthesis, as well as detoxification of reactive carbonyls in chloroplasts to be uniquely upregulated under RDS (Table 1.6).

Two notable upregulated genes in the flag-leaf of DTY-IL were also noted using the KEGG Orthology. LOC_Os02g02400 is a Catalase gene. It is well documented that Catalase is involved in scavenging reactive oxygen species. This gene, particularly mapped in the KEGG pathway, is involved in Salt/Drought stress by modulating the H_2O_2 production resulting, in a stress-tolerant response. Another gene is LOC_Os05g44570, a histidine-containing phosphotransfer protein, and this gene is involved in cell division/shoot initiation.

Panicle transcriptome under moderate RDS

A total of 4799 genes were found to be drought-responsive in panicles of both Swarna and DTY-IL (Figure 1.7 (B); Table 1.2). Details of the G.O. classifications of the differentially expressed common genes in DTY-Il and Swarna in the panicle tissue were shown in Tables 1.7 to 1.8. Under moderate water stress, the most significant upregulated G.O. terms that were over-represented in the two genotypes with 1775 differentially expressed common genes were as follows: 'post-translational protein modification,' 'phosphorylation,' and 'response to stress' (Table 1.7). The 3024 downregulated differentially expressed common genes, on the other hand, mainly were related to 'transmembrane transport,' 'carbohydrate metabolic process,' and 'localization' (Table 1.8).

In Swarna panicles, a total of 487 (184 up and 303 downregulated) genes were found uniquely drought-responsive (Table 1.2). No significant G.O. categories were identified within the uniquely upregulated DEGs of Swarna. For the uniquely downregulated genes in Swarna panicles, significant G.O. terms included 'oxidation-reduction' as well as 'monooxygenase activity,' 'tetrapyrrole binding,' and 'heme-binding' (Figure 1.11). Most of the genes with 'oxidoreductase activity' are cytochrome P450 with two dehydrogenase, oxidoreductase, and peroxidase precursor genes. Significantly enriched pathways associated with downregulated DEGs were DNA replication, diterpenoid biosynthesis, phenylpropanoid biosynthesis, and photosynthesis (Table 1.9).

Notable in the panicle downregulated genes in Swarna were also listed as per KEGG Orthology. LOC_Os07g22770 is an Ethylene-responsive Transcription Factor 1, and this gene was annotated to be involved in defense and wounding responses. Downregulation of this gene in Swarna panicle would also hinder fruit ripening as per KEGG Orthology. Thus, its upregulation in DTY-IL would promote fruit ripening. Another interesting downregulated gene in Swarna is LOC_Os01g12160, a Jasmonic acid-amino synthetase found upstream of the alpha-Linolenic acid metabolism is involved in senescence and stress response.

DEGs were uniquely drought-responsive in DTY-IL panicle 164 (108 up and 56 downregulated) (Table 1.2). No significant G.O. enrichment was identified among the uniquely downregulated DEGs of DTY-IL. Prevalent G.O. terms of upregulated DEGs in DTY-IL for the

panicle tissue were related to ‘protein amino acid phosphorylation’ as well as ‘oxidation-reduction’ and ‘carbohydrate metabolic process’ (Figure 1.12). Interestingly, three putative transposable Elements (TEs) were included in the DEGs under the ‘oxidation-reduction’ category, one retrotransposon and two transposon proteins. Most of the genes upregulated in the panicle of DTY-IL under the ‘protein phosphorylation’ category were receptor proteins (wall-associated kinases, receptor-like protein kinases, and DUF26 kinases), most likely involved in the signal transduction pathway. Protein phosphorylation in PTMs plays a crucial role in plant stress tolerance by transmitting intracellular signals from the cell surface to the nucleus to regulate proteins’ cellular functions (Zhang et al., 2020). The upregulated gene expression of several protein kinases involved in protein phosphorylation in the panicle of DTY-IL under reproductive-stage drought stress could positively contribute to improved reproductive-stage drought tolerance in our study. The most significantly enriched pathways in the panicle tissue of DTY-IL upregulated DEGs were related to propanoate metabolism, methylerythritol phosphate pathway, diterpenoid biosynthesis, camalexin biosynthesis, and circadian rhythm in plants (Table 1.10).

Few notable panicle upregulated genes in the DTY-IL were also noted. LOC_Os09g33850, annotated as a Flowering Locus T is essentially involved in flowering. This gene was significantly downregulated in the Swarna panicle. Two upregulated genes involved in defense response and cell death were also noted. LOC_Os04g52780, an LRR receptor-like Serine/threonine-protein kinase, and LOC_Os03g30470, a basic chitinase B. This also implies potential crosstalk between pathogen infection, phytohormones response, and drought stress tolerance.

Transcriptome characterization in the flag-leaf and panicle tissues of the DTY-IL and the parent Swarna

Many genes were differentially regulated in the flag-leaf and panicle tissues of the DTY-IL and the recurrent parent Swarna under moderate reproductive-stage drought stress, suggesting the two genotypes’ high background similarity. The number of drought-responsive genes (both up-and downregulated) that were differentially expressed under RDS in the panicle tissue for both genotypes was more significant than the flag-leaf. An almost similar number of up-and downregulated DEGs were observed in the flag-leaf but almost doubled downregulated DEGs

were identified in the panicle tissue signifying a tissue-specific response to reproductive-stage drought stress.

Main Differences in Molecular Functions of the DEGs in the Flag-leaf and Panicle tissues of Swarna and DTY-IL under RDS

GO analysis was done to differentiate between the DEGs' molecular functions in the flag-leaf and panicle tissues for the two genotypes under RDS. Differences were noted in the molecular functions of the up-and downregulated DEGs. For the upregulated DEGs, the leaf transcriptome profile of the DTY-IL was enriched for genes involved in 'oxidoreductase activity.' In the panicle profile of the 'DTY-IL, upregulated DEGs with the molecular functions' protein serine/threonine kinase activity,' 'phosphotransferase activity,' and 'hydrolase activity.' When we analyzed the downregulated DEGs of Swarna in flag-leaf, 'protein serine/threonine kinase activity,' 'adenyl nucleotide-binding,' and 'nucleoside binding' were uniquely enriched GO terms. Most of the repressed DEGs in the panicle of Swarna under RDS were involved in the 'binding' GO category, such as 'tetrapyrrole,' monooxygenase,' and 'heme/iron.'

A better understanding of the molecular function and quantities of genes commonly regulated by water-deficit stress will help identify the adaptive responses to drought in plants. The genes with altered expression are likely those involved in the pathways that underlie plant response to water deficit. We observed that various genes related to 'hydrolase activity' were induced in the panicle of DTY-IL in response to moderate RDS. These gene families play essential roles in plants' stress tolerance through diverse physiological activities (Shankar et al.,2013), and their expression is activated by drought stress in rice. Heme-binding (peroxidase precursors and cytochrome P450) were noted to be downregulated in the panicle of Swarna in the present study. This may lead to the accumulation of hydrogen peroxide in guard cells. Furthermore, the downregulation of genes in Swarna flag-leaf and panicle belonging to the electron-carrier activity and photosystem categories may be the result of a reduction of photosynthetic activity under drought, which could be due to reductions in stomatal conductance and Rubisco activities, leading to lower carbon fixation, which consequently results in the over-reduction of components within the electron transport chain and the generation of reactive oxygen species (Moumeni et al., 2015).

Validation of Differential Gene Expression

RNA-Seq results were validated using ten genes from different response categories (increased, decreased, and non-differentially expressed genes upon treatment in both flag-leaf and panicle) for qRT-PCR (Figure 1.13). Four selected genes from within the *qDTY1.1* region (LOC_Os01g66120, LOC_Os01g66180, LOC_Os01g66820, and LOC_Os01g67030) showed differential expression. LOC_Os01g66120 (no apical meristem protein) was upregulated in both genotypes and both tissues under drought. LOC_Os01g66180 (cytochrome c) is upregulated in DTY1.1-IL and downregulated in Swarna in both tissues under RDS. The DTY-IL dramatically maintains its expression of LOC_Os01g66820 in drought stress panicles, but not in flag-leaves. LOC_Os01g67030 (auxin-responsive protein) was upregulated under RDS in DTY-IL panicles and downregulated in Swarna panicles but not affected by RDS in flag-leaves. A high correlation between qRT-PCR results and RNA-Seq results was observed for flag-leaf (R^2 = 0.88) and panicle (R^2 = 0.91) tissues (Figure 1.13), supporting RNA-Seq-based findings and interpretations. Targeted transcripts and respective primer sets used were shown in Table 1.11.

Significance of the regulatory motifs of the unique groups of DEGs in DTY-IL and Swarna

In silico analysis of 2-kb regions of promoters of the unique DEGs groups in DTY-IL and Swarna under RDS was performed using ELEMENT (version 2.0). ELEMENT is a web-based tool that identifies statistically over-represented motifs across groups of promoters.

Numerous overrepresented *cis*-elements were found in 327 promoters of uniquely downregulated DEGs in Swarna in flag-leaf, primarily binding sites for dehydration responsive genes. These include ACGTATERD1, IBOX, PREATPRODH, MYCATERD1, MYCATRD22, CCAATBOX1, and MYB2AT (Table 1.12). The overrepresented motifs in a set of 74 promoters in the uniquely upregulated DEGs in DTY-IL in flag-leaf were mostly functioning upon induction of dehydration stress through the ACGTATERD1 motif. Other overrepresented *cis*-acting elements were GT1GMSCAM4, BIHD10s, and WRKY10S (Table 1.13).

Overrepresented *cis*-acting elements in 303 promoters of the uniquely downregulated DEGs in Swarna in panicle tissue mainly involved dehydration response like the ACGTATERD1 MYBCOREATCYB1, ABRELATEDRD1, and IBOX motifs (Table 1.14). Overrepresented *cis*-elements in a set of 108 promoters of uniquely upregulated DEGs in DTY-IL in panicle tissue

mainly were related to dehydration response like the MYB2AT, MYBCOREATCYCB1, and ACGTABOX (Table 1.15).

The regulatory *cis*-elements present in promoter regions are one of the remarkable aspects of gene regulation. They provide a detailed explanation for the co-expression of a group of co-expressed genes (Moumeni et al., 2015). Under moderate RDS, the essential regulatory motifs identified in the promoters of the unique upregulated DEGs in DTY-IL and downregulated DEGs in Swarna were mainly involved as binding sites for dehydration responsive genes, potentially suggesting the differential response of Swarna and DTY-IL under reproductive-stage drought stress. Some of the identified over-represented *cis*-elements in the promoter region of the specific DEGs in Swarna and DTY-IL were related to MYB Transcription Factor. Drought responsive genes in rice have been reported to contain MYB (C/TAACG/TG) consensus elements. A MYBCOREATCYCB1 motif was a binding site of at least two plant MYB proteins ATMYB1 and ATMYB2, and the latter is involved in the regulation of genes that are responsive to water stress in Arabidopsis (Solano et al., 1995) with MYB2AT motif as binding site as well. Binding sites of the MYC transcription factor in *Arabidopsis thaliana* erd1 (early responsive to dehydration) and dehydration-response gene rd22 were also overrepresented, signifying the importance of the MYC recognition sequence necessary for the expression of these genes (Shinozaki, 1997). Other regulatory elements are related to ACGTATERD1 and ABRELATERD1 motifs with a core sequence of ACGT and ACGTG, and these sequences were required for etiolation-induced expression of erd1 in Arabidopsis (Yamaguchi-Shinozaki, 2003). This study's information may further analyze the putative novel regulatory elements through mutation/deletion analysis to uncover more TFs.

CONCLUSION

The study provided a comprehensive overview of the molecular and gene-expression changes under water-deficit treatments in the flag-leaf and panicle tissue of rice as a source and sink machinery, respectively using three particular elements: 1) a drought-introgression line and its recurrent parent Swarna, 2) an Illumina Hi-Seq platform covering all the entire rice genome, and 3) water deficit treatments via a soil moisture content/field capacity method in the

reproductive-stage almost mimicking field conditions. This set-up allowed us to carry out transcriptional profiling in the flag-leaf and panicle tissue of rice and identified putative drought-responsive genes and genes involved in tolerance to drought stress. Despite having a similar genetic background, we reported that these two genotypes with contrasting drought responses have different potential mechanisms/pathways based on the transcriptome data from the flag-leaf and panicle tissues. The present study provided insight into the gene-expression profiles of the flag-leaf and panicle tissues, including the main functional categories of drought-responsive genes and those involved in drought tolerance mechanisms and potentially affect the plant phenotype in response to water stress. This work will help breeders improve the drought tolerance of rice cultivars. In the meantime, further work is needed on the physiological aspects of the flag-leaf and panicle reactions of rice DTY-IL under reproductive-stage drought stress, such as stomal closure, conductance, and density, and agronomic characterization, especially the grain yield and yield-related components.

TABLES AND FIGURES

Table 1.1. Mapping results of RNA-Seq reads of Swarna and Introgression Line (DTY-IL) under reproductive-stage drought stress and control conditions.

Samples	Flag-leaf			Panicle		
	Total fragments	Total read counts	Mapping rate	Total fragments	Total read counts	Mapping rate
IL_C_FL1	18647745	17139189	91.9102%	32407311	29931901	92.3616%
IL_C_FL2	19672858	18079752	91.9020%	32708248	29897712	91.4073%
IL_C_FL3	21197153	19367167	91.3668%	32450231	30031141	92.5452%
IL_C_FL4	16497328	15140321	91.7744%	28337665	26308525	92.8394%
IL_D_FL1	18192316	16835349	92.5410%	27841197	25360191	91.0887%
IL_D_FL2	15714912	14250563	90.6818%	31783306	27958965	87.9675%
IL_D_FL3	18993072	17325378	91.2195%	28181167	25596954	90.8300%
IL_D_FL4	16727725	15437176	92.2850%	30321220	27358715	90.2296%
S_C_FL1	20351631	20351631	91.9808%	32056573	29674988	92.5707%
S_C_FL2	17734494	16451522	92.7657%	33576990	31080099	92.5637%
S_C_FL3	18143450	16674788	91.9053%	31532581	29034816	92.0788%
S_C_FL4	17899529	16634750	92.9340%	29940903	27453849	91.6935%
S_D_FL1	18791386	17136288	91.1923%	30751211	27971547	90.9608%
S_D_FL2	17203402	15656064	91.0056%	29178726	26244026	89.9423%
S_D_FL3	16414736	14854107	90.4925%	29973948	27191513	90.7172%
S_D_FL4	19943244	15503358	77.7374%	27615112	24677602	89.3627%

Note: C indicates well-watered control; D indicates drought stress; 1-4 in the first column indicate four replicates of each sample. IL_C_FL = DTY-IL Control Flag-leaf; IL_D_FL = DTY-IL Drought Flag-leaf; S_C_FL = Swarna Drought Flag-leaf; S_D_FL = Swarna Drought Flag-leaf

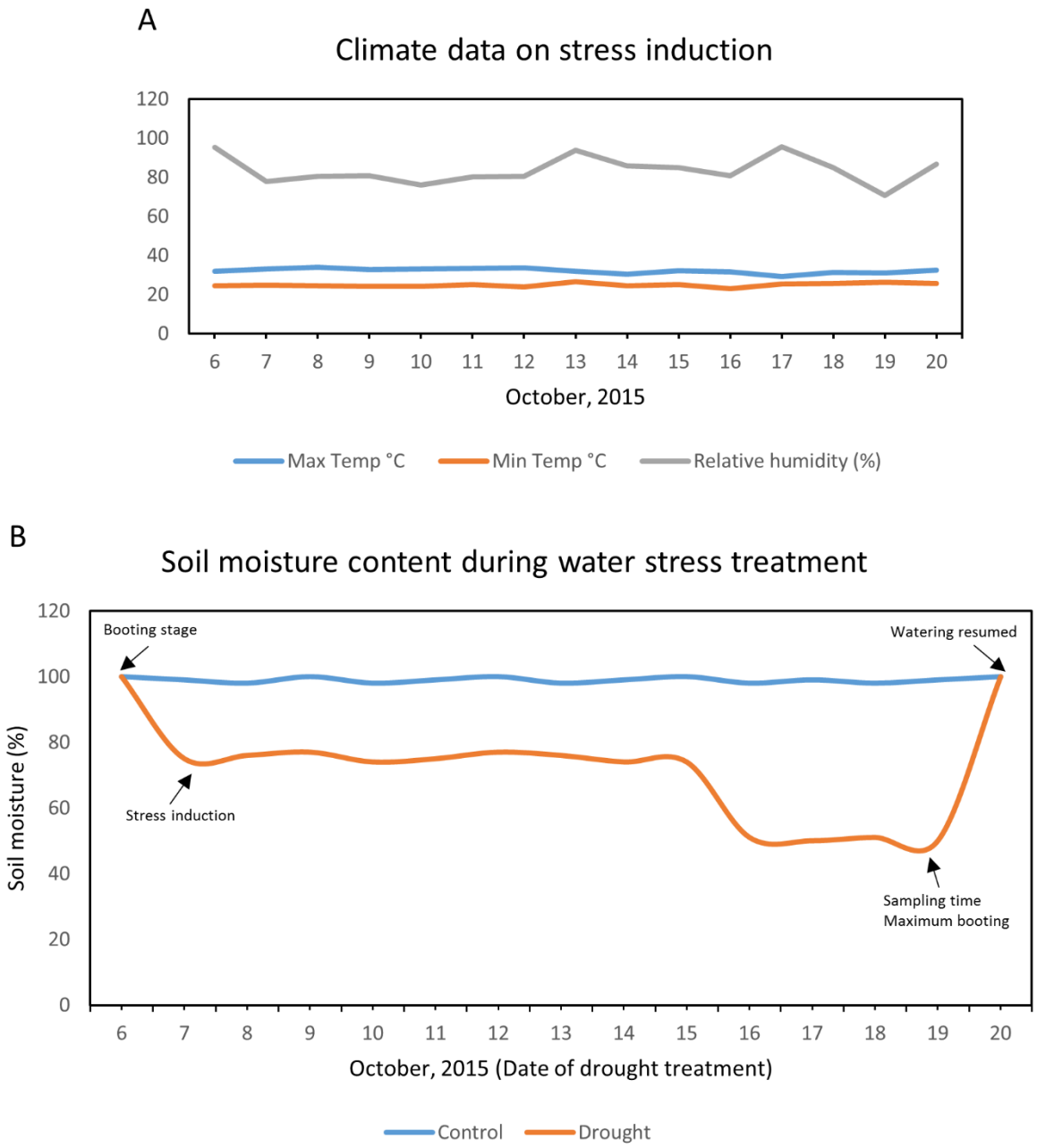

Figure 1.1. Climate data (A) and soil water content (B) during water stress treatment.

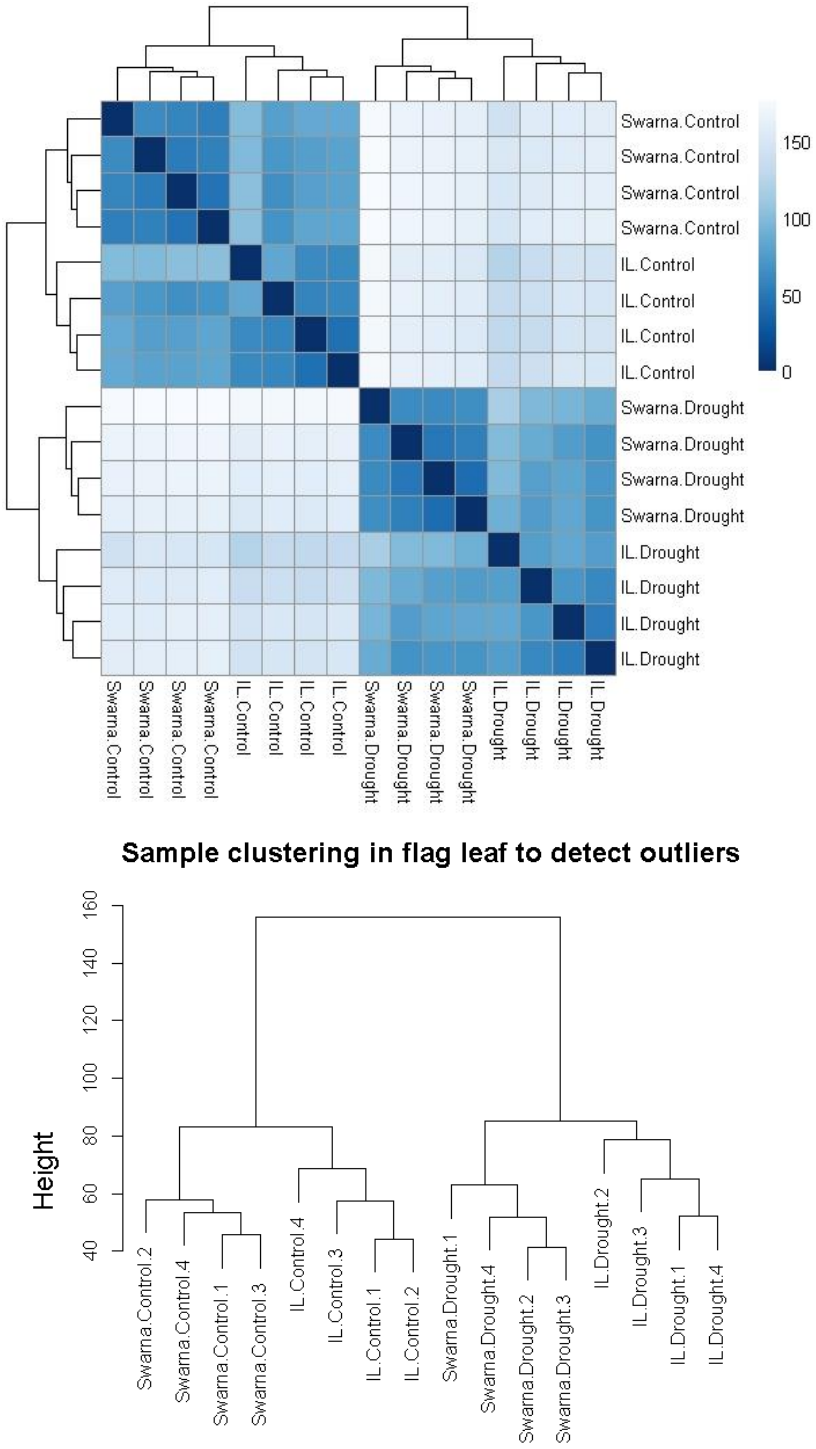

Figure 1.2. Quality control assessment for 16 flag-leaf tissue samples. Visualization of *vst*-transformed values through heatmap (A) and clustering by Euclidean distance (B) was used to display similarity and dissimilarity between samples. IL = DTY-IL.

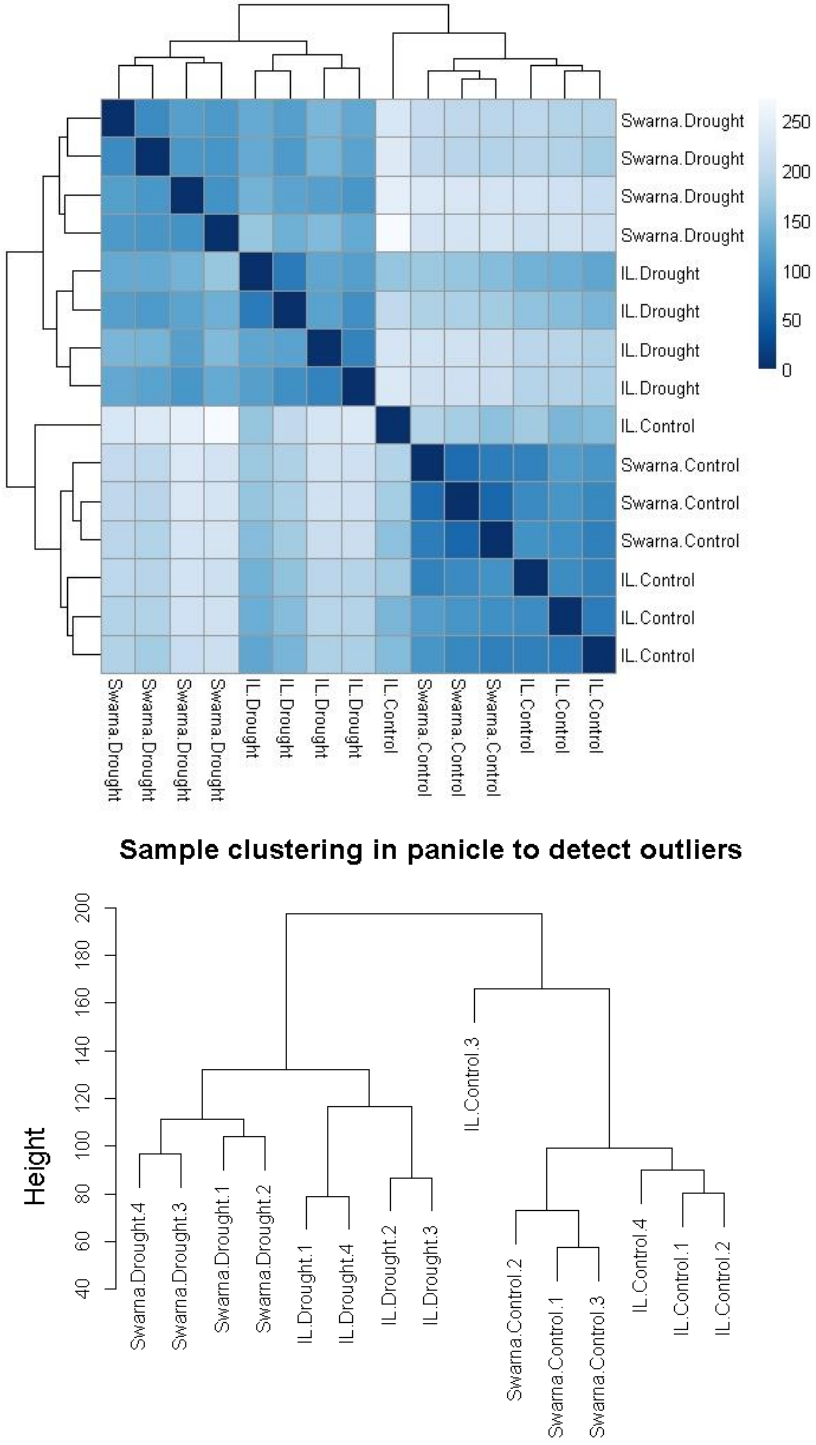

Figure 1.3. Quality control assessment for 15 panicle tissue samples, with one Swarna control outlier removed (See Figure 1.4). Visualization of *vst*-transformed values through heatmap (A) and clustering by Euclidean distance (B) was used to display similarity and dissimilarity between samples. IL = DTY-IL.

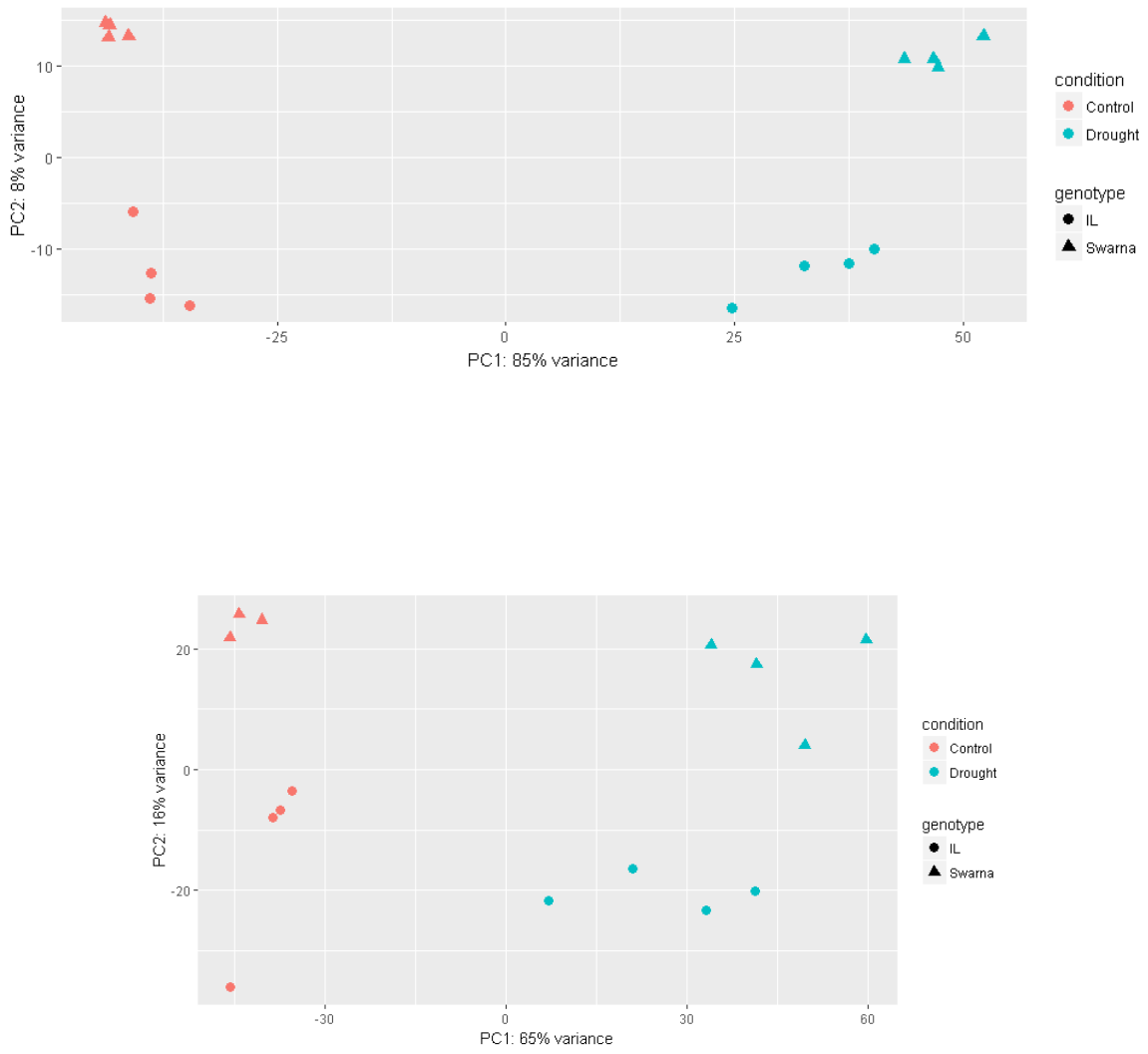

Figure 1.4. Principal component analysis of the flag-leaf and panicle samples under RDS. 2D PCA plot in flag-leaf (A) and panicle (B) was used for visualizing the overall effect of experimental covariates. IL= DTY-IL.

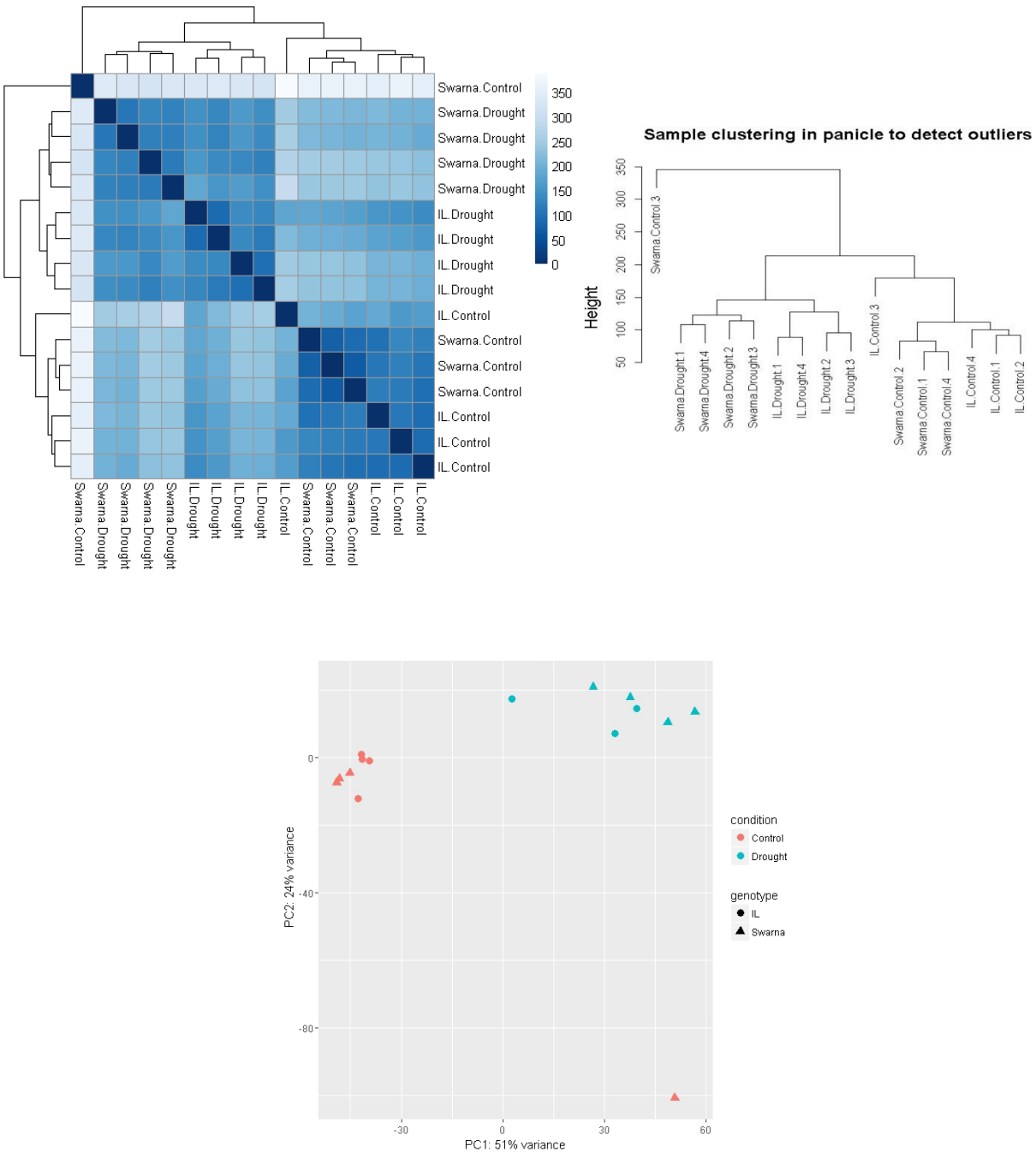

Figure 1.5. Quality control assessment for 16 panicle tissue samples. Visualization of *vst*-transformed values through heatmap (A) and clustering by Euclidean distance (B) was used to display similarity and dissimilarity between samples. PCA plot (C) was used for visualizing the overall effect of experimental covariates. The sample dendrogram (B) and PCA (C) indicated sample Swana.Control 3 was an obvious outlier and was removed before DE analysis (See **Figures 1.3 and 1.4**). IL = DTY-IL.

A

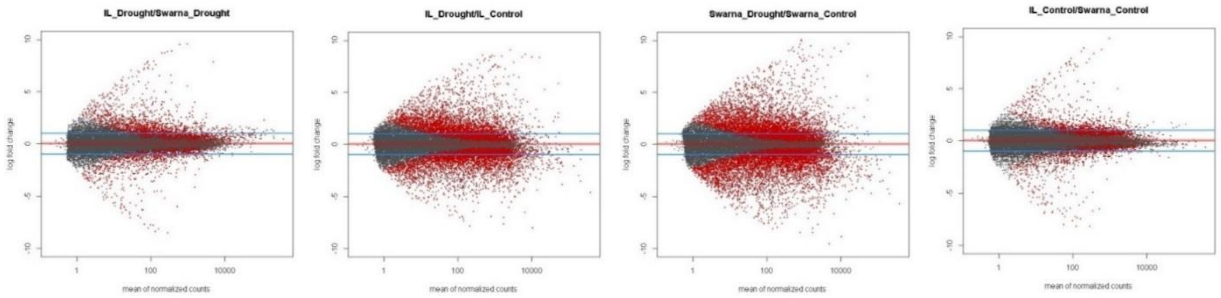

B

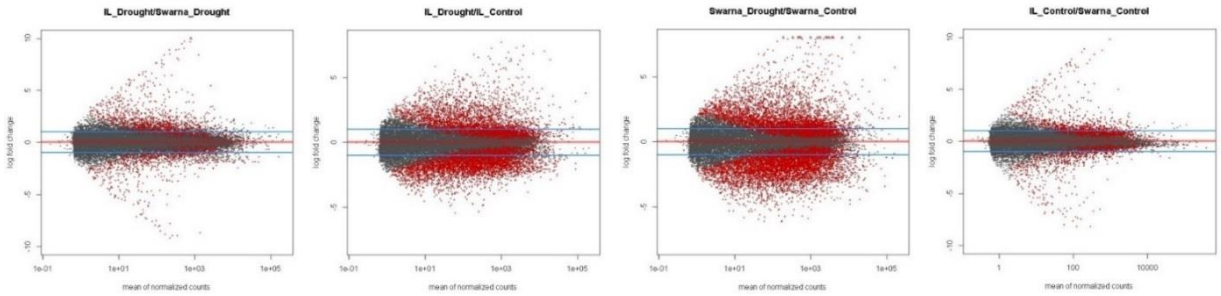

Figure 1.6. DEGs identification. Mean-difference plots showing the result of the different pairwise differential expression analyses for (A) flag-leaf and (B) panicle tissues, respectively. The X-axis represents the mean of normalized counts, and the Y-axis represents the fold change (on a $\log_2$ scale). Red dots indicate an adjusted *p*-value of less than 0.05. Red dots outside of the blue line indicate DEGs for which the $\log_2$ fold change was significantly higher than +/- 1. IL = DTY-IL.

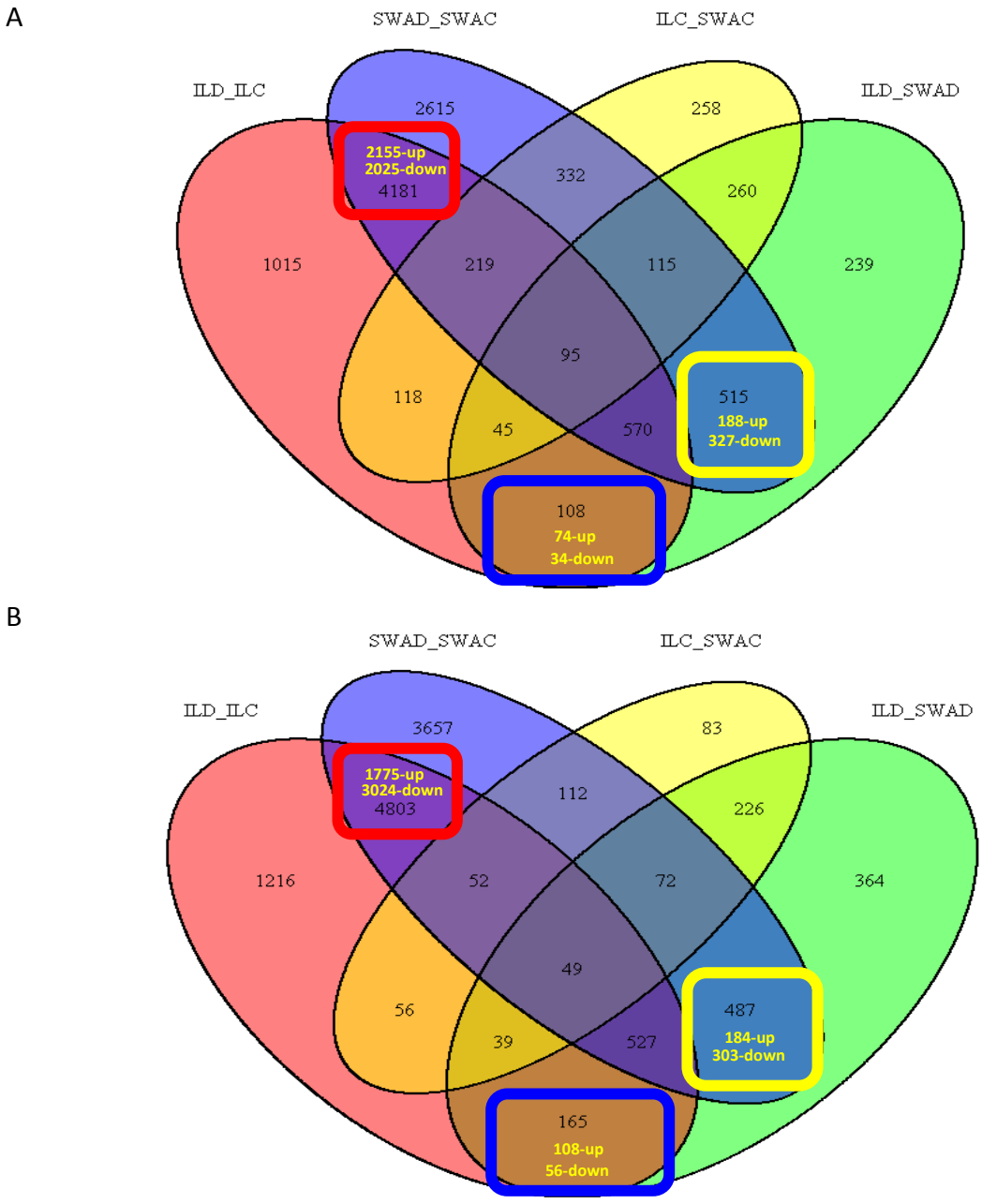

Figure 1.7. Gene differential expression and identification. Venn diagram of differentially expressed genes (upregulated and downregulated DEGs) for flag-leaf (A) and panicle (B) tissues in Swarna and DTY-IL under RDS at an FDR adjusted *P*-value < 0.05 and -1 ≤ log2-ratio ≤ +1 (fold change ≥ 2 and ≤ 0.5). The three highlighted boxes for each tissue represent the common DEGs (Red), the unique response of Swarna (Yellow) under RDS, and the unique response of DTY-IL (Blue) under RDS. SWAC = Swarna control, SWAD = Swarna under RDS, ILC = DTY-IL control, ILD = DTY-IL under RDS.

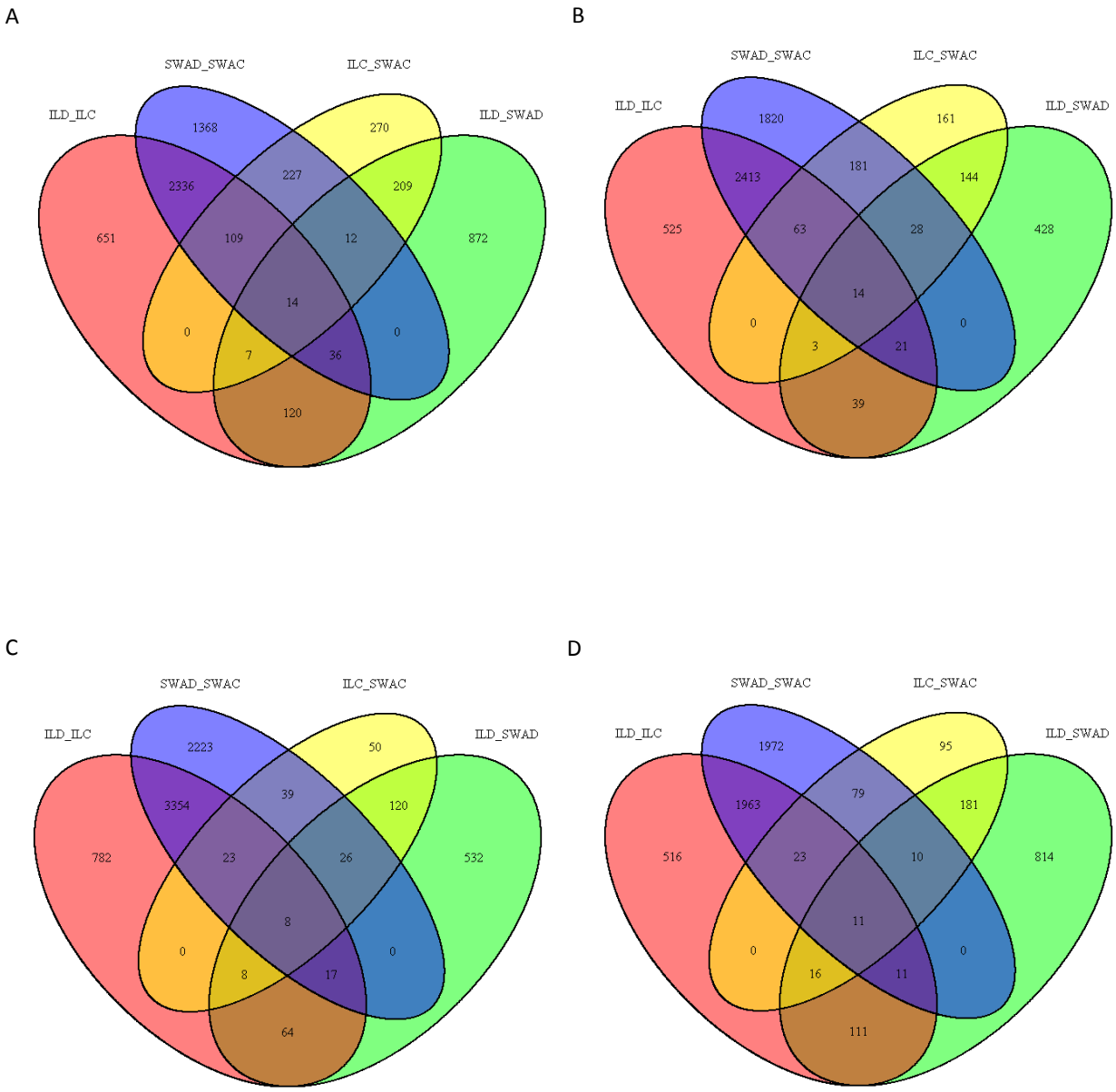

Figure 1.8. Venn diagrams of differentially expressed genes (DEGs) upregulated (A) and downregulated (B) in flag-leaf as well as upregulated (C) and downregulated D) in panicle tissues at FDR adjusted *P*-value < 0.05 and -1 ≤ log2-ratio ≤ +1 (fold change ≥ 2. SWAC = Swarna control, SWAD = Swarna under RDS, ILC = DTY-IL control, ILD = DTY-IL under RDS.

Table 1.2. A summary of GO enrichment analysis of differentially expressed genes (DEGs) common to both genotypes and unique to DTY-IL and Swarna for flag-leaf and panicle tissues under RDS.

DEGs of Interest	Expression	Genes		GO Terms		Significant GO Terms	
		Flag-leaf	Panicle	Flag-leaf	Panicle	Flag-leaf	Panicle
Common responses of DTY-IL and Swarna DEGs to drought	Upregulated	2155	1775	409	324	88	110
	Downregulated	2025	3024	482	525	171	135
	Sub-total	4180	4799	891	849	259	245
Unique responses of Swarna DEGs to drought	Upregulated	188	184	92	89	0	0
	Downregulated	327	303	134	141	**35**	**13**
	Sub-total	515	487	226	230	35	13
Unique responses of DTY-IL DEGs to drought	Upregulated	74	108	31	58	**4**	**36**
	Downregulated	34	56	19	22	0	0
	Sub-total	108	164	50	80	4	36

Table 1.3. GO enrichment analysis of the commonly upregulated genes in DTY-IL and Swarna under RDS in the flag-leaf tissue.

GO term	Ontology	Description	Number in input list	Number in BG/Ref	*P*-value	FDR
GO:0045449	P	regulation of transcription	119	1513	9.90E-09	8.80E-07
GO:0019219	P	regulation of nucleobase, nucleoside, nucleotide metabolic process	119	1520	1.30E-08	8.80E-07
GO:0051171	P	regulation of nitrogen compound metabolic process	119	1520	1.30E-08	8.80E-07
GO:0009889	P	regulation of biosynthetic process	120	1564	3.10E-08	0.00000093
GO:0010556	P	regulation of macromolecule biosynthetic process	120	1564	3.10E-08	0.00000093
GO:0031326	P	regulation of cellular biosynthetic process	120	1564	3.10E-08	0.00000093
GO:0005975	P	carbohydrate metabolic process	76	833	2.60E-08	9.30E-07
GO:0031323	P	regulation of cellular metabolic process	121	1593	4.50E-08	1.10E-06
GO:0010468	P	regulation of gene expression	120	1577	4.70E-08	1.10E-06
GO:0050794	P	regulation of cellular process	140	1955	1.00E-07	2.10E-06
GO:0080090	P	regulation of primary metabolic process	121	1626	1.30E-07	2.20E-06
GO:0065007	P	biological regulation	149	2125	1.20E-07	0.0000022
GO:0060255	P	regulation of macromolecule metabolic process	121	1640	1.90E-07	3.10E-06
GO:0019222	P	regulation of metabolic process	122	1664	2.30E-07	3.30E-06
GO:0006350	P	transcription	120	1629	2.40E-07	3.30E-06
GO:0050789	P	regulation of biological process	141	2027	4.30E-07	5.70E-06
GO:0055114	P	oxidation reduction	102	1351	7.30E-07	9.00E-06
GO:0006355	P	regulation of transcription, DNA-dependent	60	737	2.10E-05	2.40E-04
GO:0051252	P	regulation of RNA metabolic process	60	740	2.30E-05	2.60E-04
GO:0044282	P	small molecule catabolic process	20	146	3.30E-05	3.40E-04
GO:0006970	P	response to osmotic stress	6	12	7.50E-05	7.50E-04
GO:0051234	P	establishment of localization	108	1638	8.70E-05	7.60E-04
GO:0006810	P	transport	108	1638	8.70E-05	7.60E-04
GO:0009628	P	response to abiotic stimulus	13	74	0.000086	0.00076
GO:0006351	P	transcription, DNA-dependent	60	786	0.00011	0.00093
GO:0032774	P	RNA biosynthetic process	60	788	0.00012	0.00093

Table 1.3. (Continued)

GO term	Ontology	Description	Number in input list	Number in BG/Ref	*P*-value	FDR
GO:0051179	P	localization	108	1651	0.00012	0.00093
GO:0016054	P	organic acid catabolic process	8	31	0.00021	0.0015
GO:0016052	P	carbohydrate catabolic process	17	131	0.00022	0.0015
GO:0046395	P	carboxylic acid catabolic process	8	31	0.00021	0.0015
GO:0042221	P	response to chemical stimulus	28	301	0.00051	0.0033
GO:0009056	P	catabolic process	36	433	0.00063	0.004
GO:0006950	P	response to stress	61	873	0.00084	0.0052
GO:0050896	P	response to stimulus	69	1026	0.001	0.0058
GO:0015833	P	peptide transport	12	86	0.001	0.0058
GO:0006857	P	oligopeptide transport	12	86	0.001	0.0058
GO:0044262	P	cellular carbohydrate metabolic process	32	385	0.0012	0.0068
GO:0005976	P	polysaccharide metabolic process	16	143	0.0014	0.0077
GO:0006470	P	protein amino acid dephosphorylation	11	78	0.0015	0.0079
GO:0051258	P	protein polymerization	6	24	0.0015	0.0079
GO:0000272	P	polysaccharide catabolic process	7	37	0.0026	0.013
GO:0009112	P	nucleobase metabolic process	5	18	0.0026	0.013
GO:0009063	P	cellular amino acid catabolic process	6	28	0.003	0.014
GO:0016311	P	dephosphorylation	11	86	0.003	0.014
GO:0009310	P	amine catabolic process	6	28	0.003	0.014
GO:0006869	P	lipid transport	12	103	0.004	0.017
GO:0010876	P	lipid localization	12	103	0.004	0.017
GO:0016070	P	RNA metabolic process	69	1088	0.004	0.017
GO:0006725	P	cellular aromatic compound metabolic process	15	145	0.0039	0.017
GO:0010467	P	gene expression	137	2424	0.0043	0.018
GO:0006558	P	L-phenylalanine metabolic process	5	21	0.0045	0.018
GO:0016998	P	cell wall macromolecule catabolic process	7	42	0.0048	0.019
GO:0005996	P	monosaccharide metabolic process	15	150	0.0052	0.02

Table 1.3. (Continued)

GO term	Ontology	Description	Number in input list	Number in BG/Ref	*P*-value	FDR
GO:0033036	P	macromolecule localization	31	411	0.0056	0.021
GO:0044036	P	cell wall macromolecule metabolic process	7	45	0.0066	0.025
GO:0006066	P	alcohol metabolic process	18	202	0.0071	0.026
GO:0006026	P	aminoglycan catabolic process	5	26	0.0098	0.033
GO:0006030	P	chitin metabolic process	5	26	0.0098	0.033
GO:0006032	P	chitin catabolic process	5	26	0.0098	0.033
GO:0019318	P	hexose metabolic process	13	133	0.011	0.035
GO:0044281	P	small molecule metabolic process	63	1034	0.012	0.04
GO:0016051	P	carbohydrate biosynthetic process	12	121	0.012	0.04
GO:0034622	P	cellular macromolecular complex assembly	12	121	0.012	0.04
GO:0044248	P	cellular catabolic process	25	337	0.014	0.043
GO:0044275	P	cellular carbohydrate catabolic process	10	94	0.014	0.043
GO:0046164	P	alcohol catabolic process	10	94	0.014	0.043
GO:0006022	P	aminoglycan metabolic process	5	29	0.014	0.043
GO:0034621	P	cellular macromolecular complex subunit organization	13	142	0.017	0.049
GO:0006979	P	response to oxidative stress	15	174	0.017	0.049
GO:0004553	F	hydrolase activity, hydrolyzing O-glycosyl compounds	44	424	0.0000012	0.00018
GO:0016798	F	hydrolase activity, acting on glycosyl bonds	46	480	0.0000048	0.00025
GO:0016491	F	oxidoreductase activity	117	1672	0.0000036	0.00025
GO:0048037	F	cofactor binding	48	543	0.000021	0.00083
GO:0003700	F	transcription factor activity	54	651	0.000034	0.00088
GO:0050662	F	coenzyme binding	37	382	0.000032	0.00088
GO:0008289	F	lipid binding	14	85	0.000086	0.0019
GO:0004722	F	protein serine/threonine phosphatase activity	10	54	0.00038	0.0075
GO:0030528	F	transcription regulator activity	66	987	0.0015	0.026
GO:0043565	F	sequence-specific DNA binding	35	453	0.0024	0.034
GO:0005506	F	iron ion binding	50	713	0.0022	0.034

Table 1.3. (Continued)

GO term	Ontology	Description	Number in input list	Number in BG/Ref	*P*-value	FDR
GO:0050660	F	FAD binding	16	156	0.0032	0.042
GO:0016209	F	antioxidant activity	19	203	0.0036	0.043
GO:0016757	F	transferase activity, transferring glycosyl groups	42	595	0.0043	0.048
GO:0016020	C	membrane	132	2115	0.00014	0.006
GO:0008287	C	protein serine/threonine phosphatase complex	10	67	0.0017	0.035

Table 1.4. GO enrichment analysis of the commonly downregulated genes in DTY-IL and Swarna under RDS in the flag-leaf tissue.

GO term	Ontology	Description	Number in input list	Number in BG/Ref	*P*-value	FDR
GO:0055085	P	transmembrane transport	101	701	1.50E-17	3.60E-15
GO:0051234	P	establishment of localization	168	1638	3.60E-15	2.20E-13
GO:0006810	P	transport	168	1638	3.60E-15	2.20E-13
GO:0051179	P	localization	169	1651	3.50E-15	2.20E-13
GO:0055114	P	oxidation reduction	129	1351	6.00E-10	3.00E-08
GO:0006811	P	ion transport	56	408	1.40E-09	5.60E-08
GO:0006812	P	cation transport	50	348	2.70E-09	9.60E-08
GO:0016310	P	phosphorylation	143	1695	1.00E-07	3.10E-06
GO:0030001	P	metal ion transport	34	214	1.10E-07	3.10E-06
GO:0006796	P	phosphate metabolic process	148	1795	2.20E-07	4.90E-06
GO:0006793	P	phosphorus metabolic process	148	1795	2.20E-07	4.90E-06
GO:0043687	P	post-translational protein modification	148	1815	4.00E-07	7.60E-06
GO:0006468	P	protein amino acid phosphorylation	132	1570	4.00E-07	7.60E-06
GO:0006464	P	protein modification process	150	1929	4.00E-06	7.10E-05
GO:0044281	P	small molecule metabolic process	91	1034	5.40E-06	8.90E-05
GO:0006629	P	lipid metabolic process	55	528	6.30E-06	9.70E-05
GO:0043412	P	macromolecule modification	150	1979	1.40E-05	0.00021
GO:0050794	P	regulation of cellular process	148	1955	1.70E-05	0.00024
GO:0065007	P	biological regulation	158	2125	2.20E-05	0.00027
GO:0050789	P	regulation of biological process	152	2027	2.10E-05	0.00027
GO:0006720	P	isoprenoid metabolic process	11	41	4.50E-05	0.00051
GO:0008299	P	isoprenoid biosynthetic process	11	41	4.50E-05	0.00051
GO:0006066	P	alcohol metabolic process	26	202	8.90E-05	0.00096
GO:0034641	P	cellular nitrogen compound metabolic process	44	435	9.50E-05	0.00098
GO:0044271	P	cellular nitrogen compound biosynthetic process	28	231	0.00012	0.0012
GO:0045449	P	regulation of transcription	112	1513	0.00042	0.004

Table 1.4. (Continued)

GO term	Ontology	Description	Number in input list	Number in BG/Ref	*P*-value	FDR
GO:0051171	P	regulation of nitrogen compound metabolic process	112	1520	0.0005	0.0044
GO:0015672	P	monovalent inorganic cation transport	20	155	0.00054	0.0044
GO:0044255	P	cellular lipid metabolic process	26	229	0.00053	0.0044
GO:0005975	P	carbohydrate metabolic process	68	833	0.00059	0.0047
GO:0009064	P	glutamine family amino acid metabolic process	9	41	0.00078	0.006
GO:0080090	P	regulation of primary metabolic process	117	1626	0.00084	0.0061
GO:0031323	P	regulation of cellular metabolic process	115	1593	0.00083	0.0061
GO:0019222	P	regulation of metabolic process	119	1664	0.00093	0.0066
GO:0044283	P	small molecule biosynthetic process	32	320	0.00096	0.0066
GO:0051188	P	cofactor biosynthetic process	14	94	0.001	0.007
GO:0060255	P	regulation of macromolecule metabolic process	117	1640	0.0011	0.0071
GO:0009309	P	amine biosynthetic process	19	153	0.0011	0.0071
GO:0009889	P	regulation of biosynthetic process	112	1564	0.0013	0.0074
GO:0010556	P	regulation of macromolecule biosynthetic process	112	1564	0.0013	0.0074
GO:0031326	P	regulation of cellular biosynthetic process	112	1564	0.0013	0.0074
GO:0008652	P	cellular amino acid biosynthetic process	17	133	0.0015	0.0086
GO:0010468	P	regulation of gene expression	112	1577	0.0016	0.0092
GO:0006350	P	transcription	115	1629	0.0017	0.0093
GO:0044106	P	cellular amine metabolic process	32	333	0.0017	0.0093
GO:0006813	P	potassium ion transport	10	57	0.0018	0.0096
GO:0009308	P	amine metabolic process	35	380	0.0021	0.011
GO:0005996	P	monosaccharide metabolic process	18	150	0.0021	0.011
GO:0043436	P	oxoacid metabolic process	41	473	0.0026	0.013
GO:0019752	P	carboxylic acid metabolic process	41	473	0.0026	0.013
GO:0006082	P	organic acid metabolic process	41	474	0.0027	0.013
GO:0023052	P	signaling	39	447	0.0029	0.014
GO:0019318	P	hexose metabolic process	16	133	0.0035	0.014

Table 1.4. (Continued)

GO term	Ontology	Description	Number in input list	Number in BG/Ref	*P*-value	FDR
GO:0045454	P	cell redox homeostasis	16	132	0.0033	0.014
GO:0023046	P	signaling process	27	279	0.0035	0.014
GO:0042180	P	cellular ketone metabolic process	41	480	0.0033	0.014
GO:0006790	P	sulfur metabolic process	10	63	0.0035	0.014
GO:0023060	P	signal transmission	27	279	0.0035	0.014
GO:0006519	P	cellular amino acid and derivative metabolic process	35	391	0.0032	0.014
GO:0006108	P	malate metabolic process	5	17	0.0041	0.017
GO:0046483	P	heterocycle metabolic process	29	312	0.0043	0.017
GO:0006644	P	phospholipid metabolic process	11	77	0.0046	0.018
GO:0046488	P	phosphatidylinositol metabolic process	5	18	0.005	0.019
GO:0010035	P	response to inorganic substance	5	18	0.005	0.019
GO:0009108	P	coenzyme biosynthetic process	9	56	0.0051	0.019
GO:0006520	P	cellular amino acid metabolic process	28	303	0.0053	0.02
GO:0019725	P	cellular homeostasis	16	140	0.0055	0.02
GO:0046486	P	glycerolipid metabolic process	9	58	0.0062	0.022
GO:0019953	P	sexual reproduction	5	19	0.0061	0.022
GO:0006650	P	glycerophospholipid metabolic process	9	58	0.0062	0.022
GO:0006563	P	L-serine metabolic process	6	28	0.0064	0.022
GO:0033014	P	tetrapyrrole biosynthetic process	6	28	0.0064	0.022
GO:0044262	P	cellular carbohydrate metabolic process	33	385	0.0074	0.025
GO:0019637	P	organophosphate metabolic process	11	84	0.0082	0.027
GO:0042592	P	homeostatic process	16	147	0.0083	0.027
GO:0006006	P	glucose metabolic process	13	109	0.0085	0.027
GO:0055086	P	nucleobase, nucleoside and nucleotide metabolic process	23	244	0.0088	0.028
GO:0000160	P	two-component signal transduction system	8	51	0.0091	0.029
GO:0006753	P	nucleoside phosphate metabolic process	21	218	0.0096	0.029
GO:0009117	P	nucleotide metabolic process	21	218	0.0096	0.029
GO:0033013	P	tetrapyrrole metabolic process	6	31	0.0098	0.029

Table 1.4. (Continued)

GO term	Ontology	Description	Number in input list	Number in BG/Ref	*P*-value	FDR
GO:0016053	P	organic acid biosynthetic process	21	222	0.011	0.034
GO:0046394	P	carboxylic acid biosynthetic process	21	222	0.011	0.034
GO:0015979	P	photosynthesis	13	115	0.012	0.036
GO:0043648	P	dicarboxylic acid metabolic process	8	55	0.013	0.038
GO:0009084	P	glutamine family amino acid biosynthetic process	5	24	0.014	0.039
GO:0051186	P	cofactor metabolic process	15	143	0.014	0.039
GO:0009070	P	serine family amino acid biosynthetic process	5	25	0.016	0.044
GO:0065008	P	regulation of biological quality	17	176	0.018	0.05
GO:0005215	F	transporter activity	112	941	4.50E-14	8.20E-12
GO:0016301	F	kinase activity	157	1750	4.60E-10	4.20E-08
GO:0022857	F	transmembrane transporter activity	76	643	8.40E-10	5.20E-08
GO:0016491	F	oxidoreductase activity	150	1672	1.20E-09	5.40E-08
GO:0016773	F	phosphotransferase activity, alcohol group as acceptor	148	1726	2.30E-08	8.60E-07
GO:0022891	F	substrate-specific transmembrane transporter activity	61	517	4.20E-08	1.30E-06
GO:0001883	F	purine nucleoside binding	240	3247	1.50E-07	3.40E-06
GO:0030554	F	adenyl nucleotide binding	240	3247	1.50E-07	3.40E-06
GO:0001882	F	nucleoside binding	240	3257	1.90E-07	3.90E-06
GO:0015075	F	ion transmembrane transporter activity	48	389	3.60E-07	6.60E-06
GO:0004672	F	protein kinase activity	132	1575	4.70E-07	7.80E-06
GO:0032559	F	adenyl ribonucleotide binding	227	3087	5.20E-07	7.90E-06
GO:0017076	F	purine nucleotide binding	249	3456	5.90E-07	8.30E-06
GO:0005524	F	ATP binding	226	3085	7.20E-07	9.40E-06
GO:0000166	F	nucleotide binding	271	3874	1.60E-06	1.90E-05
GO:0032555	F	purine ribonucleotide binding	236	3292	1.80E-06	1.90E-05
GO:0032553	F	ribonucleotide binding	236	3292	1.80E-06	1.90E-05
GO:0008324	F	cation transmembrane transporter activity	37	280	1.90E-06	1.90E-05
GO:0022892	F	substrate-specific transporter activity	61	593	2.90E-06	2.80E-05
GO:0004674	F	protein serine/threonine kinase activity	120	1478	6.60E-06	6.00E-05

Table 1.4. (Continued)

GO term	Ontology	Description	Number in input list	Number in BG/Ref	*P*-value	FDR
GO:0060089	F	molecular transducer activity	24	152	8.80E-06	7.30E-05
GO:0004871	F	signal transducer activity	24	152	8.80E-06	7.30E-05
GO:0046873	F	metal ion transmembrane transporter activity	19	112	3.10E-05	0.00025
GO:0022804	F	active transmembrane transporter activity	36	333	0.00012	0.00094
GO:0009055	F	electron carrier activity	52	599	0.00073	0.0053
GO:0048037	F	cofactor binding	48	543	0.00081	0.0057
GO:0004497	F	monooxygenase activity	42	458	0.00087	0.0059
GO:0016655	F	oxidoreductase activity, acting on NADH or NADPH	8	34	0.001	0.0067
GO:0042578	F	phosphoric ester hydrolase activity	26	244	0.0012	0.0077
GO:0016651	F	oxidoreductase activity, acting on NADH or NADPH	11	64	0.0013	0.0078
GO:0005506	F	iron ion binding	58	713	0.0016	0.009
GO:0016903	F	oxidoreductase activity, acting on the aldehyde	7	28	0.0016	0.009
GO:0015291	F	secondary active transmembrane transporter activity	17	136	0.0018	0.01
GO:0030528	F	transcription regulator activity	75	987	0.002	0.011
GO:0050662	F	coenzyme binding	35	382	0.0023	0.012
GO:0008374	F	O-acyltransferase activity	7	33	0.0035	0.018
GO:0016667	F	oxidoreductase activity, acting on sulfur group of donors	11	75	0.0039	0.019
GO:0016829	F	lyase activity	29	309	0.0038	0.019
GO:0016298	F	lipase activity	12	87	0.0041	0.019
GO:0016615	F	malate dehydrogenase activity	5	17	0.0041	0.019
GO:0050661	F	NADP or NADPH binding	9	55	0.0046	0.02
GO:0015297	F	antiporter activity	13	101	0.0048	0.021
GO:0016307	F	phosphatidylinositol phosphate kinase activity	5	18	0.005	0.021
GO:0015300	F	solute:solute antiporter activity	7	36	0.0053	0.022
GO:0016597	F	amino acid binding	8	47	0.006	0.023
GO:0016709	F	oxidoreductase activity, acting on paired donors	7	37	0.006	0.023
GO:0042626	F	ATPase activity, coupled to transmembrane movement	16	142	0.0062	0.023
GO:0043176	F	amine binding	8	47	0.006	0.023

Table 1.4. (Continued)

GO term	Ontology	Description	Number in input list	Number in BG/Ref	*P*-value	FDR
GO:0043492	F	ATPase activity, coupled to movement of substances	16	142	0.0062	0.023
GO:0001727	F	lipid kinase activity	5	20	0.0073	0.026
GO:0016620	F	oxidoreductase activity, acting on the aldehyde	5	20	0.0073	0.026
GO:0004197	F	cysteine-type endopeptidase activity	9	60	0.0075	0.027
GO:0008137	F	NADH dehydrogenase (ubiquinone) activity	6	30	0.0086	0.028
GO:0050136	F	NADH dehydrogenase (quinone) activity	6	30	0.0086	0.028
GO:0003954	F	NADH dehydrogenase activity	6	30	0.0086	0.028
GO:0016820	F	hydrolase activity, acting on acid anhydrides	16	147	0.0083	0.028
GO:0043565	F	sequence-specific DNA binding	37	453	0.0095	0.029
GO:0015079	F	potassium ion transmembrane transporter activity	6	31	0.0098	0.029
GO:0004428	F	inositol or phosphatidylinositol kinase activity	6	31	0.0098	0.029
GO:0015299	F	solute:hydrogen antiporter activity	6	31	0.0098	0.029
GO:0015298	F	solute:cation antiporter activity	6	31	0.0098	0.029
GO:0004806	F	triglyceride lipase activity	8	52	0.01	0.03
GO:0008081	F	phosphoric diester hydrolase activity	7	42	0.011	0.032
GO:0022890	F	inorganic cation transmembrane transporter activity	18	180	0.011	0.033
GO:0020037	F	heme binding	46	600	0.012	0.033
GO:0004499	F	flavin-containing monooxygenase activity	6	33	0.013	0.035
GO:0015399	F	primary active transmembrane transporter activity	17	170	0.014	0.037
GO:0015405	F	P-P-bond-hydrolysis-driven transmembrane	17	170	0.014	0.037
GO:0004607	F	phosphatidylcholine-sterol O-acyltransferase activity	5	24	0.014	0.037
GO:0046906	F	tetrapyrrole binding	46	608	0.014	0.037
GO:0005509	F	calcium ion binding	27	316	0.015	0.038
GO:0004553	F	hydrolase activity, hydrolyzing O-glycosyl compounds	34	424	0.016	0.04
GO:0016616	F	oxidoreductase activity	12	107	0.017	0.042
GO:0003700	F	transcription factor activity	48	651	0.019	0.046
GO:0031406	F	carboxylic acid binding	9	71	0.019	0.046
GO:0016020	C	membrane	205	2115	4.60E-16	2.40E-14

Table 1.4. (Continued)

GO term	Ontology	Description	Number in input list	Number in BG/Ref	*P*-value	FDR
GO:0016021	C	integral to membrane	88	752	6.00E-11	1.60E-09
GO:0031224	C	intrinsic to membrane	89	775	1.10E-10	1.90E-09
GO:0044425	C	membrane part	103	1007	1.40E-09	1.80E-08
GO:0009536	C	plastid	8	37	0.0016	0.017
GO:0009507	C	chloroplast	6	23	0.0028	0.024

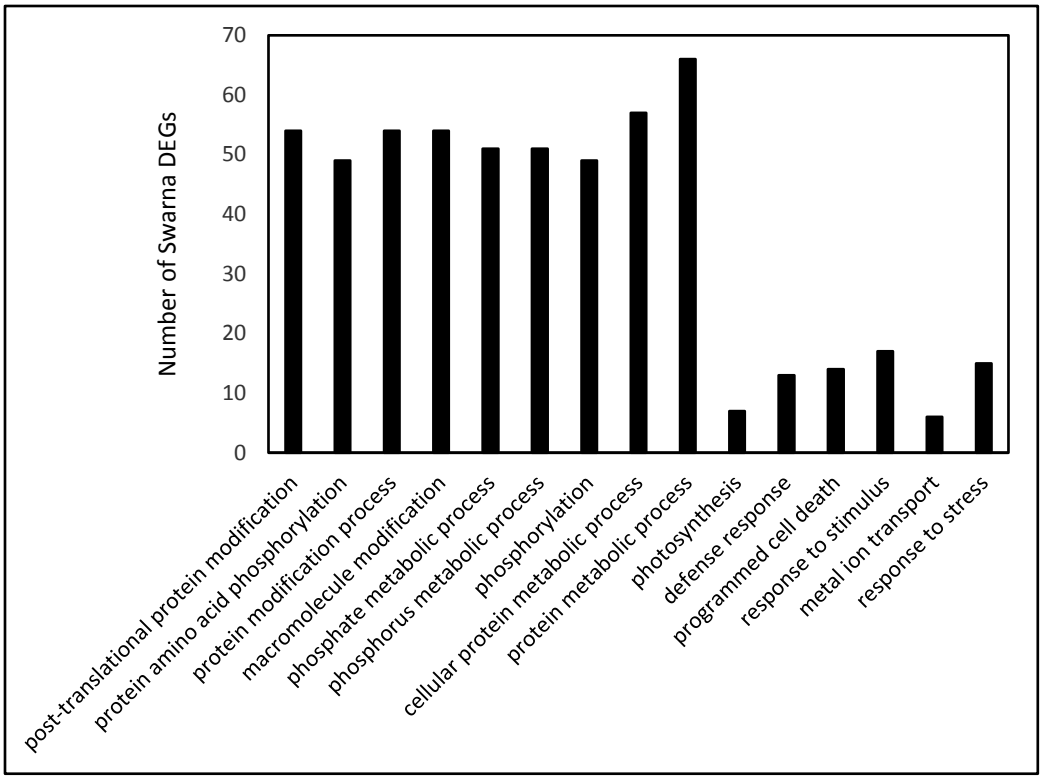

Figure 1.9. Flag-leaf significant GO terms of biological processes that are down-regulated in Swarna under RDS. The X-axis represents the significant GO terms, and the Y-axis represents the number of DEGs for each significant GO term.

Table 1.5. Pathway enrichment analysis of Swarna downregulated DEGs in flag-leaf under drought stress.

Pathway	Database	# of genes	*P*-values
Photosynthesis	KEGG PATHWAY	6	0.000182619
Ubiquinone and other terpenoid-quinone biosynthesis	KEGG PATHWAY	4	0.000599608
superpathway of plastoquinol biosynthesis	BioCyc	2	0.002004193
glutathione-mediated detoxification II	BioCyc	4	0.002051747
phenylalanine biosynthesis (cytosolic, plants)	BioCyc	2	0.00265473
tyrosine degradation I	BioCyc	2	0.003390856
Tyrosine biosynthesis	PANTHER	2	0.005112877
glycerophosphodiester degradation	BioCyc	2	0.008294788
glycerol and glycerophosphodiester degradation	BioCyc	2	0.009508492
Phenylalanine metabolism	KEGG PATHWAY	3	0.010159843
Glutathione metabolism	KEGG PATHWAY	4	0.016145902
cytokinin-O-glucosides biosynthesis	BioCyc	2	0.016653422
flavonoid biosynthesis	BioCyc	2	0.021746795
Photosynthesis - antenna proteins	KEGG PATHWAY	2	0.023570214
Isoquinoline alkaloid biosynthesis	KEGG PATHWAY	2	0.025454103
Cysteine and methionine metabolism	KEGG PATHWAY	4	0.028874824
Cutin, suberine and wax biosynthesis	KEGG PATHWAY	2	0.035733207

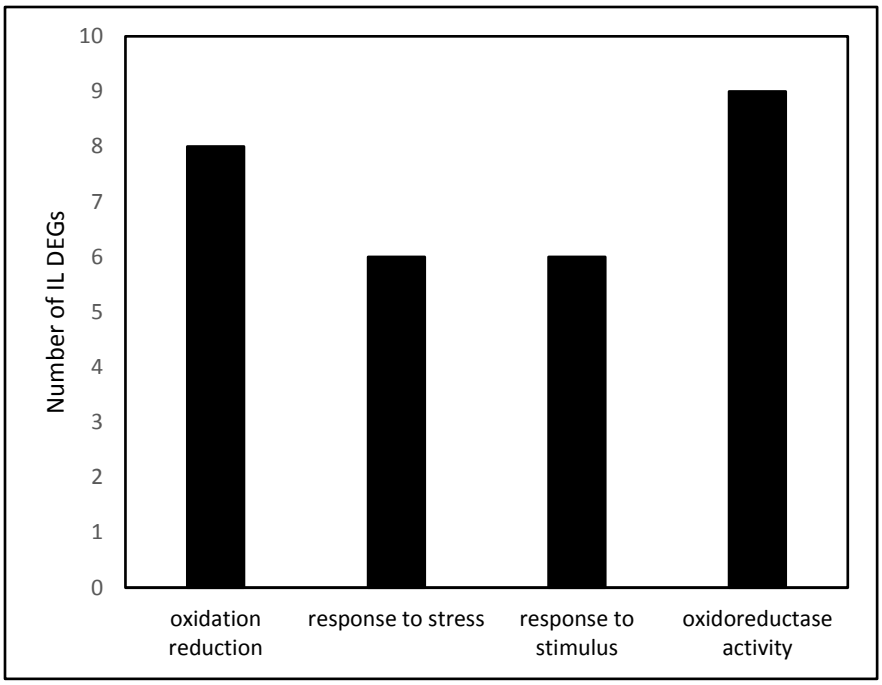

Figure 1.10. Flag-leaf significant GO terms of biological processes that were upregulated in DTY-IL under RDS. The X-axis represents the significant GO terms, and the Y-axis represents the number of DEGs for each significant GO term. IL = DTY-IL.

Table 1.6. Pathway enrichment analysis of DTY-IL upregulated DEGs in flag-leaf under drought stress.

Pathway	Database	# of genes	*P*-value
Phenylpropanoid biosynthesis	KEGG PATHWAY	4	0.000327058
@@phenylpropanoid biosynthesis	BioCyc	1	0.076418538
Biosynthesis of secondary metabolites	KEGG PATHWAY	8	0.00149698
dhurrin biosynthesis	BioCyc	1	0.018168211
xylan biosynthesis	BioCyc	1	0.020166779
scopoletin biosynthesis	BioCyc	1	0.020166779
detoxification of reactive carbonyls in chloroplasts	BioCyc	1	0.024151934
methylglyoxal degradation III	BioCyc	1	0.024151934
Biotin metabolism	KEGG PATHWAY	1	0.030099836
choline biosynthesis III	BioCyc	1	0.030099836
Cytoskeletal regulation by Rho GTPase	PANTHER	1	0.036012128
chlorogenic acid biosynthesis I	BioCyc	1	0.036012128
Other glycan degradation	KEGG PATHWAY	1	0.037975015
Metabolic pathways	KEGG PATHWAY	8	0.039317698
suberin monomers biosynthesis	BioCyc	1	0.039933977
Flavonoid biosynthesis	KEGG PATHWAY	1	0.043840153
Diterpenoid biosynthesis	KEGG PATHWAY	1	0.045787384
Plant-pathogen interaction	KEGG PATHWAY	2	0.046515138
Zeatin biosynthesis	KEGG PATHWAY	1	0.04773072
superpathway of choline biosynthesis	BioCyc	1	0.04773072
phosphatidate metabolism, as a signaling molecule	BioCyc	1	0.049670169

Table 1.7. GO enrichment analysis of the commonly upregulated genes in DTY-IL and Swarna under RDS in the panicle tissue.

GO term	Ontology	Description	Number in input list	Number in BG/Ref	*P*-value	FDR
GO:0043687	P	post-translational protein modification	171	1815	2.00E-24	3.10E-22
GO:0043412	P	macromolecule modification	178	1979	2.20E-23	1.30E-21
GO:0006464	P	protein modification process	175	1929	2.40E-23	1.30E-21
GO:0006468	P	protein amino acid phosphorylation	153	1570	4.00E-23	1.6E-21
GO:0006796	P	phosphate metabolic process	165	1795	1.60E-22	4.3E-21
GO:0006793	P	phosphorus metabolic process	165	1795	1.60E-22	4.3E-21
GO:0016310	P	Phosphorylation	155	1695	6.50E-21	1.50E-19
GO:0044267	P	cellular protein metabolic process	190	2877	5.90E-12	1.20E-10
GO:0016998	P	cell wall macromolecule catabolic process	14	42	1.70E-08	2.90E-07
GO:0044036	P	cell wall macromolecule metabolic process	14	45	3.50E-08	5.40E-07
GO:0051704	P	multi-organism process	21	120	9.80E-08	1.40E-06
GO:0000272	P	polysaccharide catabolic process	12	37	2.30E-07	0.000003
GO:0006950	P	response to stress	68	873	4.00E-07	4.80E-06
GO:0006026	P	aminoglycan catabolic process	10	26	6.50E-07	6.40E-06
GO:0006030	P	chitin metabolic process	10	26	6.50E-07	6.40E-06
GO:0006032	P	chitin catabolic process	10	26	6.50E-07	6.40E-06
GO:0032501	P	multicellular organismal process	22	154	1.10E-06	1.00E-05
GO:0006952	P	defense response	42	452	1.30E-06	1.20E-05
GO:0006022	P	aminoglycan metabolic process	10	29	1.50E-06	1.20E-05
GO:0009875	P	pollen-pistil interaction	18	114	2.90E-06	1.90E-05
GO:0008037	P	cell recognition	18	114	2.90E-06	1.90E-05
GO:0048544	P	recognition of pollen	18	114	2.90E-06	1.90E-05
GO:0022414	P	reproductive process	18	114	2.90E-06	1.90E-05
GO:0009856	P	pollination	18	114	0.0000029	0.000019
GO:0000003	P	reproduction	19	133	0.0000058	0.000037
GO:0050896	P	response to stimulus	72	1026	0.0000061	0.000037

Table 1.7. (Continued)

GO term	Ontology	Description	Number in input list	Number in BG/Ref	*P*-value	FDR
GO:0009607	P	response to biotic stimulus	7	16	0.000017	0.000097
GO:0045449	P	regulation of transcription	94	1513	0.000025	0.00014
GO:0019219	P	regulation of nucleobase, nucleoside, nucleotide metabolic process	94	1520	0.00003	0.00016
GO:0051171	P	regulation of nitrogen compound metabolic process	94	1520	0.00003	0.00016
GO:0009889	P	regulation of biosynthetic process	95	1564	0.000051	0.00024
GO:0010556	P	regulation of macromolecule biosynthetic process	95	1564	0.000051	0.00024
GO:0031326	P	regulation of cellular biosynthetic process	95	1564	0.000051	0.00024
GO:0019538	P	protein metabolic process	221	4333	0.000058	0.00027
GO:0010468	P	regulation of gene expression	95	1577	0.000069	0.00031
GO:0031323	P	regulation of cellular metabolic process	95	1593	0.000097	0.00042
GO:0016265	P	death	41	544	0.00016	0.00065
GO:0008219	P	cell death	41	544	0.00016	0.00065
GO:0080090	P	regulation of primary metabolic process	95	1626	0.00019	0.00078
GO:0060255	P	regulation of macromolecule metabolic process	95	1640	0.00025	0.001
GO:0006350	P	transcription	94	1629	0.00031	0.0012
GO:0005975	P	carbohydrate metabolic process	55	833	0.00033	0.0012
GO:0007154	P	cell communication	18	170	0.00034	0.0012
GO:0012501	P	programmed cell death	39	532	0.00037	0.0013
GO:0006915	P	apoptosis	39	532	0.00037	0.0013
GO:0019222	P	regulation of metabolic process	95	1664	0.0004	0.0014
GO:0071554	P	cell wall organization or biogenesis	16	148	0.00057	0.0019
GO:0050794	P	regulation of cellular process	107	1955	0.00073	0.0024
GO:0065007	P	biological regulation	114	2125	0.00096	0.0031
GO:0006355	P	regulation of transcription, DNA-dependent	48	737	0.001	0.0031
GO:0016567	P	protein ubiquitination	12	98	0.001	0.0032
GO:0070647	P	protein modification by small protein conjugation or removal	12	99	0.0011	0.0032
GO:0032446	P	protein modification by small protein conjugation	12	99	0.0011	0.0032

Table 1.7. (Continued)

GO term	Ontology	Description	Number in input list	Number in BG/Ref	*P*-value	FDR
GO:0051252	P	regulation of RNA metabolic process	48	740	0.0011	0.0032
GO:0055085	P	transmembrane transport	45	701	0.0018	0.0053
GO:0050789	P	regulation of biological process	107	2027	0.0023	0.0063
GO:0055114	P	oxidation reduction	75	1351	0.0032	0.0089
GO:0016052	P	carbohydrate catabolic process	13	131	0.0036	0.0092
GO:0032774	P	RNA biosynthetic process	48	788	0.0035	0.0092
GO:0016311	P	dephosphorylation	10	86	0.0037	0.0092
GO:0015833	P	peptide transport	10	86	0.0037	0.0092
GO:0006857	P	oligopeptide transport	10	86	0.0037	0.0092
GO:0006470	P	protein amino acid dephosphorylation	9	78	0.006	0.015
GO:0005976	P	polysaccharide metabolic process	13	143	0.007	0.017
GO:0006810	P	Transport	84	1638	0.013	0.03
GO:0051234	P	establishment of localization	84	1638	0.013	0.03
GO:0051179	P	Localization	84	1651	0.015	0.035
GO:0023052	P	Signaling	28	447	0.016	0.037
GO:0004672	F	protein kinase activity	153	1575	5.4E-23	7.2E-21
GO:0030554	F	adenyl nucleotide binding	242	3247	1.5E-21	4.9E-20
GO:0001883	F	purine nucleoside binding	242	3247	1.5E-21	4.9E-20
GO:0004674	F	protein serine/threonine kinase activity	144	1478	9.8E-22	4.9E-20
GO:0001882	F	nucleoside binding	242	3257	2.1E-21	5.7E-20
GO:0005524	F	ATP binding	232	3085	4.8E-21	9.3E-20
GO:0016773	F	phosphotransferase activity, alcohol group as acceptor	157	1726	5.6E-21	9.3E-20
GO:0032559	F	adenyl ribonucleotide binding	232	3087	5.2E-21	9.3E-20
GO:0016301	F	kinase activity	158	1750	8E-21	1.2E-19
GO:0017076	F	purine nucleotide binding	246	3456	1.8E-19	2.4E-18
GO:0032555	F	purine ribonucleotide binding	236	3292	5.8E-19	6.5E-18
GO:0032553	F	ribonucleotide binding	236	3292	5.8E-19	6.5E-18
GO:0000166	F	nucleotide binding	260	3874	1.6E-17	1.7E-16

Table 1.7. (Continued)

GO term	Ontology	Description	Number in input list	Number in BG/Ref	*P*-value	FDR
GO:0004568	F	chitinase activity	10	26	6.5E-07	0.0000063
GO:0003700	F	transcription factor activity	54	651	0.0000011	0.00001
GO:0030246	F	carbohydrate binding	26	219	0.0000028	0.000024
GO:0004497	F	monooxygenase activity	40	458	0.0000092	0.000069
GO:0004553	F	hydrolase activity, hydrolyzing O-glycosyl compounds	38	424	0.000009	0.000069
GO:0004866	F	endopeptidase inhibitor activity	13	72	0.00002	0.00013
GO:0005529	F	sugar binding	20	166	0.000032	0.0002
GO:0016798	F	hydrolase activity, acting on glycosyl bonds	39	480	0.000052	0.00032
GO:0004867	F	serine-type endopeptidase inhibitor activity	11	60	0.000076	0.00044
GO:0009055	F	electron carrier activity	45	599	0.000082	0.00046
GO:0005506	F	iron ion binding	51	713	0.00009	0.00048
GO:0020037	F	heme binding	44	600	0.00016	0.00083
GO:0030528	F	transcription regulator activity	64	987	0.00017	0.00086
GO:0046906	F	tetrapyrrole binding	44	608	0.00021	0.001
GO:0001871	F	pattern binding	5	11	0.00025	0.0011
GO:0008061	F	chitin binding	5	11	0.00025	0.0011
GO:0030247	F	polysaccharide binding	5	11	0.00025	0.0011
GO:0004722	F	protein serine/threonine phosphatase activity	9	54	0.00062	0.0026
GO:0016491	F	oxidoreductase activity	93	1672	0.001	0.0041
GO:0043565	F	sequence-specific DNA binding	33	453	0.0011	0.0044
GO:0004842	F	ubiquitin-protein ligase activity	12	101	0.0013	0.005
GO:0004857	F	enzyme inhibitor activity	15	157	0.0026	0.0096
GO:0016887	F	ATPase activity	26	355	0.0034	0.012
GO:0005215	F	transporter activity	54	941	0.0064	0.022
GO:0004721	F	phosphoprotein phosphatase activity	10	98	0.0084	0.029
GO:0000151	C	ubiquitin ligase complex	13	92	0.00019	0.0061
GO:0008287	C	protein serine/threonine phosphatase complex	9	67	0.0024	0.04

Table 1.8. GO enrichment analysis of the commonly downregulated genes in DTY-IL and Swarna under RDS in the panicle tissue.

GO term	Ontology	Description	Number in input list	Number in BG/Ref	*P*-value	FDR
GO:0055085	P	transmembrane transport	101	701	1.00E-10	2.60E-08
GO:0006629	P	lipid metabolic process	82	528	2.80E-10	2.60E-08
GO:0005975	P	carbohydrate metabolic process	113	833	2.00E-10	2.60E-08
GO:0051234	P	establishment of localization	185	1638	4.70E-10	2.60E-08
GO:0006810	P	Transport	185	1638	4.70E-10	2.60E-08
GO:0051179	P	localization	185	1651	8.20E-10	3.80E-08
GO:0015979	P	photosynthesis	30	115	1.20E-08	5.00E-07
GO:0009765	P	photosynthesis, light harvesting	12	16	6.10E-08	2.10E-06
GO:0055114	P	oxidation reduction	148	1351	1.60E-07	5.10E-06
GO:0006811	P	ion transport	60	408	3.60E-07	1.00E-05
GO:0006812	P	cation transport	52	348	1.40E-06	3.60E-05
GO:0007018	P	microtubule-based movement	16	63	4.00E-05	9.30E-04
GO:0019684	P	photosynthesis, light reaction	13	47	1.00E-04	2.20E-03
GO:0030001	P	metal ion transport	32	214	1.40E-04	2.80E-03
GO:0065007	P	biological regulation	192	2125	2.10E-04	3.90E-03
GO:0007017	P	microtubule-based process	16	79	3.80E-04	6.70E-03
GO:0008610	P	lipid biosynthetic process	27	180	4.20E-04	0.007
GO:0050789	P	regulation of biological process	180	2027	7.10E-04	0.011
GO:0009416	P	response to light stimulus	10	38	8.70E-04	0.012
GO:0009314	P	response to radiation	10	38	8.70E-04	0.012
GO:0044281	P	small molecule metabolic process	100	1034	1.10E-03	0.013
GO:0019953	P	sexual reproduction	7	19	1.10E-03	0.013
GO:0050794	P	regulation of cellular process	173	1955	1.00E-03	0.013
GO:0006633	P	fatty acid biosynthetic process	15	81	1.30E-03	0.015
GO:0042221	P	response to chemical stimulus	37	301	0.0013	0.015
GO:0009628	P	response to abiotic stimulus	14	74	0.0015	0.016

Table 1.8. (Continued)

GO term	Ontology	Description	Number in input list	Number in BG/Ref	*P*-value	FDR
GO:0044255	P	cellular lipid metabolic process	30	229	0.0015	0.016
GO:0071555	P	cell wall organization	15	83	0.0016	0.016
GO:0046394	P	carboxylic acid biosynthetic process	29	222	0.0019	0.016
GO:0044262	P	cellular carbohydrate metabolic process	44	385	0.0018	0.016
GO:0006091	P	generation of precursor metabolites and energy	31	243	0.0019	0.016
GO:0030036	P	actin cytoskeleton organization	8	29	0.0022	0.018
GO:0030029	P	actin filament-based process	8	29	0.0022	0.018
GO:0046417	P	chorismate metabolic process	8	30	0.0026	0.02
GO:0009073	P	aromatic amino acid family biosynthetic process	8	30	0.0026	0.02
GO:0045449	P	regulation of transcription	135	1513	0.0028	0.021
GO:0006576	P	cellular biogenic amine metabolic process	10	46	0.0029	0.022
GO:0044283	P	small molecule biosynthetic process	37	320	0.0034	0.022
GO:0043648	P	dicarboxylic acid metabolic process	11	55	0.0033	0.022
GO:0007010	P	cytoskeleton organization	10	47	0.0034	0.022
GO:0019219	P	regulation of nucleobase, nucleoside, nucleotide metabolic process	135	1520	0.0033	0.022
GO:0051171	P	regulation of nitrogen compound metabolic process	135	1520	0.0033	0.022
GO:0042439	P	ethanolamine and derivative metabolic process	5	12	0.0037	0.023
GO:0046470	P	phosphatidylcholine metabolic process	5	12	0.0037	0.023
GO:0006066	P	alcohol metabolic process	26	202	0.0037	0.023
GO:0019222	P	regulation of metabolic process	145	1664	0.0044	0.026
GO:0044264	P	cellular polysaccharide metabolic process	16	103	0.0043	0.026
GO:0006073	P	cellular glucan metabolic process	15	95	0.0049	0.026
GO:0060255	P	regulation of macromolecule metabolic process	143	1640	0.0046	0.026
GO:0044042	P	glucan metabolic process	15	95	0.0049	0.026
GO:0034637	P	cellular carbohydrate biosynthetic process	17	114	0.0048	0.026
GO:0010468	P	regulation of gene expression	138	1577	0.0047	0.026
GO:0080090	P	regulation of primary metabolic process	141	1626	0.0058	0.029

Table 1.8. (Continued)

GO term	Ontology	Description	Number in input list	Number in BG/Ref	*P*-value	FDR
GO:0009063	P	cellular amino acid catabolic process	7	28	0.0064	0.029
GO:0010556	P	regulation of macromolecule biosynthetic process	136	1564	0.0061	0.029
GO:0006631	P	fatty acid metabolic process	15	97	0.0058	0.029
GO:0009310	P	amine catabolic process	7	28	0.0064	0.029
GO:0031326	P	regulation of cellular biosynthetic process	136	1564	0.0061	0.029
GO:0031323	P	regulation of cellular metabolic process	138	1593	0.0065	0.029
GO:0071554	P	cell wall organization or biogenesis	20	148	0.0063	0.029
GO:0006694	P	steroid biosynthetic process	5	15	0.0078	0.034
GO:0016051	P	carbohydrate biosynthetic process	17	121	0.0081	0.035
GO:0006575	P	cellular amino acid derivative metabolic process	14	92	0.0086	0.035
GO:0006979	P	response to oxidative stress	22	174	0.0086	0.035
GO:0033692	P	cellular polysaccharide biosynthetic process	12	73	0.0086	0.035
GO:0042545	P	cell wall modification	9	46	0.0084	0.035
GO:0005976	P	polysaccharide metabolic process	19	143	0.0089	0.036
GO:0009072	P	aromatic amino acid family metabolic process	10	56	0.0097	0.038
GO:0009250	P	glucan biosynthetic process	11	65	0.0097	0.038
GO:0008202	P	steroid metabolic process	6	23	0.0096	0.038
GO:0006350	P	transcription	139	1629	0.0099	0.038
GO:0016054	P	organic acid catabolic process	7	31	0.01	0.038
GO:0046395	P	carboxylic acid catabolic process	7	31	0.01	0.038
GO:0000271	P	polysaccharide biosynthetic process	12	76	0.011	0.041
GO:0019438	P	aromatic compound biosynthetic process	9	50	0.013	0.048
GO:0043436	P	oxoacid metabolic process	47	473	0.014	0.048
GO:0019752	P	carboxylic acid metabolic process	47	473	0.014	0.048
GO:0006082	P	organic acid metabolic process	47	474	0.014	0.049
GO:0016491	F	oxidoreductase activity	184	1672	3.2E-09	4.4E-07
GO:0016757	F	transferase activity, transferring glycosyl groups	85	595	4.6E-09	4.4E-07

Table 1.8. (Continued)

GO term	Ontology	Description	Number in input list	Number in BG/Ref	*P*-value	FDR
GO:0004091	F	carboxylesterase activity	36	172	6.3E-08	4E-06
GO:0030599	F	pectinesterase activity	26	100	1.2E-07	5.8E-06
GO:0005215	F	transporter activity	112	941	1.5E-07	5.8E-06
GO:0016758	F	transferase activity, transferring hexosyl groups	69	489	0.0000002	6.2E-06
GO:0004553	F	hydrolase activity, hydrolyzing O-glycosyl compounds	61	424	5.6E-07	1.5E-05
GO:0022857	F	transmembrane transporter activity	81	643	0.0000012	2.8E-05
GO:0015299	F	solute:hydrogen antiporter activity	13	31	0.0000027	4.6E-05
GO:0015298	F	solute:cation antiporter activity	13	31	2.70E-06	4.60E-05
GO:0016798	F	hydrolase activity, acting on glycosyl bonds	64	480	3.00E-06	4.70E-05
GO:0022891	F	substrate-specific transmembrane transporter activity	67	517	4.20E-06	6.10E-05
GO:0015291	F	secondary active transmembrane transporter activity	27	136	6.30E-06	8.60E-05
GO:0022892	F	substrate-specific transporter activity	73	593	8.00E-06	1.00E-04
GO:0015297	F	antiporter activity	22	101	1.30E-05	1.50E-04
GO:0022804	F	active transmembrane transporter activity	47	333	1.70E-05	1.90E-04
GO:0008092	F	cytoskeletal protein binding	15	52	2.00E-05	2.10E-04
GO:0003779	F	actin binding	14	50	4.90E-05	4.90E-04
GO:0016620	F	oxidoreductase activity, acting on the aldehyde or oxo group of donors	9	20	6.10E-05	5.80E-04
GO:0015075	F	ion transmembrane transporter activity	50	389	8.00E-05	7.20E-04
GO:0048037	F	cofactor binding	64	543	9.00E-05	7.80E-04
GO:0016903	F	oxidoreductase activity, acting on the aldehyde or oxo group of donors	10	28	1.10E-04	9.40E-04
GO:0003774	F	motor activity	15	69	3.00E-04	2.40E-03
GO:0005507	F	copper ion binding	22	130	3.30E-04	2.50E-03
GO:0003777	F	microtubule motor activity	13	55	3.80E-04	2.60E-03
GO:0016298	F	lipase activity	17	87	3.70E-04	2.60E-03
GO:0008324	F	cation transmembrane transporter activity	37	280	4.00E-04	2.70E-03
GO:0005515	F	protein binding	214	2460	6.10E-04	4.00E-03
GO:0004857	F	enzyme inhibitor activity	24	157	6.80E-04	4.30E-03

Table 1.8. (Continued)

GO term	Ontology	Description	Number in input list	Number in BG/Ref	*P*-value	FDR
GO:0050662	F	coenzyme binding	45	382	9.50E-04	5.80E-03
GO:0030234	F	enzyme regulator activity	33	255	1.10E-03	6.50E-03
GO:0004620	F	phospholipase activity	8	29	2.20E-03	0.013
GO:0008194	F	UDP-glycosyltransferase activity	18	118	0.0031	0.017
GO:0046527	F	glucosyltransferase activity	13	73	0.0035	0.019
GO:0004630	F	phospholipase D activity	5	12	0.0037	0.019
GO:0051287	F	NAD or NADH binding	12	65	0.0039	0.02
GO:0005506	F	iron ion binding	69	713	0.0059	0.029
GO:0016747	F	transferase activity, transferring acyl groups other than amino-acyl groups	38	348	0.007	0.032
GO:0004601	F	peroxidase activity	23	181	0.007	0.032
GO:0004650	F	polygalacturonase activity	9	45	0.0075	0.034
GO:0016020	C	membrane	264	2115	5.7E-19	3.2E-17
GO:0044425	C	membrane part	124	1007	5.5E-09	1.5E-07
GO:0031224	C	intrinsic to membrane	99	775	4.2E-08	7.8E-07
GO:0016021	C	integral to membrane	96	752	6.9E-08	9.6E-07
GO:0005576	C	extracellular region	39	251	0.000013	0.00014
GO:0009521	C	photosystem	14	72	0.0012	0.011
GO:0030312	C	external encapsulating structure	17	107	0.0027	0.018
GO:0044464	C	cell part	464	5945	0.0028	0.018
GO:0005623	C	cell	464	5945	0.0028	0.018
GO:0009522	C	photosystem I	6	18	0.0036	0.018
GO:0005618	C	cell wall	14	82	0.0035	0.018
GO:0009579	C	thylakoid	15	93	0.0042	0.019
GO:0034357	C	photosynthetic membrane	14	89	0.0067	0.029

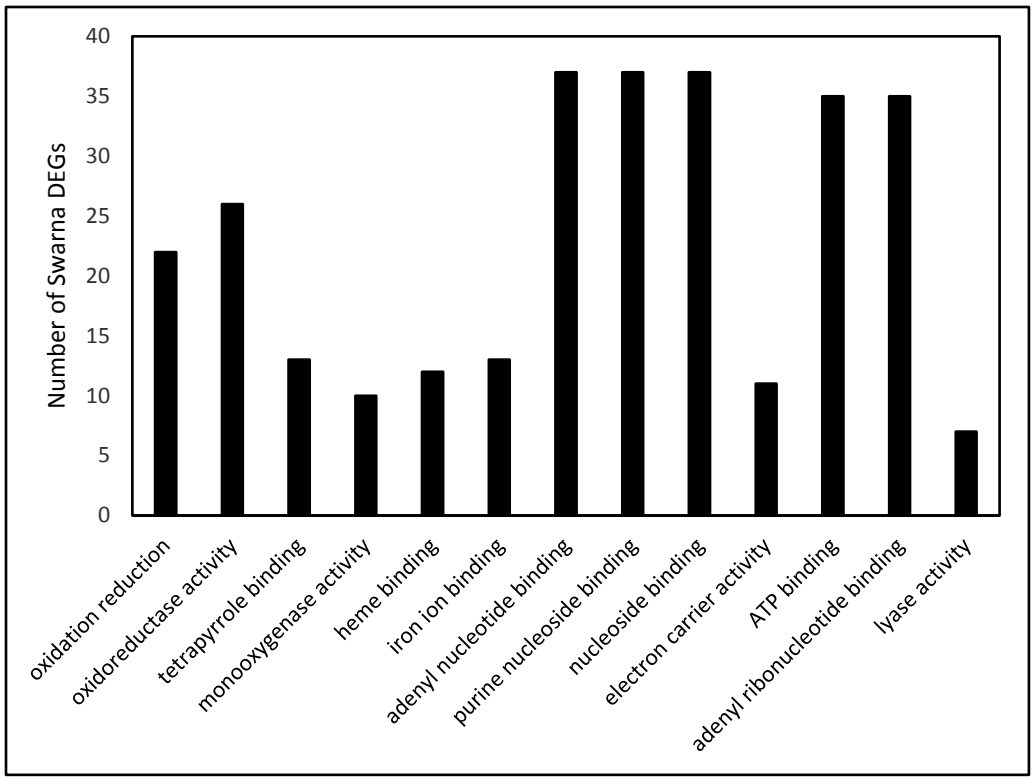

Figure 1.11. Panicle significant GO terms of biological processes that were downregulated in Swarna under RDS. The X-axis represents the significant GO terms, and the Y-axis represents the number of DEGs for each significant GO term.

Table 1.9. Pathway enrichment analysis of Swarna downregulated DEGs in panicle under drought stress.

Pathway	Database	# of genes	*P*-value
DNA replication	KEGG PATHWAY	7	9.17E-07
Biosynthesis of secondary metabolites	KEGG PATHWAY	22	0.00055964
Diterpenoid biosynthesis	KEGG PATHWAY	3	0.001523557
Phenylpropanoid biosynthesis	KEGG PATHWAY	6	0.004085611
@@phenylpropanoid biosynthesis	BioCyc	2	0.052311582
Photosynthesis	KEGG PATHWAY	4	0.006690571
glutathione-mediated detoxification II	BioCyc	3	0.012850934
cytokinin-O-glucosides biosynthesis	BioCyc	2	0.014360666
Metabolic pathways	KEGG PATHWAY	27	0.020620659
phosphate acquisition	BioCyc	2	0.029072565
Ubiquinone and other terpenoid-quinone biosynthesis	KEGG PATHWAY	2	0.045468759
alpha-Linolenic acid metabolism	KEGG PATHWAY	2	0.04771046

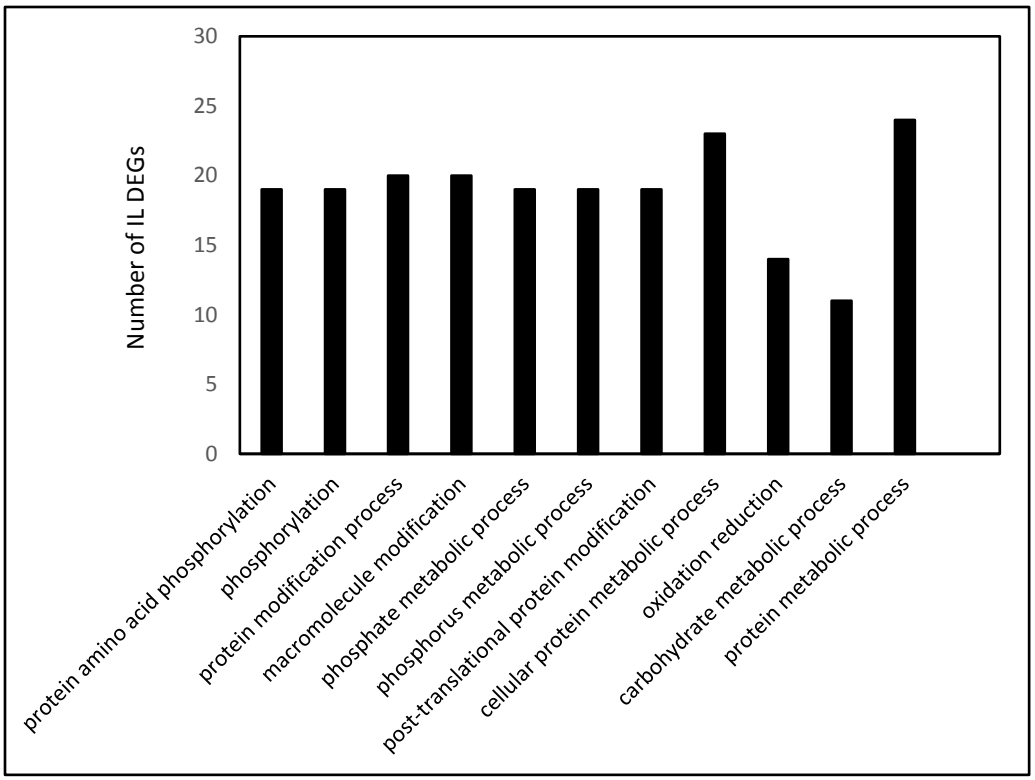

Figure 1.12. Panicle significant GO terms of biological processes that were upregulated in DTY-IL under RDS. The X-axis represents the significant GO terms, and the Y-axis represents the number of DEGs for each significant GO term. IL = DTY-IL.

Table 1.10. Pathway enrichment analysis of DTY-IL upregulated DEGs in panicle under drought stress.

Pathway	Database	# of genes	*P*-value
Metabolic pathways	KEGG PATHWAY	19	2.01E-05
Propanoate metabolism	KEGG PATHWAY	3	0.000245068
Biosynthesis of secondary metabolites	KEGG PATHWAY	12	0.00029564
methylerythritol phosphate pathway I	BioCyc	2	0.000498177
methylerythritol phosphate pathway II	BioCyc	2	0.000607546
chitin degradation II	BioCyc	2	0.001149706
valine degradation I	BioCyc	2	0.001856002
superpathway of geranylgeranyl diphosphate biosynthesis II	BioCyc	2	0.002722023
Diterpenoid biosynthesis	KEGG PATHWAY	2	0.002962976
camalexin biosynthesis	BioCyc	2	0.005892144
Circadian rhythm – plant	KEGG PATHWAY	2	0.007319294
beta-Alanine metabolism	KEGG PATHWAY	2	0.008886367
Valine, leucine and isoleucine degradation	KEGG PATHWAY	2	0.012424629
Carbon metabolism	KEGG PATHWAY	4	0.012677424
Phenylpropanoid biosynthesis	KEGG PATHWAY	3	0.017032696
Terpenoid backbone biosynthesis	KEGG PATHWAY	2	0.017566105
cutin biosynthesis	BioCyc	1	0.026685174
fatty acid biosynthesis initiation I	BioCyc	1	0.026685174
Photosynthesis	KEGG PATHWAY	2	0.029343791
ethanol degradation I	BioCyc	1	0.033245639
Thiamine metabolism	KEGG PATHWAY	1	0.039762357
octanoyl-ACP biosynthesis (mitochondria, yeast)	BioCyc	1	0.043004401
glycerophosphodiester degradation	BioCyc	1	0.043004401
glycerol and glycerophosphodiester degradation	BioCyc	1	0.046235616
acetaldehyde biosynthesis I	BioCyc	1	0.046235616
pyruvate fermentation to ethanol II	BioCyc	1	0.046235616
flavonoid biosynthesis (in equisetum)	BioCyc	1	0.046235616

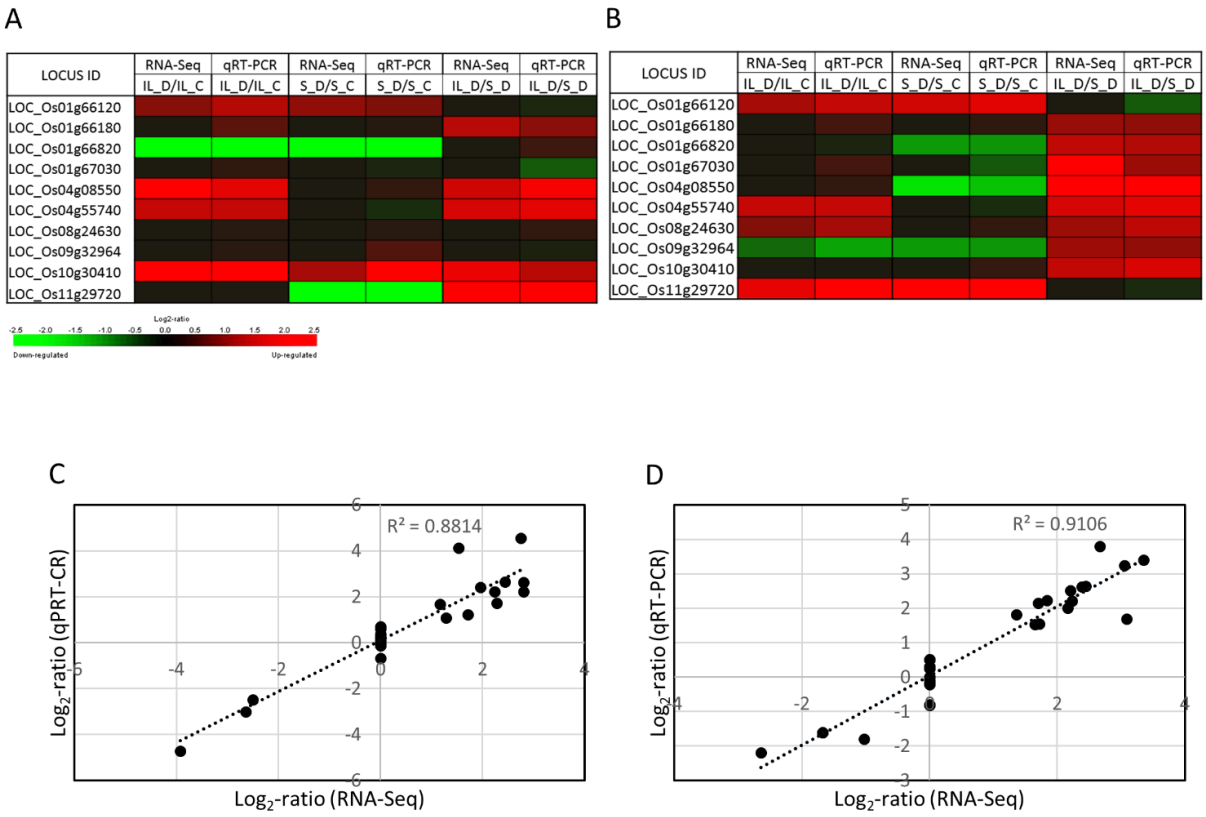

Figure 1.13. qRT-PCR validation of candidate genes. The selected genes from the different pairwise comparisons in (A) flag-leaf and (B) panicle tissues under the reproductive-stage drought stress were shown in heat-maps representing their expression profile. RNA-Seq values used are the calculated $\log_2$ fold change for each contrast. The scale from qPCR represents a $\log_2$ fold change in expression. *ELF* and *ATU* were used as an endogenous control for flag-leaf and panicle tissues, respectively.

Table 1.11. Primers used for qRT-PCR analysis.

Gene ID	Forward Sequence	Reverse Sequence
LOC_Os01g66120	AGAAGAACAGCCTCAGGTTGGATG	AGCCCGCCCTTCTTGTTGTAAATC
LOC_Os01g66180	AAGTACACTCCTGCCAAGATGGG	TGTGGCGTTCTTCAGGTATGCG
LOC_Os01g66820	TGACATCGGATCAGTCGGTCAC	GGTGGGCTAGAAACAGACAGTTCG
LOC_Os01g67030	TGGAACTGGTACCACCACAACG	TGTTGAGGCCGATGAAGATGTTGG
LOC_Os04g08550	ATGCAAGACGATCGCTCAGGTG	ATGTCCATGTTCTGCTTCATCCG
LOC_Os04g55740	TCCACGACTGCTTTGTCAATGGG	AGGGAGTTCTTGTTCGGCTTCG
LOC_Os08g24630	TTTGTGGTGCTGCTACCGAAGG	ACCAACTTGCGAGCAACCTCTG
LOC_Os09g32964	CGGGAAGCATGGAGAGATCAGAAG	ACCAACTTGCGAGCAACCTCTG
LOC_Os10g30410	TGGACTTGTTGGGCCTAAACGC	ACACTGCTTGGAGCAACACGAG
LOC_Os11g29720	TACATGCTCTCCATGCCACAGG	TCTCCCAGAGGACAGCAATGAC

REFERENCES

Baldoni, E., Bagnaresi, P., Locatelli, F., Mattana, M., and Genga, A. 2016. Comparative Leaf and Root Transcriptomic Analysis of two Rice Japonica Cultivars Reveals Major Differences in the Root Early Response to Osmotic Stress. *Rice,9*(1). doi:10.1186/s12284-016-0098-1

Basu, S., Ramegowda, V., Kumar, A., and Pereira, A. 2016. Plant adaptation to drought stress. *F1000Research, 5*, 1554. doi:10.12688/f1000research.7678.1

Benjamini, Yoav, and Yosef Hochberg. 1995. "Controlling the False Discovery Rate: A Practical and Powerful Approach to Multiple Testing." *Journal of the Royal Statistical Society. Series B (Methodological)*57 (1): 289–300. http://www.jstor.org/stable/2346101.

Bernier, J., Kumar, A., Ramaiah, V., Spaner, D., and Atlin, G. 2007. A Large-Effect QTL for Grain Yield under Reproductive-Stage Drought Stress in Upland Rice. *Crop Science,47*(2), 507. doi:10.2135/cropsci2006.07.0495

Bolger, A. M., Lohse, M., and Usadel, B. 2014. Trimmomatic: a flexible trimmer for Illumina sequence data. *Bioinformatics, 30*(15), 2114-2120. doi:10.1093/bioinformatics/btu170

Borah, P., Sharma, E., Kaur, A., Chandel, G., Mohapatra, T., Kapoor, S., and Khurana, J. P. 2017. Analysis of drought-responsive signalling network in two contrasting rice cultivars using transcriptome-based approach. *Scientific Reports,7*(1). doi:10.1038/srep42131

Counce, P. A., Keisling, T. C., and Mitchell, A. J. 2000. A Uniform, Objective, and Adaptive System for Expressing Rice Development. *Crop Science,40*(2), 436. doi:10.2135/cropsci2000.402436x

Cruz, R. T., and O'Toole, J. C. 1984. Dryland Rice Response to an Irrigation Gradient at Flowering Stage. *Agronomy Journal,76*(2),178. doi:10.2134/agronj1984.00021962007600200031xs

Degenkolbe, T., Do, P. T., Zuther, E., Repsilber, D., Walther, D., Hincha, D. K., and Köhl, K. I. 2009. Expression profiling of rice cultivars differing in their tolerance to long-term drought stress. *Plant Molecular Biology,69*(1-2), 133-153. doi:10.1007/s11103-008-9412-7

Ding, X., Li, X., and Xiong, L. 2013. Insight into Differential Responses of Upland and Paddy Rice to Drought Stress by Comparative Expression Profiling Analysis. *International Journal of Molecular Sciences,14*(3), 5214-5238. doi:10.3390/ijms14035214

Dixit, S.; Biswal, A.K.; Min, A.; Henry, A.; Oane, R.H.; Raorane, M.L.; Longkumer, T.; Pabuayon, I.M.; Mutte, S.K.; Vardarajan, A.R.; et al. 2015. Action of multiple intra-QTL genes concerted around a co-localized transcription factor underpins a large effect QTL. *Sci. Rep.*, *5*, 15183.

Ehrlich, P. R., and Harte, J. 2015. Opinion: To feed the world in 2050 will require a global revolution. *Proceedings of the National Academy of Sciences, 112*(48), 14743-14744. doi:10.1073/pnas.1519841112

FAOs Director-General on How to Feed the World in 2050. 2009. *Population and Development Review, 35*(4), 837-839. doi:10.1111/j.1728-4457.2009.00312.x

FAO Rice Market Monitor (RMM). (n.d.). Retrieved July 11, 2017, from http://www.fao.org/economic/est/publications/rice-publications/rice-market-monitor-rmm/en/

Franceschini, A., Szklarczyk, D., Frankild, S., Kuhn, M., Simonovic, M., Roth, A., and Jensen, L. J. 2013. STRING v9.1: Protein-protein interaction networks, with increased coverage and integration. *Nucleic Acids Research,41*(D1). doi:10.1093/nar/gks1094

Fukao, T., and Xiong, L. 2013. Genetic mechanisms conferring adaptation to submergence and drought in rice: simple or complex? *Current Opinion in Plant Biology,16*(2), 196-204. doi:10.1016/j.pbi.2013.02.003

Ghimire, K. H., Quiatchon, L. A., Vikram, P., Swamy, B. M., Dixit, S., Ahmed, H., and Kumar, A. 2012. Identification and mapping of a QTL (qDTY1.1) with a consistent effect on grain yield under drought. *Field Crops Research,131*, 88-96. doi:10.1016/j.fcr.2012.02.028

Guo, C., Ge, X., and Ma, H. 2013. The rice OsDIL gene plays a role in drought tolerance at vegetative and reproductive stages. *Plant Molecular Biology,82*(3), 239-253. doi:10.1007/s11103-013-0057-9

Guo, C., Yao, L., You, C., Wang, S., Cui, J., Ge, X., and Ma, H. 2016. *MID1* plays an important role in response to drought stress during reproductive development. *The Plant Journal, 88*(2), 280-293. doi:10.1111/tpj.13250

He, H., and Serraj, R. 2012. Involvement of peduncle elongation, anther dehiscence and spikelet sterility in upland rice response to reproductive-stage drought stress. *Environmental and Experimental Botany,75*, 120-127. doi:10.1016/j.envexpbot.2011.09.004

Hu, H., and Xiong, L. 2014. Genetic Engineering and Breeding of Drought-Resistant Crops. *Annual Review of Plant Biology,65*(1), 715-741. doi:10.1146/annurev-arplant-050213-040000

Huang, L., Zhang, F., Zhang, F., Wang, W., Zhou, Y., Fu, B., and Li, Z. 2014. Comparative transcriptome sequencing of tolerant rice introgression line and its parents in response to drought stress. *BMC Genomics,15*(1), 1026. doi:10.1186/1471-2164-15-1026

IRRI (International Rice Research Institute). IRRI Rice Facts; IRRI (International Rice Research Institute): Los Baños, Philippines, 1995.

Iizumi, T., Sakuma, H., Yokozawa, M., Luo, J., Challinor, A. J., Brown, M. E., and Yamagata, T. 2013. Prediction of seasonal climate-induced variations in global food production. *Nature Climate Change,3*(10), 904-908. doi:10.1038/nclimate1945

Jin, Y., Yang, H., Wei, Z., Ma, H., and Ge, X. 2013) Rice Male Development under Drought Stress: Phenotypic Changes and Stage-Dependent Transcriptomic Reprogramming. *Molecular Plant,6*(5), 1630-1645. doi:10.1093/mp/sst067

Kawahara, Y., De la Bastide, M., Hamilton, J. P., Kanamori, H., McCombie, W. R., Ouyang, S., and Matsumoto, T. 2013. Improvement of the Oryza sativa Nipponbare reference genome using next generation sequence and optical map data. *Rice*, *6*(1), 4. doi:10.1186/1939-8433-6-4

Kim, W., T. Iizumi, and Nishimori, M. 2019: Global Patterns of Crop Production Losses Associated with Droughts from 1983 to 2009. *J. Appl. Meteor. Climatol.*, **58**, 1233–1244, https://doi.org/10.1175/JAMC-D-18-0174.1.

Krishnan, A., Gupta, C., Ambavaram, M. M. R., and Pereira, A. 2017. RECoN: Rice Environment Coexpression Network for Systems Level Analysis of Abiotic-Stress Response. *Frontiers in Plant Science*, *8*. doi: 10.3389/fpls.2017.01640

Kumar, A., Bernier, J., Verulkar, S., Lafitte, H., and Atlin, G. 2008. Breeding for drought tolerance: Direct selection for yield, response to selection and use of drought-tolerant donors in upland and lowland-adapted populations. *Field Crops Research,107*(3), 221-231. doi:10.1016/j.fcr.2008.02.007

Kumar, A., Dixit, S., Ram, T., Yadaw, R. B., Mishra, K. K., and Mandal, N. P. 2014. Breeding high-yielding drought-tolerant rice: genetic variations and conventional and molecular approaches. *Journal of Experimental Botany,65*(21), 6265-6278. doi:10.1093/jxb/eru363

Kumar, A.; Sandhu, N.; Dixit, S.; Yadaw, S.; Swamy, M.P.; Shamsudin, N.A. 2018. Marker-assisted selection strategy to pyramid two or more QTLs for quantitative trait-grain yield under drought. *Rice*, *11*, 35.

Lafitte, H. R., Price, A. H., and Courtois, B. 2004. Yield response to water deficit in an upland rice mapping population: associations among traits and genetic markers. *Theoretical and Applied Genetics,109*(6), 1237-1246. doi:10.1007/s00122-004-1731-8

Lenka, S. K., Katiyar, A., Chinnusamy, V., and Bansal, K. C. 2011. Comparative analysis of drought-responsive transcriptome in Indica rice genotypes with contrasting drought tolerance. *Plant Biotechnology Journal,9*(3), 315-327. doi:10.1111/j.1467-7652.2010.00560.x

Lesk, C., Rowhani, P. and Ramankutty, N. 2016. Influence of extreme weather disasters on global crop production. *Nature* **529,** 84–87. https://doi.org/10.1038/nature16467.

Li, Z.K.; Xu, J.L. Breeding for drought and salt tolerant rice (Oryza sativa L.): Progress and perspectives. In Advances in Molecular Breeding toward Drought and Salt Tolerant Crops; Jenks, M.A., Hasegawa, P.M., Jain, S.M., Eds.; Springer: Dordrecht, The Netherlands, 2007; pp. 531–564.

Li, F., Liu, W., Tang, J., Chen, J., Tong, H., Hu, B., and Chu, C. 2010. Rice DENSE AND ERECT PANICLE 2 is essential for determining panicle outgrowth and elongation. *Cell Research, 20*(7), 838-849. doi:10.1038/cr.2010.69

Liseron-Monfils, C., and Ware, D. 2015. Revealing gene regulation and associations through biological networks. *Current Plant Biology,3-4*, 30-39. doi:10.1016/j.cpb.2015.11.001

Liu, J., and Bennett, J. 2011. Reversible and Irreversible Drought-Induced Changes in the Anther Proteome of Rice (Oryza sativa L.) Genotypes IR64 and Moroberekan. *Molecular Plant,4*(1), 59-69. doi:10.1093/mp/ssq039

Livak, K. J., and Schmittgen, T. D. 2001. Analysis of Relative Gene Expression Data Using Real-Time Quantitative PCR and the 2−ΔΔCT Method. *Methods, 25*(4), 402–408. doi: 10.1006/meth.2001.1262

Love, M. I., Huber, W., and Anders, S. 2014. Moderated estimation of fold change and dispersion for RNA-seq data with DESeq2. *Genome Biology, 15*(12). doi:10.1186/s13059-014-0550-8

Marguerat, S., & Bähler, J. 2010. RNA-seq: From technology to biology. *Cellular and Molecular Life Sciences,67*(4), 569-579. doi:10.1007/s00018-009-0180-6

Mickelbart, M. V., Hasegawa, P. M., and Bailey-Serres, J. 2015. Genetic mechanisms of abiotic stress tolerance that translate to crop yield stability. *Nature Reviews Genetics,16*(4), 237-251. doi:10.1038/nrg3901

Moumeni, A., Satoh, K., Venuprasad, R., Serraj, R., Kumar, A., Leung, H., and Kikuchi, S. 2015. Transcriptional profiling of the leaves of near-isogenic rice lines with contrasting drought tolerance at the reproductive stage in response to water deficit. *BMC Genomics,16*(1). doi:10.1186/s12864-015-2335-1

Pandey, S. 2009. Economic costs of drought and rice farmers' coping mechanisms. *International Rice Research Notes,32*(1). doi:10.3860/irrn.v32i1.1078

Pantuwan, G., Fukai, S., Cooper, M., Rajatasereekul, S., and O'Toole, J. 2002. Yield response of rice (Oryza sativa L.) genotypes to drought under rainfed lowland. *Field Crops Research,73*(2-3), 181-200. doi:10.1016/s0378-4290(01)00194-0

Patro, R., Duggal, G., Love, M. I., Irizarry, R. A., and Kingsford, C. 2017. Salmon provides fast and bias-aware quantification of transcript expression. *Nature Methods, 14*(4), 417-419. doi:10.1038/nmeth.4197

Peng, S.; Cassman, K.G.; Virmani, S.S.; Sheehy, J.; Khush, G.S. 1999. Yield Potential Trends of Tropical Rice since the Release of IR8 and the Challenge of Increasing Rice Yield Potential. *Crop Sci*., *39*, 1552–1559.

Raorane, M.L.; Pabuayon, I.M.; Varadarajan, A.R.; Mutte, S.K.; Kumar, A.; Treumann, A.; Kohli, A. 2015. Proteomic insights into the role of the large-effect QTL qDTY 12.1 for rice yield under drought. *Mol. Breed.*, *35*, 6.

Ray, S., Dansana, P. K., Giri, J., Deveshwar, P., Arora, R., Agarwal, P., and Tyagi, A. K. 2011. Modulation of transcription factor and metabolic pathway genes in response to water-deficit stress in rice. *Functional & Integrative Genomics,11*(1), 157-178. doi:10.1007/s10142-010-0187-y

Ray, D. K., Mueller, N. D., West, P. C., and Foley, J. A. 2013. Yield Trends Are Insufficient to Double Global Crop Production by 2050. *PLoS ONE, 8*(6). doi:10.1371/journal.pone.0066428

Robert, C., and Watson, M. 2015. Errors in RNA-Seq quantification affect genes of relevance to human disease. *Genome Biology, 16*(1). doi:10.1186/s13059-015-0734-x

Ronald, P.C. 2014. Lab to Farm: Applying Research on Plant Genetics and Genomics to Crop Improvement. PLoS Biol 12(6): e1001878. https://doi.org/10.1371/journal.pbio.1001878

Sandhu, N., and Kumar, A. 2017. Bridging the Rice Yield Gaps under Drought: QTLs, Genes, and their Use in Breeding Programs. *Agronomy,7*(2), 27. doi:10.3390/agronomy7020027

Shankar, R., Bhattacharjee, A., and Jain, M. 2016. Transcriptome analysis in different rice cultivars provides novel insights into desiccation and salinity stress responses. *Scientific Reports,6*, 23719. doi:10.1038/srep23719

Shinozaki K. 1997. Isolation and functional analysis of arabidopsis stress-inducible NAC transcription factors that bind to a drought-responsive cis-element in the early responsive to dehydration stress 1promoter.Role of Arabidopsis MYC and MYB homologs in drought- and abscisic acid-regulated gene expression. *Plant Cell 9:1859-1868*

Solano R, Nieto C, Avila J, Canas L, Diaz I, Paz-Ares J. 1995. An Arabidopsis myb homolog is induced by dehydration stress andits gene product binds to the conserved MYB recognition sequence Dual DNA binding specificity of a petal epidermis-specific MYB transcription factor (MYB.Ph3) from Petunia hybrida. *EMBO J 14:1773-1784*

Soneson, C., Love, M. I., and Robinson, M. D. 2016. Differential analyses for RNA-seq: transcript-level estimates improve gene-level inferences. *F1000Research, 4*, 1521. doi:10.12688/f1000research.7563.2

Srivastava, A., Sarkar, H., Gupta, N., and Patro, R. 2016. RapMap: a rapid, sensitive and accurate tool for mapping RNA-seq reads to transcriptomes. *Bioinformatics*, *32*(12), i192-i200. doi:10.1093/bioinformatics/btw277

Szklarczyk, D., Morris, J. H., Cook, H., Kuhn, M., Wyder, S., Simonovic, M., and Von Mering, C. 2017. The STRING database in 2017: Quality-controlled protein–protein association networks, made broadly accessible. *Nucleic Acids Research, 45*(D1). doi:10.1093/nar/gkw937

Tian, T., Liu, Y., Yan, H., You, Q., Yi, X., Du, Z., and Su, Z. 2017. agriGO v2.0: a GO analysis toolkit for the agricultural community, 2017 update. *Nucleic Acids Research, 45*(W1), W122-W129. doi:10.1093/nar/gkx382

Todaka, D., Shinozaki, K., and Yamaguchi-Shinozaki, K. 2015. Recent advances in the dissection of drought-stress regulatory networks and strategies for development of drought-tolerant transgenic rice plants. *Frontiers in Plant Science,6*. doi:10.3389/fpls.2015.00084

Trapnell, C., Hendrickson, D. G., Sauvageau, M., Goff, L., Rinn, J. L., and Pachter, L. 2013. Differential analysis of gene regulation at transcript resolution with RNA-seq. *Nature Biotechnology, 31*(1), 46-53. doi:10.1038/nbt.2450

Venuprasad, R., Lafitte, H. R., and Atlin, G. N. 2007. Response to Direct Selection for Grain Yield under Drought Stress in Rice. *Crop Science,47*(1), 285. doi:10.2135/cropsci2006.03.0181

Venuprasad, R., Bool, M. E., Quiatchon, L., and Atlin, G. N. 2011. A QTL for rice grain yield in aerobic environments with large effects in three genetic backgrounds. *Theoretical and Applied Genetics,124*(2), 323-332. doi:10.1007/s00122-011-1707-4

Vikram, P., Swamy, B., Dixit, S., Ahmed, H., Cruz, M. T., Singh, A., and Kumar, A. 2011. QDTY1.1, a major QTL for rice grain yield under reproductive-stage drought stress with a consistent effect in multiple elite genetic backgrounds. *BMC Genetics,12*(1), 89. doi:10.1186/1471-2156-12-89

Wang, Z., Gerstein, M., and Snyder, M. 2009. RNA-Seq: a revolutionary tool for transcriptomics. *Nature Reviews Genetics,10*(1), 57-63. doi:10.1038/nrg2484

Wang, D., Pan, Y., Zhao, X., Zhu, L., Fu, B., and Li, Z. 2011. Genome-wide temporal-spatial gene expression profiling of drought responsiveness in rice. *BMC Genomics,12*(1). doi:10.1186/1471-2164-12-149

Wang et al. 2014. The concordance between RNA-seq and microarray data depends on chemical treatment and transcript abundance. *Nat Biotechnol, 32*(9), 926-932. doi:10.1038/nbt.3001

Wei, H., Chen, C., Ma, X., Zhang, Y., Han, J., Mei, H., and Yu, S. 2017. Comparative Analysis of Expression Profiles of Panicle Development among Tolerant and Sensitive Rice in Response to Drought Stress. *Frontiers in Plant Science, 08*. doi:10.3389/fpls.2017.00437

Weng, X., Wang, L., Wang, J., Hu, Y., Du, H., Xu, C., and Zhang, Q. 2014. Grain Number, Plant Height, and Heading Date7 Is a Central Regulator of Growth, Development, and Stress Response. *Plant Physiology,164*(2), 735-747. doi:10.1104/pp.113.231308

Xing, Y., and Zhang, Q. 2010. Genetic and Molecular Bases of Rice Yield. *Annual Review of Plant Biology,61*(1), 421-442. doi:10.1146/annurev-arplant-042809-112209

Xiong, J., Zhang, L., Fu, G., Yang, Y., Zhu, C., and Tao, L. 2011. Drought-induced proline accumulation is uninvolved with increased nitric oxide, which alleviates drought stress by decreasing transpiration in rice. *Journal of Plant Research,125*(1), 155-164. doi:10.1007/s10265-011-0417-y

Yadaw, R. B., Dixit, S., Raman, A., Mishra, K. K., Vikram, P., Swamy, B. M., and Kumar, A. 2013. A QTL for high grain yield under lowland drought in the background of popular rice variety Sabitri from Nepal. *Field Crops Research,144*, 281-287. doi:10.1016/j.fcr.2013.01.019

Yamaguchi-Shinozaki K. 2003. Two different novel cis-acting elements of erd1, a clpAhomologous Arabidopsis gene function in induction by dehydrationstress and dark-induced senescence. *Plant J. 33: 259-270.*

Yuan, L. L., Zhang, M., Yan, X., Bian, Y. W., Zhen, S. M., and Yan, Y. M. 2016. Dynamic Phosphoproteome Analysis of Seedling Leaves in Brachypodium distachyon L. Reveals Central Phosphorylated Proteins Involved in the Drought Stress Response. *Scientific reports*, *6*, 35280. https://doi.org/10.1038/srep35280

Yue, B., Xue, W., Luo, L., and Xing, Y. 2008. Identification of quantitative trait loci for four morphologic traits under water stress in rice (Oryza sativa L.). *Journal of Genetics and Genomics,35*(9), 569-575. doi:10.1016/s1673-8527(08)60077-6

Zhang, Z., Li, Y., and Xiao, B. 2016. Comparative transcriptome analysis highlights the crucial roles of photosynthetic system in drought stress adaptation in upland rice. *Scientific Reports,6*(1). doi:10.1038/srep19349

Zhang, X., Zhuang, L., Liu, Y., Yang, Z., and Huang, B. 2020. Protein phosphorylation associated with drought priming-enhanced heat tolerance in a temperate grass species. *Horticulture Research, 7*(1). doi:10.1038/s41438-020-00440-8

CHAPTER 2

GENE CO-EXPRESSION NETWORK ANALYSIS OF FLAG-LEAF AND PANICLE TISSUES UNDER MODERATE REPRODUCTIVE-STAGE DROUGHT STRESS IN RICE

ABSTRACT

Convincing concepts on how drought-stress-related genes are regulated are still in their infancy. Differential expression analysis, based on single-genes, often failed to result in meaningful biological interpretations prompting the development of network-based techniques that consider complex relationships among genes. Advances in gene co-expression networks analysis can explore the system-level functionality of genes. This research's objectives were to identify drought-responsive modules and hub genes in the flag-leaf and panicle tissues and identify putative DTY-IL dependent drought tolerance mechanisms and pathways related to these modules. We applied a co-expression network approach to independently analyzed the transcriptome profiles of flag-leaf and panicle tissues, using WGCNA in drought-stressed and control plants, and identified modules of putatively co-regulated genes within each network. We presented the gene modules analysis to identify tissue-specific drought-responsive gene modules based on differential expression profiles of genes comprising these modules. Two contrasting modules (designated as M), M14 and M16 in flag-leaf and M10 and M15 in panicle tissue, were identified as drought-responsive modules. Specifically, protein turnover and efficient reactive oxygen species scavenging were the driving factors in both tissues. In the flag-leaf, the responses further included maintenance of photosynthesis and cell wall reorganization, while in the panicle, biosynthesis of secondary metabolites was found to play additional roles. Hub genes in differential drought responses included an expansin in the flag leaf and two peroxidases in the panicle.

INTRODUCTION

Cellular activities and biological functions are executed through complex physical and regulatory interactions of genes that resemble a network (Ma et al., 2014). The recent surge of omics data has opened the door to a system-wide understanding of biological information's flow

underlying complex traits (Serin et al., 2016). The corresponding large data sets represent a challenging endeavor that leads to the construction and analysis of gene networks. Such networks are often used for the genome-wide representation of biological systems' complex functional organization (Serin et al., 2016). Transcriptomic profiling technologies such as microarray and high-throughput sequencing (RNA-Seq) enable functional association based on co-expression networks (You et al., 2016).

Our knowledge of biological mechanisms related to drought stress is still limited despite numerous transcriptome studies (Hadiarto and Tran, 2011). Transcriptional profiling is a prevalent and robust approach for capturing crop plants' response to environmental stresses, e.g., rice response to drought. However, functionally interpreting the resulting genome-wide gene expression changes is severely hampered by the significant gaps in our genomic knowledge about which genes work together in cellular pathways/processes in rice (Krishan et al., 2017). We have not investigated thoroughly how drought-stress-related genes are regulated. Understanding the functions, communication, and interactions of drought-stress-related genes is critical for understanding how plants respond to drought stress (Ahn et al., 2017). The widely used differential expression (DE) analysis, one of the single-gene analyses, is often limited in deducing meaningful biological interpretations since it does not consider relationships among genes (dela Fuente, 2010; Shojaie and Michailidis, 2009). Fortunately, there has been significant progress in network-based analysis techniques that consider complex relationships among genes (Ma et al., 2014; Gitter et al., 2013).

Gene-co-expression analysis has emerged in the past five years as a powerful tool for gene function prediction. Co-expression analysis asks the question, “what are the co-expressed genes, that is, those that show similar expression profiles across experiments (Usadel et al., 2009). Gene co-expression networks (GCNs) are increasingly used to explore the system-level functionality of genes and have been useful for describing the pairwise relationships among genes (Zhang and Horvath, 2005). GCNs provide a pathway structure for extracting modular responses that are often missed by DE or ANOVA approaches (Gehan et al., 2015). Co-expression networks allow the possibility to shift focus from single candidate gene search to groups of related genes that are likely to operate together within a tissue or respond to stress (Liseron-Monfils and Ware, 2015). Genes clustered together in a module provide insight into potential regulatory functions (Sircar and

Parekh, 2015; Gehan et al., 2015; Segal et al., 2003). Therefore, co-expression can allow a modularized analysis of biological processes and mimic gene regulatory mechanisms *in vivo* to discover regulatory genes or modules of essential traits (You et al., 2016).

One of the essential GCN analysis applications is identifying functional gene modules, a group of nodes with high topological overlap (Horvath and Dong, 2008). Weighted gene co-expression network analysis is a system biology method describing the correlation patterns among genes across different transcriptomic samples. Weighted Gene Correlation Network Analysis (WGCNA) can be used for co-expression network analysis of gene expression data to find modules of highly correlated genes (Langfelder and Horvath, 2008). This approach has been used in plant systems to gain in-depth knowledge on the biotic and abiotic stress responses using whole transcriptome sequencing of potato (Masa et al., 2013), understand seed germination in Arabidopsis (Bassel et al., 2011), identify modules of new and conserved co-expressed miRNA highlighting potential miRNA-regulated biological pathways relevant to pathogenic and symbiotic interactions in *Medicago truncatula* (Formey et al., 2014), organize genes into transcriptional modules and explore their functions (Mao et al., 2009), to name a few. In rice GCN analysis provided some insights into gene regulation under drought stress, including (i) consensus modules of downregulated and upregulated genes (Shaik and Ramakrishna, 2013); (ii) a module enriched for genes involved in water homeostasis and embryonic development, including a heat shock TF (Zhang et al., 2012) and (iii) new candidates involved in drought response (Smita et al., 2013).

In the present study, we utilized the processed Illumina RNA-Sequencing from differential expression analysis results and applied a co-expression network approach to independently analyzed the transcriptome profiles of flag-leaf and panicle tissues, using WGCNA, a package in R (Langfelder and Horvath, 2008), in drought-stressed and control plants. By applying a gene co-expression network analysis and focusing on key source (flag-leaf) and sink (emerging panicle) tissues at reproductive stages, which had previously been demonstrated as critical for drought response (Sircar and Parekh, 2015), we speculated that adaptive mechanisms that drive yield under reproductive-stage drought stress could be captured. We identified modules of putatively co-regulated genes within each network possessing similar expression patterns and highly correlated with each other within different metabolic networks. We presented the gene modules analysis to

identify tissue-specific drought-responsive gene modules based on differential expression profiles of genes comprising these modules.

MATERIALS AND METHODS

Dataset Preprocessing

The flag-leaf and panicle datasets were filtered to remove non-varying or low-abundance genes introducing noise into the network analysis. Pre-filtering the low count's genes of the raw counts were done to keep only rows with at least ten reads total. The pre-filtered raw counts were used for transformation on the $\log_2$ scale, which has been normalized concerning library size using *vst* function in the *DESeq2* package. Differential expression analysis was performed using the pre-filtered raw counts. *DESeq2* uses each gene's average expression strength, across all samples, as its filter criterion, and it omits all genes with normalized mean counts below a filtering threshold from multiple testing adjustments (Love et al., 2014). The *results* function of the *DESeq2* package using the *filtered_p* function of the genefilter package (version 1.56.0) performs independent filtering by default using the mean of normalized counts as a filtered statistic. *DESeq2*, by default, chose a threshold that maximizes the number of genes found at a user-specified target FDR. The sum of the nonredundant/unique genes whose expression levels showed significant changes across different groups at FDR adjusted *P-value* <0.05 was identified. To generate separate co-expression networks for flag-leaf and panicle tissue using the WGCNA package in R, we extracted the pre-filtered, log2-transformed, normalized, and differentially expressed at FDR adjusted *P-value* <0.05 gene expression values of each sample as processed by *DESeq2*. After preprocessing, 17,616 and 18,614 unique genes for flag-leaf and panicle tissue were imported into WGCNA to construct the gene-coexpression network.

Network Construction and Module Detection

The WGCNA (version 1.6.1) software package in R was used to construct independent signed networks of flag-leaf and panicle tissue from the pre-filtered, $\log_2$-transformed, normalized expression matrix of 17,616 and 18,614 genes respectively from drought-tolerant and drought-sensitive samples. The use of soft thresholding is essential for the TOM calculations that measure

the strength of two genes' correlations based not just on their direct correlation value but also on all their common neighbors (Zhang and Horvath, 2005). The parameter ß was chosen such that low correlations that typically arise due to noise will be sufficiently suppressed (Langfelder et al., 2013). The pickSoftThreshold function in the WGCNA package was used to determine the smallest value of ß, which best approximates a scale-free topology model fit (signed R^2 >0.8) of the resultant network. An adjacency matrix was constructed using a soft threshold power of 6 and 9 for flag-leaf and panicle, respectively, the lowest power for a good fit of the scale-free topology index. Subsequently, the blockwiseModules function of the WGCNA package was used to detect and generate modules, which are groups of cotranscribed nodes (genes) that have high topological overlap. Network interconnectedness was measured by calculating the topological overlap using the TOMdist function with a "signed" TOM-type. Average hierarchical clustering using the hclust function was performed to group the genes based on the topological overlap dissimilarity measure (1-TOM) of their connection strengths. Network modules were identified using a dynamic tree cut algorithm (version 1.63.1) with minimum and maximum module sizes of 20 and 20000, respectively, merging threshold function at 0.15 and deep split parameter set at level 2. Genes inside a given module were summarized with the module eigengene, which can be defined as the first principal component of the expression matrix and represent the weighted average of each module's expression profile (Langfelder and Horvath, 2008). Heatmaps were constructed to depict the eigengenes from each identified module. To visualize the modules' expression profiles, each group's mean eigengene value for each module plus the contrasts and FDR adjusted *P*-value was plotted using a customized barplot function in R.

Functional Enrichment Analysis

Gene co-expression modules were tested for gene ontology and functional enrichment using the KOBAS web server and Over-Representation Analysis to identify modules that may have some functional interpretation. KOBAS (http://kobas.cbi.pku.edu.cn) is a web-server that annotates an input set of genes with putative pathways and disease relationships based on mapping to genes with known annotations (Xie et al., 2011). It allows for both ID mapping and cross-species sequence similarity mapping. It then performs statistical tests to identify statistically significantly enriched pathways and diseases. KOBAS also integrated nine gene set enrichment

(GSE) methods, including set-based methods (GSEA, GSA, PADOG, PLAGE, GAGE, GLOBAL TEST) and net-based methods (GANPA, GGEA, CEPA). KOBAS integrates the nine methods' results, giving gene set enrichment scores and the probability of being enriched sets based on nine gene set enrichment methods. Functional gene set enrichment was performed using KOBAS (version 3.0) using a hypergeometric test.

Module Hub Genes Identification

Hub genes are loosely defined as an abbreviation of highly connected genes within a module (Langfelder and Horvath, 2013). Selecting intramodular hub genes in a relevant module often leads to gene lists with a cleaner biological annotation which is typically evaluated using functional enrichment analysis (Langfelder et al., 2013). This is relevant for studying candidate biological processes associated with the trait of interest. To identify hub genes within the modules, the module membership (MM) values for each gene, also known as module eigengene-based connectivity (kME), were calculated first based on the Pearson correlation between each gene's actual expression values and the module eigengene values. The MM is highly related to intramodular connectivity (kIM), so highly connected intramodular hub genes tend to have high MM values to the respective module (Langfelder and Horvath, 2008). Genes within the module with the highest MM are highly connected within that module. To incorporate external information into the co-expression network, we used the gene significance (GS) measures. Abstractly speaking, the higher the absolute value of GSi, the more biologically significant is the i-th gene. A gene significance measure could also be defined by the minus log of a p-value (Langfelder and Horvath, 2008). We calculated GS measures for any contrast of interest using the –log10(p-value) from the DE analysis. The kME and GS values were plotted, and hub genes were identified with kME >0.9 and GS >10 for each contrast of interest within a module.

Module Preservation

In network applications, one is often interested in studying whether modules are preserved across multiple networks. For example, to determine whether a pathway of genes is perturbed in a specific condition, one can study whether its connectivity pattern is no longer preserved (Langfelder et al., 2011). Non-preserved modules can either be biologically uninteresting (e.g.,

reflecting data outliers) or interesting (e.g., reflecting tissue or stage-specific modules). An intuitive approach for studying module preservation is to cross-tabulate module membership.

A consensus network to identify modules shared between the two networks were generated as previously described to examine network topology conservation between the flag-leaf and panicle tissue transcriptomes (Langfelder and Horvath, 2008). Since the gene names were directly comparable, we first extracted the common genes present in flag-leaf and panicle tissue networks. These were the expression profiles of genes common to flag-leaf and panicle tissue utilized to detect consensus modules that would reveal sets of genes with similar co-expression patterns in both tissues. Each module from each network was used for sub-setting, so the genes are in the correct order. An in-house R function was used for overlap counting and statistical testing. The consensus network matrix for the flag-leaf and panicle tissue networks was plotted to show the significant overlap in gene count of two modules based on Fisher's exact test with the –log(p) of the *p-value*.

Over-representation Analysis

Generating many experimental results calls for an automated tool to generate a high-level view of inter-relations between existing biological knowledge and new experimental results. Over-Representation Analysis (ORA) helps in identifying pathways or gene sets that are over-represented (present more than would be expected) in a subset of your data, thus helping biologists to discover novel functional genetic mechanisms (Dong et al., 2016). One common application of GO is to categorize genes by a relatively small set of high-level GO terms, and this involves mapping a set of annotations for the genes of interest to a specified subset of high-level GO terms called a GO slim ontology (Rhee et al., 2008). This is a typical way of providing an overview of the broad biology encoded by a genome or differential expression patterns.

Using the GO slim assignment and the Interpro domains from Rice Genome Annotation Project Release 7 with the multiple gene sets in each module, ORA of gene ontology terms and protein families and domains were performed. The kegga function under the goana package in R utilized the user-supplied GO slim assignment and Interpro domains independently in the form of data.frame annotation alongside the entire group of filtered genes that went into statistical testing.

Gene.pathway was the data.frame linking genes to pathways and the pathway.names was the data.frame giving full names of pathways. The universe was the vector specifying the set of gene identifiers to be the background and not the whole genome. GO terms and Interpro domains were called significantly over-represented in the gene set if the *P*-value is <0.05.

RESULTS

Drought-stress related gene modules within the transcriptional map

The weighted gene co-expression network analysis (WGCNA) is a systems biology method used to describe the correlation patterns among genes across transcriptomic libraries and screen candidate genes related to phenotypic traits. WGCNA was employed to construct two independent signed networks for flag-leaf and panicle tissue from the expression matrix of a drought-tolerant and a susceptible genotype under well-watered and drought stress conditions during the reproductive stage. We analyzed the co-expression network of the pre-filtered, $\log_2$-transformed, normalized gene expression matrix of 17,616 and 18,614 unique genes with adjusted *P-value* <0.05 across four different groups of samples for each tissue totaling 16 samples.

A power value of 6 and 9 for flag-leaf and panicle, respectively, predicted a gene co-expression network that exhibited scale-free topology with inherent modular features (Figure 2.1). A total of 21 distinct co-expressed modules with different expression patterns in flag-leaf (designated as M1-M21, capturing 17,616 genes) and 23 distinct modules for panicle tissues (designated as M1-M23, capturing 18,614 genes) were identified via hierarchical clustering, which was displayed by different colors according to the WGCNA package function. The resulting gene dendrogram and respective module colors are shown (Figure 2.2; Table 2.1). The number of genes per module (module size) ranged from 28 to 6,403 highly co-expressed genes in the flag-leaf and 22 to 7,684 highly co-expressed genes in the panicle tissue (Table 2.1). Modules were defined as clusters of highly interconnected genes, and genes within the same module were highly correlated. The module eigengene calculated as the first principal component of a given module could represent gene expression levels among these samples in a module.

More than 70% of genes were distributed in the M1 (6403 and 7684) and M2 (6177 and 7390) for flag-leaf and panicle tissues, respectively (Table 2.1). While genes in the M1 had higher expression profiles under drought conditions and lower expression in control conditions for both genotypes in the flag-leaf and panicle tissues (Figure 2.3), genes in the M2 showed the opposite expression pattern, lower under drought and higher under control conditions for both tissues (Figure 2.3). The condition effect for each genotype was similar. It could be assumed to a large extent that the genes clustered in both modules in the flag-leaf and panicle tissues signify the high background similarity of the two genotypes and could play a fundamental role in drought response.

In the flag-leaf tissue, network genes in the M1 and M2 displayed similarities in GO terms. Under the biological processes, both modules showed localization and transport as the most significantly abundant GO term. Under cellular components, major categories, including membrane and cell part, were significantly enriched in both modules. Differences were found under molecular function, where protein binding, oxidoreductase activity, and cofactor binding were highly represented in the M1, while nucleotide and nucleoside binding were highly represented in the M2 (Table 2.2).

In the panicle, network genes in the M1 and M2 displayed a different trend regarding GO terms. Under biological processes, RNA processing and macromolecule modification were the most abundant GO terms in the M1, while localization and transport were significantly enriched in the M2. Under cellular components, major categories in the M1 included nuclear part, intracellular organelle lumen, and protein complex, while membrane, cell part, and cell were significantly enriched in the M2. In molecular function, nucleotide binding, purine nucleotide binding, and purine ribonucleotide binding were the most abundant in the M1. At the same time, oxidoreductase activity, transporter activity, and transmembrane transporter activity were highly represented in the M2 (Table 2.3).

Flag-leaf Specific Modules

Two specific modules with a contrasting expression pattern were investigated in more detail for implications in the two genotypes' differential performance under RDS. M14 (cyan)

consisting of 140 genes (Table 2.4) had significantly higher expression profiles in all samples of the DTY-IL genotype under RDS, whereas a lower expression across the three other groups of samples was observed (Figure 2.4). M16 (light-cyan) consisting of 102 genes (Table 2.5) had significantly lower expression in Swarna under RDS, whereas the three other groups of samples had a higher expression (Figure 2.5). There were 40 and 18 genes unannotated in the M14 and M16, respectively, 15 and 1 of which were annotated as Transposable elements (TEs).

M14 (high in DTY-IL under RDS) enriched biological process GO terms were cellular amino acid biosynthetic process, carboxylic acid biosynthetic process, as well as cell wall organization. Pathway enrichment suggested biosynthesis of secondary metabolites, phagosome, and fatty acid elongation as the most significant. Overrepresented Interpro domains included Expansins; Monooxygenase, FAD-binding, Glycosyltransferase, family 43; as well as Plant peroxidase (Figure 2.6). M14 hub genes included Amidase, Oxidoreductase, and Expansin (Table 2.6).

Notably, Module 14 contained four transcription factors (2 bHLH, 1 Zinc finger, and 1 Homeobox-leucine zipper), six genes involved in protein degradation (2 F-box domain, 1 E3 ubiquitin ligase, and 3 peptidases), four genes involved in ROS metabolism/scavenging (1 Glutathione S-transferase, and 3 Peroxidase precursors), all of which were significantly upregulated in the DTY-IL and significantly downregulated in Swarna under RDS (Table 2.4).

M16 (low in Swarna under RDS) was enriched in single-organism metabolic process, oxidation-reduction process, and cellular carbohydrate metabolic process, with enriched pathways including photosynthesis, Vitamin B6 metabolism, and folate biosynthesis. Overrepresented Interpro domains in Module 16 included Ferrodoxin—NAP reductase, Photosystem antenna protein-like, and Multicopper oxidase, type 1 (Figure 2.7). M16 hub genes included OsSub37 – Putative subtilisin homolog, Acetamidase, and Cytochrome P450 (Table 2.7).

Notably, Module 16 contained three transcription factors (1 Zinc finger, 1 MYB, and 1 TCP family TF-bHLH), two peptidases, a plastidial peroxiredoxin, a plant NADPH oxidase, and six photosynthesis-related genes, all of which were significantly upregulated in the DTY-IL and significantly downregulated in Swarna under drought RDS (Table 2.5).

Of particular interest in M14 is plant cell wall remodeling's potential involvement as one of the significant adaptation responses of the drought-tolerant genotype (DTY-IL). Significant upregulation of cell wall organization or biogenesis genes in DTY-IL in M14 was observed (Table 2.4; Figure 2.8). These included expansins, class III peroxidases, and cytoskeleton and cell cycle genes. This set of genes were significantly downregulated in Swarna under RDS. Leaf rolling was also observed for Swarna in the greenhouse experiment. While there was no visible difference in flag-leaf morphology between both genotypes under the well-watered condition, a prominent leaf rolling phenotype in Swarna was observed after ten days of reproductive-stage drought stress with complete leaf-rolling on the 13th day of drought stress (Figure 2.8).

Panicle Specific Modules

M10 (purple) consisting of 138 genes (Table 2.8) and M15 (midnight-blue) consisting of 73 genes (Table 2.9) were significantly associated with drought response. M10 had significantly higher expression profiles in all samples of the DTY-IL genotype under RDS and had a lower expression across the other three groups of samples (Figure 2.9). M15 had significantly lower expression profiles in all samples in the Swarna genotype under RDS, whereas the three other groups of samples had a higher expression (Figure 2.10). There were 22 unannotated genes for both modules. 6 and 5 of which were Transposable elements for M10 and M15, respectively.

M10 (high in DTY-IL under RDS) most significantly abundant biological process GO terms were calcium ion transmembrane transport, isoprenoid biosynthetic process, and lipid biosynthetic process, and pathway enrichment suggesting terpenoid backbone biosynthesis, glutathione metabolism, L-ascorbate degradation, and phenylpropanoid biosynthesis to be significant. Overrepresented Interpro domains were Protein kinase, catalytic domain; Serine/threonine-protein kinase; EF hand-like domain; as well as Plant peroxidase (Figure 2.11). M10 hub genes included OsWAK receptor-like cytoplasmic kinase, a peroxidase precursor, and a serine-type peptidase (Supplementary Table 2.10).

Notably, M10 contained three transcription factors (1 NAC, 1 MYB TF, 1 Zinc finger), the negative ABA regulator phosphatase 2C *(PP2C),* two LOX pathway genes (lipoxygenase, and dehydration stress-induced protein), six ROS scavenging genes (1 Stromal ascorbate peroxidase,

1 L-ascorbate peroxidase, and four Peroxidase precursors), six hydrolases (Glycosyl hydrolases and beta-glucosidases), five ribosomal protein-related, four protein degradation-related genes (2 peptidases, 1 F-box domain, and 1 U-box domain), and numerous receptor kinases (22), all of which were significantly upregulated in DTY-IL and significantly downregulated in Swarna under RDS (Table 2.8).

The identities of plant cell-wall stress sensors are unclear. However, plants have hundreds of receptor-like kinases and other kinases with an extracellular domain, a transmembrane domain, and a cytoplasmic kinase domain. So many candidates exist to sense cell-wall perturbations (Zhu, 2016). At the initial stage of stress transduction, receptors and sensor proteins localized on cell membranes perceive stress bridging the gap between perception and transmission of the signals to the target genes, conveying information to their cytoplasmic target proteins via catalytic processes, such as phosphorylation, and contributing to plant survival (Osakabe et al., 2014). In this study, numerous cell surface receptors were identified in M10 as upregulated in DTY-IL and downregulated in Swarna as rice response to RDS, including receptor protein kinases and wall-associated receptor kinases (Figure 2.12).

M15 (low in Swarna under RDS) was GO enriched for carboxylic acid metabolic process, small molecule metabolic process, and coenzyme metabolic process, and pathway enriched for carbon metabolism, Glutathione metabolism, Biosynthesis of amino acids, and Sulfur metabolism. Overrepresented Interpro domains included Cysteine synthase, Pyridoxal phosphate (Vit B6)-dependent enzyme, and Thiolase-like subgroup (Figure 2.13). M15 hub genes included Acyl-coenzyme A thioesterase 10, Glycosyl hydrolase family 29, and Dehydrogenase/reductase (Table 2.11).

Notably, M15 contained two transcription factors (1 WRKY protein, 1 AP2/EREBP family), a putative 12-oxophytodienoate reductase gene, three ROS scavenging genes (1 Glutathione S-transferase, 1 Glutathione peroxidase, and 1 Stromal ascorbate peroxidase), three heat shock proteins and two peptidases, all of which were significantly downregulated in Swarna and upregulated in the IL under RDS (Table 2.9).

Being essential for cellular signaling, maintenance of ROS level depends on the balance between ROS production and scavenging. Thus, ROS detoxification's kinetics reflects the tissue's ability to acclimate the energy imbalance caused due to rising ROS levels (Miller et al., 2010). Analysis of genome-scale metabolic pathways in the DTY-IL revealed up-regulation of genes involved in the biosynthesis of antioxidant enzymes and metabolites in M10 (Figure 2.14). Metabolic pathways such as glutathione metabolism, terpenoid backbone biosynthesis, ascorbate degradation and metabolism, phenylpropanoid biosynthesis, genes with sulfur-containing amino acids as well as genes for protein biosynthesis and normal protein processing in the endoplasmic reticulum (ER) were uniquely expressed at a higher level in the DTY-IL compared to Swarna under RDS.

To examine the conservation in network topology between the flag-leaf and panicle transcriptomes, a consensus network to identify modules shared between the two networks was generated as previously described (Langfelder and Horvath, 2008). The consensus network contained few significant overlaps in module classifications between the flag-leaf and panicle networks, consistent with the tissue-specific expression under drought (Figure 2.15). Similarly, colored modules between the flag-leaf and panicle networks contained a few significant overlaps of genes with a common consensus network module, consistent with their similar eigengenes profiles. The significant overlap portrays a common expression pattern for each condition of both genotypes (M1 and M2) and a common expression pattern for each genotype on both conditions (M6 and M7, and M5 and M6) in the flag-leaf and panicle networks, respectively.

DISCUSSION

Source-sink relationships largely determine the grain yield of cereal crops, with developing grains being primary sinks. In particular, the top two leaves, the flag-leaf, serve as the primary source (Hirota et al., 1990; Biswal and Kohli, 2013). Source sink regulation is orchestrated through intricate metabolic signaling (Lawlor and Paul, 2014), of which key players in sucrose sensing (e.g., trehalose-6-phosphate) and signal integration (e.g., SnRK1) are beginning to emerge (Lawlor and Paul, 2014). Drought stress affects these relationships by reducing both source and sink strengths. In source organs, carbon fixation and primary metabolism limitations reduce resource

allocation to developing sinks, causing yield reduction characterized by suboptimal grain filling (Basu et al., 2016). In sink organs, drought reduces fertility, causing yield reductions through suboptimal seed setting (Guo et al., 2016).

While DTY-QTLs have demonstrated effects to improve rice grain yields under RDS, knowledge about underlying molecular mechanisms is limited. Functional studies of *qDTY12.1* suggested an intricate pattern of below-ground contributions (Dixit et al., 2015) while physiological studies of *qDTY1.1* suggested above-ground implications (Vikram et al., 2015). Though confined to a single time point at the late booting stage (close to anthesis) after two weeks of RDS, our study suggested that DTY controlled mechanisms improve yield under drought by acting at both source and sink organs. At the flag-leaf, a coordinated response to sustain primary metabolism through cell wall loosening and maintained photosynthetic rates seemed to allow for sufficient carbon and energy allocation to the developing panicle, which in turn enabled reproductive structures to invest in protective mechanisms, including protein stabilization and turnover, ROS scavenging and production of protective secondary metabolites. While proximate effects in the panicle are suggested as improved male fertility and improved sink strength under RDS, the ultimate effects are improved seed setting and grain filling, and consequently, drought-tolerant yield (DTY) (Figure 2.16).

Source Effects—Flag-Leaf-Specific Differences between DTY-IL and Swarna

Collectively WGCNA and DE analyses suggested a complex interplay of a range of processes in the flag-leaf to contribute to the observed differences in RDS tolerance between DTY-IL and Swarna. These included specific protein turn-over, cell wall loosening, efficient ROS scavenging, and photosynthesis maintenance (Figures 4–6 and S12).

Stress causes perturbations in various cellular components such as cell walls, generating signals integrated into the nuclear gene expression and other cellular activities, which helps restore cellular homeostasis (Zhu, 2016). Cell wall perturbations significantly affect plant stress resistance. A direct consequence of drought is impaired cell turgor (Farooq et al., 2009), which is countered by the stiffening of cell walls to provide structural resistance (Moore et al., 2008; Tenhaken, 2015). Prolonged drought stress challenges plants to modify their cell walls, resulting

in cell wall tightening and loosening. Tightening occurs in tissues of relevance to structural integrity, while loosening occurs in tissues that need to be maintained in a growing and metabolically active mode (Moore et al., 2008). Although the cell wall is affected by drought stress, surprisingly, little is known about drought-induced cell wall composition changes (Tenhaken, 2015).

Cell wall organization or biogenesis genes showed an increase in expression in M14. A total of 12 cell wall-related genes were significantly upregulated in the DTY-IL and significantly downregulated in Swarna (Figure 6). These included two glycosyltransferase family 43 proteins, previously reported being involved in the synthesis of glucuronoxylan hemicellulose of secondary cell walls (Szklarczyk et al., 2017) and two expansin genes. Expansins facilitate loosening and extension of plant cell walls by disrupting non-covalent bonding between cellulose microfibrils and matrix glucans (Cosgrove, 2005), and implications in response to dehydration are well documented (Wu et al., 1996; Jones and Mcqueen-Mason, 2004; Harb et al., 2010; Guo et al., 2011; Li et al., 2013) and rose (Dai et al., 2012). Expansin appears to be strongly regulated by water stress deficiency (Jones and Mcqueen-Mason, 2004). Cell wall expansin activity increases during dehydration and rehydration in the resurrection plants, suggesting that expansin proteins help increase cell wall flexibility and promote leaf growth under water stress (Jones and Mcqueen-Mason, 2004). Such flexibility may be required to avoid desiccation-related damage due to mechanical strain in cells undergoing shrinkage.

Higher expression of cytoskeleton and cell cycle-related genes in DTY-IL (Figure 6) further supported the concept of maintained cell growth and stability in the tolerant flag-leaf tissue. Contrastingly, cytoskeletal genes (tubulin and formin) and a cell cycle gene (cyclin) were significantly downregulated in Swarna under drought (Table S10-1). Water deficits result in a reduced cell division rate and cell elongation (Meyer and Boyer, 1972). It is predicted that the cell wall and cytoskeleton-related proteins would change in response to drought as cytokinesis requires a new cytoskeleton and cell wall components (Wang et al., 2016). Cytoskeletal networks in the cell cortex are crucial for the plant cell wall's controlled remodeling, contributing substantially to cell growth and morphogenesis (Cvrčková, 2012). Several cytoskeleton proteins, including tubulin, reported in proteomic studies were decreased in response to drought (Wang et al., 2016).

Transcripts accumulation of actin and actin depolymerization factor were decreased in the drought-treated *H. vulgare* leaves for the tolerant and susceptible cultivar (Śniegowska-Świerk et al., 2015).

Several classes of enzymes control ROS production in the cell wall, most prominently plasma membrane NADPH oxidases (Torres and Dangl, 2005) and class III peroxidases (CIII Prxs) (Shigeto and Tsutsumi, 2016). CIII Prxs are secreted in the extracellular space, where they perform either cell wall stiffening through the peroxidative cycle (Passardi et al., 2004) or cell wall loosening through the hydroxylic cycle in which H_2O_2 and O_2^- are used in a Fenton-type reaction to generate hydroxyl radicals, including $^{\bullet}OH$, that lead to nonenzymatic cleavage of polysaccharides (Kunieda et al., 2013; Passardi et al., 2004). ROS-mediated wall loosening likely plays a vital role during drought and other abiotic stresses to maintain cell growth even in cases of variable turgor pressure (Novaković et al., 2018). Hydroxyl radicals ($^{\bullet}OH$), produced in the cell wall, are capable of cleaving wall polymers by attacking cell wall polysaccharides leading to breakage of load-bearing structures and can thus mediate cell wall loosening and extension growth (Skirycz and Inzé, 2010; Müller et al., 2009; Almagro et al., 2008; Liszkay et al., 2003). Interestingly, $^{\bullet}OH$ generated by a CIII Prx-mediated reaction was shown to play a role in plant extension growth by the degradation of cell wall polysaccharides (Liszkay et al., 2003). In the present study, three CIII Prxs (LOC_Os03g13200, LOC_Os07g01370, and LOC_Os07g48020) were present in M14 (Table S10-1), with LOC_Os03g13200 and LOC_Os07g48020 significantly upregulated in DTY-IL and significantly downregulated in Swarna (Figure 6). High CIII Prxs expression in DTY-IL could support the generation of $^{\bullet}OH$ for cell-wall loosening through cell wall polymers' cleavage (Tenhaken, 2015). Notably, evidence is emerging for similar mechanisms acting in leaves growing under low turgor pressure. Superoxide levels were exclusively elevated in the expanding leaves of Arabidopsis (Skirycz et al., 2010), consistent with earlier findings showing that the generation of hydroxyl radicals from superoxide and hydrogen peroxide plays a direct role in cell wall loosening via polysaccharide cleavage under both favorable and drought stress conditions (Liszkay et al., 2003). Since the experiment was a long (2 weeks) of moderate drought, we could assume that ROS levels by this time are high. The reported gene expression of CIII Prxs genes in the DTY-IL from our transcriptome analysis could potentially help generate $^{\bullet}OH$, which in turn could be an additional cell-wall loosening agent through overcoming growth

arrest by using ROS-mediated cleavage of cell wall polymers. This hypothesis needs to be validated by biochemical and physiological analysis. Interestingly, decreased expression of a calcium-dependent NADPH oxidase in Swarna and increased in activity of the DTY-IL in M16 (Table S10-2) were also observed. It is also known as respiratory burst oxidase and is a well-studied enzymatic source of superoxide (Miller et al., 2010; You and Chan, 2015), which had previously been implicated in drought and high-temperature stability (You and Chan, 2015). Hence, loosening the cell wall and synthesis of structural constituents together is suggested to contribute to water-deficit tolerance in the flag-leaf of DTY-IL.

Leaf rolling, a standard indicator of drought stress in rice (Cal et al., 2019), was prominent in Swarna under drought but nearly absent in DTY-IL (Figure 1D). Leaf rolling likely relates to aberrant cell turgor and cell wall homeostasis and phenotypically reflects findings in the flag-leaf specific module M14. The evident complete leaf rolling of the flag-leaf of Swarna signified that cell walls were either stiffened or arrested during RDS, resulting in suppressed growth through an apparent downregulation of cell wall loosening genes, and cytoskeleton and cell-cycle related genes during RDS. In the present study, the $^{\bullet}OH$ mediated cell wall loosening could potentially contribute to the loosening process. However, a thorough examination in the broader sense that considers the peroxidase activity, substrates, and ROS generated should be undertaken to verify such claims.

Another potential layer of regulation for the cell wall and cytoskeleton-related genes was the upregulation of an HD-Zip class II Transcription Factor (LOC_Os08g36220) in DTY-IL and downregulation in Swarna under RDS. HD-Zip proteins are transcription factors unique to plants characterized by a homeodomain and a leucine zipper motif. Despite these structural similarities, HD-Zip proteins participate in diverse and sometimes overlapping events ranging from stress responses to morphogenesis and development (Elhiti and Stasolla, 2009). It appears that HD-Zip I and HD-Zip II TFs contribute to the regulation of plant cell expansion, division, and differentiation. There is little functional evidence to suggest a role for HD-Zip II TFs in plant growth adaptation responses to water deficit. However, expression studies using microarrays have shown that *HAT2* (Homeobox from *Arabidopsis thaliana* 2) and *HAT22* expression are up-regulated under drought in Arabidopsis (Huang *et al.*, 2008). Both families bind similar 9-bp

pseudopalindromic *cis*-elements, CAATNATTG, under *in vitro* conditions. Among the 12-cell wall and cytoskeleton-related genes, 6 and 8 genes recognized the *cis*-elements of HD-Zip II and HD-Zip I, respectively, which could trigger these genes' activity or inactivity. This signifies that the upregulation of LOC_Os08g36220 regulates the induction of these cell wall organization genes in DTY-IL and repression in Swarna under drought.

More effective ROS scavenging, in general, seemed to be an essential mechanism differentiating drought responses of Swarna and DTY-IL. Higher expression of peroxiredoxin in DTY-IL (Table S10-2) suggests increased reduction capacity for H_2O_2, indicating enhanced detoxification in drought-stressed leaves (Wang et al., 2016).

The ubiquitin-26S proteasome system (UPS) plays a vital role in plants' resistance to abiotic stress by affecting cellular proteins' stability (Kong et al., 2016). E3 acts as a central component in the ubiquitination process in the UPS, which confirms the target proteins' specificity (Zhou et al., 2015). Many studies have shown that E3 ubiquitin ligases were positively related to plant drought tolerance (Wang et al., 2016). A higher expression profile of several genes involved in protein degradation of related proteins in the DTY-IL and lower basal expression in Swarna under RDS was observed in M14 and M16. Such findings indicate that the enhancement of UPS is essential for plants to cope with drought.

A primary detrimental effect of water stress in source tissues is impaired photosynthesis (Patro et al., 2014). Reduced abundance of photosynthesis-related proteins in response to RDS had previously been reported (Wang et al., 2016) and was indeed reflected in drought-stressed leaves of RDS-susceptible Swarna (M16). Components of the light reaction (two photosystem genes, components of the core complex of photosystem II (PSII) involved the primary light-induced photochemical processes), the dark reaction (ribulose bisphosphatase and the fructose-1,6 bisphosphatase), and photorespiration (ribulose bisphosphate carboxylase large chain precursor) were found to be consistently downregulated in Swarna (Table S10-2), suggesting functional impairments of general photosynthesis. Protection of photosynthesis from photoinhibition through photorespiration is a well-characterized drought response and prevents ROS accumulation in green tissues (Voss et al., 2013). Also, Swarna showed a lower expression of two ferredoxin-NADP genes involved in thylakoid electron transport, suggesting reduced capacity in regulating the

relative amounts of cyclic and non-cyclic electron for ATP and redox homeostasis (Szklarczyk et al., 2017). Consequently, it is argued that the physiological environment in DTY-IL under RDS supports relatively higher rates of photosynthesis, which in turn might sustain higher rates of energy and carbon production to support primary metabolism and source strength, ultimately leading to improved grain filling.

Sink Effects—Panicle Specific Differences between DTY-IL and Swarna

Collectively WGCNA and DE suggested several distinct mechanisms to contribute to RDS tolerance differences between DTY-IL and Swarna in panicles. They included protein stabilization and turnover, ROS scavenging, biosynthesis of secondary metabolites to protect reproductive organs, and hormonal signaling presumably to adapt reproductive developmental processes to drought. Under field conditions, they resulted in an approximate doubling of yield under drought for DTY-IL compared to Swarna (Figure 1A), at no significant difference in plant height (Figure 1B).

Dehydration stress enhances ROS and ROS-associated peroxidation production, causing damage to cellular structures (Noctor et al., 2014). Being essential for cellular signaling, ROS homeostasis depends on the balance between ROS production and scavenging (Miller et al., 2010). Analysis of genome-scale metabolic pathways in the DTY-IL revealed the up-regulation of genes involved in the biosynthesis of antioxidant enzymes and metabolites (Figures 8, 9, and S14).

Secondary metabolite production is crucial in stress-adaptive mechanisms (Nakabayashi et al., 2014). Genes in pathways involved in secondary metabolite biosynthesis, lipid biosynthesis, redox homeostasis, amino acid metabolism, carbohydrate metabolism, and protein metabolism were upregulated at the maximum booting stage under RDS in DTY-IL and downregulated in Swarna for M10 and M15 (Figure 9). Several metabolic pathways found to be shared between the two modules include glutathione, terpenoid, and ascorbate metabolism.

De novo protein synthesis and turnover are fundamental for plants to cope with drought stress (Wang et al., 2016). Translational efficiency is affected by ribosome composition. Thus relative ribosomal protein abundance can modulate plant environmental responses (Wang et al., 2016). Several proteins involved in protein biosynthesis, such as ribosomal proteins, exhibited an

increased activity under drought, which would be beneficial for protein synthesis in response to specific drought conditions (Wang et al., 2016). Five ribosomal protein-related genes involved in protein biosynthesis have a higher expression profile in the DTY-IL and lower expression in Swarna under RDS in M10. Ribosome was found to influence plant environmental response by controlling transcripts' translational efficiency through ribosome composition alterations (Wang et al., 2013).

Protein that function to maintain normal protein folding, repairing, and renaturation of the stress-damaged proteins showed significant upregulation of two protein processing genes in the DTY-IL and significant downregulation in Swarna under RDS in M10. Three genes related to protein processing, including a heat shock protein, had a lower expression pattern in Swarna and a higher expression profile in DTY-IL under RDS in M15. Heat shock proteins (HSP) function in protein folding during drought tolerance have been extensively studied in several plant species (Masand and Yadav, 2016). Overexpression of *MuHSP70* plays an essential role in improving abiotic stress tolerance, including drought in the transgenic Arabidopsis (Masand and Yadav, 2016). These data suggest that maintaining correct protein folding is important for panicles to cope with reproductive-stage drought stress.

Protein degradation is essential to remove abnormal or damaged proteins and control specific regulatory proteins' levels during drought stress (Wang et al., 2016). Degradation-related proteins showed an increase of expression profile (4 peptidases, 1 F-box domain, and 1 U-box domain) in the DTY-IL under RDS were observed in M10. The two peptidases (glutamate carbopeptidase and carboxyl-terminal peptidase) and the F-box and U-box domain are significantly upregulated in the DTY-IL and significantly downregulated in Swarna under RDS. A decrease in basal expression of 2 peptidases in Swarna and an increase of expression pattern in the DTY-IL under RDS in M15 was also observed. Some peptidases such as serine carbopeptidase in *G. herbaecum* and oligopeptidase in *O. sativa* were increased in drought-stressed leaves, and aminopeptidases (APs), were generally increased in drought-tolerant plant species and decreased in drought-sensitive plant species (Wang et al., 2016). The carbopeptidase activity in wheat seedlings increased in response to water deficit, and AP activity increased in dehydrated seedlings (Miazek and Zagdańska, 2008). The U-box domain is a known E3 ligase family and the Skp1-

Cullin-F-box complex (SCF), which have been found to play an important role in abiotic stress responses via the ubiquitin pathway (Zhou et al., 2015). A major subunit of the SCF complex is the F-box protein. Overexpression of an F-box protein gene, named *TaFBA1* from wheat confers enhanced tolerance to oxidative stress with the tobacco plants, and the enhanced tolerance of oxidative stress may be associated with higher activities of the antioxidant enzymes, which may have resulted from the regulation of the antioxidant gene expression (Zhou et al., 2015). Collectively this suggested that panicles of DTY-IL were more responsive and had the necessary energy to adapt their proteome to reproductive-stage drought conditions than Swarna.

In M10, six genes involved in the ROS scavenging (two ascorbate peroxidases and four peroxidase precursors) had elevated expression profiles in the DTY-IL (Figure 9; Table S12-1). Efficient reduction of H_2O_2 by peroxidases had previously been implicated with drought-tolerance in rice (Raorane et al., 2015). Specifically, plant ascorbate peroxidases (APXs) are crucial for ROS homeostasis (Zhang et al., 2013) and free radical detoxification through the ascorbate-glutathione cycle (Cramer et al., 2013), and their functional role in rice drought tolerance was demonstrated through transgenic approaches (Zhang et al., 2013). In M15, three ROS scavenging genes (1 glutathione *S*-transferase, one glutathione peroxidase, and one stromal ascorbate peroxidase) had a lower expression profile in Swarna (Figure 9; Table S12-2). Glutathione peroxidase (GPX) catalyzes the reduction of H_2O_2 using thioredoxin (Trx), while glutathione *S*-transferases (GSTs) are key to the removal of xenobiotic compounds (Wang et al., 2016). Ectopic expression of a GST in *Arabidopsis* (Xu et al., 2015) and a GPX in rice (Islam et al., 2015) resulted in enhanced drought tolerance, suggesting functional implications.

Interestingly, an ABC function gene with AP2 domain-containing protein (LOC_Os07g22770) controlling floral organ identity was downregulated in Swarna RDS under P-M15 (Table S12-2) suggesting a link to aberrant Swarna floral development under drought (Su et al., 2013). TFs belonging to AP2 and MYB family are involved in panicle development and water-deficit stress response, implying that they may represent a crosstalk component between redevelopment and stress.

A negative regulator of plant drought tolerance in abscisic acid (ABA) signaling, protein phosphatase 2C (PP2C) (Bhaskara et al., 2012), was upregulated in the DTY-IL in M10 (Table

S12-1). PP2C inhibits the activity of sucrose non fermenting 1 related kinase 1 (SnRK1) (Gosti et al., 1999), a central integrator of metabolic signaling and regulator of starvation response. Thus, the higher expression of PP2C in DTY-IL might correlate with reduced SnRK1 activity, indicative of anabolism rather than catabolism and growth rather than the starvation mode in panicles of DTY-IL.

Biosynthetic pathways that lead to the formation of these oxylipins in plants have been investigated. Such compounds are produced via the lipoxygenase (LOX) pathway (Chen et al., 2015). Significant upregulation of two genes involved in the LOX pathway (lipoxygenase and dehydration stress-induced protein) in the DTY-IL under RDS was observed in M10. These genes were significantly downregulated in Swarna under RDS. In plants, some oxylipins and their derivatives, such as jasmonic acid (JA), leaf aldehydes, and divinyl ethers, have been suggested to be involved in plant defense against pests. Plant lipoxygenase (LOX) may be involved in several diverse aspects of plant physiology, including growth and development, pest resistance, senescence, or wounding responses. It catalyzes the hydroperoxidation of lipids containing a cis, cis-1,4-pentadiene structure (Porta, 2002). LOX gene expression is regulated by different effectors such as Jasmonic acid (JA) and water deficiency (Porta et al., 1999). A LOX mRNA increase in *P. vulgaris* could be required for JA synthesis in response to drought stress (Porta et al., 1999).

Brassinosteroids (BRs) are growth-promoting steroid hormones important for male fertility and pollen development (Mandava, 1998). BR catabolism is controlled by BAS1, a cytochrome P450 monooxygenase (Neff et al., 1999). BRs bind to a cell-surface receptor kinase's extracellular domain, BRASSINOSTEROID INSENSITIVE1 (BRI1), to activate kinase activity (Belkhadur and Chory, 2006; Clouse, 2011). In P-M10, a BAS1-orthologue and two BRI1 genes were found to be upregulated in DTY-IL, suggesting a role for BR signaling in the maintenance of male fertility as part of the *qDTY*1.1-mediated RDS responses.

CONCLUSION

To obtain more information about the RNA-Seq data on drought-stressed flag-leaf and panicle tissues, the WGCNA package was employed to independently dissect the drought co-

expression gene modules from the filtered 17,818 and 18,616 genes in flag-leaf and panicle, respectively, across 16 RNA-Seq samples. This study provided novel insight into global transcriptional responses in rice under moderate RDS in a DTY-dependent manner and highlighted associated physiological mechanisms that allow DTY-IL to better cope with RDS. In DTY-IL flag leaves, structural and metabolic integrity associated with cell wall re-organization and active ROS metabolism allowed for the maintenance of cellular growth and homeostasis under RDS, supporting sustained rates of photosynthetic activity, consequently provisioning of energy and carbon to developing sinks. In the developing panicles close to anthesis, sustained energy and carbon allocation enabled to minimize the damage of reproductive structures due to RDS through protective mechanisms, including ROS homeostasis, post-transcriptional modifications, detoxification, and secondary metabolite production. Ultimately this results in improved yields under moderate RDS. Physiological and biochemical analysis would be needed to validate the identified putative drought-responsi0ve modules and better understand plant responses to reproductive-stage drought stress.

TABLES AND FIGURES

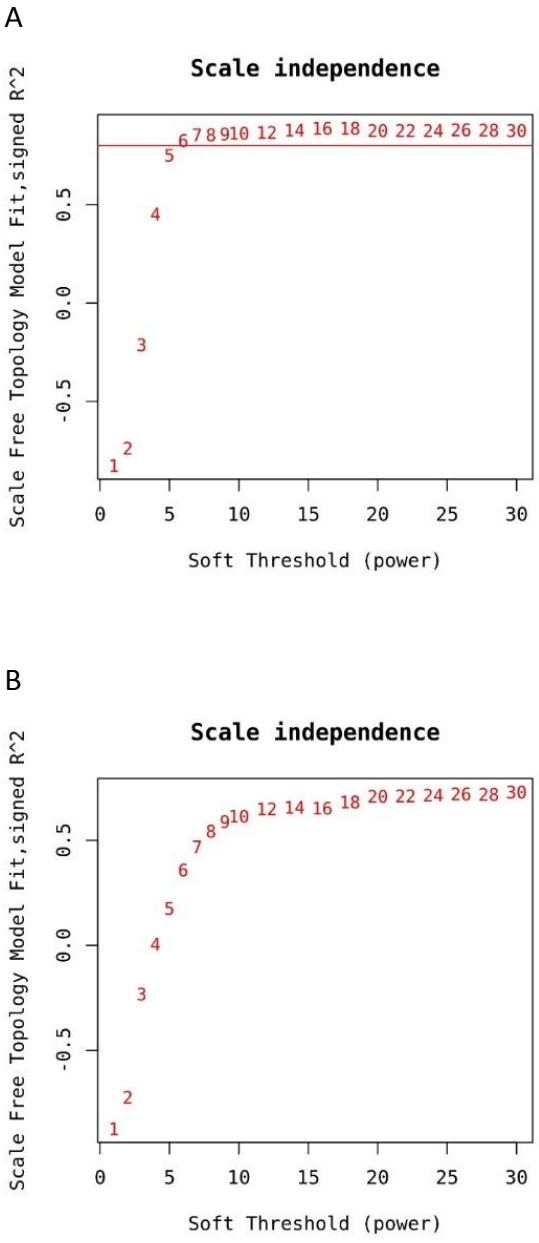

Figure 2.1. Identification of gene co-expression modules in the flag-leaf and panicle transcriptome under RDS. Selection of soft-thresholding power in WGCNA. The y-axis shows the scale-free topology index as a function of the Soft Threshold on the x-axis. The graph reaches a saturation point at threshold ß value = 6 in flag-leaf (A) and ß value = 9 and panicle (B) networks.

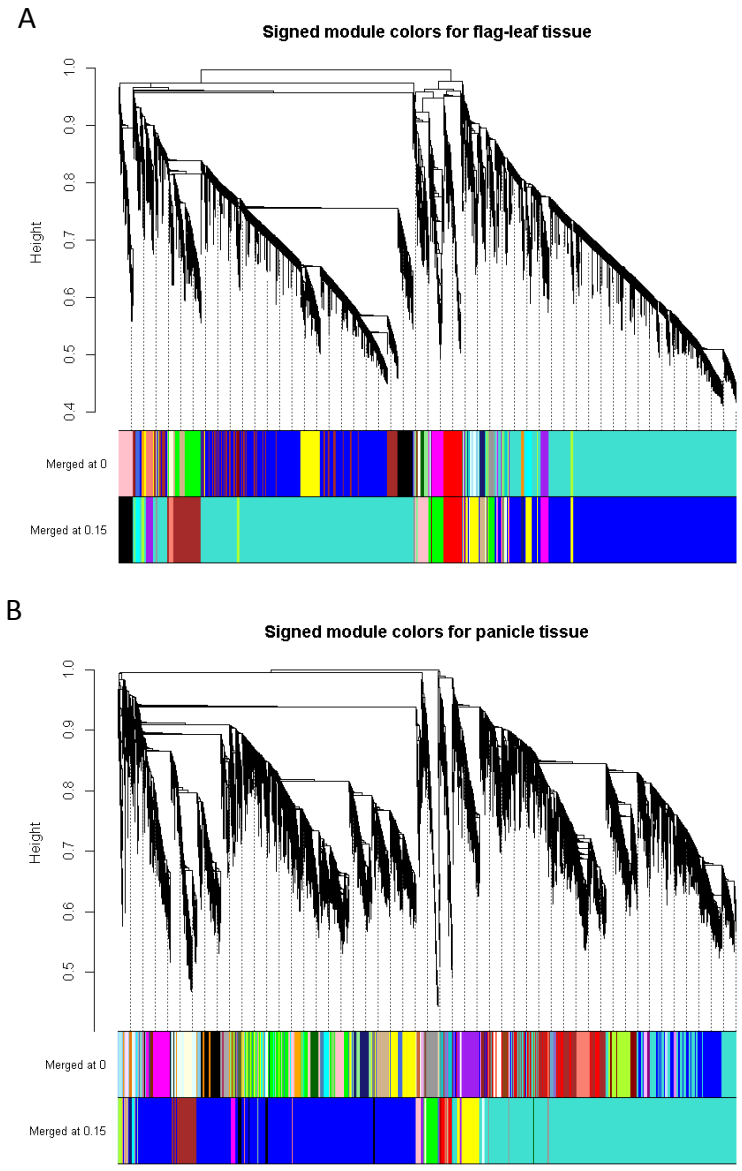

Figure 2.2. Identification of gene co-expression modules in the flag-leaf and panicle transcriptome under RDS. Properties and topologies of gene co-expression networks in flag-leaf and panicle tissues. Hierarchical cluster dendrogram showing co-expression modules from WGCNA in flag-leaf (A) and panicle (B) tissues. The *y*-axis denotes the co-expression distance, and the *x*-axis corresponds to genes. Genes were clustered based on a dissimilarity measure (1-TOM). Dynamic tree cutting was applied with a 0.15 threshold to identify modules by dividing the dendrogram at significant branch points. The branches correspond to modules of highly interconnected groups of genes. Modules corresponding to branches are displayed with different colors in the horizontal bar immediately below the dendrogram, with gray representing unassigned genes. Each vertical line a.k.a "leaf" in the tree, represents a gene.

Table 2.1. List of different module colors and sizes generated in flag-leaf and emerging panicle tissue under RDS using WGCNA.

Module No.	Module Color	Number of genes_Flag-leaf	Number of genes_Panicle
0	Grey	24	7
1	Turquoise	6403	7684
2	Blue	6177	7390
3	Brown	841	668
4	Yellow	691	598
5	Green	565	363
6	Red	515	288
7	Black	388	270
8	Pink	338	163
9	Magenta	307	138
10	Purple	229	138
11	Greenyellow	199	126
12	Tan	192	102
13	Salmon	146	99
14	Cyan	140	79
15	Midnightblue	126	73
16	Lightcyan	102	72
17	Grey60	88	69
18	Lightgreen	53	65
19	Lightyellow	34	60
20	Royalblue	30	55
21	Darkred	28	47
22	Darkgreen	.	38
23	Darkturquoise	.	22
Total		**17616**	**18614**

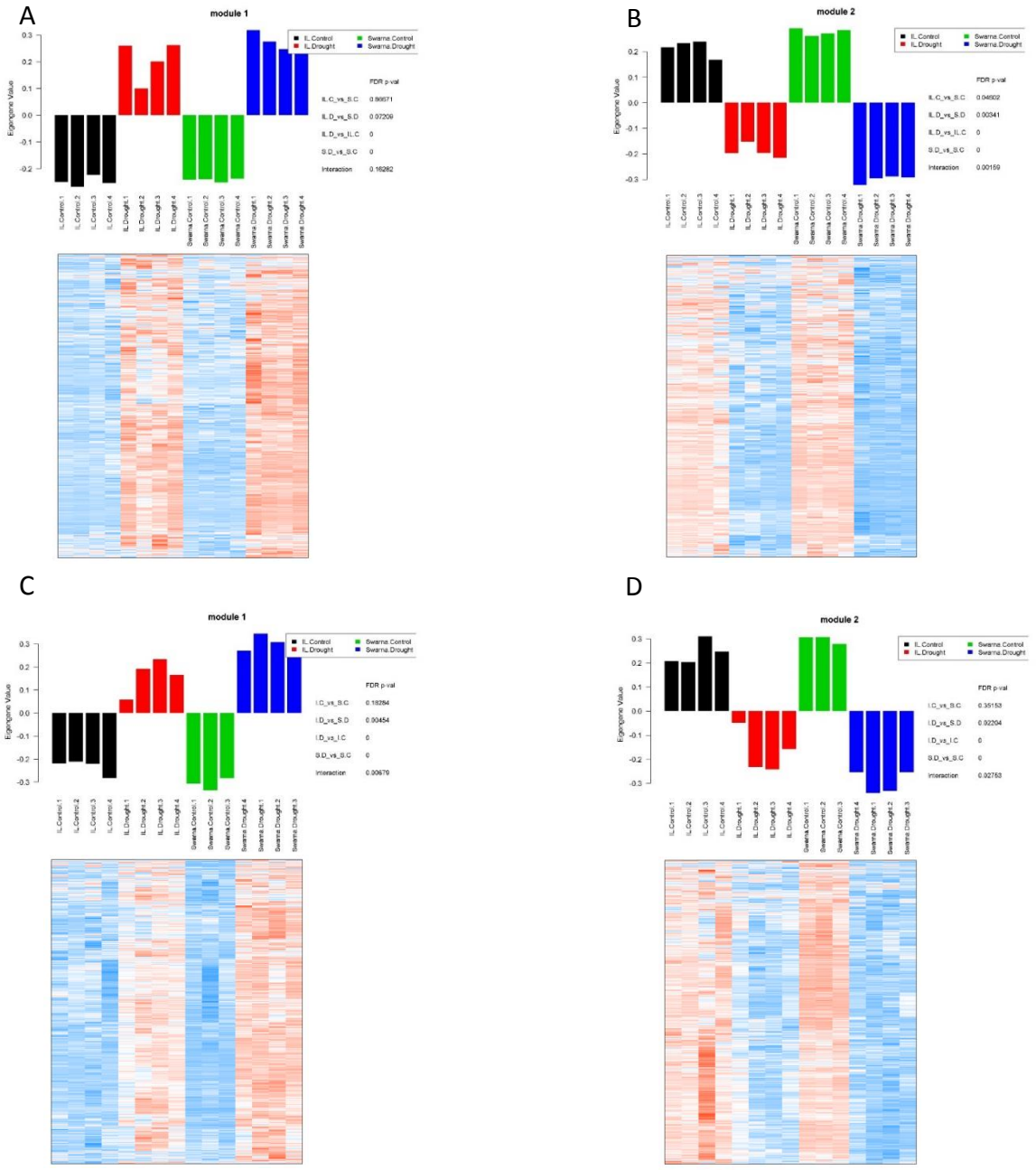

Figure 2.3. Bar graphs and Heatmaps of M1 and M2 in flag-leaf and panicle tissues under RDS correspond to a similar expression profile of both genotypes to drought. Bar plot of the module eigengene across different samples of M1 and M2 in flag-leaf (A & B) and panicle (C & D) tissues, respectively. The four different pairwise comparisons and the interaction term were used to assess changes in expression profiles. The X-axis represents the different samples across four different groups. The Y-axis corresponds to the Eigengene Value. The Eigengene Value can be considered a representative of the gene expression profiles in a module. Heatmaps showing gene expression levels of the genes and the number of genes within M1 and M2 in flag-leaf (A & B) and panicle (C & D) tissues, respectively, across the different samples. Each column represents different samples. Each row corresponds to one gene in the module. Red is a positive expression, and blue is a negative expression profile.

Table 2.2. The top 10 Go terms in biological process, molecular function, and cellular component categories in M1 and M2 in the flag-leaf tissue.

Class	M1		M2	
	GO ID	**Description**	**GO ID**	**Description**
Biological Process	GO:0051179	localization	GO:0051234	establishment of localization
	GO:0051234	establishment of localization	GO:0006810	transport
	GO:0006810	transport	GO:0055085	transmembrane transport
	GO:0008104	protein localization	GO:0051179	localization
	GO:0065007	biological regulation	GO:0043687	post-translational protein modification
	GO:0033036	macromolecule localization	GO:0006464	protein modification process
	GO:0045184	establishment of protein localization	GO:0043412	macromolecule modification
	GO:0015031	protein transport	GO:0006796	phosphate metabolic process
	GO:0005975	carbohydrate metabolic process	GO:0006793	phosphorus metabolic process
	GO:0051641	cellular localization	GO:0016310	phosphorylation
Molecular Function	GO:0005515	protein binding	GO:0001883	purine nucleoside binding
	GO:0016491	oxidoreductase activity	GO:0030554	adenyl nucleotide binding
	GO:0048037	cofactor binding	GO:0001882	nucleoside binding
	GO:0003924	GTPase activity	GO:0000166	nucleotide binding
	GO:0019001	guanyl nucleotide binding	GO:0017076	purine nucleotide binding
	GO:0032561	guanyl ribonucleotide binding	GO:0032559	adenyl ribonucleotide binding
	GO:0005525	GTP binding	GO:0005524	ATP binding
	GO:0050662	coenzyme binding	GO:0032555	purine ribonucleotide binding
	GO:0004553	hydrolase activity	GO:0032553	ribonucleotide binding
	GO:0004722	protein serine/threonine phosphatase activity	GO:0005215	transporter activity
Cellular Component	GO:0016020	membrane	GO:0016020	membrane
	GO:0044464	cell part	GO:0044425	membrane part
	GO:0005623	cell	GO:0016021	integral to membrane
	GO:0043234	protein complex	GO:0031224	intrinsic to membrane
	GO:0044425	membrane part	GO:0044464	cell part
	GO:0031224	intrinsic to membrane	GO:0005623	cell
	GO:0016021	integral to membrane	GO:0034357	photosynthetic membrane
	GO:0005783	endoplasmic reticulum	GO:0009579	thylakoid
	GO:0012505	endomembrane system	GO:0009521	photosystem
	GO:0031090	organelle membrane	GO:0009507	chloroplast

Table 2.3. The top 10 Go terms in biological process, molecular function, and cellular component categories in M1 and M2 in the panicle tissue.

Class	M1		M2	
	GO ID	**Description**	**GO ID**	**Description**
Biological Process	GO:0006396	RNA processing	GO:0051234	establishment of localization
	GO:0016070	RNA metabolic process	GO:0051179	localization
	GO:0043412	macromolecule modification	GO:0006810	Transport
	GO:0006464	protein modification process	GO:0044281	small molecule metabolic process
	GO:0043687	post-translational protein modification	GO:0005975	carbohydrate metabolic process
	GO:0010467	gene expression	GO:0006629	lipid metabolic process
	GO:0044267	cellular protein metabolic process	GO:0055114	oxidation reduction
	GO:0006796	phosphate metabolic process	GO:0065007	biological regulation
	GO:0006793	phosphorus metabolic process	GO:0006091	generation of precursor metabolites and energy
	GO:0006468	protein amino acid phosphorylation	GO:0055085	transmembrane transport
Molecular Function	GO:0000166	nucleotide binding	GO:0016491	oxidoreductase activity
	GO:0017076	purine nucleotide binding	GO:0005215	transporter activity
	GO:0032555	purine ribonucleotide binding	GO:0022857	transmembrane transporter activity
	GO:0032553	ribonucleotide binding	GO:0022892	substrate-specific transporter activity
	GO:0001882	nucleoside binding	GO:0022891	substrate-specific transmembrane transporter activity
	GO:0001883	purine nucleoside binding	GO:0048037	cofactor binding
	GO:0030554	adenyl nucleotide binding	GO:0016757	transferase activity, transferring glycosyl groups
	GO:0005524	ATP binding	GO:0015075	ion transmembrane transporter activity
	GO:0032559	adenyl ribonucleotide binding	GO:0008324	cation transmembrane transporter activity
	GO:0004386	helicase activity	GO:0016758	transferase activity, transferring hexosyl groups
Cellular Component	GO:0044428	nuclear part	GO:0016020	Membrane
	GO:0070013	intracellular organelle lumen	GO:0044464	cell part
	GO:0043234	protein complex	GO:0005623	Cell
	GO:0043233	organelle lumen	GO:0044425	membrane part
	GO:0031981	nuclear lumen	GO:0031224	intrinsic to membrane
	GO:0005654	nucleoplasm	GO:0016021	integral to membrane
	GO:0031974	membrane-enclosed lumen	GO:0043234	protein complex
	GO:0044451	nucleoplasm part	GO:0009521	photosystem
	GO:0000151	ubiquitin ligase complex	GO:0034357	photosynthetic membrane
	GO:0005635	nuclear envelope	GO:0005737	cytoplasm

Table 2.4. The list of 140 genes with their putative functions and expression profiles in the DTY-IL and Swarna under RDS in M14 in the flag-leaf tissue.

Model	Putative function	IL_D/SWA_D Log_2FC
LOC_Os01g02060	TOO MANY MOUTHS precursor, putative, expressed	1.314100904
LOC_Os01g06680	Retrotransposon protein, putative, unclassified, expressed	2.31823922
LOC_Os01g08470	Retrotransposon protein, putative, unclassified, expressed	1.331563436
LOC_Os01g21620	Conserved hypothetical protein	2.588586755
LOC_Os01g36060	Expressed protein	2.931649312
LOC_Os01g38510	Protein transport protein Sec61 subunit beta, putative	1.156520647
LOC_Os01g43110	Expressed protein	0.840385657
LOC_Os01g56150	OsProCP1 – Putative Lysosomal Pro-x Carboxypeptidase	0.51202901
LOC_Os01g56235	Expressed protein	5.235670129
LOC_Os01g57350	Diacylglycerol kinase, putative, expressed	0.535834835
LOC_Os01g59720	Expressed protein	1.502755075
LOC_Os01g61710	Coatomer subunit delta, putative, expressed	0.582880135
LOC_Os01g67540	AMP-binding domain containing protein, expressed	1.1661468
LOC_Os01g70770	Glutathione S-transferase, putative, expressed	0.939526348
LOC_Os01g71700	Amino acid permease family protein, putative, expressed	3.234463411
LOC_Os02g01590	Glycosyl hydrolases, putative, expressed (GH family 28)	3.13633334
LOC_Os02g06580	Formin, putative, expressed	1.045036235
LOC_Os02g06670	Retrotransposon protein, putative, unclassified, expressed	2.489695685
LOC_Os02g07670	URED, putative, expressed	0.997868041
LOC_Os02g12070	Hypothetical protein	2.715942672
LOC_Os02g33400	OsFBL9 – F-box domain and LRR containing protein, expressed	0.534275064
LOC_Os02g36020	Transposon protein, putative, CACTA, En/Spm sub-class,	3.556322523
LOC_Os02g37940	CRP12 – Cysteine-rich family protein precursor, expressed	0.410429123
LOC_Os02g44155	Expressed protein	0.854747637
LOC_Os02g50410	Hypothetical protein	
LOC_Os02g51610	CRAL/TRIO domain containing protein, expressed	0.803308862
LOC_Os02g52460	Zinc knuckle domain containing protein, expressed	1.498387892
LOC_Os02g53790	Adenylate kinase, putative, expressed	0.710587862
LOC_Os02g58730	Ras-related protein, putative, expressed	0.456183536
LOC_Os03g01150	Palmitoyl-protein thioesterase 1 precursor, putative, expressed	0.345495528
LOC_Os03g05910	Expressed protein	2.832273915
LOC_Os03g05920	Expressed protein	2.787701927
LOC_Os03g06460	Type I inositol-1,4,5-trisphosphate 5-phosphatase, putative	3.246292891
LOC_Os03g13200	Peroxidase precursor, putative, expressed	2.519840485
LOC_Os03g14820	Hypothetical protein	3.98008513
LOC_Os03g17120	Arginine biosynthesis bifunctional protein argJ 1, putative	0.73682532
LOC_Os03g20800	Hypothetical protein	3.975952036

Table 2.4. (Continued)

Model	Putative function	IL_D/SWA_D Log_2FC
LOC_Os03g21820	Expansin precursor, putative, expressed	3.897085967
LOC_Os03g29360	Expressed protein	1.635262513
LOC_Os03g44420	tubulin/FtsZ domain containing protein, putative, expressed	0.967733592
LOC_Os03g46040	Expressed protein	1.814563466
LOC_Os03g48840	Ribosomal L18p/L5e family protein, putative, expressed	0.867275544
LOC_Os03g51580	Helix-loop-helix DNA-binding domain containing protein	0.823513522
LOC_Os03g63310	Cytochrome P450 71E1, putative, expressed	
LOC_Os03g63900	1-aminocyclopropane-1-carboxylate oxidase 2, putative	0.669420538
LOC_Os04g01160	Zinc finger family protein, putative, expressed	0.894835161
LOC_Os04g03120	Retrotransposon protein, putative, unclassified	1.918410579
LOC_Os04g10350	1-aminocyclopropane-1-carboxylate oxidase homolog 2, putative	0.742277928
LOC_Os04g10530	Amidase, putative, expressed	7.035495573
LOC_Os04g13364	Transposon protein, putative, CACTA, En/Spm sub-class	2.249907028
LOC_Os04g20070	Tropinone reductase 2, putative, expressed	1.442349326
LOC_Os04g26240	OsFBDUF21 – F-box and DUF domain containing protein	1.272547673
LOC_Os04g26910	Oxidoreductase, aldo/keto reductase family protein, putative,	1.721871678
LOC_Os04g27670	Terpene synthase family, metal binding domain	3.94916513
LOC_Os04g31924	Nodulin, putative, expressed	0.650696809
LOC_Os04g34320	S-domain receptor-like protein kinase, putative	1.28844896
LOC_Os04g34530	Integral membrane protein DUF6 containing protein, expressed	2.640460074
LOC_Os04g38026	Transporter family protein, putative, expressed	0.899400616
LOC_Os04g44530	Expressed protein	0.967569306
LOC_Os04g45470	Vacuolar-processing enzyme precursor, putative, expressed	0.388287438
LOC_Os04g46100	Expressed protein	0.416316374
LOC_Os04g48020	3-hexulose-6-phosphate isomerase, putative, expressed	0.718060442
LOC_Os04g55670	Glycosyltransferase family 43 protein, putative, expressed	0.64200949
LOC_Os04g57590	DJ-1 family protein, putative, expressed	0.58221609
LOC_Os04g58580	Phosphomannomutase, putative, expressed	0.60096795
LOC_Os05g04584	Transferase family protein, putative, expressed	0.567765942
LOC_Os05g06660	OsSCP26 – Putative Serine Carboxypeptidase homologue	1.05673699
LOC_Os05g07880	Phospholipase D, putative, expressed	1.250134626
LOC_Os05g15340	Retrotransposon protein, putative, unclassified	1.417348642
LOC_Os05g19010	Expressed protein	1.531966347
LOC_Os05g19974	Endonuclease/exonuclease/phosphatase family protein, putative	0.571138023
LOC_Os05g35080	Hypothetical protein	
LOC_Os05g47780	E3 ubiquitin ligase, putative, expressed	0.582594853
LOC_Os05g47860	Expressed protein	1.688003042
LOC_Os05g48600	Glycosyltransferase family 43 protein, putative, expressed	0.430297521
LOC_Os05g49050	CobW/P47K family protein, putative, expressed	1.031247904

Table 2.4. (Continued)

Model	Putative function	IL_D/SWA_D Log_2FC
LOC_Os06g04990	Early nodulin 93 ENOD93 protein, putative, expressed	1.461931021
LOC_Os06g08910	Glutamate receptor 2.8 precursor, putative, expressed	0.530293018
LOC_Os06g12790	Ras-related protein, putative, expressed	0.702124689
LOC_Os06g13680	B12D protein, putative, expressed	0.52454175
LOC_Os06g15420	Asparagine synthetase, putative, expressed	0.651440284
LOC_Os06g15500	Retrotransposon protein, putative, unclassified	1.243554093
LOC_Os06g34830	Amino acid permease family protein, putative, expressed	0.459493191
LOC_Os06g36650	ABC transporter family protein, putative, expressed	1.755997985
LOC_Os06g40530	Transposon protein, putative, CACTA, En/Spm sub-clas	3.206314904
LOC_Os06g48510	Choline monooxygenase, chloroplast precursor, putative	1.251976301
LOC_Os06g50400	Expansin precursor, putative, expressed	2.990692297
LOC_Os06g51470	Expressed protein	
LOC_Os07g01100	Legume lectins beta domain containing protein, putative	
LOC_Os07g01370	Peroxidase precursor, putative, expressed	
LOC_Os07g05470	AIR9 protein, putative, expressed	1.142922402
LOC_Os07g13770	UDP-glucoronosyl and UDP-glucosyl transferase domain	2.245742717
LOC_Os07g30330	cytokinin-O-glucosyltransferase 2, putative, expressed	1.09948689
LOC_Os07g33240	Endoribonuclease, putative, expressed	0.619103598
LOC_Os07g34598	tyrosyl-DNA phosphodiesterase 1, putative, expressed	0.967181088
LOC_Os07g37010	Cyclin, putative, expressed	1.143335111
LOC_Os07g42960	Phospho-2-dehydro-3-deoxyheptonate aldolase	1.326717634
LOC_Os07g44350	Sec20 domain containing protein, expressed	0.520304006
LOC_Os07g48020	Peroxidase precursor, putative, expressed	2.791891
LOC_Os08g01490	Cytochrome P450, putative, expressed	0.701460288
LOC_Os08g08680	Transposon protein, putative, CACTA, En/Spm sub-class	0.758523343
LOC_Os08g10440	NBS-LRR disease resistance protein, putative, expressed	
LOC_Os08g20544	Expressed protein	0.618060531
LOC_Os08g20670	Retrotransposon protein, putative, unclassified, expressed	2.404020283
LOC_Os08g23410	Rubredoxin family protein, putative, expressed	0.674744662
LOC_Os08g24320	Retrotransposon protein, putative, unclassified	1.8665231
LOC_Os08g30480	Clathrin adaptor complex small chain domain containing protein	0.442263205
LOC_Os08g31940	Expressed protein	0.806394718
LOC_Os08g34000	Glycosyl transferase family 1 protein, putative	4.057637898
LOC_Os08g36220	Homeobox associated leucine zipper, putative, expressed	1.50645049
LOC_Os08g37300	Expressed protein	2.143444286
LOC_Os08g38210	Transcription factor BIM2, putative, expressed	0.823421806
LOC_Os08g40210	Expressed protein	1.408051322
LOC_Os09g07020	Oxidoreductase, putative, expressed	0.434456454
LOC_Os09g28810	RNA recognition motif containing protein, putative, expressed	0.89578189

Table 2.4. (Continued)

Model	Putative function	IL_D/SWA_D Log_2FC
LOC_Os09g32470	Membrane protein, putative, expressed	1.754793182
LOC_Os09g32810	Ribulose-phosphate 3-epimerase, putative, expressed	0.3843307
LOC_Os09g32988	POEI18 – Pollen Ole e I allergen and 103xtension family protein precursor	0.610773659
LOC_Os09g33920	Expressed protein	1.298903064
LOC_Os09g34150	NBS-LRR disease resistance protein, putative, expressed	2.060943806
LOC_Os09g34160	Resistance protein, putative, expressed	2.713693409
LOC_Os10g04720	TKL_IRAK_DUF26-la.5 – DUF26 kinases	0.877258068
LOC_Os10g07229	Dehydrogenase, putative, expressed	0.802203636
LOC_Os10g28094	Retrotransposon protein, putative, unclassified, expressed	3.060346217
LOC_Os10g30410	Cytochrome P450 71D7, putative, expressed	2.275268795
LOC_Os10g30880	Expressed protein	1.868699097
LOC_Os10g36210	valyl-tRNA synthetase, putative	1.506127238
LOC_Os10g37350	Expressed protein	1.070601108
LOC_Os10g42240	Kinase, pfkB family, putative, expressed	0.289560208
LOC_Os11g21804	Expressed protein	0.478655366
LOC_Os11g28770	Retrotransposon protein, putative, unclassified	4.194780979
LOC_Os11g34624	TKL_IRAK_DUF26-lc.29 – DUF26 kinases	3.62636909
LOC_Os11g35660	Leucine-rich repeat receptor protein kinase EXS precursor	4.124589968
LOC_Os11g42030	Expressed protein	1.639229337
LOC_Os12g02640	Cytochrome P450 72A1, putative, expressed	1.161609881
LOC_Os12g04260	Astaxanthin synthase KC28, putative	0.562909849
LOC_Os12g09590	Leafbladeless1, putative, expressed	0.426674253
LOC_Os12g10784	2-dehydro-3-deoxyphosphooctonate aldolase, putative	0.914919511
LOC_Os12g37840	Boron transporter protein, putative, expressed	0.675213879

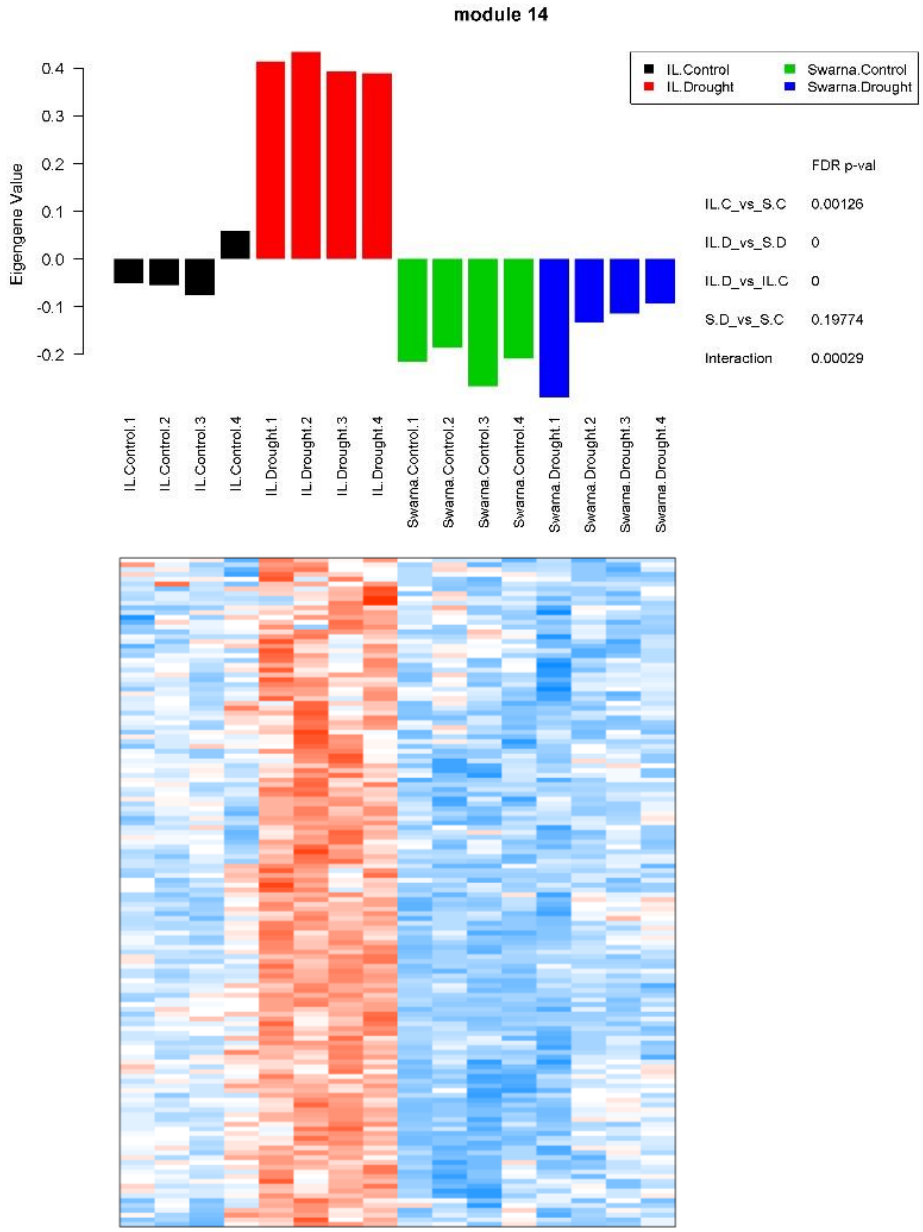

Figure 2.4. Gene co-expression network analysis in flag-leaf under RDS. Bar plots of the module eigengene as representatives of gene expression profiles across samples in M14. The X-axis represents 16 different samples across four different groups, while Y-axis corresponds to the Eigengene Value. Heatmaps showing gene expression levels of genes in M14. Columns represent samples, while rows correspond to genes in the module. Red indicates positive and blue negative expression profile. S.C = Swarna control, S.D = Swarna under RDS, IL.C = DTY-IL control, IL.D = DTY-IL under RDS.

Table 2.5. The list of 102 genes with their putative functions and expression profiles in the DTY-IL and Swarna under RDS in M16 in the flag-leaf tissue.

Model	Putative Function	IL_D/SWA_D Log_2FC
LOC_Os01g14890	Expressed protein	0.849946851
LOC_Os01g24090	TPR repeat, putative, expressed	0.831045658
LOC_Os01g25820	Respiratory burst oxidase, putative, expressed	0.561022709
LOC_Os01g29820	Expressed protein	
LOC_Os01g39280	Conserved hypothetical protein	1.29997984
LOC_Os01g41870	Protein kinase, putative, expressed	1.702487111
LOC_Os01g42800	MEE18, putative, expressed	
LOC_Os01g47450	OsCttP1 – Putative C-terminal processing peptidase homologue	
LOC_Os01g51020	60S ribosomal protein L28-1, putative, expressed	1.328641197
LOC_Os01g55950	Acetamidase, putative, expressed	1.42778977
LOC_Os01g58690	Endonuclease/exonuclease/phosphatase family domain	0.615989523
LOC_Os01g63870	Nucleobase-ascorbate transporter, putative, expressed	0.772808204
LOC_Os01g64980	Ion channel DMI1, chloroplast precursor, putative, expressed	0.361617106
LOC_Os01g65060	S-domain receptor-like protein kinase, putative	
LOC_Os02g03050	Dimethyladenosine transferase, putative, expressed	
LOC_Os02g05030	Sucrose-phosphatase, putative, expressed	0.465915285
LOC_Os02g05744	Endoglucanase, putative, expressed	2.173742804
LOC_Os02g32780	Pentatricopeptide, putative, expressed	0.594400735
LOC_Os02g33450	Peroxiredoxin, putative, expressed	
LOC_Os02g33500	threonyl-tRNA synthetase, putative, expressed	0.512279379
LOC_Os02g35310	12-oxophytodienoate reductase, putative, expressed	0.769890729
LOC_Os02g49326	SET domain-containing protein, putative, expressed	
LOC_Os02g52450	Regulator of ribonuclease, putative, expressed	1.308353692
LOC_Os02g52940	Soluble inorganic pyrophosphatase, putative, expressed	0.473888378
LOC_Os03g02030	Folylpolyglutamate synthase, mitochondrial precursor, putative	0.540522539
LOC_Os03g02640	Methylthioribose kinase, putative, expressed	0.704623435
LOC_Os03g04580	Expressed protein	0.844650662
LOC_Os03g06230	Galactose mutarotase-like, putative, expressed	0.63424949
LOC_Os03g10230	Expressed protein	0.644611244
LOC_Os03g21830	Appr-1-p processing enzyme family protein, putative, expressed	0.655903401
LOC_Os03g29170	Sterol-4-alpha-carboxylate 3-dehydrogenase, decarboxylating	0.421756742
LOC_Os03g42530	Retrotransposon, putative, centromere-specific	1.40663863
LOC_Os03g44040	Hypothetical protein	0.920104365
LOC_Os03g56782	Hypothetical protein	
LOC_Os03g57120	ferredoxin–NADP reductase, chloroplast precursor, putative	
LOC_Os03g60350	Leaf senescence related protein, putative, expressed	0.830663847

Table 2.5. (Continued)

Model	Putative Function	IL_D/SWA_D Log_2FC
LOC_Os03g61900	Hypothetical protein	0.500994518
LOC_Os04g01140	Cytochrome P450 93A2, putative, expressed	1.633704239
LOC_Os04g03180	Disease resistance protein, putative, expressed	3.042598521
LOC_Os04g03796	OsSub37 – Putative Subtilisin homologue, expressed	6.591975753
LOC_Os04g10924	Hypothetical protein	1.454101695
LOC_Os04g20960	Expressed protein	1.068071534
LOC_Os04g39930	Receptor-like protein kinase, putative	
LOC_Os04g40530	Methyltransferase domain containing protein, expressed	1.060854456
LOC_Os04g44110	Hydrolase, putative, expressed	0.452424622
LOC_Os04g49440	RNA recognition motif containing protein, putative, expressed	
LOC_Os04g51330	Maltose excess protein 1-like, chloroplast precursor, putative	0.581064178
LOC_Os04g51350	Pentatricopeptide, putative, expressed	0.677143767
LOC_Os04g57560	Amine oxidase, flavin-containing, domain containing protein,	1.099388323
LOC_Os05g11010	Harpin-induced protein 1 domain containing protein, expressed	1.217834852
LOC_Os05g13860	Hypothetical protein	0.88787681
LOC_Os05g43760	TCP family transcription factor, putative, expressed	0.586516969
LOC_Os06g01850	ferredoxin–NADP reductase, chloroplast precursor, putative	1.156290083
LOC_Os06g02610	Folic acid binding protein, putative	1.870087066
LOC_Os06g03520	DUF581 domain containing protein, expressed	1.248672436
LOC_Os06g03640	BAG domain containing protein, expressed	1.167511316
LOC_Os06g09240	Anthocyanidin 3-O-glucosyltransferase, putative, expressed	1.212802397
LOC_Os06g09450	Sucrose synthase, putative, expressed	0.42336964
LOC_Os06g12600	Kinase, pfkB family, putative, expressed	
LOC_Os06g23190	Receptor-like protein kinase 5 precursor, putative, expressed	1.105550757
LOC_Os06g33810	Zinc finger protein, putative, expressed	0.792654678
LOC_Os06g36840	Cysteine synthase, putative, expressed	1.032642855
LOC_Os06g39708	Photosystem II P680 chlorophyll A apoprotein, putative	1.185016919
LOC_Os06g40450	Targeting protein for Xklp2, putative, expressed	0.488144726
LOC_Os06g45370	Fructose-1,6-bisphosphatase, putative, expressed	0.783285411
LOC_Os06g45660	Histidine triad family protein, putative, expressed	0.658416756
LOC_Os06g50120	Novel plant SNARE 11, putative, expressed	1.649776439
LOC_Os07g07230	Protein kinase, putative, expressed	1.496089547
LOC_Os07g18720	Tetratricopeptide repeat containing protein, putative, expressed	0.531160512
LOC_Os07g32590	Peptidase, M24 family protein, putative, expressed	0.818137547
LOC_Os07g39750	GDSL-like lipase/acylhydrolase, putative, expressed	1.133451775
LOC_Os08g03630	Acyl-activating enzyme 14, putative, expressed	1.443497287
LOC_Os08g06380	CSLF6 – cellulose synthase-like family F; beta1,3;1,4 glucan synthase	0.84323323
LOC_Os08g33900	CAAX amino terminal protease family protein, putative	0.415109127
LOC_Os08g36860	Cytochrome P450, putative, expressed	1.516110808

Table 2.5. (Continued)

Model	Putative Function	IL_D/SWA_D Log_2FC
LOC_Os08g38400	Oligopeptide transporter, putative, expressed	2.279177944
LOC_Os08g40890	Spermidine synthase-related, putative, expressed	0.764258693
LOC_Os08g40919	Expressed protein	
LOC_Os08g42480	Expressed protein	1.091967104
LOC_Os08g42530	SFC, putative, expressed	0.494223276
LOC_Os08g44210	Dihydroneopterin aldolase, putative, expressed	1.068021549
LOC_Os09g07350	Fasciclin-like arabinogalactan protein 8 precursor, putative, expressed	3.543528593
LOC_Os09g30410	Expressed protein	
LOC_Os09g34214	UDP-glucoronosyl and UDP-glucosyl transferase domain	1.9863297
LOC_Os09g34890	Expressed protein	3.833997392
LOC_Os09g35990	Expressed protein	0.800999938
LOC_Os09g39034	Expressed protein	0.554291372
LOC_Os10g21268	Ribulose bisphosphate carboxylase large chain precursor, putative	1.790221788
LOC_Os10g21310	Photosystem II P680 chlorophyll A apoprotein, putative, expressed	1.16236184
LOC_Os10g25090	STRUBBELIG-RECEPTOR FAMILY 6 precursor, putative, expressed	0.542432824
LOC_Os10g29620	Tyrosine protein kinase domain containing protein, putative, expressed	0.813702189
LOC_Os10g32600	MYB family transcription factor, putative	1.384765523
LOC_Os10g33730	Pentatricopeptide, putative, expressed	0.470733613
LOC_Os10g37330	Oxidoreductase, aldo/keto reductase family protein, putative	0.616658334
LOC_Os10g41980	RALFL26 – Rapid Alkalinization Factor RALF family protein	
LOC_Os11g05556	Signal recognition particle 54 kDa protein, putative, expressed	0.393570813
LOC_Os11g17970	POT family protein, expressed	1.066225305
LOC_Os11g29720	Cytochrome P450, putative, expressed	2.800656472
LOC_Os11g34110	Heparan-alpha-glucosaminide N-acetyltransferase, putative	1.69981274
LOC_Os11g40840	Receptor-like protein kinase 2 precursor, putative, expressed	1.764750664
LOC_Os12g34890	Acyl carrier protein, putative, expressed	0.713615397

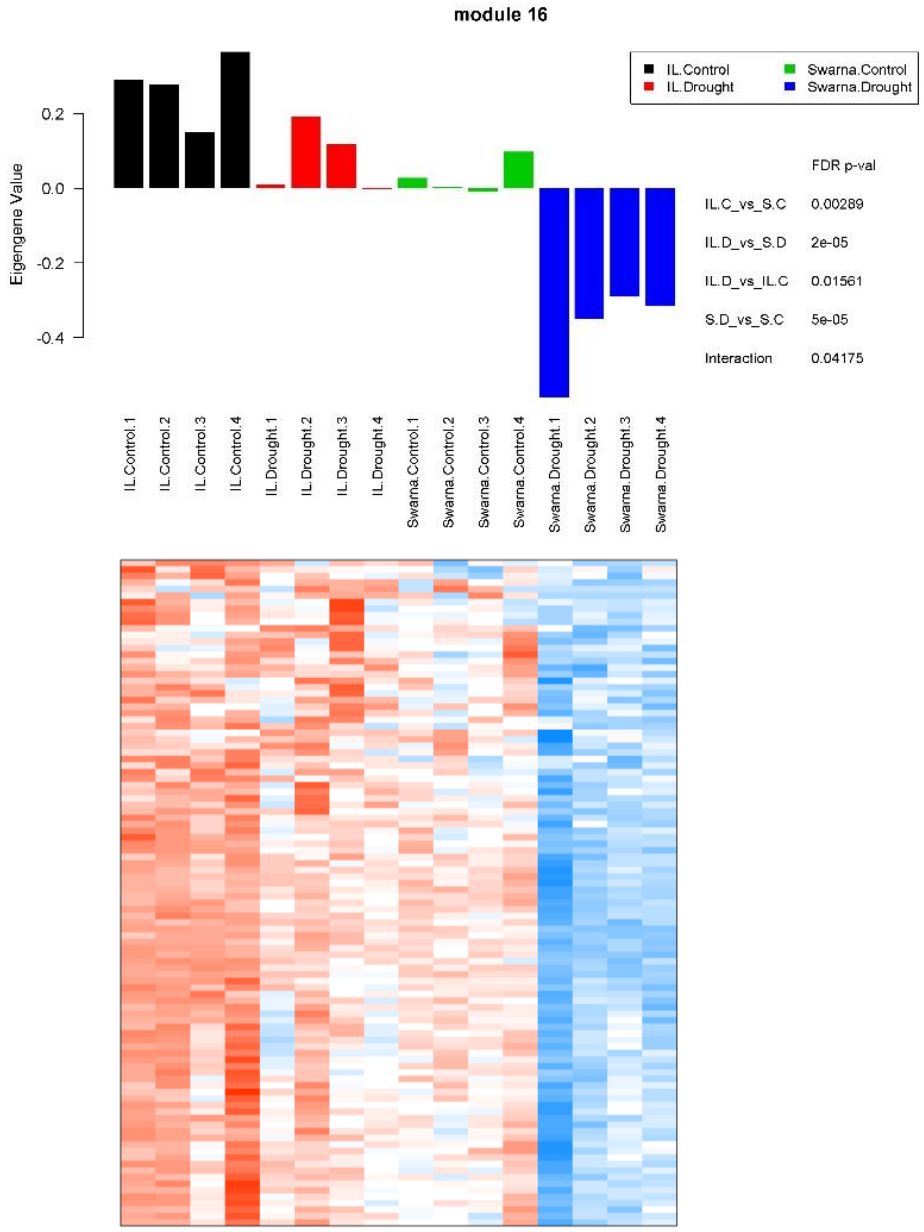

Figure 2.5. Gene co-expression network analysis in flag-leaf under RDS. Bar plots of the module eigengene as representatives of gene expression profiles across samples in M16. The X-axis represents 16 different samples across four different groups, while Y-axis corresponds to the Eigengene Value. Heatmaps showing gene expression levels of genes in M16. Columns represent samples, while rows correspond to genes in the module. Red indicates positive and blue negative expression profile. S.C = Swarna control, S.D = Swarna under RDS, IL.C = DTY-IL control, IL.D = DTY-IL under RDS.

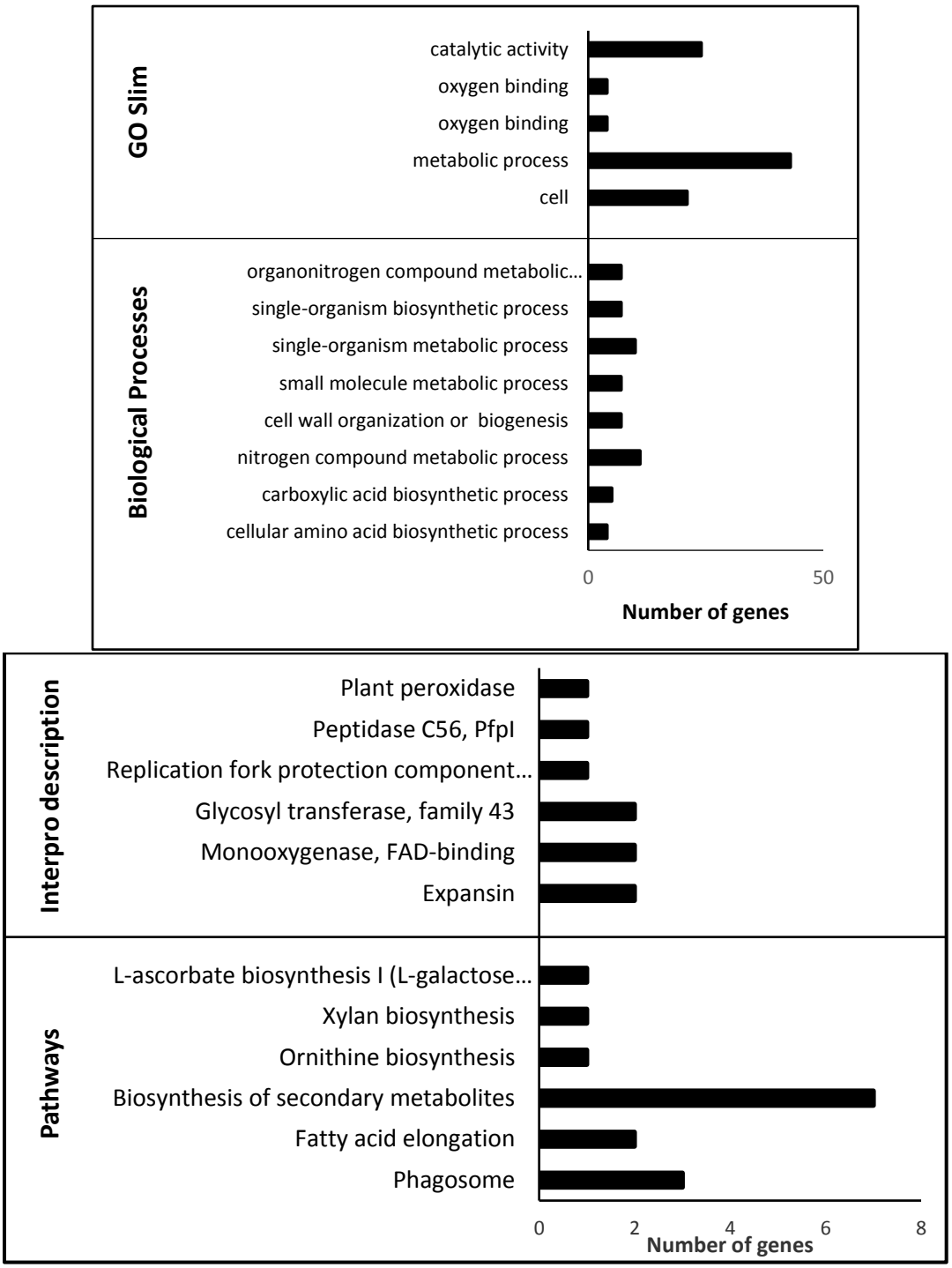

Figure 2.6. Enrichment analysis of the functional categories in M14. Major BP, Over-represented GO Slim description, Interpro domains, and enriched pathways in M14in flag-leaf under RDS. Top significant BP, GO Slim, Pathways, and Interpro domains are shown in Y-axis with the number of represented genes on the X-axis.

Table 2.6. Identified hub genes in M14 in the flag-leaf tissue between the DTY-IL and Swarna under RDS.

ID	module	kME	negLogPValue	Annotation	IL_D/SWA_D Log_2FC
LOC_Os04g46100	14	0.905460158	5.33342159	expressed protein	0.416316374
LOC_Os02g52460	14	0.940317512	6.146430856	zinc knuckle domain containing protein; expressed	1.498387892
LOC_Os09g32470	14	0.9311385	6.98329703	membrane protein; putative; expressed	1.754793182
LOC_Os06g15420	14	0.925345026	7.047822142	asparagine synthetase; putative; expressed	0.651440284
LOC_Os08g24320	14	0.91110619	7.20363343	retrotransposon protein; putative; unclassified; expressed	1.8665231
LOC_Os05g49050	14	0.955632791	7.807535842	CobW/P47K family protein; putative; expressed	1.031247904
LOC_Os02g51610	14	0.914681827	8.139774081	CRAL/TRIO domain containing protein; expressed	0.803308862
LOC_Os09g34160	14	0.947515836	8.334868607	resistance protein; putative; expressed	2.713693409
LOC_Os12g02640	14	0.928944251	10.4520702	cytochrome P450 72A1; putative; expressed	1.16161
LOC_Os04g34530	14	0.942497865	10.55553945	integral membrane protein DUF6 containing protein; expressed	2.64046
LOC_Os09g33920	14	0.913268803	11.63405229	expressed protein	1.298903
LOC_Os03g05910	14	0.909910923	12.95393082	expressed protein	2.832274
LOC_Os01g56235	14	0.939303472	15.61934817	expressed protein	5.23567
LOC_Os03g21820	14	0.961522738	20.73818436	expansin precursor; putative; expressed	3.897086
LOC_Os04g26910	14	0.956039897	21.63456924	oxidoreductase; aldo/keto reductase family protein; putative; expressed	1.721872
LOC_Os04g10530	14	0.960466686	24.42571759	amidase; putative; expressed	7.035496
LOC_Os03g05920	14	0.935217153	29.14943131	expressed protein	2.787702

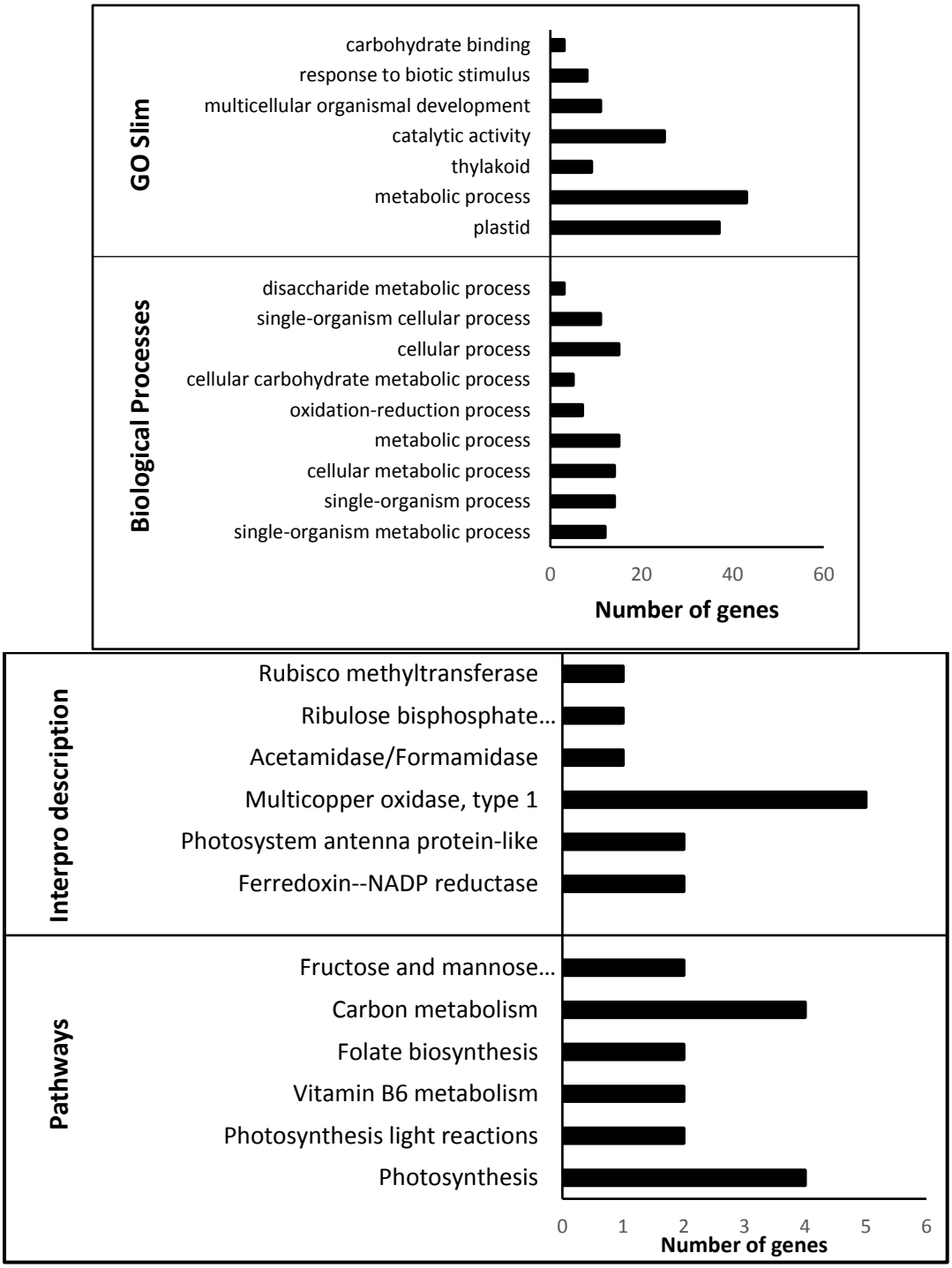

Figure 2.7. Enrichment analysis of the functional categories in M16. Major BP, Over-represented GO Slim description, Interpro domains, and enriched pathways in M14in flag-leaf under RDS. Top significant BP, GO Slim, Pathways, and Interpro domains are shown in Y-axis with the number of represented genes on the X-axis.

Table 2.7. Identified hub genes in M16 in the flag-leaf tissue between the DTY-IL and Swarna under RDS.

ID	module	kME	negLogPValue	Annotation	IL_D/SWA_D Log_2FC
LOC_Os01g39280	16	0.919212824	5.097365926	expressed protein	1.29997984
LOC_Os08g44210	16	0.908742965	5.137025668	dihydroneopterin aldolase; putative	1.068021549
LOC_Os04g40530	16	0.928405595	5.562749562	methyltransferase domain containing protein; expressed	1.060854456
LOC_Os03g04580	16	0.915236398	6.147130683	expressed protein	0.844650662
LOC_Os04g20960	16	0.929761767	6.591017748	expressed protein	1.068071534
LOC_Os02g52450	16	0.951518949	6.647200744	regulator of ribonuclease; putative; expressed	1.308353692
LOC_Os03g60350	16	0.910061607	6.747889859	leaf senescence related protein; putative; expressed	0.830663847
LOC_Os06g33810	16	0.918162604	7.040252446	zinc finger protein; putative; expressed	0.792654678
LOC_Os04g10924	16	0.920216901	7.180194767	expressed protein	1.454101695
LOC_Os11g17970	16	0.919492003	7.24453701	POT family protein; expressed	1.066225305
LOC_Os04g57560	16	0.910645153	7.700212375	amine oxidase; flavin-containing; domain containing protein; expressed	1.099388323
LOC_Os02g05744	16	0.924325767	8.136086929	endoglucanase; putative; expressed	2.173742804
LOC_Os06g01850	16	0.926973991	8.636463229	ferredoxin--NADP reductase; chloroplast precursor; putative; expressed	1.156290083
LOC_Os04g01140	16	0.94409875	8.657172602	cytochrome P450 93A2; putative; expressed	1.633704239
LOC_Os11g34110	16	0.948426086	9.106674349	heparan-alpha-glucosaminide N-acetyltransferase; putative; expressed	1.69981274
LOC_Os08g37940	16	0.953000314	10.15301442	HAD-superfamily hydrolase subfamily IA; variant 3; putative; expressed	2.0132557
LOC_Os06g50120	16	0.941781186	11.18223253	novel plant SNARE 11; putative; expressed	1.6497764
LOC_Os06g36840	16	0.933390467	12.06035151	cysteine synthase; putative; expressed	1.0326429
LOC_Os10g29620	16	0.953653762	12.83499923	tyrosine protein kinase domain containing protein; putative; expressed	0.8137022
LOC_Os08g36860	16	0.906694498	12.95941484	cytochrome P450; putative; expressed	1.5161108
LOC_Os01g41870	16	0.926675036	20.25175887	protein kinase; putative; expressed	1.7024871
LOC_Os11g29720	16	0.94802708	20.65762302	cytochrome P450; putative; expressed	2.8006565
LOC_Os01g55950	16	0.95208327	26.27136431	acetamidase; putative; expressed	1.4277898
LOC_Os09g34890	16	0.923503887	44.13913457	expressed protein	3.8339974
LOC_Os04g03796	16	0.933481941	54.04411749	OsSub37 - Putative Subtilisin homologue; expressed	6.5919758

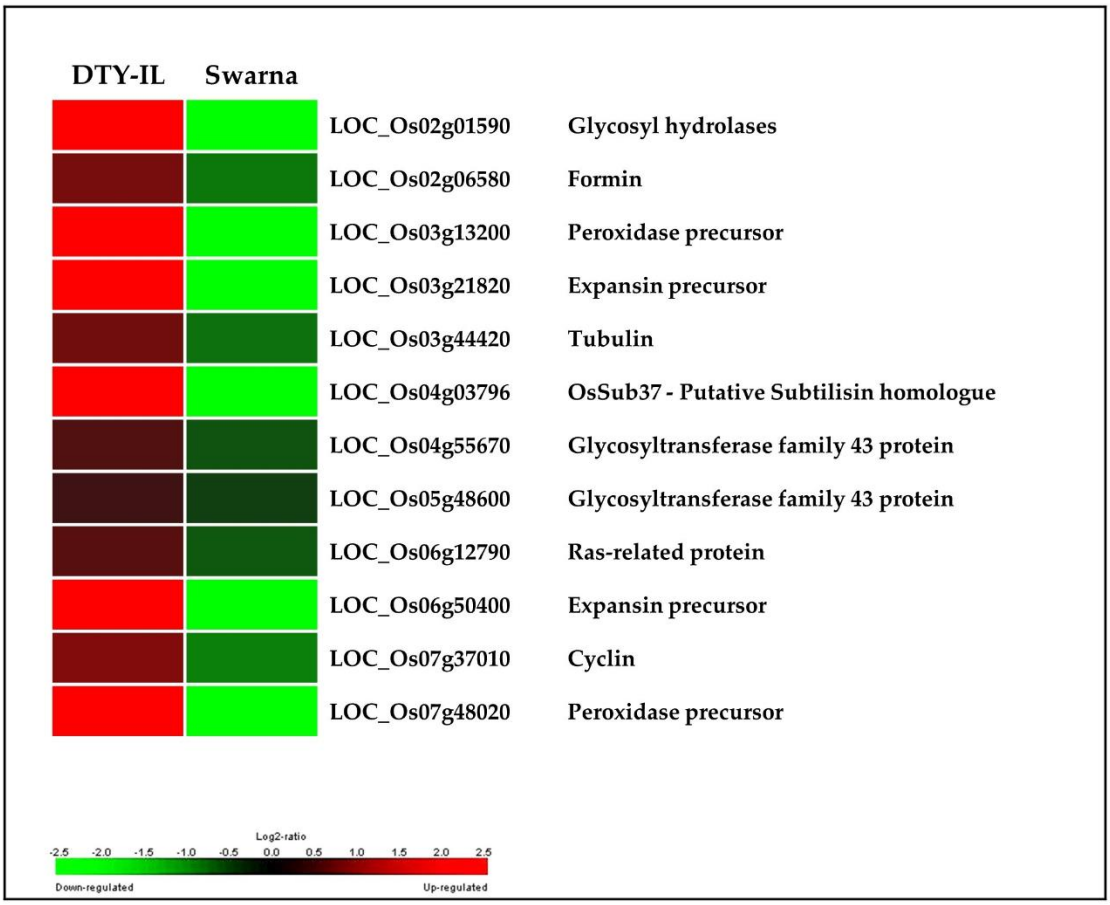

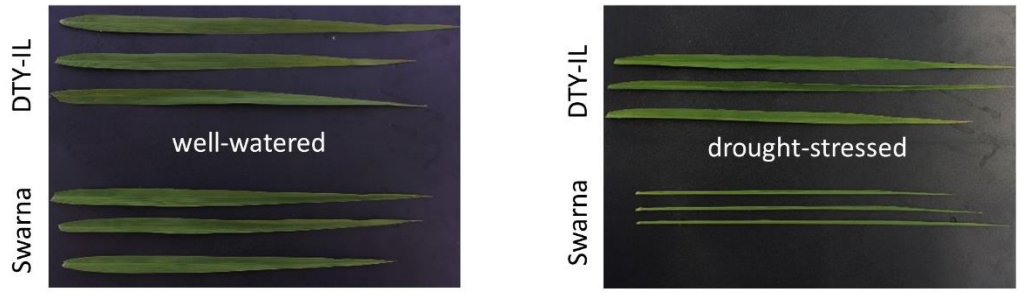

Figure 2.8. Cell wall organization and biogenesis during RDS in the flag-leaf tissue. Expression of genes in drought-responsive modules between DTY-IL and Swarna are shown as log_2-fold change heat-maps. Flag-leaf phenotypes of the DTY-IL and Swarna under the well-watered condition and the leaf-rolling phenotype during drought-stress under controlled greenhouse conditions.

Table 2.8. The list of 138 genes with their putative functions and expression profiles in the DTY-IL and Swarna under RDS in M10 in the panicle tissue.

Model	Putative function	IL_D/SWA_D Log_2FC
LOC_Os01g01710	1-deoxy-D-xylulose 5-phosphate reductoisomerase, chloroplast precursor, putative, expressed	0.928511739
LOC_Os01g04560	Conserved hypothetical protein	2.776411162
LOC_Os01g05870	Receptor kinase, putative, expressed	1.345120501
LOC_Os01g06490	OsSCP1 - Putative Serine Carboxypeptidase homologue, expressed	0.576949236
LOC_Os01g24980	Naringenin,2-oxoglutarate 3-dioxygenase, putative, expressed	0.917436079
LOC_Os01g41360	Expressed protein	3.028208064
LOC_Os01g42330	Retrotransposon protein, putative, unclassified	0.996839298
LOC_Os01g42980	Ribosomal protein L22, putative, expressed	0.481851001
LOC_Os01g48760	THAP domain-containing protein 4, putative, expressed	0.796196176
LOC_Os01g51570	Glycosyl hydrolases family 17, putative, expressed	2.478256576
LOC_Os01g53450	Aminotransferase, classes I and II, domain containing protein, expressed	0.755009871
LOC_Os01g53800	Glutamate carboxypeptidase 2, putative, expressed	1.340790928
LOC_Os01g61814	40S ribosomal protein S23, putative, expressed	0.604899437
LOC_Os01g64110	Glycosyl hydrolase, putative, expressed	1.739980612
LOC_Os01g70210	CRAL/TRIO domain containing protein, expressed	1.041396098
LOC_Os01g71790	NAM, putative, expressed	1.232363479
LOC_Os01g72710	Expressed protein	0.878390485
LOC_Os01g72870	BAS1, putative, expressed	0.713299651
LOC_Os01g73170	Peroxidase precursor, putative, expressed	1.262839087
LOC_Os01g74160	Carboxyl-terminal peptidase, putative, expressed	3.040690073
LOC_Os02g01510	Lactate/malate dehydrogenase, putative, expressed	1.409736902
LOC_Os02g06070	Phytosulfokine receptor precursor, putative	0.690245654
LOC_Os02g06205	Phytosulfokine receptor precursor, putative, expressed	0.96501549
LOC_Os02g11680	Glucosyltransferase, putative, expressed	1.706219564
LOC_Os02g12070	Hypothetical protein	2.307469349
LOC_Os02g29600	Conserved hypothetical protein	2.733818362
LOC_Os02g33240	OsFBX51 - F-box domain containing protein, expressed	1.488939084
LOC_Os02g34650	Expressed protein	0.930817441
LOC_Os02g36070	Cytochrome P450, putative, expressed	
LOC_Os02g37290	Heavy metal associated domain containing protein, expressed	1.526420299
LOC_Os02g37320	Heavy metal associated domain containing protein, expressed	1.833076724
LOC_Os02g37330	Heavy metal associated domain containing protein, expressed	1.974831331
LOC_Os02g38840	Glucose-6-phosphate 1-dehydrogenase, cytoplasmic isoform, putative, expressed	1.557084849

Table 2.8. (Continued)

Model	Putative function	IL_D/SWA_D Log_2FC
LOC_Os02g39160	Hydroxymethylbutenyl 4-diphosphate synthase, putative, expressed	1.232206203
LOC_Os02g42370	Receptor-like protein kinase 2 precursor, putative, expressed	0.616621676
LOC_Os02g42406	DEAD-box ATP-dependent RNA helicase, putative, expressed	0.584714235
LOC_Os02g52940	Soluble inorganic pyrophosphatase, putative, expressed	0.566553173
LOC_Os02g58260	Metallo-beta-lactamase family protein, putative, expressed	0.660745412
LOC_Os03g02030	Folylpolyglutamate synthase, mitochondrial precursor, putative, expressed	0.589730243
LOC_Os03g05920	Expressed protein	1.744785713
LOC_Os03g15120	Imidazole glycerol phosphate synthase hisHF, chloroplast precursor, putative, expressed	0.437911327
LOC_Os03g16950	Cysteine-rich repeat secretory protein 55 precursor, putative, expressed	3.945820047
LOC_Os03g21940	60S ribosomal protein L19-3, putative, expressed	0.682492479
LOC_Os03g32040	Phenazine biosynthesis protein, putative, expressed	1.061149776
LOC_Os03g36160	DNAJ heat shock N-terminal domain-containing protein, putative, expressed	3.422911844
LOC_Os03g37970	Ribosomal protein L13, putative, expressed	0.524787492
LOC_Os03g49620	BRASSINOSTEROID INSENSITIVE 1-associated receptor kinase 1 precursor, putative, expressed	0.763521939
LOC_Os03g59880	Expressed protein	0.744716246
LOC_Os04g01240	Serine-type peptidase, putative, expressed	0.720270167
LOC_Os04g03180	Disease resistance protein, putative, expressed	2.139301506
LOC_Os04g11910	Transposon protein, putative, unclassified	2.365499154
LOC_Os04g22120	Protein kinase, putative, expressed	2.996413632
LOC_Os04g27540	Terpene synthase, putative	4.29137385
LOC_Os04g29990	OsWAK44 - OsWAK receptor-like protein kinase	5.037513928
LOC_Os04g30010	OsWAK45 - OsWAK receptor-like protein kinase, expressed	1.754807427
LOC_Os04g34370	Serine/threonine-protein kinase receptor precursor, putative, expressed	0.954148045
LOC_Os04g35520	OsAPx7 - Stromal Ascorbate Peroxidase encoding gene 5,8, expressed	0.964298279
LOC_Os04g39880	Os4bglu12 - beta-glucosidase, exo-beta-glucanase, expressed	1.305299275
LOC_Os04g41380	Leucine Rich Repeat family protein, expressed	0.89143764
LOC_Os04g42920	Dehydrogenase, putative, expressed	0.355475435
LOC_Os04g47890	MYB family transcription factor, putative, expressed	1.832811967
LOC_Os04g48200	Cytochrome P450, putative, expressed	2.582122212
LOC_Os04g51030	Wall-associated kinase 1, putative, expressed	1.373995356
LOC_Os04g52780	Leucine-rich repeat receptor protein kinase EXS precursor, putative, expressed	1.743609023
LOC_Os05g03770	Expressed protein	1.88368902

Table 2.8. (Continued)

Model	Putative function	IL_D/SWA_D Log_2FC
LOC_Os05g13800	Transposon protein, putative, unclassified	2.140766906
LOC_Os05g25430	Receptor-like protein kinase At3g46290 precursor, putative, expressed	1.377521001
LOC_Os05g29710	RING-H2 finger protein, putative, expressed	1.263801663
LOC_Os05g36360	U-box domain containing protein, expressed	1.046808717
LOC_Os05g43170	Calreticulin precursor protein, putative, expressed	1.913292369
LOC_Os05g43360	NADH dehydrogenase flavoprotein 2, mitochondrial precursor, putative, expressed	
LOC_Os05g44060	Expressed protein	
LOC_Os05g49250	hhH-GPD superfamily base excision DNA repair protein, putative, expressed	0.540964885
LOC_Os05g51610	Sodium/calcium exchanger protein, putative, expressed	1.27809255
LOC_Os06g01350	Transferase family protein, putative, expressed	0.84824452
LOC_Os06g03720	Ribonucleoside-diphosphate reductase small chain, putative, expressed	1.028676595
LOC_Os06g12120	BRASSINOSTEROID INSENSITIVE 1-associated receptor kinase 1 precursor, putative, expressed	1.003148149
LOC_Os06g12250	Sphingolipid C4-hydroxylase SUR2, putative, expressed	0.900064337
LOC_Os06g19370	Cadmium tolerance factor, putative, expressed	1.441819399
LOC_Os06g20920	SAM dependent carboxyl methyltransferase, putative, expressed	1.402759554
LOC_Os06g45960	Cytochrome P450, putative, expressed	2.906176907
LOC_Os06g46340	Glycosyl hydrolase, family 31, putative, expressed	2.359467997
LOC_Os07g09190	Transketolase, putative, expressed	1.803440818
LOC_Os07g18230	Lectin-like receptor kinase, putative, expressed	2.559464752
LOC_Os07g22710	CAMK_CAMK_like.32 - CAMK includes calcium/calmodulin depedent protein kinases, expressed	0.66807568
LOC_Os07g31250	OsWAK69 - OsWAK receptor-like cytoplasmic kinase OsWAK-RLCK, expressed	0.545460928
LOC_Os07g32380	Protein phosphatase 2C, putative, expressed	0.653995861
LOC_Os07g33240	Endoribonuclease, putative, expressed	0.760562986
LOC_Os07g34280	CXE carboxylesterase, putative, expressed	
LOC_Os07g35004	TKL_IRAK_DUF26-la.4 - DUF26 kinases have homology to DUF26 containing loci, expressed	1.496082205
LOC_Os07g35480	Glucan endo-1,3-beta-glucosidase precursor, putative, expressed	2.973603617
LOC_Os07g36800	UPF0041 domain containing protein, putative, expressed	1.305671784
LOC_Os07g48010	Peroxidase precursor, putative, expressed	4.00808614
LOC_Os07g48020	Peroxidase precursor, putative, expressed	5.55539429
LOC_Os07g49080	COBRA-like protein 7 precursor, putative, expressed	1.579379127
LOC_Os08g04230	Cysteine-rich repeat secretory protein 55 precursor, putative, expressed	2.606377882
LOC_Os08g08440	Hypothetical protein	0.860771864
LOC_Os08g24630	Protein kinase domain containing protein, expressed	1.703678682

Table 2.8. (Continued)

Model	Putative function	IL_D/SWA_D Log_2FC
LOC_Os08g26820	Plant protein of unknown function domain containing protein, expressed	1.536840005
LOC_Os08g32690	Expressed protein	0.973013233
LOC_Os08g36220	Homeobox associated leucine zipper, putative, expressed; Probable transcription factor	0.517077054
LOC_Os08g39850	Lipoxygenase, chloroplast precursor, putative, expressed	1.91441181
LOC_Os09g01880	Transposon protein, putative, unclassified	2.720542609
LOC_Os09g04339	Expressed protein	2.363957703
LOC_Os09g19160	Serine/threonine-protein kinase, putative, expressed	1.840497025
LOC_Os09g20500	Transporter, putative, expressed	0.974803558
LOC_Os09g29600	OsWAK85 - OsWAK receptor-like cytoplasmic kinase OsWAK-RLCK	2.195489447
LOC_Os09g36750	L-ascorbate peroxidase 4, putative, expressed	0.752163729
LOC_Os10g21670	Dehydration stress-induced protein, putative, expressed	4.287191167
LOC_Os10g26940	BURP domain containing protein, expressed	3.920979316
LOC_Os10g30880	Expressed protein	0.874887182
LOC_Os10g33690	GDSL-like lipase/acylhydrolase, putative, expressed	0.383330555
LOC_Os11g03840	D-mannose binding lectin family protein, expressed	1.313274343
LOC_Os11g04370	Ribosomal protein L24, putative, expressed	0.508429644
LOC_Os11g04460	Calcium-transporting ATPase, plasma membrane-type, putative, expressed	0.663741243
LOC_Os11g06230	Expressed protein	0.844640647
LOC_Os11g06570	Transposon protein, putative, CACTA, En/Spm sub-class	1.88582335
LOC_Os11g07440	Plant neutral invertase domain containing protein, expressed	
LOC_Os11g10290	S-domain receptor-like protein kinase, putative, expressed	1.537062433
LOC_Os11g11780	Cysteine-rich receptor-like protein kinase 21 precursor, putative, expressed	2.647802191
LOC_Os11g14150	Transposon protein, putative, Pong sub-class	0.986779797
LOC_Os11g34624	TKL_IRAK_DUF26-lc.29 - DUF26 kinases have homology to DUF26 containing loci	4.509944153
LOC_Os11g37010	Expressed protein	0.543333587
LOC_Os11g37700	Pleiotropic drug resistance protein, putative, expressed	1.708640581
LOC_Os11g45130	Pollen signalling protein with adenylyl cyclase activity, putative, expressed	1.600109057
LOC_Os11g46860	Wall-associated receptor kinase-like 4 precursor, putative, expressed	2.357719243
LOC_Os11g46870	Protein kinase, putative	
LOC_Os11g46900	Wall-associated receptor kinase 3 precursor, putative	1.779994305
LOC_Os12g02060	Peroxidase precursor, putative	1.427166736
LOC_Os12g04220	Calcium-transporting ATPase, plasma membrane-type, putative	0.82000135
LOC_Os12g13320	Argininosuccinate synthase, chloroplast precursor, putative, expressed	0.575883838

Table 2.8. (Continued)

Model	Putative function	IL_D/SWA_D Log_2FC
LOC_Os12g19304	Fe-S metabolism associated domain containing protein, expressed	0.658816127
LOC_Os12g24330	Expressed protein	1.351298488
LOC_Os12g28710	ATPase 3, putative, expressed	1.337533848
LOC_Os12g39860	Phosphoribosyl transferase, putative, expressed	0.543462447
LOC_Os12g41710	Protein kinase domain containing protein, expressed	1.15235857
LOC_Os12g43664	FGGY family of carbohydrate kinases, putative, expressed	0.713732813

Table 2.9. The list of 73 genes with their putative functions and expression profiles in the DTY-IL and Swarna under RDS in M15 in the panicle tissue.

Model	Putative Function	IL_D/SWA_D Log_2FC
LOC_Os01g01369	3-beta-hydroxysteroid-Delta-isomerase, putative, expressed	0.374950798
LOC_Os01g09080	WRKY DNA-binding domain containing protein, expressed	1.593670023
LOC_Os01g11160	Amino acid permease family protein, putative, expressed	1.335262436
LOC_Os01g14580	Dehydrogenase, putative, expressed	0.576832127
LOC_Os01g17000	Expressed protein	0.861455383
LOC_Os01g23580	Inorganic H+ pyrophosphatase, putative, expressed	1.201598102
LOC_Os01g27240	12-oxophytodienoate reductase, putative, expressed	1.583249626
LOC_Os01g27340	Glutathione S-transferase, putative, expressed	2.062712986
LOC_Os01g38510	Protein transport protein Sec61 subunit beta, putative	0.736886469
LOC_Os01g42400	STE_MEK_ste7_MAP2K.3 - STE kinases	2.427613837
LOC_Os01g47550	Kinase, pfkB family, putative, expressed	0.545637085
LOC_Os01g53460	Anthocyanidin 5,3-O-glucosyltransferase, putative, expressed	0.70555624
LOC_Os01g59140	DNA-directed RNA polymerases I, II, and III subunit RPABC1	0.449926919
LOC_Os01g66360	2-C-methyl-D-erythritol 4-phosphate cytidylyltransferase	0.84382116
LOC_Os01g69190	Regulatory protein, putative, expressed	1.224440768
LOC_Os02g01280	T-complex protein, putative, expressed	
LOC_Os02g01920	GHMP kinases ATP-binding protein, putative, expressed	0.719880585
LOC_Os02g13965	Lectin protein kinase family protein, putative, expressed	0.890037843
LOC_Os02g33060	Expressed protein	1.210709683
LOC_Os03g04650	Cytochrome P450 protein, putative, expressed	1.067572796
LOC_Os03g05620	Inorganic phosphate transporter, putative, expressed	1.338210488
LOC_Os03g06670	Core histone H2A/H2B/H3/H4 domain containing protein	1.207167782
LOC_Os03g35720	Retrotransposon protein, putative, Ty3-gypsy subclass	1.883100407
LOC_Os03g36650	Cysteine-rich repeat secretory protein 55 precursor, putative	2.265163096
LOC_Os03g44300	Transketolase, putative, expressed	0.33253876
LOC_Os03g55400	Expressed protein	2.090427381
LOC_Os03g56590	Expressed protein	0.862511338
LOC_Os03g58260	Indole-3-glycerol phosphate lyase, chloroplast precursor, putative	0.489358572
LOC_Os04g08350	Cysteine synthase, chloroplast/chromoplast precursor, putative	0.992588415
LOC_Os04g31700	Methylisocitrate lyase 2, putative, expressed	0.493594106
LOC_Os04g31790	Expressed protein	1.747254817
LOC_Os04g39460	NBS-LRR type disease resistance protein, putative, expressed	
LOC_Os04g47310	Expressed protein	0.806785726
LOC_Os04g52770	Helix-loop-helix DNA-binding domain containing protein	0.899864824
LOC_Os05g20900	Retrotransposon protein, putative, unclassified	2.88720326
LOC_Os05g41180	Peptidase, T1 family, putative, expressed	0.616780586
LOC_Os06g02144	6-phosphogluconate dehydrogenase, decarboxylating, putative	0.617897111

Table 2.9. (Continued)

Model	Putative Function	IL_D/SWA_D Log_2FC
LOC_Os06g06820	Hydrolase, alpha/beta fold family domain containing protein	0.430201034
LOC_Os06g28880	Retrotransposon protein, putative, unclassified, expressed	1.646736984
LOC_Os06g36880	Cysteine synthase, putative, expressed	1.445584055
LOC_Os06g39344	enoyl-CoA hydratase/isomerase family protein, putative	0.481583948
LOC_Os06g50300	Heat shock protein, putative, expressed	0.746315365
LOC_Os06g51410	OsPOP15 - Putative Prolyl Oligopeptidase homologue, expressed	0.725566644
LOC_Os07g22770	AP2 domain containing protein, expressed	1.9068753
LOC_Os07g28850	Retrotransposon protein, putative, unclassified, expressed	1.285184511
LOC_Os07g31430	Phosphate-induced protein 1 conserved region domain	1.273964698
LOC_Os07g35330	TKL_IRAK_DUF26-lc.13 - DUF26 kinases	2.285879599
LOC_Os07g47040	Expressed protein	0.654947055
LOC_Os08g05830	Transaldolase, putative, expressed	0.571072657
LOC_Os08g15130	Retrotransposon, putative, centromere-specific	2.43138404
LOC_Os09g26730	Chaperonin, putative, expressed	0.724137214
LOC_Os09g26980	Cytochrome P450, putative, expressed	2.244730478
LOC_Os09g27830	OsPDIL2-3 protein disulfide isomerase PDIL2-3, expressed	0.880916849
LOC_Os09g29480	2-aminoethanethiol dioxygenase, putative, expressed	4.153995123
LOC_Os09g31466	Expressed protein	0.954531605
LOC_Os09g34190	Acyl-coenzyme A thioesterase 10, mitochondrial precursor	0.977573732
LOC_Os09g34920	Glycosyl hydrolase family 29, putative, expressed	1.273853791
LOC_Os10g05220	Queuine tRNA-ribosyltransferase, putative, expressed	0.503672862
LOC_Os10g20350	MATE efflux family protein, putative, expressed	1.627710347
LOC_Os10g26690	Structural constituent of ribosome, putative, expressed	0.885931741
LOC_Os10g28200	NAD dependent epimerase/dehydratase family protein, putative	0.677068599
LOC_Os11g17504	Retrotransposon protein, putative, Ty1-copia subclass, expressed	1.516654207
LOC_Os11g18170	Glutathione peroxidase, putative, expressed	0.842925634
LOC_Os11g30560	Dehydrogenase/reductase, putative, expressed	1.402416343
LOC_Os11g34850	Maf, putative, expressed	0.846168026
LOC_Os11g35210	NB-ARC domain containing protein	1.881633718
LOC_Os11g37270	AMBP1 - Antimicrobial peptide MBP-1 family protein precursor	2.065293268
LOC_Os11g42030	Expressed protein	1.330195836
LOC_Os12g03260	MATE efflux family protein, putative, expressed	0.8671577
LOC_Os12g07820	OsAPx6 - Stromal Ascorbate Peroxidase encoding gene 5,8,	0.302648226
LOC_Os12g37160	Expressed protein	1.089483723
LOC_Os12g42980	Cysteine synthase, putative, expressed	0.630954545
LOC_Os12g43750	Expressed protein	0.902324122

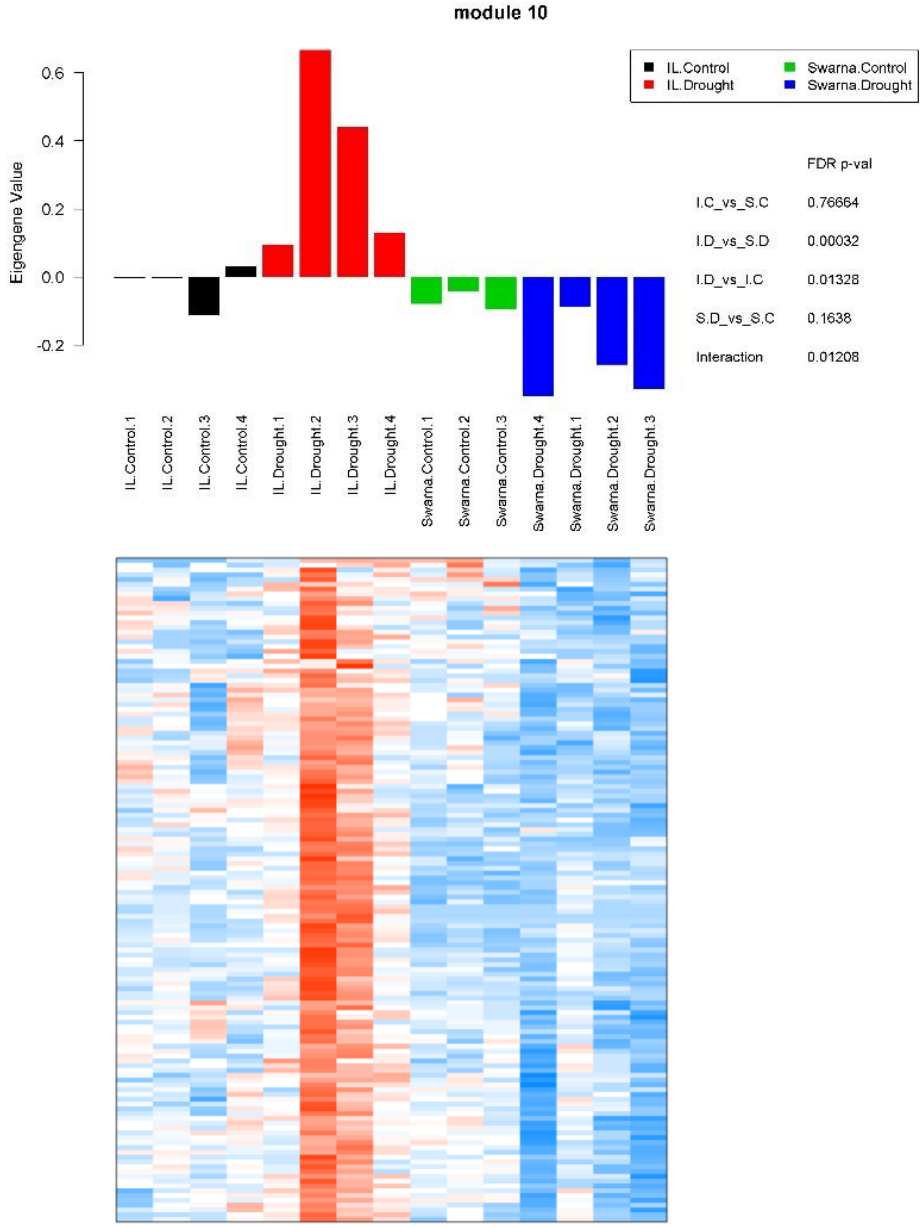

Figure 2.9. Gene co-expression network analysis in panicle under RDS. Bar plots of the module eigengene as representatives of gene expression profiles across samples in M10. The X-axis represents 15 different samples across four different groups, while Y-axis corresponds to the Eigengene Value. Heatmaps showing gene expression levels of genes in M10. Columns represent samples, while rows correspond to genes in the module. Red indicates positive and blue negative expression profile. S.C = Swarna control, S.D = Swarna under RDS, IL.C = DTY-IL control, IL.D = DTY-IL under RDS.

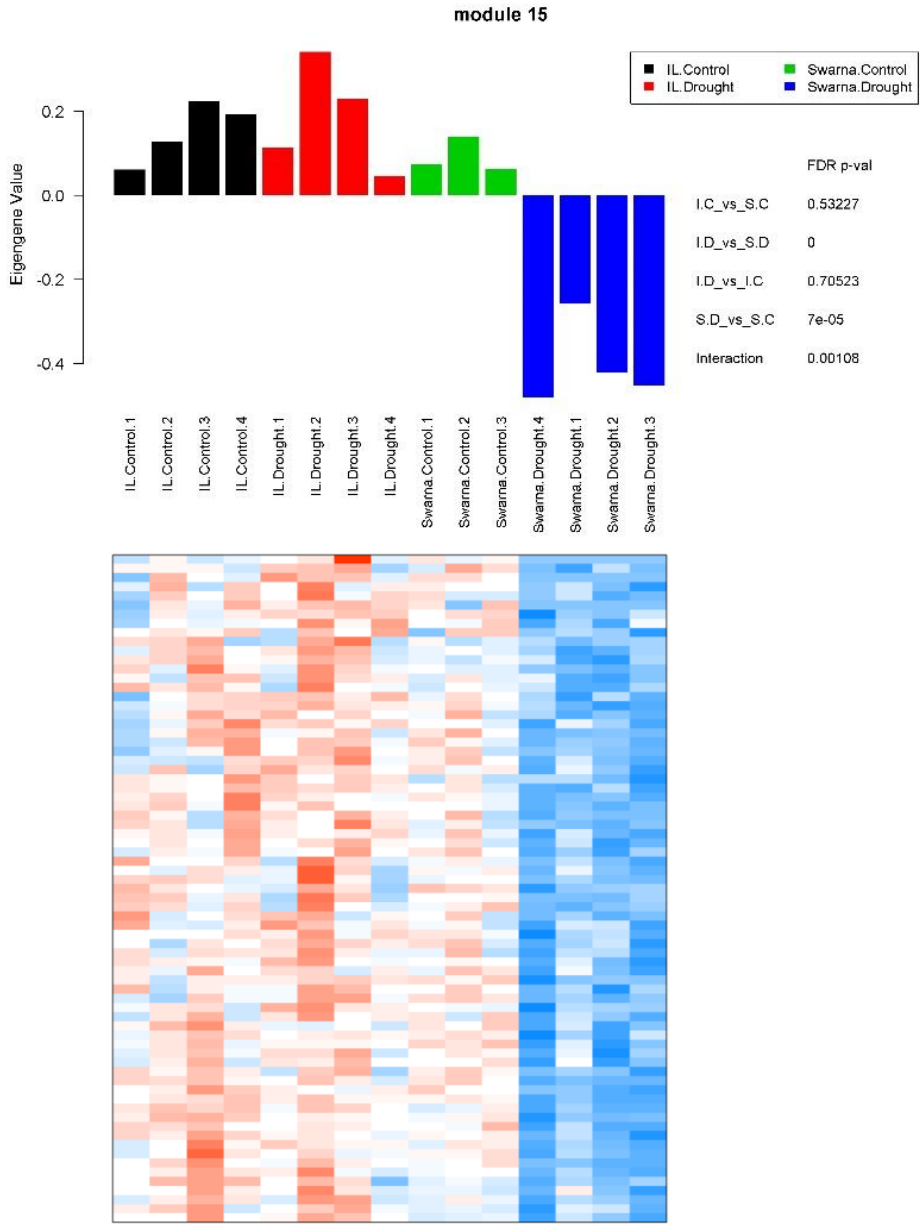

Figure 2.10. Gene co-expression network analysis in panicle under RDS. Bar plots of the module eigengene as representatives of gene expression profiles across samples in M15. The X-axis represents 15 different samples across four different groups, while Y-axis corresponds to the Eigengene Value. Heatmaps showing gene expression levels of genes in M15. Columns represent samples, while rows correspond to genes in the module. Red indicates positive and blue negative expression profile. S.C = Swarna control, S.D = Swarna under RDS, IL.C = DTY-IL control, IL.D = DTY-IL under RDS.

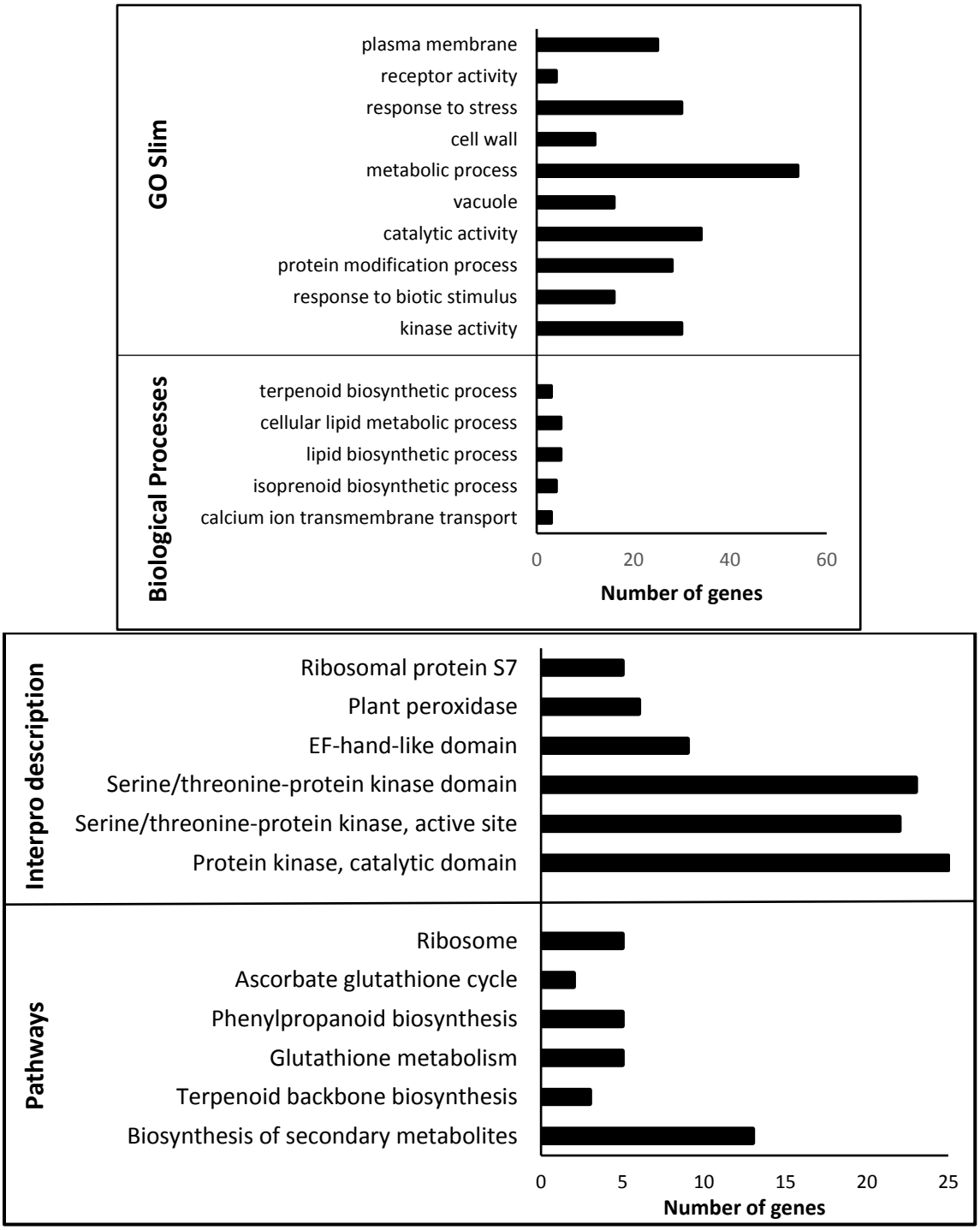

Figure 2.11. Enrichment analysis of the functional categories in M10. Major BP, Over-represented GO Slim description, Interpro domains, and enriched pathways in M14in flag-leaf under RDS. Top significant BP, GO Slim, Pathways, and Interpro domains are shown in Y-axis with the number of represented genes on the X-axis.

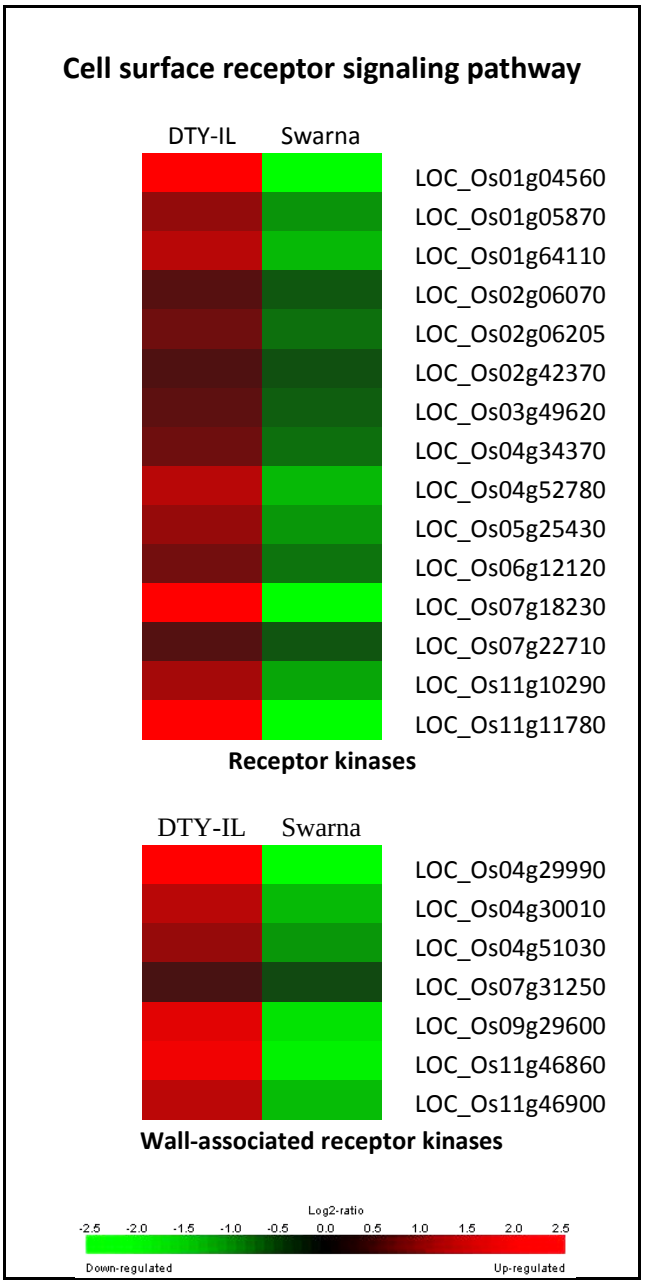

Figure 2.12. Sensing cell-wall perturbations during drought stress in the panicle tissue. The cell surface receptor signaling pathway enriched in the drought-responsive M10 between DTY-IL and Swarna under the reproductive-stage drought stress are shown in heat-maps representing their expression profile. The scale represents a $\log_2$ fold change in expression.

Table 2.10. Identified hub genes in M10 in the panicle tissue between the DTY-IL and Swarna under RDS.

ID	module	kME	negLogPValue	Annotation	IL_D/SWA_D Log_2FC
LOC_Os04g22120	10	0.917668722	5.257652371	protein kinase; putative; expressed	2.996413632
LOC_Os01g73170	10	0.93181306	5.343441498	peroxidase precursor; putative; expressed	1.262839087
LOC_Os01g72870	10	0.934970547	5.884580202	BAS1; putative; expressed	0.713299651
LOC_Os06g19370	10	0.922868491	6.185733491	cadmium tolerance factor; putative; expressed	1.441819399
LOC_Os06g46340	10	0.957089142	6.275271295	glycosyl hydrolase; family 31; putative; expressed	2.359467997
LOC_Os11g34624	10	0.905535015	6.714955934	TKL_IRAK_DUF26-lc_29 - DUF26 kinases have homology to DUF26 containing loci; expressed	4.509944153
LOC_Os04g27540	10	0.902044043	6.782197352	terpene synthase; putative; expressed	4.29137385
LOC_Os02g12070	10	0.915031834	6.892907946	expressed protein	2.307469349
LOC_Os03g05920	10	0.975870326	7.722306559	expressed protein	1.744785713
LOC_Os04g01240	10	0.904204941	8.077463459	serine-type peptidase; putative; expressed	0.7202702
LOC_Os07g48020	10	0.927220412	12.19954665	peroxidase precursor; putative; expressed	5.555394
LOC_Os09g29600	10	0.922209404	12.34628081	OsWAK85 - OsWAK receptor-like cytoplasmic kinase OsWAK-RLCK; expressed	2.195489

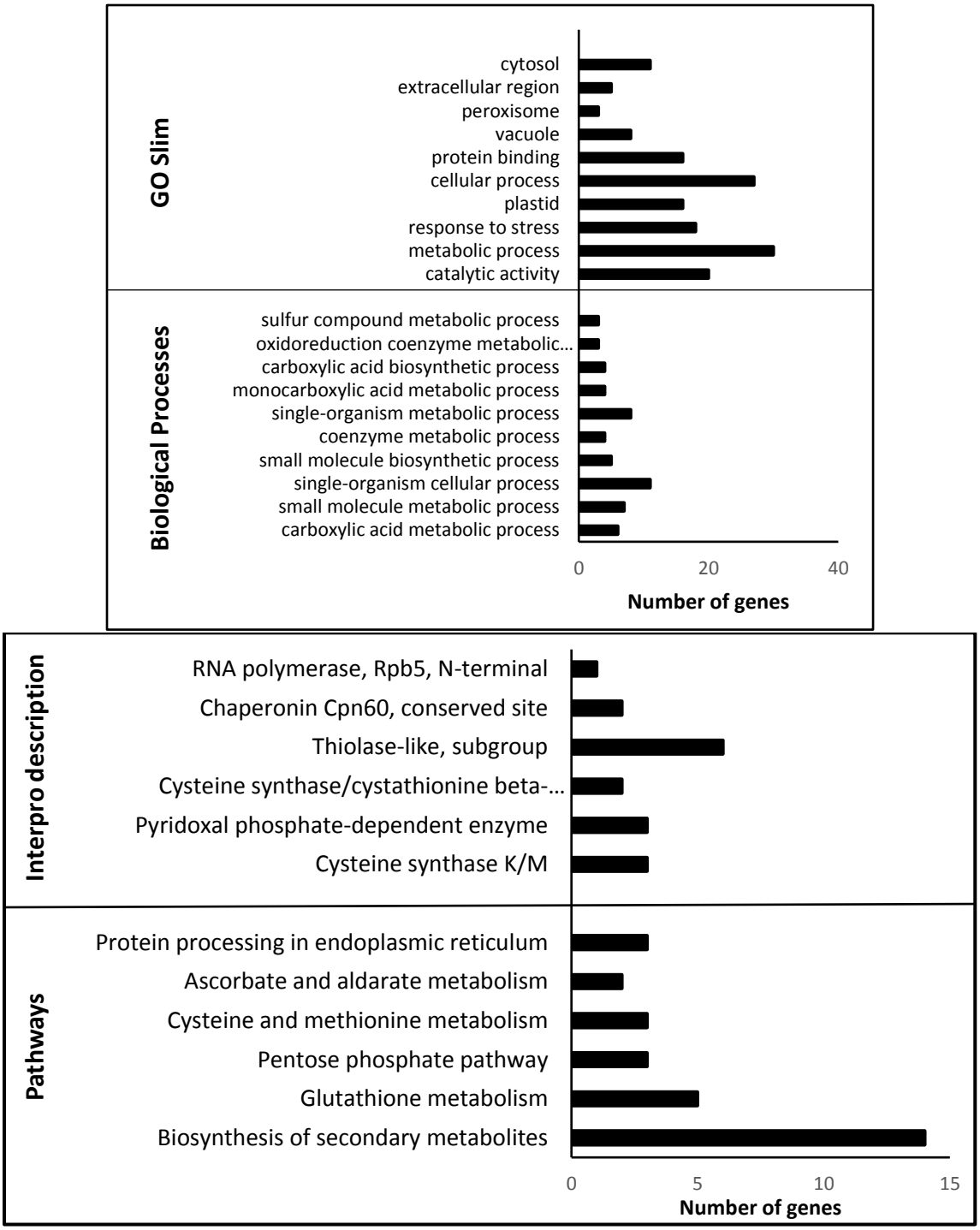

Figure 2.13. Enrichment analysis of the functional categories in M15. Major BP, Over-represented GO Slim description, Interpro domains, and enriched pathways in M14in flag-leaf under RDS. Top significant BP, GO Slim, Pathways, and Interpro domains are shown in Y-axis with the number of represented genes on the X-axis.

Table 2.11. Identified hub genes in M15 in the panicle tissue between the DTY-IL and Swarna under RDS.

ID	module	kME	negLogPValue	Annotation	IL_D/SWA_D Log_2FC
LOC_Os03g36650	15	0.942684871	5.191226228	cysteine-rich repeat secretory protein 55 precursor; putative; expressed	2.265163096
LOC_Os08g05830	15	0.929504956	5.348932747	transaldolase; putative; expressed	0.571072657
LOC_Os03g05620	15	0.909565724	5.808987251	inorganic phosphate transporter; putative; expressed	1.338210488
LOC_Os11g30560	15	0.920104197	6.523438827	dehydrogenase/reductase; putative; expressed	1.4024163
LOC_Os07g28850	15	0.910551435	6.750263383	retrotransposon protein; putative; unclassified; expressed	1.285184511
LOC_Os09g34920	15	0.901524723	8.666228705	glycosyl hydrolase family 29; putative; expressed	1.2738538
LOC_Os09g34190	15	0.918579447	9.71069502	acyl-coenzyme A thioesterase 10; mitochondrial precursor; putative; expressed	0.9775737
LOC_Os06g28880	15	0.95091667	11.48249859	retrotransposon protein; putative; unclassified; expressed	1.646737
LOC_Os11g17504	15	0.977689528	19.72362551	retrotransposon protein; putative; Ty1-copia subclass; expressed	1.5166542

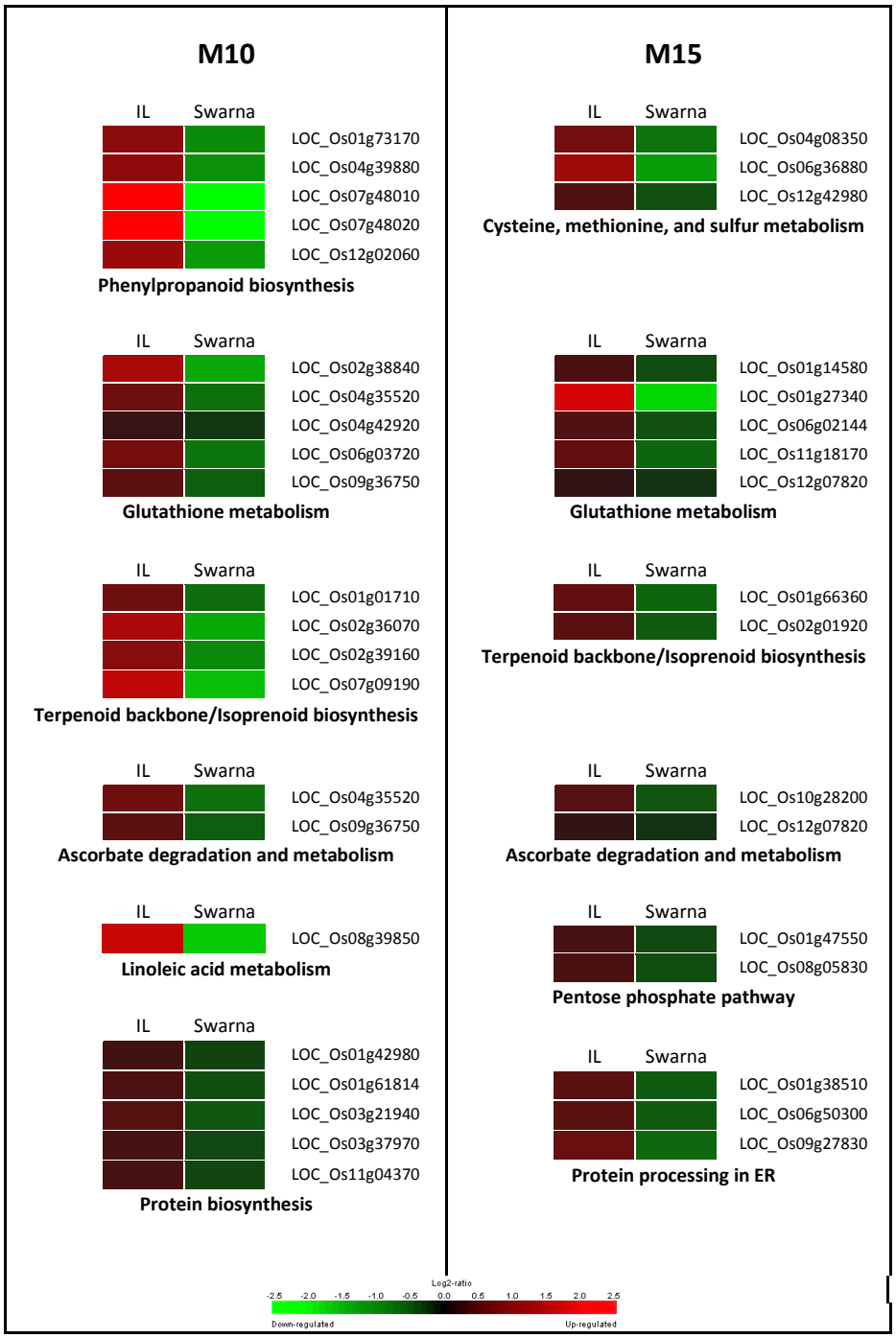

Figure 2.14. Regulation of metabolic pathways during RDS in the panicle. The metabolic pathways enriched in the drought-responsive modules between DTY-IL and Swarna under RDS are shown in heat-maps representing their expression profile. The scale represents a $\log_2$-fold change in expression. IL = DTY-IL.

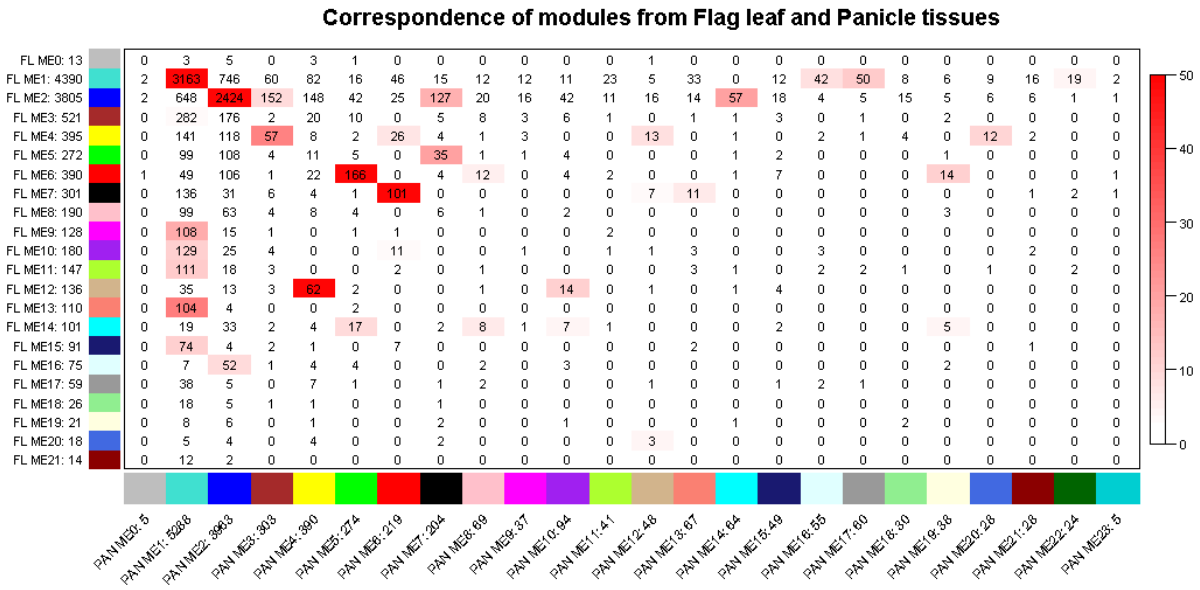

Figure 2.15. The tissue-specific expression under RDS. Consensus network matrix for the flag-leaf and panicle networks. The X-axis represents all the panicle modules, and the Y-axis represents all the flag-leaf modules. Numbers beside the module number are the total gene counts for that module. Numbers inside the matrix are the number of genes common between the flag-leaf and panicle modules. Red numbers have significant overlap in gene count based on Fisher's exact test with the –log(p) of the p-value encoding the coloring (0 = -log(1) and 50 = -log(1E-50)).

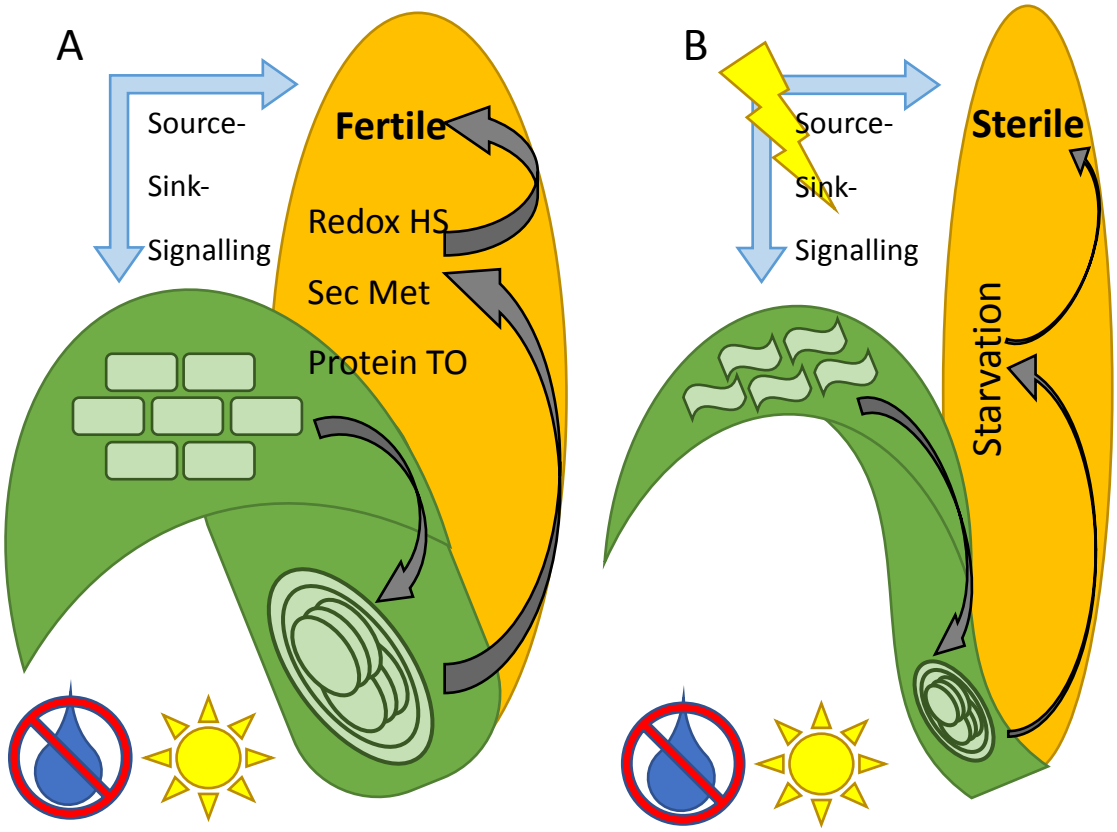

Figure 2.16. Model of suggested DTY-IL dependent drought tolerance mechanism. (A) In DTY-IL, flag leaves (green), maintained, and drought-adapted cell wall homeostasis (solid green bricks) under drought (no water and sun icons) supports sustained photosynthetic activity (large green chloroplast icon). This, in turn, allows for strong source strength and the allocation of energy and carbon in the form of photo-assimilates to emerging panicles. A strong sink is established, and energy and carbon available for Redox-homeostasis (Redox HS), protective secondary metabolism (Sec Met), and high rates of protein turnover (Protein TO) enable the emerging panicle to cope with drought stress and remain fertile, ultimately leading to successful grain filling and drought-tolerant yield (DTY). This is proposed to be in part accomplished through efficient source-sink signaling (blue arrow) suggested being modulated through the identified candidate genes. (B) In Swarna flag leaves (green), failure to maintain cell wall integrity (wavy green bricks) under drought results in leaf rolling and impaired photosynthetic activity (small chloroplast icon). This, in turn, negatively affects source strength and severely limits the allocation of energy and carbon in the form of photo-assimilates to emerging panicles. Consequently, the emerging panicle is in starvation mode and fails to establish a strong sink. There is insufficient carbon energy available to counter drought stress successfully, and the results are sterility and failure to fill grain and yield under drought. This is proposed to be in part due to failure to modulate source-sink signaling in response to drought stress (yellow lightning across blue arrow) and unfavorable alleles on the identified candidate genes suggested to contribute.

REFERENCES

Ahn, H., Jung, I., Shin, S., Park, J., Rhee, S., Kim, J., and Kim, S. 2017. Transcriptional Network Analysis Reveals Drought Resistance Mechanisms of AP2/ERF Transgenic Rice. *Frontiers in Plant Science,8*. doi:10.3389/fpls.2017.01044

Almagro, L., Ros, L. V., Belchi-Navarro, S., Bru, R., Barceló, A. R., and Pedreño, M. A. 2008. Class III peroxidases in plant defence reactions. *Journal of Experimental Botany,60*(2), 377-390. doi:10.1093/jxb/ern277

Bassel, G. W., Lan, H., Glaab, E., Gibbs, D. J., Gerjets, T., Krasnogor, N., and Provart, N. J. 2011. Genome-wide network model capturing seed germination reveals coordinated regulation of plant cellular phase transitions. *Proceedings of the National Academy of Sciences,108*(23), 9709-9714. doi:10.1073/pnas.1100958108

Basu, S., Ramegowda, V., Kumar, A., and Pereira, A. 2016. Plant adaptation to drought stress. *F1000Research, 5*, 1554. doi:10.12688/f1000research.7678.1

Belkhadir, Y.; Chory, J. 2006. Brassinosteroid Signaling: A Paradigm for Steroid Hormone Signaling from the Cell Surface. *Science, 314*, 1410–1411.

Bhaskara, G. B., Nguyen, T. T., and Verslues, P. E. 2012. Unique Drought Resistance Functions of the Highly ABA-Induced Clade A Protein Phosphatase 2Cs. *Plant Physiology,160*(1), 379-395. doi:10.1104/pp.112.202408

Biswal, A.K. and Kohli, A. 2013. Cereal flag leaf adaptations for grain yield under drought: Knowledge status and gaps. *Mol. Breed.*, *31*, 749–766.

Cal, A.; Sanciangco, M.; Rebolledo, M.B.; Luquet, D.; Torres, R.; McnNaly, K. and Henry, A. 2019. Leaf morphology, rather than plant water status, underlies, genetic variation of rice leaf rolling under drought. *Plant Cell Environ. 42*, 1532–1544.

Chen, Z., Chen, X., Yan, H., Li, W., Li, Y., Cai, R., and Xiang, Y. 2015. The Lipoxygenase Gene Family in Poplar: Identification, Classification, and Expression in Response to MeJA Treatment. *Plos One,10*(4). doi:10.1371/journal.pone.0125526

Clouse, S.D. 2011. Brassinosteroid Signal Transduction: From Receptor Kinase Activation to Transcriptional Networks Regulating Plant Development. *Plant Cell*, *23*, 1219–1230.

Cosgrove, D. J. 2005. Growth of the plant cell wall. *Nature Reviews Molecular Cell Biology,6*(11), 850-861. doi:10.1038/nrm1746

Cramer, G. R., Van Sluyter, S. C., Hopper, D. W., Pascovici, D., Keighley, T., and Haynes, P. A. 2013. Proteomic analysis indicates massive changes in metabolism prior to the inhibition of growth and photosynthesis of grapevine (Vitis vinifera L.) in response to water deficit. BMC Plant Biol. 13:49. doi: 10.1186/1471-2229-13-49

Cvrčková, F. 2012. Formins: Emerging Players in the Dynamic Plant Cell Cortex. *Scientifica,2012*, 1-14. doi:10.6064/2012/712605

Dai, F., Zhang, C., Jiang, X., Kang, M., Yin, X., Lu, P., and Gao, J. 2012. RhNAC2 and RhEXPA4 Are Involved in the Regulation of Dehydration Tolerance during the Expansion of Rose Petals. *Plant Physiology,160*(4), 2064-2082. doi:10.1104/pp.112.207720

dela Fuente, A. 2010. From 'differential expression' to 'differential networking' – identification of dysfunctional regulatory networks in diseases. *Trends in Genetics,26*(7), 326-333. doi:10.1016/j.tig.2010.05.001

Dixit, S.; Biswal, A.K.; Min, A.; Henry, A.; Oane, R.H.; Raorane, M.L.; Longkumer, T.; Pabuayon, I.M.; Mutte, S.K.; Vardarajan, A.R.; and Kohli, A. 2015. Action of multiple intra-QTL genes concerted around a co-localized transcription factor underpins a large effect QTL. *Sci. Rep. 5*, 15183.

Dong, X., Hao, Y., Wang, X., and Tian, W. 2016. LEGO: A novel method for gene set over-representation analysis by incorporating network-based gene weights. *Scientific Reports,6*(1). doi:10.1038/srep18871

Elhiti, M., and Stasolla, C. 2009. Structure and function of homodomain-leucine zipper (HD-Zip) proteins. *Plant Signaling & Behavior, 4*(2), 86-88. doi:10.4161/psb.4.2.7692

Farooq, M., Wahid, A., Kobayashi, N., Fujita, D., and Basra, S. M. 2009. Plant Drought Stress: Effects, Mechanisms and Management. *Sustainable Agriculture,*153-188. doi:10.1007/978-90-481-2666-8_12

Formey, D., Sallet, E., Lelandais-Brière, C., Ben, C., Bustos-Sanmamed, P., Niebel, A., and Crespi, M. 2014. The small RNA diversity from Medicago truncatula roots under biotic interactions evidences the environmental plasticity of the miRNAome. *Genome Biology,15*(9), 457. doi:10.1186/preaccept-1413382507120111

Gehan, M. A., Greenham, K., Mockler, T. C., and Mcclung, C. R. 2015. Transcriptional networks — crops, clocks, and abiotic stress. *Current Opinion in Plant Biology,24*, 39-46. doi:10.1016/j.pbi.2015.01.004

Gitter, A., Carmi, M., Barkai, N., and Bar-Joseph, Z. 2012. Linking the signaling cascades and dynamic regulatory networks controlling stress responses. *Genome Research,23*(2), 365-376. doi:10.1101/gr.138628.112

Gosti, F. 1999. ABI1 Protein Phosphatase 2C Is a Negative Regulator of Abscisic Acid Signaling. *The Plant Cell Online,11*(10), 1897-1910. doi:10.1105/tpc.11.10.1897

Guo, W., Zhao, J., Li, X., Qin, L., Yan, X., and Liao, H. 2011. A soybean β-expansin gene GmEXPB2 intrinsically involved in root system architecture responses to abiotic stresses. *The Plant Journal,66*(3), 541-552. doi:10.1111/j.1365-313x.2011.04511.x

Guo, C.; Yao, L.; You, C.; Wang, S.; Cui, J.; Ge, X. and Ma, H. 2016. MID1 plays an important role in response to drought stress during reproductive development. *Plant J. 88*, 280–293.

Hadiarto, T., and Tran, L. P. 2010. Progress studies of drought-responsive genes in rice. *Plant Cell Reports,30*(3), 297-310. doi:10.1007/s00299-010-0956-z

Harb, A., Krishnan, A., Ambavaram, M. M., and Pereira, A. 2010. Molecular and Physiological Analysis of Drought Stress in Arabidopsis Reveals Early Responses Leading to Acclimation in Plant Growth. *Plant Physiology,154*(3), 1254-1271. doi:10.1104/pp.110.161752

Hirota, O., Oka, M., and Takeda, T. 1990. Sink Activity Estimation by Sink Size and Dry Matter Increase During the Ripening Stage of Barley (Hordeum vulgare) and Rice (Oryza sativa). *Annals of Botany*, *65*(4), 349–353. doi: 10.1093/oxfordjournals.aob.a087944

Horvath, S., and Dong, J. 2008. Geometric Interpretation of Gene Coexpression Network Analysis. *PLoS Computational Biology*, *4*(8). doi:10.1371/journal.pcbi.1000117

Huang DQ, Wu WR, Abrams SR, and Cutler AJ. 2008. The relationship of drought-related gene expression in *Arabidopsis thaliana* to hormonal and environmental factors. *Journal of Experimental Botany* **59**: 2991–3007.

Islam, T., Manna, M., and Reddy, M. K. 2015. Glutathione Peroxidase of Pennisetum glaucum (PgGPx) Is a Functional Cd2 Dependent Peroxiredoxin that Enhances Tolerance against Salinity and Drought Stress. *Plos One,10*(11). doi:10.1371/journal.pone.0143344

Jones, L., and Mcqueen-Mason, S. 2004. A role for expansins in dehydration and rehydration of the resurrection plantCraterostigma plantagineum. *FEBS Letters,559*(1-3), 61-65. doi:10.1016/s0014-5793(04)00023-7

Kong, X., Zhou, S., Yin, S., Zhao, Z., Han, Y., and Wang, W. 2016. Stress-Inducible Expression of an F-box Gene TaFBA1 from Wheat Enhanced the Drought Tolerance in Transgenic Tobacco Plants without Impacting Growth and Development. *Frontiers in Plant Science,7*. doi:10.3389/fpls.2016.01295

Kunieda, T., Shimada, T., Kondo, M., Nishimura, M., Nishitani, K., and Hara-Nishimura, I. 2013. Spatiotemporal Secretion of PEROXIDASE36 Is Required for Seed Coat Mucilage Extrusion in Arabidopsis. *The Plant Cell,25*(4), 1355-1367. doi:10.1105/tpc.113.110072

Krishnan, A., Gupta, C., Ambavaram, M. M. R., and Pereira, A. 2017. RECoN: Rice Environment Coexpression Network for Systems Level Analysis of Abiotic-Stress Response. *Frontiers in Plant Science, 8*. doi: 10.3389/fpls.2017.01640

Langfelder, P., and Horvath, S. 2008. WGCNA: An R package for weighted correlation network analysis. *BMC Bioinformatics,9*(1), 559. doi:10.1186/1471-2105-9-559

Langfelder, P., Luo, R., Oldham, M. C., and Horvath, S. 2011. Is My Network Module Preserved and Reproducible? *PLoS Computational Biology,7*(1). doi:10.1371/journal.pcbi.1001057

Langfelder, P., Mischel, P. S., and Horvath, S. 2013. When Is Hub Gene Selection Better than Standard Meta-Analysis? *PLoS ONE, 8*(4). doi:10.1371/journal.pone.0061505

Lawlor, D.W. and Paul, M.J. 2014. Source/sink interactions underpin crop yield: The case for trehalose 6-phosphate/SnRK1 in improvement of wheat. *Front. Plant Sci. 5*, 418.

Li, F., Han, Y., Feng, Y., Xing, S., Zhao, M., Chen, Y., and Wang, W. 2013. Expression of wheat expansin driven by the RD29 promoter in tobacco confers water-stress tolerance without impacting growth and development. *Journal of Biotechnology,163*(3), 281-291. doi:10.1016/j.jbiotec.2012.11.008

Liseron-Monfils, C., and Ware, D. 2015. Revealing gene regulation and associations through biological networks. *Current Plant Biology,3-4*, 30-39. doi:10.1016/j.cpb.2015.11.001

Liszkay, A., Kenk, B., and Schopfer, P. 2003. Evidence for the involvement of cell wall peroxidase in the generation of hydroxyl radicals mediating extension growth. *Planta,217*(4), 658-667. doi:10.1007/s00425-003-1028-1

Love, M. I., Huber, W., and Anders, S. 2014. Moderated estimation of fold change and dispersion for RNA-seq data with DESeq2. *Genome Biology*, *15*(12). doi:10.1186/s13059-014-0550-8

Ma, C., Xin, M., Feldmann, K. A., and Wang, X. 2014. Machine Learning-Based Differential Network Analysis: A Study of Stress-Responsive Transcriptomes in Arabidopsis. *The Plant Cell*, *26*(2), 520-537. doi:10.1105/tpc.113.121913

Mandava, N.B. 1998. Plant Growth-Promoting Brassinosteroids. *Annu. Rev. Plant Physiol. Plant Mol. Biol*, *39*, 23–52.

Masand, S., and Yadav, S. K. 2016. Overexpression of MuHSP70 gene from Macrotyloma uniflorum confers multiple abiotic stress tolerance in transgenic Arabidopsis thaliana. *Molecular Biology Reports,43*(2), 53-64. doi:10.1007/s11033-015-3938-y

Massa, A. N., Childs, K. L., and Buell, C. R. 2013. Abiotic and Biotic Stress Responses in Group Phureja DM1-3 516 R44 as Measured through Whole Transcriptome Sequencing. *The Plant Genome,6*(3), 0. doi:10.3835/plantgenome2013.05.0014

Meyer, R. F., and Boyer, J. S. 1972. Sensitivity of cell division and cell elongation to low water potentials in soybean hypocotyls. *Planta,108*(1), 77-87. doi:10.1007/bf00386508

Miazek, A., and Zagdańska, B. 2008. Involvement of exopeptidases in dehydration tolerance of spring wheat seedlings. *Biologia Plantarum,52*(4), 687-694. doi:10.1007/s10535-008-0133-1

Miller, G., Suzuki, N., Ciftci-Yilmaz, S., and Mittler, R. 2010. Reactive oxygen species homeostasis and signalling during drought and salinity stresses. *Plant, Cell & Environment,33*(4), 453-467. doi:10.1111/j.1365-3040.2009.02041.x

Moore, J. P., Vicré-Gibouin, M., Farrant, J. M., and Driouich, A. 2008. Adaptations of higher plant cell walls to water loss: Drought vs desiccation. *Physiologia Plantarum,134*(2), 237-245. doi:10.1111/j.1399-3054.2008.01134.x

Müller, K., Linkies, A., Vreeburg, R. A., Fry, S. C., Krieger-Liszkay, A., and Leubner-Metzger, G. 2009. In Vivo Cell Wall Loosening by Hydroxyl Radicals during Cress Seed Germination and Elongation Growth. *Plant Physiology,150*(4), 1855-1865. doi:10.1104/pp.109.139204

Nakabayashi, R.; Yonekura-Sakakibara, K.; Urano, K.; Suzuki, M.; Yamada, Y.; Nishizawa, T.; Matsuda, F.; Kojima; F; Sakakibara; H, and Shinozaki, K. 2014. Enhancement of oxidative and drought tolerance in Arabidopsis by overaccumulation of antioxidant flavonoids. *Plant J. 77*, 367–379.

Neff, M.M.; Nguyen, S.M.; Malancharuvil, E.J.; Fujioka, S.; Noguchi, T.; Seto, H.; Tsukubi, M.; Takatsuto, S.; Yoshida, S.; Chory, J. 1999. BAS1: A gene regulating brassinosteroid levels and light responsiveness in Arabidopsis. *Proc. Natl. Acad. Sci. USA, 96*, 15316–15323.

Noctor, G., Mhamdi, A., and Foyer, C. H. 2014. The Roles of Reactive Oxygen Metabolism in Drought: Not So Cut and Dried. *Plant Physiology, 164*(4), 1636–1648. doi: 10.1104/pp.113.233478

Novaković, L., Guo, T., Bacic, A., Sampathkumar, A., and Johnson, K. 2018. Hitting the Wall—Sensing and Signaling Pathways Involved in Plant Cell Wall Remodeling in Response to Abiotic Stress. *Plants,7*(4), 89. doi:10.3390/plants7040089

Osakabe, Y., Osakabe, K., Shinozaki, K., and Tran, L. P. 2014. Response of plants to water stress. *Frontiers in Plant Science,5*. doi:10.3389/fpls.2014.00086

Passardi, F., Penel, C., and Dunand, C. 2004. Performing the paradoxical: How plant peroxidases modify the cell wall. *Trends in Plant Science,9*(11), 534-540. doi:10.1016/j.tplants.2004.09.002

Patro, L., Mohapatra, P. K., Biswal, U. C., and Biswal, B. 2014. Dehydration induced loss of photosynthesis in Arabidopsis leaves during senescence is accompanied by the reversible enhancement in the activity of cell wall β-glucosidase. *Journal of Photochemistry and Photobiology B: Biology,137,* 49-54. doi:10.1016/j.jphotobiol.2014.03.018

Porta, H., Rueda-Benitez, P., Campos, F., Colmenero-Flores, J. M., Colorado, J. M., Carmona, M. J., and Rocha-Sosa, M. 1999. Analysis of Lipoxygenase mRNA Accumulation in the Common Bean (Phaseolus vulgaris L.) during Development and under Stress Conditions. *Plant and Cell Physiology,40*(8), 850-858. doi:10.1093/oxfordjournals.pcp.a029614

Porta, H. 2002. Plant Lipoxygenases. Physiological and Molecular Features. *Plant Physiology,130*(1), 15-21. doi:10.1104/pp.010787

Raorane, M. L., Pabuayon, I. M., Varadarajan, A. R., Mutte, S. K., Kumar, A., Treumann, A., and Kohli, A. 2015. Proteomic insights into the role of the large-effect QTL qDTY 12.1 for rice yield under drought. *Molecular Breeding,35*(6). doi:10.1007/s11032-015-0321-6

Rhee, S. Y., Wood, V., Dolinski, K., and Draghici, S. 2008. Use and misuse of the gene ontology annotations. *Nature Reviews Genetics,9*(7), 509-515. doi:10.1038/nrg2363

Segal, E., Shapira, M., Regev, A., Peer, D., Botstein, D., Koller, D., and Friedman, N. 2003. Module networks: Identifying regulatory modules and their condition-specific regulators from gene expression data. *Nature Genetics,34*(2), 166-176. doi:10.1038/ng1165

Serin, E. A., Nijveen, H., Hilhorst, H. W., and Ligterink, W. 2016. Learning from Co-expression Networks: Possibilities and Challenges. *Frontiers in Plant Science,7*. doi:10.3389/fpls.2016.00444

Shaik, R., and Ramakrishna, W. 2013. Genes and Co-Expression Modules Common to Drought and Bacterial Stress Responses in Arabidopsis and Rice. *PLoS ONE, 8*(10). doi:10.1371/journal.pone.0077261

Shigeto, J., and Tsutsumi, Y. 2016. Diverse functions and reactions of class III peroxidases. *New Phytologist,209*(4), 1395-1402. doi:10.1111/nph.13738

Shojaie, A., and Michailidis, G. 2009. Analysis of Gene Sets Based on the Underlying Regulatory Network. *Journal of Computational Biology,16*(3), 407-426. doi:10.1089/cmb.2008.0081

Sircar, S., and Parekh, N. 2015. Functional characterization of drought-responsive modules and genes in Oryza sativa: A network-based approach. *Frontiers in Genetics, 6*. doi:10.3389/fgene.2015.00256

Skirycz, A., and Inzé, D. 2010. More from less: Plant growth under limited water. *Current Opinion in Biotechnology,21*(2), 197-203. doi:10.1016/j.copbio.2010.03.002

Skirycz, A., Bodt, S. D., Obata, T., Clercq, I. D., Claeys, H., Rycke, R. D., and Inze, D. 2010. Developmental Stage Specificity and the Role of Mitochondrial Metabolism in the Response of Arabidopsis Leaves to Prolonged Mild Osmotic Stress. *Plant Physiology,152*(1), 226-244. doi:10.1104/pp.109.148965

Śniegowska-Świerk, K., Dubas, E., and Rapacz, M. 2015. Drought-induced changes in the actin cytoskeleton of barley (Hordeum vulgare L.) leaves. *Acta Physiologiae Plantarum,37*(4). doi:10.1007/s11738-015-1820-0

Su, Z., Ma, X., Guo, H., Sukiran, N. L., Guo, B., Assmann, S. M., and Ma, H. 2013. Flower Development under Drought Stress: Morphological and Transcriptomic Analyses Reveal Acute Responses and Long-Term Acclimation in Arabidopsis. *The Plant Cell,25*(10), 3785-3807. doi:10.1105/tpc.113.115428

Szklarczyk, D.; Morris, J.H.; Cook, H.; Kuhn; M; Wyder, S.; Simonovic, M.; Santos, A.; Doncheva, N.T.; Roth, A. and Bork, P.2017. The STRING database in 2017: Quality-controlled protein–protein association networks, made broadly accessible. *Nucleic Acids Res. 45*, D362–D368.

Tenhaken, R. 2015. Cell wall remodeling under abiotic stress. *Frontiers in Plant Science,5*. doi:10.3389/fpls.2014.00771

Torres, M. A., and Dangl, J. L. 2005. Functions of the respiratory burst oxidase in biotic interactions, abiotic stress and development. *Current Opinion in Plant Biology,8*(4), 397-403. doi:10.1016/j.pbi.2005.05.014

Usadel, B., Obayashi, T., Mutwil, M., Giorgi, F. M., Bassel, G. W., Tanimoto, M., and Provart, N. J. 2009. Co-expression tools for plant biology: Opportunities for hypothesis generation and caveats. *Plant, Cell & Environment, 32*(12), 1633-1651. doi:10.1111/j.1365-3040.2009.02040.x

Vikram, P.; Swamy, B.P.; Dixit, S.; Singh, R.; Singh, B.P.; Miro, B.; Kohli, A.; Henry, A.; Singh, N.K. and Kumar, A. 2015. Drought susceptibility of modern rice varieties: An effect of linkage of drought tolerance with undesirable traits. *Sci. Rep. 5*, 14799.

Voss, I., Sunil, B., Scheibe, R., and Raghavendra, A. S. 2013. Emerging concept for the role of photorespiration as an important part of abiotic stress response. *Plant Biology,15*(4), 713-722. doi:10.1111/j.1438-8677.2012.00710.x

Wang J, Lan P, Gao H, Zheng L, Li W, and Schmidt, W. 2013. Expression changes of ribosomal proteins in phosphate- and iron-deficient Arabidopsis roots predict stress-specific alterations in ribosome composition. BMC Genom 14:783. doi. org/10.1186/1471-2164-14-783

Wang, X., Cai, X., Xu, C., Wang, Q., and Dai, S. 2016. Drought-Responsive Mechanisms in Plant Leaves Revealed by Proteomics. *International Journal of Molecular Sciences,17*(10), 1706. doi:10.3390/ijms17101706

Wu, Y., Sharp, R. E., Durachko, D. M., and Cosgrove, D. J. 1996. Growth Maintenance of the Maize Primary Root at Low Water Potentials Involves Increases in Cell-Wall Extension Properties, Expansin Activity, and Wall Susceptibility to Expansins. *Plant Physiology,111*(3), 765-772. doi:10.1104/pp.111.3.765

Xu, J., Xing, X., Tian, Y., Peng, R., Xue, Y., Zhao, W., and Yao, Q. 2015. Transgenic Arabidopsis Plants Expressing Tomato Glutathione S-Transferase Showed Enhanced Resistance to Salt and Drought Stress. *Plos One,10*(9). doi:10.1371/journal.pone.0136960

You, J. and Chan, Z. 2015. ROS Regulation During Abiotic Stress Responses in Crop Plants. *Front. Plant Sci*. *6*, 1092.

You, Q., Zhang, L., Yi, X., Zhang, K., Yao, D., Zhang, X., and Su, Z. 2016. Co-expression network analyses identify functional modules associated with development and stress response in *Gossypium arboreum*. *Scientific Reports, 6*(1). doi:10.1038/srep38436

Zhang, B., and Horvath, S. 2005. A General Framework for Weighted Gene Co-Expression Network Analysis. *Statistical Applications in Genetics and Molecular Biology,4*(1). doi:10.2202/1544-6115.1128

Zhang, L., Yu, S., Zuo, K., Luo, L., and Tang, K. 2012. Identification of Gene Modules Associated with Drought Response in Rice by Network-Based Analysis. *PLoS ONE, 7*(5). doi:10.1371/journal.pone.0033748

Zhang, Z.; Zhang, Q.; Wu, J.; Zheng, X.; Zheng, S.; Sun, X.; Qiu, Q., and Lu, T. 2013. Gene Knockout Study Reveals That Cytosolic Ascorbate Peroxidase 2(OsAPX2) Plays a Critical Role in Growth and Reproduction in Rice under Drought, Salt and Cold Stresses. *PLoS ONE, 8*, 2.

Zhou, S., Kong, X., Kang, H., Sun, X., and Wang, W. 2015. The Involvement of Wheat F-Box Protein Gene TaFBA1 in the Oxidative Stress Tolerance of Plants. *Plos One,10*(4). doi:10.1371/journal.pone.0122117

Zhu, J. 2016. Abiotic Stress Signaling and Responses in Plants. *Cell, 167*(2), 313-324. doi:10.1016/j.cell.2016.08.029

CHAPTER 3

COMPARATIVE SEQUENCE ANALYSIS, INTROGRESSION ANALYSIS, AND *qDTYs* CONTRIBUTION TO REPRODUCTIVE-STAGE DROUGHT TOLERANCE IN RICE

ABSTRACT

The *qDTY1.1* locus was identified as a major quantitative trait locus for drought tolerance in rice based on the Nipponbare reference genome. Previous studies have found that there were functionally important genes absent in the reference Nipponbare genome but present in other rice varieties. In this chapter, a "pan-QTL" approach was undertaken to provide the best characterization of candidate gene(s) causative to the trait. Three genomes were used for pan-QTL analysis: i) Nipponbare, the best characterized and reference used in previous chapters), ii) MH63 – indica, closest to recipient parent, and iii) N22 – aus, the DTY donor parent. Size variations in the pan *qTY1.1* region were attributed mainly to retrotransposon and transposon-related elements present in all three genome sequences. Most Nipponbare genes have putative alleles in MH63 and N22. Among the unique genes, most of the predicted N22 or MH63 genes were annotated as Transposable Elements. Following on, DEGs were characterized using the pan-QTL approach. Overlaying differential expression data with allelic variation in DTY-IL quantitative trait loci allowed for the prioritization of candidate genes. They included a differentially regulated auxin-responsive protein, with DTY-IL-specific amino acid changes in conserved domains, as well as a protein kinase with a DTY-IL-specific frameshift in the C-terminal region. As an additional candidate, a gene downregulated in the DTY-IL and upregulated in Swarna under drought was considered a potentially negative regulator of drought. It was unique to the representative *indica* genome and absent from the *japonica* and *aus* references. The approach highlights how the integration of differential expression and allelic variation can help discover the mechanism and putative causal contribution underlying quantitative trait loci for drought-tolerant yield.

INTRODUCTION

Plant breeding at a global level has made remarkable contributions in improving commercially important major crops like rice, maize, wheat, and cotton. A breakthrough in rice breeding came in the late 1960s- when the International Rice Research Institute (IRRI) released

the first-ever high-yielding, semi-dwarf, modern variety (IR8). This variety carries the dwarfing allele of the *sd1* (semi-dwarfing) gene, also known as the "Green Revolution gene" (Vikram et al., 2015). Traditional rice and wheat varieties before the "Green Revolution" were tall, photoperiod-sensitive, low-yielding but highly drought-tolerant, and had a wide-range maturity duration with poor grain quality (Kumar et al., 2008). In the post- Green Revolution-era, traditional varieties adapted to rainfed conditions were replaced with a few elite cultivars that are semi-dwarf and photoperiod-insensitive, early maturing, higher yield, good grain quality, responsive to fertilizer inputs, lodging resistant, and low pest resistance (Khush, 1999; Sandhu and Kumar, 2017). The semi-dwarf modern rice varieties were originally bred for irrigated ecosystems and were never selected for drought tolerance. Thus, they suffer significant yield losses even under mild drought conditions (Kumar et al., 2008; Frei and Becker, 2004). Because of the absence of high-yielding, good quality rainfed varieties, many varieties that were developed for high-input irrigated conditions are grown in rainfed areas. Though these varieties have high yield potential, they are highly prone to yield reductions under drought because of their high sensitivity to drought (Sandhu and Kumar, 2017; Swamy et al., 2017). During the progression of the Green Revolution era, the drought tolerance contributing alleles of the traditional varieties unknowingly have not been appropriately maintained during the development of semi-dwarf varieties for the irrigated ecosystem (Sandhu and Kumar, 2017). The drought susceptibility of modern rice varieties could be partly attributed to the tight linkage between plant height and drought tolerance loci (Vikram et al., 2015). The study reported that the loss of the *qDTY1.1* allele during the GR was due to its tight linkage in repulsion with the sd1 allele. Linkage of *qDTY1.1* and *sd1* would suggest that during the development of dwarf varieties, drought tolerance could have been lost, and a strong selection for semi-dwarfism would have impeded the introduction of *qDTY1.1* into breeding pools (Vikram et al., 2015).

A significant genotypic variation in drought tolerance exists within the cultivated rice gene pool and its wild relatives (Lafitte et al., 2006). Some traditional cultivars and landraces are excellent genetic resources for drought tolerance. However, they have undesirable traits like low tillering, tall plant height, poor grain quality, and poor yield (Kumar et al., 2014; Sandhu and Kumar et al., 2017). Due to these undesirable traits, most of the drought-tolerant donors are not

directly used in breeding. The identified drought-tolerant traditional donors such as Aday Sel, Dagadeshi, Kali Aus, Aus 276, Kalia, N22, Apo, and Dular have been used in conventional breeding programs and QTL mapping studies at IRRI. Most of the quantitative trait loci (QTLs) for grain yield under drought in rice have been introgressed into the background of popular, high-yielding, drought-susceptible GR and post-GR varieties, which are preferably cultivated on large areas in rainfed regions in the absence of high-yielding, good quality, drought-tolerant varieties (Vikram et al., 2011).

Within *Oryza sativa*, the two major varietal groups, *Indica*, and *Japonica* can be further subdivided into five major subpopulations. *Indica* and *aus* share ancestry within the *Indica* varietal group, while *temperate japonica, tropical japonica*, and *Group V (aromatic)* varieties share ancestry within the *Japonica* varietal group (Garris et al., 2005; Zhao et al., 2010). However, the indica and the aus genomes are more distantly related than previously anticipated (Schatz et al., 2014). Different *Oryza sativa* subpopulations are adapted to different ecologies and geographies and harbor different alleles and traits of interest for cultivar development (Zhao et al., 2010; Schatz et al., 2014). In recent years, many key biotic and abiotic stress tolerance genes have been discovered in *aus* varieties (Garris et al., 2003; Xu et al., 2006; Bernier et al., 2009; Hattori et al., 2009; Gamuyao et al., 2012). Characterization of the *aus* subpopulation gave rise to unique *aus* alleles at loci such as *Rc*, conferring white versus colored pericarp (Takano et al., 2007), the *Snorkel* locus conferring deepwater ability (Hattori et al., 2009), the *Pstol1* locus conferring phosphorus-update efficiency (Gamuyao et al., 2012), or the *Sub1* locus conferring submergence tolerance (Xu et al., 2006). They all support the hypothesis that *aus* has a unique domestication history compared to *japonica* and *indica* and underscore the importance of recognizing genetic subpopulation structure to guide plant breeders in identifying novel sources of variation for traits of interest. The absence of these genes from modern rice varieties underlines the importance of conserving and exploring traditional germplasm.

Although the *aus* types have a historically smaller geographical distribution and receive less attention than *indica* and *japonica* rice in breeding programs, their drought tolerance, deep-rooting, and early maturity are adaptive traits that are considered usefully targeted in breeding applications (Garris et al., 2005). The Indian landrace selection Nagina 22 (N22), developed

through selection from landrace Rajbhog, is one example of a genotype that is highly tolerant to drought (Lenka et al., 2011). Belonging to the *aus* group, N22 was traditionally grown in the short summer season (Aus season) under Bangladesh's rainfed conditions. N22 remains one of the best-characterized drought-tolerant varieties. It is further considered a donor for heat tolerance (Ziska et al., 1996) as its flowers maintain high spikelet fertility during high daytime temperatures (Reddy et al., 2009).

Several examples have shown that high-resolution mapping of QTLs coupled with identifying genes in the Nipponbare reference genomes' syntenic regions may not be sufficient to identify the causative genes or variation responsible for the observed phenotype. For instance, three ethylene response factor (ERF)-type transcription factor genes (*Sub1A*, *Sub1B*, and *Sub1C*) were only identified after sequencing the rice submergence tolerance locus *Sub1* in the tolerant donor line. The *Sub1A* gene was subsequently identified as the major determinant of submergence tolerance. It was shown that the gene was absent from the Nipponbare reference genome and other submergence-intolerant genotypes (Xu *et al*., 2006; Septiningsih *et al*., 2008). A similar situation was found for the *Pup1* locus, where the sequencing of the region of the donor Kasalath revealed the presence of an ~90-kb transposon-rich insertion-deletion (INDEL) region that was absent from the Nipponbare reference genome and other intolerant rice varieties (Heuer et al., 2009). Likewise, the rye (*Secale cereale* L.) aluminum tolerance locus *Alt4* (Collins *et al*., 2008) was discovered after sequencing of the tolerant variety (M39A-1-6) revealed five copies of the tolerance-determining malate transporter gene, while only two copies were present in the intolerant variety (M77A-1). The case of aluminum tolerance in sorghum furthermore highlighted that genotype-specific changes in intergenic regions could produce a tolerance response. The size (repeat number) of a miniature inverted-repeat transposable element (MITE) transposon integration in the upstream region of the Alt_{SB} gene, rather than allelic differences within Alt_{SB}, was positively correlated with tolerance (Magalhaes *et al*., 2007). Consequently, resolving the sequence of a given QTL in the respective tolerant donor parent should be considered a crucial component of a map-based cloning strategy.

The size of the fine-mapped region of the *qDTY1.1* locus using the Nipponbare genome was roughly 480 kb. The tolerant parent came from *aus* subpopulation, and the recipient parent

was an *indica* type. It was imperative for us to consider the genes in Nipponbare and the representative genomes of *indica* and *aus*. In this chapter, we 1) did a genome-wide genotyping-based identification on introgressions in DTY-IL; 2) created and analyzed a DTY pan-QTL using three references from different subgroups, looked at the presence-absence variations and identified DEGs across the three genomes; and 3) analyzed the candidate genes by looking at the non-synonymous variations within them. We included the MH63 and N22 references for this chapter, addressing the possibility that additional genes might be present in the MH63 or N22 *qDTY1.1* locus that are more obviously related to drought tolerance.

MATERIALS AND METHODS

DNA Extraction and Sanger Sequencing

According to the manufacturer, genetic DNA was extracted from the leaves of N22, the DTY-IL qDTY donor, using the Qiagen DNeasy Kit (Qiagen, Limburg, Netherlands) 's instructions. LOC_Os01g67030 (auxin-responsive protein), including a 1.8-kb upstream promoter region, was amplified using the forward primer GAGCGTGCAGTCCACTAGGCATTATC and reverse primer GTGACACGTATTCTGATGTACTG. The amplicon was cloned into the pGEM-T Easy Vector (Promega, WI, USA), as per manufacturer's instructions, and Sanger sequenced using Macrogen, Inc. South Korea as the service provider.

Genotyping

The three rice lines DTY-IL, Swarna, and N22 were genotyped with three replications using the 7k rice Illumina assay (Morales et al., 2020). Based on the replicates, a consensus genotype (considered as the most accurate representative genotype) was generated for each line by generating a hap.map file. Genotypic frequencies for each SNP across the replicated samples were estimated, and the most frequent genotype was considered the true genotype. True genotypes were collected and used to represent the genotypic calls for each line. Missing markers and monomorphic markers between the parents N22 and Swarna were filtered. For the remaining markers (1,648 SNPs), each parent's genotypic calls were used to assign if the genotypic call in each DTY-IL line was inherited from N22 or Swarna. Introgressed genome segments from the

donor parent N22 were identified based on contiguous SNP blocks of N22-type calls. Markers that potentially represent miss-called double recombination were discarded if the probability of observing this event was smaller than 1 cM or 1 in 100 events. A graphical representation of the markers inherited from N22 and Swarna was graphed using the R package ggplot2.

Identification of the physical location of the fine-mapped *qDTY1.1* region in 3 published rice genomes

A pan-QTL approach (a pan-genome analysis restricted to a QTL region) was undertaken in order to provide the most comprehensive identification of candidate genes causative to reproductive-stage drought tolerance in rice. The pan-genome concept refers to the non-redundant collection of all DNA sequences present in the entire population of a species, which comprises a "core genome" containing sequences present in all individuals, a "dispensable genome" containing sequences present in two or more individuals, and unique sequences specific to an individual (Yao et al., 2015). At present, whole-genome sequences and annotations (gff) were available for the three rice genotypes 'Nipponbare', representing the *japonica* subspecies, 'MH63', as a proxy for Swarna, an *indica* recurrent parent used to develop the DTY-IL, and 'N22', an *aus* donor parent of DTY-IL. Respective sequences were retrieved from public databases (http://rice.plantbiology.msu.edu/pub/data/Eukaryotic_Projects/o_sativa/annotation_dbs/pseudomolecules/version_7.0/ for Nipponbare; http://rice.hzau.edu.cn/cgi-bin/rice2/download_ext for MH63; and https://www.ncbi.nlm.nih.gov/assembly/GCA_001952365.3/ for N22).

To convert the QTL position from genetic to physical coordinates, the sequences of the genetic markers flanking the fine-mapped *qDTY1.1* region were used to conduct an in-silico PCR-based analysis to extract the physical sequence underlying the QTL. The flanking markers (RM431 and id1024366) of the fine-mapped *qDTY1.1* region in the Nipponbare reference genome were used to make the QTL marker fasta file using SAMtools (version 1.7). The 100 nucleotides upstream of the SNP marker in the Nipponbare genome (RGAP 7, http://rice.plantbiology.msu.edu/) was included with the SNP marker using the 'faidx' function of SAMtools. The forward and reverse primer sequences of the RM431 marker were manually added through *vi* in Unix to have the marker fasta file. The alignment was done through Novocraft (version 3.08.00). Novoalign index was first done on the latest version of N22 and MH63 through

the function ‘novoindex’ of Novocraft. The alignment was done using the ‘novoalign’ function with the QTL marker fasta file, and the individual indexed genome of N22 and MH63. The novoalign alignment output was the lifted-over region of *qDTY1.1* in the *aus* and *indica* representative genomes. For sequence extraction in the N22 and MH63 genome, local server BLAST (version 2.9.0) was used first to create a blast database using the ‘makeblastdb’ function. The sequence of the *qDTY1.1* region in the *aus* and *indica* genomes was extracted using the ‘blastdbcmd’ function with the specific “lifted-over” region range in N22 and MH63, respectively. The chromosomal regions corresponding to the *qDTY1.1* region of the three genomes were aligned using the GEPARD (version 1.40) software (Krumsiek et al., 2007).

Pan-QTL analysis of the *qDTY1.1* region

Sequences of Nipponbare genes located within the *qDTY1.1* physical region in chromosome 1 (38.4-38.9 Mb) were downloaded from the Rice Genome Annotation Project. The lifted-over *qDTY1.1* region of N22 and MH63 were extended at 30 kbs downstream and a few kbs upstream to capture one of the candidate gene's equivalent from the Nipponbare genome. Five genes located downstream of the *qDTY1.1* physical region in Nipponbare were identified and their respective sequences downloaded. Pan-QTL genes were identified using the following workflow: 1) in order to determine the N22 and MH63 synteny and subregions that have hits versus the Nipponbare *qDTY1.1* genes, sequence-based alignment through BLAT was carried out using the cDNA of Nipponbare *qDTY1.1* genes as query, while the N22 and MH63 *qDTY1.1* lifted-over genomic regions as a reference; 2) identified predicted genes within *qDTY1.1* genome region in N22, MH63 using the respective annotations (from the respective gffs). This allows identification of gene structures within the aligned region of N22, MH63, and 3) N22 and MH63 alleles of Nipponbare genes were identified based on the overlap of alignment from step#1, the N22/MH63 gene model coordinates should overlap with the alignment. These N22 and MH63 genes were considered as alleles of Nipponbare genes and assigned with the Nipponbare gene ID. Those N22 and MH63 genes that did not map (no overlap) with the Nipponbare *qDTY1.1* genes (no Nipponbare equivalent) were also identified. The CDS of these gene sets (no Nipponbare equivalent) were aligned against each other using the Find-seq tool in Galaxy/CropGalaxy with default settings

(http://cropgalaxy.excellenceinbreeding.org/?tool_id=blat.342&version=v.01&__identifer=70mx7z89gvs). Genes with no Nipponbare homologs but had homologs in N22 and MH63 were identified. The unique N22 and MH63 genes were lastly identified as those genes without Nipponbare homologs and without gene homologs in either N22 or MH63 when aligned.

A first-pass annotation of the pan-QTL genes was carried out via NCBI and Uniprot BLAST (nucleotide and protein) using the cDNA sequences of N22 and MH63 and protein sequences for MH63 only. (https://www.uniprot.org/blast/; https://blast.ncbi.nlm.nih.gov/Blast.cgi?PAGE_TYPE=BlastSearch).

Differential expression analysis was done using the pan-QTL gene sets. The DEGs within the *qDTY1.1* region of the three representative reference genomes were identified and compared. DEG's not present in the Nipponbare genome were further investigated for a possible role in reproductive-stage drought tolerance.

Sequence Alignment and Conserved Domain Analysis

The pan-QTL region in the N22, MH63, and Nipponbare representative reference genomes were used for multiple genomic and peptide sequence alignments. Blastn and blastp with default settings in NCBI were used for the pairwise and multiple genomic and peptide sequence alignments.

Additionally, Clustal Omega (version 1.2.4) with default settings and a ClustalW output format was used for multiple protein sequence alignment for each of the two candidate genes within the Nipponbare, N22, and MH63 peptide sequences. Conserved domains of each of the two candidate genes within the peptide sequences of the pan-QTL gene set were determined through NCBI's conserved domain database using default settings.

Candidate Gene Sequence Analysis

An in-depth comparative analysis of the two candidate gene sequences from MH63 and N22 and the reference gene models from Nipponabre was carried out to characterize the differences of the putative alleles better. The gene structure of the N22 allele was predicted using

FGENESH. We later determined that the prediction was more accurate as supported by the Sanger sequencing result than the most updated N22 annotation.

The genomic sequences of the two candidate genes (LOC_Os01g67030 and LOC_Os01g03510), including the 2-kb upstream and downstream sequences of the genes, were extracted in the Nipponbare reference genome. The corresponding sequences of these Nipponbare candidates were identified via an alignment using BLASTN from the N22 and MH63 genomes and extracted for subsequent analyses.

FGENESH (Solovyev et al., 2006) with Oryza sativa Indica group (long-grained rice) as the genome-specific parameters for gene-finding was used to predict the gene structure, including the start and stop codons as well as peptide sequences of the two candidate genes in the *qDTY1.1* lifted-over sequence of the N22 genome. Annotated gene structures of the two candidate genes were already reported in the Nipponbare and MH63 genomic sequences. Experimental evidence to support the candidate genes were provided by examining the depth of RNA-Seq reads from the following samples (DTY-IL control and drought; Swarna control and drought) that align across the candidate gene sequences in Nipponbare, MH63, and N22 genomes; these were visualized in IGV (version 2.8.2) relative to MSU7 (Nipponbare) and in the latest versions of the MH63 and N22 genomes. Clustal Omega (version 1.2.4) was used for multiple protein sequence alignments. SNP-Seek (https://snp-seek.irri.org) was used to validate the nonsynonymous (NS) SNPs across the 3K genomes.

Promoter Alignment and Analysis

The 2-kb upstream region of each candidate gene within the Nipponbare, N22, and MH63 genomic sequences was extracted using the 'blastdbcmd' function of BLAST. Pairwise and multiple sequence alignment of the 2-kb upstream region of each candidate gene was done via blastn, using default settings.

The extracted 2-kb upstream region of each candidate gene for each of the three representative reference genomes was used as input queries in the PLACE database (https://www.dna.affrc.go.jp/PLACE/?action=newplace). Motifs found in plant *cis*-acting regulatory DNA elements within the 2-kb upstream of each candidate gene were listed. The

common motifs in the 2-kb upstream of each candidate gene for each of the three representative reference genomes were excluded. The unique and distinct motifs (only present in one reference genome) were listed.

RESULTS

Genotyping results and DEGs overlay

SNP genotyping revealed 16 N22-derived fragments in DTY-IL (Figure 3.1). The largest fragment was found on chromosome 1, encompassing *qDTY1.1*, followed by an introgression on chromosome 3, containing parts of *qDTY3.2*, which was also reported as N22-derived in an N22 by Swarna population (Vikram *et al*., 2011). Additional introgressions on chromosomes 4, 8, 9, and 10 did not overlap with major DTY QTL (Table 3.1). Overlaying DEGs on the N22 introgressions identified 463 DEGs in the flag-leaf (Table 3.2) and 433 DEGs in the panicle (Table 3.3), of which six overlapped with the fine-mapped region of *qDTY1.1* (Vikram *et al*., 2015) on both tissues, while 2 and 5 DEGs overlapped with the *qDTY3.2* region in the flag-leaf and panicle tissues, respectively.

The fine-mapped region of *qDTY1.1* in the Nipponbare reference genome encompassed 75 genes, of which six were differentially expressed in DTY1.1-IL and Swarna in flag-leaf (Table 3.4) and panicle tissues (Table 3.5) under RDS. Differential expression analysis on Nipponbare reference genome was done before the pan-QTL analysis as the availability of the gff of N22 was just released last 2020.

Of the 6 DEGs in the *qDTY1.1* region, LOC_Os01g67030 was upregulated in the panicle (Log_2 fold change = 3.1), which was annotated auxin-responsive protein of 418 in amino acids (AA) in Nipponbare. While LOC_Os01g67030 was annotated in the *Indica* reference MH63, it was not functionally annotated in the N22 reference genome. FGENESH-based gene prediction in N22 revealed a putative orthologue. Annotated genomic sequence alignment showed 98.6% identity between MH63 and Nipponbare in the corresponding regions, while N22 prediction showed 91.4% identity with Nipponbare and 92.3% identity with MH63. The multiple sequence alignment of the amino acid sequence, including the annotated Nipponbare sequence, was

constructed using Clustal Omega. The Nipponbare sequence has 418 AA sequence while MH63 has 381 and N22 has 380. The multiple alignments showed a high degree of similarity with several protein sequence differences (Figure 3.2). Four of the seven peptide sequence difference showed a unique N22 sequence and similar in Nipponbare and MH63 sequences. Differences were found in the 5'UTRs (including transcription start site (TSS) and start codon position), resulting in the loss of coding sequence for the first 37 AA in the MH63 and N22 alleles, as well as several nonsynonymous (NS) SNPs unique to N22 (Figure 3.3), which was further validated through RNA-Seq data. NS SNPs corresponded to four AA changes (P52L, C60F, S80T, Q137P) and G253del (Figure 3.3).

Of the 5 DEGs within *qDTY3.2*, LOC_Os03g03510, downregulated in the panicle (Log_2 fold-change = -1.11617), was annotated CAMK_KIN1/SNF1/Nim1_like.15 - calcium/calmodulin-dependent protein kinase in Nipponbare, with corresponding annotations in MH63 and predictions in N22. LOC_Os03g03510 contains a Sucrose non-fermenting 1-related kinase 3 (SnRK3) domain and a CBL-interacting serine/threonine-protein kinase 3 (CIPK3) domain. While the coding sequences were conserved mainly in multiple sequence alignment between Nipponbare, MH63, and N22 alleles, the N22 allele featured an altered stop codon resulting in a 35 AA C-terminal extension (Figure 3.4).

Characterizing the *qDTY1.1* pan-QTL genes

The size of the fine-mapped *qDTY1.1* locus, based on the Nipponbare reference genome sequence, was 480 kb, while the lifted-over locus sequence in the N22 and MH63 genomes were 506 and 491 kb, respectively. The locus size did not differ significantly across the three genomes (Table 3.6). The lifted-over sequence of the fine-mapped *qDTY1.1* locus (defined by markers RM 431 and SNP) in Nipponbare showed a high syntenic region in the N22 and MH63 genomes (Figure 3.5). The pairwise dot plot alignment between Nipponbare and N22 showed few small stretches of gaps unique to N22 and NB *qDTY1.1* locus. The same is true in the dot plot between MH63 and N22. Most of the identified gaps in the pairwise alignment showed retro-/transposons annotation upon sequence blastn based on RiTE DB (https://www.genome.arizona.edu/cgi-bin/rite/index.cgi).

To determine the Nipponbare gene equivalent in N22 and MH63 and the unique N22 and MH63 genes in the *qDTY1.1* locus, a gene-by-gene comparison was made through BLAT alignment (Figure 3.6; Table 3.7). More detailed sequence comparison of the Nipponbare fine mapped *qDTY1.1* locus to the syntenic region in the N22 and MH63 revealed a high level of gene similarity and dynamic features caused by several transposons- and retrotransposon-related elements (TEs; Table 3.7). In the N22 *qDTY1.1* region, 72 genes were identified, of which 53 had a clear Nipponbare homolog in the region. In MH63, the number of identified genes was 81, of which 60 had corresponding Nipponbare homologs (Table 3.6; Figure 3.6). Out of the 75 Nipponbare genes, 6 in *qDTY1.1* 6 did not even partially align to any N22 and MH63 genes. Most of these genes were annotated as expressed protein and TEs except for one gene which is annotated as Pentatricopeptide (LOC_Os01g66160). Four genes within the *qDTY1.1* region did not show any Nipponbare equivalent but were common between N22 and MH63. Most of these genes were annotated as hypothetical protein except for one gene annotated as OsPIF4 (phytochrome-interacting factor). On the other hand, 13 genes in N22 and 16 genes in MH63 were unique within the *qDTY1.1* locus (Figure 3.6). These genes did not have any Nipponbare equivalent, nor is it common between N22 and MH63 genomes. Of the 13 unique N22 genes, all were annotated as TEs or hypothetical proteins, except for one gene, which was annotated as beta-hexosaminidase 3. Of the 16 unique MH63 genes, 12 were annotated as TEs or hypothetical proteins, while the remaining four genes of MH63 were annotated as GRF zinc finger family protein, Receptor-like serine/threonine-protein kinase, ULP_PROTEASE domain-containing protein, and Beta-hexosaminidase precursor, putative.

There were 45, 38, and 42 genes in Nipponbare, N22, and MH63, respectively, which showed clear functional annotation (Table 3.6; Figure 3.6). In contrast, there are 21, 14, and 26 genes in Nipponbare, N22, and MH63, respectively, which showed unclear functional annotation. These unclear annotations were those genes that were either expressed or hypothetical/uncharacterized proteins excluding the TEs. In Nipponbare, 9 of the 75 genes present in the region were annotated as TEs, whereas 15 and 12 N22 and MH63 *qDTY1.1* genes were annotated as TEs based on NCBI megablast (blastn) analyses and Uniprot blast, respectively. The

genes in the N22 genome clearly showed the highest percentage of TEs (15/72 gene; 20.83%), while the Nipponbare genome showed the lowest in the genic region of *qDTY1.1* locus.

A few genes in N22 and MH63 *qDTY1.1* locus had two or more gene equivalent in Nipponbare as per blat alignment results (Figure 3.6). There were four different gene models in N22 which each had two putative homologs in Nipponbare. There was also one N22 gene model that had three putative homologs and another N22 gene model which had six putative homologs in Nipponbare. The overlap in the BLAT alignment rendered the result, and the gff of N22 gene models showed a more extended sequence compared to their Nipponbare counterparts. For MH63, there were two different gene models, each having two putative homologs in Nipponbare, and one gene model showed three gene equivalents in Nipponbare. The one gene model similar in N22 and MH63 that showed three contiguous gene equivalents in Nipponbare was annotated as pectinacetylesterase domain-containing protein in Nipponbare.

Differential expression analysis across the three genomes focusing on *qDTY1.1* locus

Differential expression analysis was done using the N22 and MH63 reference genomes similar to the Nipponbare reference-approach with a focus on the DEGs in the *qDTY1.1* syntenic region. Detailed DEGs within the locus in the panicle and flag-leaf tissues with a few genes included on the "fuzzy" border were listed in Tables 3.8 and 3.9, respectively. Two interesting DEGs were noted. The first one was annotated in MH63 (OsMH_01G0644300) and predicted in N22 (OsN22RS2_01G0429800) as a beta-hexosaminidase gene. This gene was absent in the Nipponbare *qDTY1.1* locus. DE analysis revealed that this gene in N22 was upregulated in the flag-leaf of DTY-IL and downregulated in Swarna under drought and control conditions. A similar observation was also noted on the panicle tissue but including the MH63 counterpart of the gene. Beta-hexosaminidase was an important glycosidase involved in important signal transduction, cell division, and cell integrity events and was involved in the hydrolysis processes of fruit ripening (Cao and Tan, 2019).

The other one was the MH63 OsMH_01G0644100 gene, and this gene was absent in Nipponbare and N22 *qDTY1.1* locus. This gene was downregulated in the panicle of DTY-IL and upregulated in Swarna under drought (IL_DvsSwa_D) and control condition (IL_CvsSwa_C) in the MH63 genome. Annotation of this gene in Rice Information Gateway (RIGW) was an

expressed protein. Uniprot blast of the protein sequence resulted in an annotation as ULP_Protease domain-containing protein. Conserved domain search of the protein sequence in NCBI suggested a Peptidase_C48 with a description of a Ulp1 protease family, C-terminal catalytic domain. ULP (ubiquitin-like protease) class was considered SUMO proteases in plants (Morrell and Sadanandom, 2019).

Differences in the *cis*-acting regulatory elements of a selected candidate gene

Of all the candidate genes in this study, LOC_Os01g67030 was present in all genomes and a DEG between DTY-IL and Swarna under drought. Moreover, there's also a large deletion in the 2-kb promoter region of this gene in N22 but not in Swarna and Nipponbare. Speculating that DE was due to differences in the promoter regions between N22 and Swarna, we took a closer look at the respective *cis*-acting elements.

The promoter region (2-kb upstream sequence from the start codon) of LOC_Os01g67030 in the context of Nipponbare, MH63, and N22 genome sequences was analyzed using the signal search program PLACE to identify *cis*-acting regulatory elements linked to specific abiotic stress conditions. The three genome sequences were representatives of *Japonica*, *Indica*, and *Aus* subpopulations in the rice genome, respectively.

Differences in N22 were found in the 2-kb upstream *cis*-regulatory region of N22. While the alignment of the 2-kb upstream region of LOC_Os01g67030_NB and LOC_Os01g67030_MH63 showed a 99.1% identity with only 18 nucleotide differences, N22 displayed a large deletion, including in the 5'UTR region (Figure 3.3). With an identity of less than 15% to either Nipponbare or MH63, the N22 *cis*-regulatory region of LOC_Os01g67030 was distinct with unique regulatory elements (Table 3.10) that could explain the observed expression differences.

Most *cis*-acting regulatory elements within the 2-kb upstream region of LOC_Os01g67030 were similar among the three genomic sequences. To find unique elements in the upstream region within the three genomic sequences, we listed the distinct motifs among the three representative genomes. Nipponbare showed only three, and MH63 showed only one unique and specific *cis*-acting element (Table 3.10), neither of which was associated with abiotic stress such as drought.

Two Auxin-responsive elements (AuxRe) were found in the 2-kb promoter region of Nipponbare and MH63, while only one Auxre was found in the N22 promoter region. The 2-kb upstream region of LOC_Os01g67030_N22, on the other hand, showed distinct drought-responsive elements that were absent from Nipponbare and MH63 upstream sequences. A total of six unique *cis*-acting DNA sequence elements were reported to be involved in regulating genes that are responsive to drought stress. The presence of these drought-responsive regulatory *cis*-elements in the upstream region further supports drought-stress responsiveness of this auxin-responsive protein in the *Aus* but not in the *Japonica* and *Indica* representative genomes. These results potentially signify drought tolerance of N22 and drought susceptibility of MH63 and Nipponbare genotypes.

DISCUSSION

qDTY1.1 and *qDTY3.2* Specific Contributions to Drought Tolerance

Of the 16 N22-derived introgressions in DTY-IL, two overlapped with known *qDTY*s for which N22 was a known donor (Lenka et al., 2011). While the large introgressions on chromosome 1 contained the full *qDTY*1.1 region, a smaller introgression on chromosome 3 partially overlapped with *qDTY*3.2 (Figure 3.1). Working under the assumption that the genome-wide changes in transcriptomes between the drought-tolerant and drought susceptible genotypes in both flag-leaves and panicle would at least partially trackback to either transcriptional or allelic differences of specific loci within the *qDTY* regions, we took a closer look at the *qDTY*1.1 fine mapped region and *qDTY*3.2 overlap.

Based on the Nipponbare reference, the fine-mapped *qDTY*1.1 region encompassed 75 genes, six of which were differentially expressed between DTY-IL and Swarna under RDS in either tissue (Tables 3.2 and 3.3). An auxin-responsive protein (LOC_Os01g67030), specifically upregulated in DTY-IL panicle under RDS, was considered a likely causative candidate. Generally, auxin has been shown to negatively regulate drought adaptation in plants (Basu et al., 2016). Uga et al. (2013) cloned and characterized a QTL for root growth angle in rice, *DEEPER ROOTING 1* (*DRO1*). *DRO1* is negatively regulated by auxin and functions downstream of the auxin signaling pathway and controls the gravitropic curvature in rice roots (Uga et al., 2013).

AuxRes, which contain the motif TGTCTC, were found in the promoters of some early-auxin response genes, and auxin response factors (ARFs) bind AuxRes to regulate the transcription of these genes (Hagen and Guifoyle, 2002). Specific ARF regions bind to *cis*-regulatory elements of the *DRO1*, specifically in the TGTCTC AuxRes promoter region, to regulate the expression of *DRO1* (Uga et al., 2013). While two AuxRes were found in the LOC_Os01g67030_NB and LOC_Os01g67030_MH63 promoter (-513 bp and -1606 bp), only one was found at position -1573 bp in N22. The absence of the proximal AuxRe motif, in addition to the presence of novel, putative drought-responsive elements (Figure 3.3; Table 3.10) could explain the observed differential regulation of LOC_Os01g67030 under RDS in DTY-IL.

LOC_Os01g67030 contains a cytochrome b561 (Cyt_b561) and a dopamine β-monooxygenase (DOMON) domain (Figure 3.2). Cyt_b561 proteins are involved in the regeneration of ascorbate through transmembrane electron transport (Verelst and Asard, 2003; Asard et al., 2013) and have previously been implicated in drought tolerance through redox homeostasis (Nanasato et al., 2005). The functionally uncharacterized β sheet-rich DOMON domain has been implicated in sugar and heme recognition (Lyer et al., 2007). It was predicted to be involved in protein-protein interactions, putatively functioning in metabolic signaling, redox reactions, or both. Interestingly, LOC_Os01g67030 thus has the potential to link sugar signaling and ROS signaling, both of which have emerged as essential in the DTY-IL-specific drought response.

The 5 AA differences in the N22 prediction of the LOC_Os01g67030 sequence fall under the two conserved domains (Figure 3.2). Notably, they include two proline conversions and a glycine deletion, with potential structural implications, particularly in the context of transmembrane domains and β sheets (Verelst and Asard, 2003; Asard et al., 2013). This could affect the ability of the Cyt_b561 domain to mediate transmembrane transport and the DOMON domain to mediate protein-protein interactions or ligand binding.

Efficient ROS scavenging was identified as a critical RDS tolerance mechanism in both panicles and flag-leaves of DTY-IL. In the panicle, LOC_Os01g67030 could directly contribute to ROS homeostasis, and with ROS being increasingly implicated in stress signaling, including modulation of gene expression (Choudhury et al., 2016; Mittler, 2017). LOC_Os01g67030 activity

in the panicle could be responsible for some expression changes observed in M10 and M15. LOC_Os01g67030, however, was not expressed in flag-leaves. It is possible that the ultimate positive effects of the N22 allele of LOC_Os01g67030 on seed setting in DTY-IL panicles could increase sink strength in a way that it positively affects the source strength of flag-leaves, which could contribute to maintained photosynthetic rates. A similar sink on source effects has been demonstrated by manipulating SnRK1 dependent metabolic signaling in maize under control and drought (Oszvald et al., 2018).

Unlike LOC_Os01g67030, which was present in all three genomes, OsMH_01G0644100 was a protease protein unique to the *indica* genome identified in MH63 but demonstrated to be expressed and downregulated under drought in DTY-IL and upregulated in Swarna. OTS1 and 2 (overly tolerant to salt 1/2) were initially identified in *Arabidopsis* in the screen by Kurepa et al. (2003) and named ULP1d and ULP1c (ubiquitin-like protease), respectively. In rice, knocking out OTS1/2 at the flowering-stage promoted drought tolerance while the overexpressing lines were drought-sensitive; rice OTS1-RNAi lines were much more sensitive to ABA and survived better in drought conditions losing less water. *Os*OTS1 interacted with *Os*bZIP (basic leucine zipper domain), a transcription factor that regulated ABA and drought responses. In the *Os*OTS1 RNAi lines, *Os*bZIP23 had higher levels of SUMOylation and was stabilized, leading to the transcription of more drought-tolerant genes. *Os*OTS1 was degraded by exposure to desiccation, mannitol, and ABA, working as a feedback loop to stabilized *Os*bZIP23 under drought conditions (Srivastava et al., 2017). SUMO proteases reversed SUMOylation conjugation, so-called de-SUMOylation, which lead to the removal of SUMO from its target. DeSUMOylating proteases such as OsOTS1 (Srivastava *et al*., 2016) cleaved the isopeptide bond between the terminal glycine of SUMO and the lysine of the conjugated substrate, releasing free SUMO from the target protein, thereby changing the stability of the protein and or interfering with protein-protein interactions, which led to changes in protein functionality. Conti et al. (2008; 2014) had shown that SUMOylation was a mechanism that functions as a major molecular pathway in governing Arabidopsis growth in high salinity by unraveling the function of the SUMO proteases *AtOTS1* and 2. The upregulation of OsMH_01G0644100 in Swarna under drought may have caused deSUMOylation of targets like transcription factor, which could directly suppress drought-responsive transcription of downstream

drought-responsive genes leading to drought sensitivity. The cleaving of SUMO destabilizes the target proteins or interactions, thereby affecting protein functionality, leading to drought sensitivity and decreased productivity. SUMOylation modifies the target function in many ways, including stimulating new protein-protein interactions, changing their subcellular localization, stabilizing or marking them for proteasomal degradation (Novatchkova *et al*., 2004). The downregulation of the gene in DTY-IL under drought and control conditions signified differential SUMO protease activity in the DTY-IL and Swarna. The gene in DTY-IL was potentially degraded or repressed, thus stimulating the accumulation of SUMO-conjugated targets. It could potentially promote SUMO conjugation to target proteins like transcription factors and heat shock proteins. Their activity would regulate the expression of downstream drought-responsive genes, potentially promoting drought tolerance.

One of the other *qDTY*'s that was found to introgressed into the DTY-IL was *qDTY3.2*. Of the five DEGs within the *qDTY3.2* region, one gene was a strong candidate and was downregulated in DTY-IL and upregulated in Swarna under drought. Moreover, this gene also showed an extended and altered stop codon in the C-terminal of the N22 peptide sequence. Both the CIPK_C domain (Sánchez-Barrena et al., 2007) and SnRK3 domain (Hirabak et al., 2003; Wang et al., 2019) have been implicated in abiotic stress responses, including drought tolerance. Besides, SnRK3, like SnRK1 (Oszvald et al., 2018; Lawlor and Paul, 2014), has been demonstrated to function in metabolic signaling and source-sink relationships. In sinks, SnRK1 activity has detrimental effects on grain filling (Oszvald et al., 2018). A 35 AA C-terminal extension in the N22 allele could have functional implications, which, in addition to its observed downregulation, could reduce its efficiency in DTY-IL (Figure 3.4). The postulated effect would be altered downstream phosphorylation responses with potential transcriptional changes that reflect some of the differences seen between Swarna and DTY-IL Ultimately, this could contribute to maintained sink strength of the panicle with putative effects on flag-leaf source metabolism.

In theory, all three main candidates' postulated functions could have synergistic effects that could explain a range of the observed DTY-IL specific drought responses. Gene validation studies expressing the N22 allele of LOC_Os01g67030, LOC_Os03g03510, or both, or the MH63 gene

OsMH_01G0644100, under control of their native promoters in drought susceptible Indica background, respective knockouts in DTY-IL, or both, are needed to confirm their postulated roles.

SIGNIFICANCE OF QTL SEQUENCING

Concerning QTL mapping and marker-assisted breeding, sequencing major QTLs in their respective tolerant donor parent is essential as important genes may be missing in the Nipponbare or MH63 syntenic region. As shown for the submergence tolerance QTL *Sub1*, the presence of an apparent candidate tolerance gene can be misleading. Within the Nipponbare *Sub1* syntenic region, two ERF transcription factor genes, *OsSub1B* and *OsSub1C* are present, and the latter has a tolerant-specific allele and tolerant-specific expression under submerged conditions. Yet, the actual tolerance gene, *OsSub1A*, is absent from the Nipponbare genome and was identified only after sequencing the locus in the tolerant parent (Xu *et al*., 2006). However, in several cases, tolerance genes located in QTLs are present in the Nipponbare reference genome; for instance, the sodium transporter gene *OsSKC1* in the *Saltol* QTL (Ren *et al*., 2005) and *OsPTF1* located within the intermediate phosphorus uptake QTL on chromosome 6 (Yi *et al*., 2005).

The *Sub1* and *Pup1* examples also show the limitations of candidate gene approaches, as only known genes can be tested that are selected based on our current knowledge of metabolic pathways and regulatory processes. In this regard, RNA-Seq analyses may be of limited value. They so far screen only Nipponbare and some MH63 genes but would miss potentially important genes present in N22, the tolerant donor genotype. For example, none of the highly phosphorus-responsive genes identified in transcriptome analyses (Misson *et al*., 2005) were located within or close to the *Pup1* region, which further shows the limitation of such an approach in candidate gene identification. However, transcriptome analyses could be used to detect gene networks or physiological processes affected by a specific QTL, particularly in cases like *Pup1*, where the QTL region does not contain a functional candidate. Moreover, it cannot be excluded at this point that unique non-coding genes like the *microRNA*s would be potentially present in the N22 and MH63 *qDTY1.1* locus, which might have important functions.

MARKER-ASSISTED BREEDING

Detailed knowledge of the genes present at a given QTL facilitates discovering novel tolerance alleles. It improves our understanding of tolerance mechanisms, yet one of the most significant benefits can be found in applied plant breeding. The availability of gene-specific diagnostic markers facilitates the selection of breeding lines that carry the QTL of interest with minimum flanking donor segments. This permits the breaking of linkages between the gene of interest and any undesirable linked traits. One goal of plant breeding is to introduce a donor parent's gene to improve a cultivar for a specific trait through backcrossing. Linkage drag refers to the reduction in fitness in a cultivar due to deleterious genes introduced along with the beneficial gene during backcrossing. The systematic breakage of linkage between sd1 and *qDTY1.1* led to developing a new semi-dwarf drought-tolerant genotype homozygous for *qDTY1.1* possessing high-yield potential (Vikram et al., 2015; Sandhu and Kumar, 2017).

Given the recent progress in mapping promising QTLs for important abiotic stresses and the large number of biotic stress tolerance genes already known (Ismail *et al*., 2007 and Jena and Mackill, 2008), breeders will routinely pyramid major QTLs in the future. With the marker-assisted breeding approach developed for *Sub1* and *Pup1*, QTLs can be introgressed into the genetic background of widely grown and otherwise well-adapted rice varieties without losing their desirable traits (Septiningsih *et al*., 2008). Based on the three genotypes' sequence alignment, identifying and validating regions that are highly diagnostic for *qDTY1.1* can be widely used by breeders. A germplasm survey should be conducted with the diagnostic markers to check if the *qDTY1.1* locus would be present or absent from irrigated, rainfed low, and upland rice varieties. A similar survey can be done to check on the identified candidate genes. This will suggest if breeders have unknowingly selected for *qDTY1.1* and that this QTL may have the potential to improve rice yields in unfavorable environments.

TABLES AND FIGURES

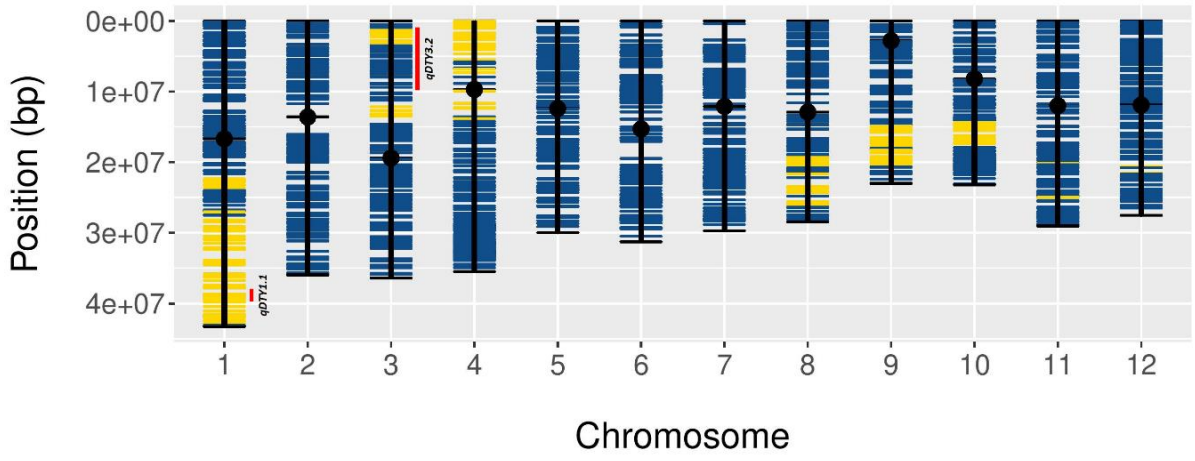

Figure 3.1. Physical map of DTY-IL. Genome-wide physical position distribution of 1648 SNPs from the 7K genotyping assay across all rice chromosomes. Swarna SNP's alleles are represented in blue. N22 SNP alleles are represented in yellow. Names and ranges of N22-derived DTY QTLs (*qDTY*1.1 and *qDTY*3.2) are shown as red bars on the sides of the chromosome. More details are provided in Tables 3.2 and 3.3.

Table 3.1. Introgressed N22 fragments in Swarna. The continuous N22 SNPs in each chromosome represent an introgressed fragment.

rs.	alleles	chrom	pos	cM	N22	SWARNA	IL4	IL6	gvIL4	gvIL6	Fragments
SNP-1.22352640.	C/T	1	22353686	0.11	CC	TT	CC	CC	N22	N22	1
id1012746	T/C	1	22494508	0.64	TT	CC	TT	TT	N22	N22	1
753735	G/A	1	22523562	0.13	GG	AA	GG	GG	N22	N22	1
757255	C/T	1	22612838	0.41	TT	CC	CC	CC	N22	N22	1
760644	C/A	1	22723681	0.5	CC	AA	CC	CC	N22	N22	1
SNP-1_22828195	C/A	1	22829240	0.48	AA	CC	CC	CC	N22	N22	1
SNP-1.23170758.	G/A	1	23171803	1.56	AG	GG	AG	AG	N22	N22	1
784044	T/C	1	23348983	0.81	TT	CC	TT	TT	N22	N22	1
801364	T/C	1	23731002	1.74	TT	CC	TT	TT	N22	N22	1
907175	C/T	1	27047209	0.92	CC	TT	CC	CC	N22	N22	2
id1015742	A/T	1	27052085	0.02	TT	AA	AA	AA	N22	N22	2
913506	G/A	1	27330724	1.27	GG	AA	GG	GG	N22	N22	2
939001	A/G	1	28183638	3.13	AA	GG	AA	AA	N22	N22	3
id1016674	C/T	1	28478660	1.34	CC	TT	CC	CC	N22	N22	3
968772	T/G	1	29153943	3.07	TT	GG	TT	TT	N22	N22	3
971777	A/G	1	29250090	0.44	AA	AG	AA	AA	N22	N22	3
SNP-1.29586481.	C/A	1	29587527	1.53	CC	AA	CC	CC	N22	N22	3
SNP-1.29621768.	G/A	1	29622814	0.16	GG	AA	GG	GG	N22	N22	3
986948	G/A	1	29758130	0.62	GG	AA	GG	GG	N22	N22	3
1011161	G/A	1	30499880	3.37	GG	AA	GG	GG	N22	N22	3
id1018601	A/C	1	30853170	1.61	AA	CC	AA	AA	N22	N22	3
1027660	G/A	1	30970379	0.53	GG	AA	GG	GG	N22	N22	3
1040379	G/T	1	31474094	2.29	GG	TT	GG	GG	N22	N22	3
1058637	A/G	1	32090338	2.8	AA	GG	AA	AA	N22	N22	3
1059782	T/C	1	32141932	0.23	TT	CC	TT	TT	N22	N22	3
SNP-1.32376151.	G/A	1	32377196	1.07	GG	AA	GG	GG	N22	N22	3
1108154	G/T	1	33901317	6.93	GG	TT	GG	GG	N22	N22	3
1117341	G/A	1	34201543	1.36	GG	AA	GG	GG	N22	N22	3
1123262	A/C	1	34363755	0.74	AA	CC	AA	AA	N22	N22	3
1129633	A/G	1	34553900	0.86	AA	GG	AA	AA	N22	N22	3
1163456	G/T	1	35825579	5.78	GG	TT	GG	GG	N22	N22	3
1165109	T/C	1	35913322	0.4	TT	CC	TT	TT	N22	N22	3
SNP-1.36204066.	C/T	1	36205110	1.33	CC	TT	CC	CC	N22	N22	3
1176291	A/G	1	36251646	0.21	AA	GG	AA	AA	N22	N22	3
1189290	C/T	1	36734765	2.2	CC	TT	CC	CC	N22	N22	3
SNP-1.37415410.	A/G	1	37416454	3.1	AA	GG	AA	AA	N22	N22	3
1212517	C/T	1	37692801	1.26	CC	TT	CC	CC	N22	N22	3
id1023824	C/T	1	37725124	0.15	CC	TT	CC	CC	N22	N22	3
SNP-1.37834974.	C/T	1	37836018	0.5	CC	TT	CC	CC	N22	N22	3

Table 3.1. (Continued)

rs.	alleles	chrom	pos	cM	N22	SWARNA	IL4	IL6	gvIL4	gvIL6	Fragments
1237300	T/C	1	38652270	3.71	TT	CC	TT	TT	N22	N22	3
1238760	C/T	1	38706387	0.25	CC	TT	CC	CC	N22	N22	3
1240276	G/A	1	38760678	0.25	GG	AG	GG	GG	N22	N22	3
1243398	C/T	1	38847770	0.4	CC	TT	CC	CC	N22	N22	3
SNP-1.38961387.	A/G	1	38962431	0.52	AA	GG	AA	AA	N22	N22	3
SNP-1.38969685.	G/A	1	38970729	0.04	GG	AA	GG	GG	N22	N22	3
SNP-1.39020597.	T/A	1	39021641	0.23	TT	AA	TT	TT	N22	N22	3
1250974	G/A	1	39076741	0.25	GG	AA	GG	GG	N22	N22	3
SNP-1.39133884.	C/A	1	39134928	0.26	CC	AA	CC	CC	N22	N22	3
id1024973	G/A	1	39369209	1.06	GG	AA	GG	GG	N22	N22	3
1261519	A/G	1	39420824	0.23	AA	GG	AA	AA	N22	N22	3
1264940	C/A	1	39541771	0.55	CC	AA	CC	CC	N22	N22	3
SNP-1.39553792.	G/A	1	39554836	0.06	GG	AA	GG	GG	N22	N22	3
1265337	G/A	1	39556216	0.01	GG	AA	GG	GG	N22	N22	3
id1025292	A/C	1	39799820	1.11	AA	CC	AA	AA	N22	N22	3
1286531	C/T	1	40425312	2.84	CC	TT	CC	CC	N22	N22	3
1305247	C/T	1	41042727	2.81	CC	TT	CC	CC	N22	N22	3
id1026236	T/G	1	41065438	0.1	TT	GG	TT	TT	N22	N22	3
1306630	A/G	1	41089199	0.11	AA	GG	AA	AA	N22	N22	3
1319354	C/T	1	41538923	2.04	CC	TT	CC	CC	N22	N22	3
1323950	G/A	1	41726149	0.85	GG	AA	GG	GG	N22	N22	3
id1026832	C/T	1	41780923	0.25	CC	TT	CC	CC	N22	N22	3
SNP-1.41823942.	A/G	1	41824986	0.2	AA	GG	AA	AA	N22	N22	3
SNP-1.41889669.	C/T	1	41890713	0.3	CC	TT	CC	CC	N22	N22	3
1329596	G/A	1	41917762	0.12	GG	AA	GG	GG	N22	N22	3
1331935	C/T	1	41985829	0.31	CC	TT	CC	CC	N22	N22	3
1332365	T/C	1	41997238	0.05	TT	CC	TT	TT	N22	N22	3
SNP-1.42049603.	T/C	1	42050647	0.24	TT	CC	TT	TT	N22	N22	3
1344024	A/C	1	42397588	1.58	AA	CC	AA	AA	N22	N22	3
1344376	G/T	1	42408243	0.05	GG	TT	GG	GG	N22	N22	3
1345014	G/A	1	42425574	0.08	GG	AA	GG	GG	N22	N22	3
1347413	C/T	1	42492399	0.3	CC	TT	CC	CC	N22	N22	3
SNP-1.42818286.	G/A	1	42819331	1.49	GG	AA	GG	GG	N22	N22	3
SNP-1.43103895.	C/A	1	43104940	1.3	AC	CC	AC	AC	N22	N22	3
SNP-3.1358710.	A/G	3	1359713	0.4	AA	GG	AA	AA	N22	N22	4
2511880	G/T	3	1380055	0.09	GG	TT	GG	GG	N22	N22	4
2513833	C/T	3	1469412	0.41	CC	TT	CC	CC	N22	N22	4
2515335	C/T	3	1524051	0.25	CC	TT	CC	CC	N22	N22	4
id3000892	G/A	3	1640734	0.53	GG	AA	GG	GG	N22	N22	4
id3000913	G/A	3	1670761	0.14	GG	AA	GG	GG	N22	N22	4

Table 3.1. (Continued)

rs.	alleles	chrom	pos	cM	N22	SWARNA	IL4	IL6	gvIL4	gvIL6	Fragments
id3001137	A/C	3	2067580	1.8	AA	CC	AA	AA	N22	N22	4
2530217	A/G	3	2230854	0.74	AA	GG	AA	AA	N22	N22	4
2543372	A/G	3	2794807	2.56	AA	GG	AA	AA	N22	N22	4
2551624	T/C	3	3192451	1.81	TT	CC	TT	TT	N22	N22	4
id3001869	G/A	3	3484027	1.33	GG	AA	GG	GG	N22	N22	4
id3006195	G/A	3	12154662	4.16	GG	AA	GG	GG	N22	N22	5
id3006542	G/A	3	12694073	2.45	GG	AA	GG	GG	N22	N22	5
id3006790	C/T	3	13193644	2.27	CC	TT	CC	CC	N22	N22	5
2813329	G/A	3	13456686	1.2	GG	AA	GG	GG	N22	N22	5
2813334	T/C	3	13457112	0	TT	CC	TT	TT	N22	N22	5
id4000001	G/A	4	59946	0	GG	AA	GG	GG	N22	N22	6
id4000082	C/A	4	222177	0.74	CC	AA	CC	CC	N22	N22	6
SNP-4.266396.	T/G	4	267397	0.21	TT	GG	TT	TT	N22	N22	6
SNP-4.411921.	A/C	4	412924	0.66	AA	CC	AA	AA	N22	N22	6
SNP-4.437072.	T/A	4	438075	0.11	TT	AA	TT	TT	N22	N22	6
SNP-4.487171.	G/A	4	488174	0.23	GG	AG	AG	AG	N22	N22	6
SNP-4.658734.	T/C	4	659736	0.78	TT	CT	CT	CT	N22	N22	6
3606371	G/T	4	796549	0.62	GG	TT	GG	GG	N22	N22	6
ud4000058	A/T	4	856605	0.27	AA	TT	AA	AA	N22	N22	6
SNP-4.955413.	A/G	4	959862	0.47	AA	GG	AA	AA	N22	N22	6
id4000585	A/G	4	1022225	0.28	AA	GG	AA	AA	N22	N22	6
3619998	A/G	4	1047515	0.11	AA	GG	AA	AA	N22	N22	6
SNP-4.1707723.	C/G	4	1712175	3.02	CC	GG	CC	CC	N22	N22	6
3647009	G/A	4	1713004	0	GG	AA	GG	GG	N22	N22	6
3647133	A/G	4	1714897	0.01	AA	GG	AA	AA	N22	N22	6
SNP-4.1713540.	G/A	4	1717992	0.01	GG	AA	GG	GG	N22	N22	6
3647336	T/C	4	1718310	0	TT	CC	TT	TT	N22	N22	6
3647403	T/C	4	1719865	0.01	TT	CC	TT	TT	N22	N22	6
id4000869	T/G	4	1841708	0.55	TT	GG	TT	TT	N22	N22	6
wd4000229	C/T	4	2032639	0.87	CC	CT	CC	CC	N22	N22	6
3674743	A/G	4	2284046	1.14	AA	GG	AA	AA	N22	N22	6
3682819	T/G	4	2394889	0.5	TT	GG	TT	TT	N22	N22	6
SNP-4.2658232.	C/T	4	2662629	1.22	CT	CC	CT	CT	N22	N22	6
SNP-4.3249846.	T/C	4	3254244	2.69	TT	CC	TT	TT	N22	N22	6
SNP-4.3413760.	T/A	4	3418158	0.75	TT	AT	TT	TT	N22	N22	6
id4001482	C/T	4	3632546	0.97	CC	TT	CC	CC	N22	N22	6
SNP-4.3762512.	T/C	4	3766907	0.61	TT	CT	TT	TT	N22	N22	6
3780340	A/C	4	4053209	1.3	AA	CC	AA	AA	N22	N22	6
id4001963	G/A	4	4648133	2.7	GG	AA	GG	GG	N22	N22	6
3857681	G/A	4	5475158	3.76	GG	AA	GG	GG	N22	N22	6

Table 3.1. (Continued)

rs.	alleles	chrom	pos	cM	N22	SWARNA	IL4	IL6	gvIL4	gvIL6	Fragments
3921623	G/A	4	6835634	0.8	GG	AA	GG	GG	N22	N22	7
SNP-4_7299682	T/G	4	7304413	2.13	TT	GG	TT	TT	N22	N22	7
id4003259	G/A	4	9943752	5	GG	AA	GG	GG	N22	N22	8
4085815	C/T	4	11645506	7.74	CC	TT	CC	CC	N22	N22	8
SNP-4.11667412.	G/A	4	11676705	0.14	GG	AG	AG	AG	N22	N22	8
wd4001738	T/C	4	12297152	2.82	TT	CC	TT	TT	N22	N22	8
4112998	G/T	4	12370219	0.33	GG	TT	GT	NA	N22	N22	8
8784145	A/G	8	19380564	0.13	AA	GG	AA	AA	N22	N22	9
SNP-8.19541265.	G/A	8	19543979	0.74	AG	GG	AG	AG	N22	N22	9
SNP-8.19589245.	G/A	8	19591959	0.22	AA	GG	GG	GG	N22	N22	9
8803052	T/C	8	19807854	0.98	TT	CC	TT	TT	N22	N22	9
id8005359	C/A	8	19833397	0.12	CC	AA	CC	CC	N22	N22	9
8815450	C/T	8	20045845	0.97	TT	CC	NA	NA	N22	N22	9
8815799	T/C	8	20053642	0.04	TT	CC	TT	TT	N22	N22	9
SNP-8.20108950.	C/T	8	20111664	0.26	CC	TT	CC	CC	N22	N22	9
8822667	A/G	8	20213731	0.46	AG	AA	AA	AA	N22	N22	9
id8005525	G/A	8	20391635	0.81	GG	AA	GG	GG	N22	N22	9
8832534	G/A	8	20488257	0.44	GG	AA	GG	GG	N22	N22	9
8918570	T/C	8	23434376	5.61	TT	CC	TT	TT	N22	N22	10
8922165	T/C	8	23546811	0.51	TT	CC	TT	TT	N22	N22	10
8926819	G/A	8	23719048	0.78	GG	AA	GG	GG	N22	N22	10
id8006789	A/G	8	24125399	1.85	AG	AA	AG	AG	N22	N22	10
8938168	A/G	8	24205833	0.37	AA	GG	AA	AA	N22	N22	10
SNP-8.24280386.	G/T	8	24283101	0.35	GG	TT	GG	GG	N22	N22	10
SNP-8.25593253.	A/T	8	25595968	3.53	AA	TT	AA	AA	N22	N22	11
8983572	G/T	8	25757847	0.74	GG	TT	GG	GG	N22	N22	11
8990744	A/G	8	26038950	1.28	AA	GG	AA	AA	N22	N22	11
id9004168	C/A	9	14889045	1.09	CC	AA	CC	CC	N22	N22	12
9665317	A/G	9	15076425	0.85	AA	GG	AA	AA	N22	N22	12
id9004406	G/A	9	15322775	1.12	GG	AA	GG	GG	N22	N22	12
9677553	A/G	9	15446817	0.56	AA	GG	AA	AA	N22	N22	12
9680263	A/G	9	15510883	0.29	AA	GG	AA	AA	N22	N22	12
9688613	T/C	9	15752720	1.1	TT	CC	TT	TT	N22	N22	12
9711583	T/C	9	16505404	3.42	TT	CC	TT	TT	N22	N22	12
9712393	A/C	9	16532043	0.12	AA	CC	AA	AA	N22	N22	12
9722273	T/G	9	16838761	1.39	GT	TT	GT	GT	N22	N22	12
id9005502	G/A	9	17184526	1.57	GG	AA	GG	GG	N22	N22	12
9744557	A/G	9	17528366	1.56	AA	GG	AA	AA	N22	N22	12
9753048	T/C	9	17767194	1.09	TT	CC	TT	TT	N22	N22	12
id9006187	T/C	9	17924577	0.72	TT	CC	TT	TT	N22	N22	12

Table 3.1. (Continued)

rs.	alleles	chrom	pos	cM	N22	SWARNA	IL4	IL6	gvIL4	gvIL6	Fragments
9766886	A/G	9	18307070	1.15	AA	GG	AA	AA	N22	N22	13
id9006377	A/C	9	18366555	0.27	AA	CC	AA	AA	N22	N22	13
9775864	G/A	9	18648513	1.28	GG	AG	GG	GG	N22	N22	13
9776646	G/A	9	18670151	0.1	GG	AA	GG	GG	N22	N22	13
9793479	A/G	9	19208050	2.44	AA	GG	AA	AA	N22	N22	13
9796547	G/A	9	19322095	0.52	GG	AA	GG	GG	N22	N22	13
id9007001	C/T	9	19667346	1.57	CC	TT	CC	CC	N22	N22	13
9815257	A/G	9	19967561	1.36	AA	GG	AA	AA	N22	N22	13
9819278	C/A	9	20138665	0.78	CC	AA	CC	CC	N22	N22	13
9833069	C/A	9	20547765	1.86	CC	AA	CC	CC	N22	N22	13
10555615	A/G	10	14428360	1.55	AA	GG	AA	AA	N22	N22	14
SNP-10.14377038.	G/T	10	14448273	0.09	GG	TT	GG	GG	N22	N22	14
10559364	G/A	10	14559932	0.51	GG	AA	GG	GG	N22	N22	14
10563128	T/C	10	14651937	0.42	TT	CC	TT	TT	N22	N22	14
id10003885	A/G	10	14777004	0.57	AA	GG	AA	AA	N22	N22	14
10579252	G/T	10	15128247	1.6	GG	TT	GG	GG	N22	N22	14
10585903	G/A	10	15365576	1.08	GG	AA	GG	GG	N22	N22	14
10586997	G/A	10	15399261	0.15	GG	AA	GG	GG	N22	N22	14
10591126	G/A	10	15524547	0.57	GG	AA	GG	GG	N22	N22	14
10618874	G/T	10	16229530	3.2	GG	TT	GG	GG	N22	N22	14
10635878	G/T	10	16645172	1.89	GG	TT	GG	GG	N22	N22	14
10638230	G/A	10	16742656	0.44	GG	AA	GG	GG	N22	N22	14
10651050	G/A	10	17152794	1.86	GG	AA	GG	GG	N22	N22	14
id10004845	G/A	10	17179336	0.12	GG	AA	GG	GG	N22	N22	14
10659848	G/A	10	17397576	0.99	GG	AA	GG	GG	N22	N22	14
SNP-11.19713488.	C/T	11	20179567	0.48	CC	TT	CC	CC	N22	N22	15
11603884	G/A	11	20239426	0.27	AA	AG	GG	GG	N22	N22	15
11606526	A/G	11	20313437	0.34	AA	GG	AA	AA	N22	N22	15
12852637	A/G	12	20626088	4.76	AA	GG	AA	AA	N22	N22	16
12884255	T/C	12	21562147	3.51	TT	CC	TT	TT	N22	N22	16

Table 3.2. Information on introgressed chromosome segments and the differentially expressed genes in flag-leaf in the DTY-IL compared with Swarna under control and reproductive-drought stress conditions and overlapping *qDTY*'s in flag-leaf.

Introgressed fragment ID	Introgressed fragment position (bp)	DEG's located in the introgressed fragment	IL_drought vs Swarna_drought _flag leaf	*qDTY*s located in/near the introgressed fragment	Functional Annotation
fragment 1	22353686-24722142	LOC_Os01g39650	up		Programmed cell death protein 2, putative
Chr01		LOC_Os01g39670	down		OsFBD1 - F-box and FBD domain containing protein
		LOC_Os01g39770	down		Calcineurin B, putative, expressed
		LOC_Os01g39830	down		Beta-galactosidase, putative, expressed
		LOC_Os01g39840	up		Expressed protein
		LOC_Os01g39890	up		Transposon protein, putative, unclassified, expressed
		LOC_Os01g40260	up		OsWRKY77 - Superfamily of TFs having WRKY and zinc finger domains, expressed
		LOC_Os01g40280	down		Integral membrane protein, putative, expressed
		LOC_Os01g40560	up		Hypersensitive-induced response protein, putative
		LOC_Os01g40730	down		Hypothetical protein
		LOC_Os01g40830	down		Transposon protein, putative, Mutator sub-class
		LOC_Os01g40860	up		Aldehyde dehydrogenase, putative, expressed
		LOC_Os01g40870	up		Aldehyde dehydrogenase, putative, expressed
		LOC_Os01g40980	down		Helicase, putative, expressed
		LOC_Os01g41050	down		Sulfate transporter, putative, expressed
		LOC_Os01g41260	up		OsFBD2 - F-box and FBD domain containing protein
		LOC_Os01g41290	up		OsFBD5 - F-box and FBD domain containing protein
		LOC_Os01g41565	up		ATP-binding domain-containing protein, putative
		LOC_Os01g41710	up		Chlorophyll A-B binding protein, putative, expressed
		LOC_Os01g41770	down		Leucine rich repeat protein, putative, expressed
		LOC_Os01g41790	down		Hypothetical protein

Table 3.2. (Continued)

Introgressed fragment ID	Introgressed fragment position (bp)	DEG's located in the introgressed fragment	IL_drought vs Swarna_drought _flag leaf	*qDTY*s located in/near the introgressed fragment	Functional Annotation
		LOC_Os01g41810	down		Cytochrome P450 72A1, putative, expressed
		LOC_Os01g41820	down		Cytochrome P450 72A1, putative, expressed
		LOC_Os01g41850	down		Transposon protein, putative, unclassified
		LOC_Os01g41870	up		Protein kinase, putative, expressed
		LOC_Os01g41910	up		Receptor-like protein kinase 5 precursor, putative
		LOC_Os01g42070	down		Kinesin motor domain containing protein, putative
		LOC_Os01g42350	down		Pleiotropic drug resistance protein, putative; May be a general defense protein
		LOC_Os01g42860	down		Inhibitor I family protein, putative, expressed
		LOC_Os01g43080	up		Exonuclease, putative, expressed
		LOC_Os01g43230	up		Expressed protein
		LOC_Os01g43270	up		Hydroquinone glucosyltransferase, putative
fragment 2 Chr01	27047209-27330724	LOC_Os01g47370	up		MYB family transcription factor, putative, expressed
		LOC_Os01g47510	up		Retrotransposon protein, putative, unclassified
fragment 3 Chr01	28183638-43104940	LOC_Os01g49120	up		MATE efflux family protein, putative, expressed
		LOC_Os01g49160	down		MYB family transcription factor, putative, expressed
		LOC_Os01g49210	up		Expressed protein
		LOC_Os01g49560	down		Expressed protein
		LOC_Os01g49580	down		Protein kinase domain containing protein, expressed
		LOC_Os01g49614	up		Protein kinase domain containing protein, expressed
		LOC_Os01g50720	up		MYB family transcription factor, putative, expressed
		LOC_Os01g50730	up		Conserved hypothetical protein
		LOC_Os01g51020	up		60S ribosomal protein L28-1, putative, expressed

Table 3.2. (Continued)

Introgressed fragment ID	Introgressed fragment position (bp)	DEG's located in the introgressed fragment	IL_drought vs Swarna_drought _flag leaf	*qDTY*s located in/near the introgressed fragment	Functional Annotation
		LOC_Os01g51030	down		Expressed protein
		LOC_Os01g51400	up		Leucine Rich Repeat family protein, expressed
		LOC_Os01g51410	up		Glycine dehydrogenase, putative, expressed
		LOC_Os01g52010	up		Alliin lyase precursor, putative, expressed
		LOC_Os01g52230	up		Phosphoethanolamine/phosphocholine phosphatase, putative,expressed
		LOC_Os01g52240	up		Chlorophyll A-B binding protein, putative, expressed
		LOC_Os01g52690	down		Retrotransposon protein, putative, unclassified, expressed
		LOC_Os01g52730	down		DUF584 domain containing protein, putative, expressed
		LOC_Os01g52760	up		Expressed protein
		LOC_Os01g52864	down		Transmembrane protein, putative, expressed
		LOC_Os01g52980	down		OsFBX23 - F-box domain containing protein, expressed
		LOC_Os01g53090	down		Pathogen-related protein, putative, expressed
		LOC_Os01g53140	down		Expressed protein
		LOC_Os01g53255	down		Expressed protein
		LOC_Os01g53330	up		Anthocyanidin 5,3-O-glucosyltransferase, putative
		LOC_Os01g53370	up		Anthocyanidin 5,3-O-glucosyltransferase, putative
		LOC_Os01g53420	up		Anthocyanidin 5,3-O-glucosyltransferase, putative
		LOC_Os01g53460	up		Anthocyanidin 5,3-O-glucosyltransferase, putative
		LOC_Os01g53470	up		Harpin-induced protein 1 domain containing protein
		LOC_Os01g53560	up		Phosphoesterase, putative, expressed
		LOC_Os01g53630	up		Ulp1 protease family protein, putative, expressed
		LOC_Os01g53680	up		6-phosphofructokinase, putative, expressed
		LOC_Os01g53750	up		Glucan endo-1,3-beta-glucosidase precursor, putative,

Table 3.2. (Continued)

Introgressed fragment ID	Introgressed fragment position (bp)	DEG's located in the introgressed fragment	IL_drought vs Swarna_drought _flag leaf	*qDTY*s located in/near the introgressed fragment	Functional Annotation
		LOC_Os01g53800	up		Glutamate carboxypeptidase 2, putative, expressed
		LOC_Os01g53920	up		Receptor-like protein kinase 5 precursor, putative
		LOC_Os01g54030	down		NADP-dependent malic enzyme, putative, expressed
		LOC_Os01g54090	down		Expressed protein
		LOC_Os01g54190	up		Expressed protein
		LOC_Os01g54300	up		OsMan02 - Endo-Beta-Mannanase
		LOC_Os01g54424	up		Expressed protein
		LOC_Os01g54490	up		osFTL9 FT-Like9 homologous to Flowering Locus T gene
		LOC_Os01g54590	down		Ras-related protein, putative, expressed
		LOC_Os01g54740	up		Transposon protein, putative, unclassified, expressed
		LOC_Os01g54750	up		Conserved hypothetical protein
		LOC_Os01g54800	up		Hypothetical protein
		LOC_Os01g54980	up		Expressed protein
		LOC_Os01g55110	down		RING-H2 finger protein, putative, expressed
		LOC_Os01g55120	down		Conserved hypothetical protein
		LOC_Os01g55570	up		Expressed protein
		LOC_Os01g55620	up		Transposon protein, putative, unclassified
		LOC_Os01g55670	up		Expressed protein
		LOC_Os01g55750	up		TCP family transcription factor, putative, expressed
		LOC_Os01g55940	down		OsGH3.2 - Probable indole-3-acetic acid-amido synthetase,expressed
		LOC_Os01g55950	up		Acetamidase, putative, expressed
		LOC_Os01g56080	up		Expressed protein
		LOC_Os01g56220	down		Expressed protein
		LOC_Os01g56235	up		Expressed protein

Table 3.2. (Continued)

Introgressed fragment ID	Introgressed fragment position (bp)	DEG's located in the introgressed fragment	IL_drought vs Swarna_drought _flag leaf	*qDTY*s located in/near the introgressed fragment	Functional Annotation
		LOC_Os01g56330	up		TKL_IRAK_CrRLK1L-1.5 - The CrRLK1L-1 subfamily has homology to the CrRLK1L homolog
		LOC_Os01g56420	up		Ctr copper transporter family protein, putative, expressed
		LOC_Os01g56850	down		Expressed protein
		LOC_Os01g57370	down		Cyclic nucleotide-gated ion channel 2, putative, expressed
		LOC_Os01g57480	down		Serine/threonine-protein kinase receptor precursor, putative expressed
		LOC_Os01g57540	up		Protein kinase, putative, expressed
		LOC_Os01g57560	up		Serine/threonine-protein kinase receptor precursor, putative expressed
		LOC_Os01g57700	up		Membrane protein, putative, expressed
		LOC_Os01g57710	up		Membrane protein, putative, expressed
		LOC_Os01g57854	down		Pectinesterase, putative, expressed
		LOC_Os01g58000	up		ATP synthase epsilon chain, putative, expressed
		LOC_Os01g58020	up		Ribulose bisphosphate carboxylase large chain precursor, putative
		LOC_Os01g58240	up		OsSub6 - Putative Subtilisin homologue, expressed
		LOC_Os01g58280	up		OsSub8 - Putative Subtilisin homologue, expressed
		LOC_Os01g58290	up		OsSub9 - Putative Subtilisin homologue, expressed
		LOC_Os01g58330	up		Hypothetical protein
		LOC_Os01g58335	up		Expressed protein
		LOC_Os01g58340	down		Conserved hypothetical protein
		LOC_Os01g58640	down		Nucleotide pyrophosphatase/phosphodiesterase, putative, expressed
		LOC_Os01g58760	up		bZIP transcription factor domain containing protein
		LOC_Os01g58850	up		Circadian clock coupling factor-related, putative

Table 3.2. (Continued)

Introgressed fragment ID	Introgressed fragment position (bp)	DEG's located in the introgressed fragment	IL_drought vs Swarna_drought _flag leaf	*qDTY*s located in/near the introgressed fragment	Functional Annotation
		LOC_Os01g59000	down		Cytochrome P450, putative, expressed
		LOC_Os01g59350	up		Transcription factor, putative, expressed
		LOC_Os01g59570	up		Senescence-induced receptor-like serine/threonine-protein kinase precursor
		LOC_Os01g59720	up		Expressed protein
		LOC_Os01g60020	down		NAC domain transcription factor, putative, expressed
		LOC_Os01g60090	down		Retrotransposon protein, putative, unclassified
		LOC_Os01g60100	down		Transposon protein, putative, unclassified
		LOC_Os01g60340	down		NTMC2Type1.1 protein, putative
		LOC_Os01g60810	up		DUF623 domain containing protein, expressed
		LOC_Os01g61070	down		Heavy metal-associated domain containing protein
		LOC_Os01g61080	up		OsWRKY24 - Superfamily of TFs having WRKY and zinc finger domains, expressed
		LOC_Os01g61170	up		Prenylated rab acceptor, putative
		LOC_Os01g61200	down		GDSL-like lipase/acylhydrolase, putative, expressed
		LOC_Os01g61370	up		Expressed protein
		LOC_Os01g61440	up		Expressed protein
		LOC_Os01g61620	up		Protein kinase family protein, putative, expressed
		LOC_Os01g61700	down		ATP-dependent Clp protease adaptor protein ClpS containing protein
		LOC_Os01g61880	up		Respiratory burst oxidase, putative, expressed
		LOC_Os01g62200	up		Domain of unknown function DUF966 domain containing protein, expressed
		LOC_Os01g62380	up		Fasciclin-like arabinogalactan protein, putative, expressed
		LOC_Os01g62430	up		C2 domain containing protein, putative, expressed
		LOC_Os01g62450	up		Conserved hypothetical protein

Table 3.2. (Continued)

Introgressed fragment ID	Introgressed fragment position (bp)	DEG's located in the introgressed fragment	IL_drought vs Swarna_drought _flag leaf	*qDTY*s located in/near the introgressed fragment	Functional Annotation
		LOC_Os01g62490	up		Laccase precursor protein, putative, expressed
		LOC_Os01g62570	up		ATP/GTP/Ca++ binding protein, putative
		LOC_Os01g62584	up		Peptidase aspartic family protein, putative, expressed
		LOC_Os01g62740	down		Expressed protein
		LOC_Os01g62750	down		Expressed protein
		LOC_Os01g62770	down		Expressed protein
		LOC_Os01g62810	down		Regulator of chromosome condensation, putative
		LOC_Os01g62900	down		Amino acid kinase, putative, expressed
		LOC_Os01g63240	up		Reticulon domain containing protein, putative, expressed
		LOC_Os01g63690	up		Hs1, putative, expressed
		LOC_Os01g63930	up		Cytochrome P450, putative, expressed
		LOC_Os01g64100	up		Glycosyl hydrolase, putative, expressed
		LOC_Os01g64270	up		Expressed protein
		LOC_Os01g64440	up		Expressed protein
		LOC_Os01g64660	up		Fructose-1,6-bisphosphatase, putative, expressed
		LOC_Os01g64670	down		Soluble inorganic pyrophosphatase, putative, expressed
		LOC_Os01g64920	up		Nuclear matrix protein 1, putative, expressed
		LOC_Os01g65030	up		S-locus-specific glycoprotein precursor, putative
		LOC_Os01g65080	up		ZOS1-18 - C2H2 zinc finger protein, expressed
		LOC_Os01g65150	down		Proton-dependent oligopeptide transport, putative
		LOC_Os01g65420	down		Expressed protein
		LOC_Os01g65630	up		Expressed protein
		LOC_Os01g65650	up		Receptor-like protein kinase HAIKU2 precursor, putative,expressed
		LOC_Os01g65660	down		Amino acid transporter, putative, expressed

Table 3.2. (Continued)

Introgressed fragment ID	Introgressed fragment position (bp)	DEG's located in the introgressed fragment	IL_drought vs Swarna_drought _flag leaf	*qDTY*s located in/near the introgressed fragment	Functional Annotation
		LOC_Os01g66180	**up**	***qDTY1.1***	**Cytochrome c, putative, expressed**
		LOC_Os01g66240	**down**	***qDTY1.1***	**Mitochondrion protein, putative, expressed**
		LOC_Os01g66440	**up**	***qDTY1.1***	**Hypothetical protein**
		LOC_Os01g66690	**down**	***qDTY1.1***	**ZIP4/SPO22, putative, expressed**
		LOC_Os01g66720	**up**	***qDTY1.1***	**NADP-dependent oxidoreductase, putative, expressed**
		LOC_Os01g66810	**up**	***qDTY1.1***	**Conserved hypothetical protein**
		LOC_Os01g67070	down		Hypothetical protein
		LOC_Os01g67160	down		Cyclin-dependent kinase B1-1, putative, expressed
		LOC_Os01g67190	down		Ribonuclease T2 family domain containing protein
		LOC_Os01g67314	up		Expressed protein
		LOC_Os01g67520	up		VTC2, putative, expressed
		LOC_Os01g67540	up		AMP-binding domain containing protein, expressed
		LOC_Os01g68290	down		Expressed protein
		LOC_Os01g69200	up		Regulatory protein, putative, expressed
		LOC_Os01g69840	up		Expressed protein
		LOC_Os01g69960	up		Expressed protein
		LOC_Os01g70110	up		No apical meristem protein, putative, expressed
		LOC_Os01g70260	up		Receptor-like protein kinase 2 precursor, putative
		LOC_Os01g70280	down		Hypothetical protein
		LOC_Os01g70500	down		Expressed protein
		LOC_Os01g70520	down		Os1bglu5 - beta-glucosidase homologue, similar to G. max isohydroxyurate hydrolase
		LOC_Os01g70720	down		Expressed protein
		LOC_Os01g70730	up		Flowering promoting factor-like 1, putative, expressed
		LOC_Os01g70830	up		Esterase PIR7A, putative, expressed

Table 3.2. (Continued)

Introgressed fragment ID	Introgressed fragment position (bp)	DEG's located in the introgressed fragment	IL_drought vs Swarna_drought _flag leaf	*qDTY*s located in/near the introgressed fragment	Functional Annotation
		LOC_Os01g70850	up		Esterase, putative, expressed
		LOC_Os01g70930	up		Leucoanthocyanidin dioxygenase, putative, expressed
		LOC_Os01g71094	up		Basic 7S globulin 2 precursor, putative, expressed
		LOC_Os01g71340	up		Glycosyl hydrolases family 17, putative, expressed
		LOC_Os01g71700	up		Amino acid permease family protein, putative, expressed
		LOC_Os01g71710	down		Amino acid permease family protein, putative, expressed
		LOC_Os01g71740	up		Amino acid permease family protein, putative, expressed
		LOC_Os01g71760	up		Amino acid permease family protein, putative
		LOC_Os01g71790	up		NAM, putative, expressed
		LOC_Os01g72120	up		Glutathione S-transferase, putative, expressed
		LOC_Os01g72130	up		Glutathione S-transferase, putative, expressed
		LOC_Os01g72170	up		Glutathione S-transferase, putative, expressed
		LOC_Os01g72230	up		Stromal membrane-associated protein, putative,
		LOC_Os01g72270	down		Cytochrome P450, putative, expressed
		LOC_Os01g72360	up		Expressed protein
		LOC_Os01g72390	down		NBS type disease resistance protein, putative
		LOC_Os01g72490	down		LRP1, putative, expressed
		LOC_Os01g72520	up		Phosphoesterase family protein, putative, expressed
		LOC_Os01g72570	down		Expressed protein
		LOC_Os01g72940	up		Phosphatidylserine decarboxylase, putative, expressed
		LOC_Os01g73170	up		Peroxidase precursor, putative, expressed
		LOC_Os01g73220	down		Peroxidase precursor, putative, expressed
		LOC_Os01g73290	up		Hypothetical protein
		LOC_Os01g73310	up		Actin, putative, expressed

Table 3.2. (Continued)

Introgressed fragment ID	Introgressed fragment position (bp)	DEG's located in the introgressed fragment	IL_drought vs Swarna_drought _flag leaf	*qDTY*s located in/near the introgressed fragment	Functional Annotation
		LOC_Os01g73644	up		Expressed protein
		LOC_Os01g73650	up		Hypothetical protein
		LOC_Os01g73656	up		Expressed protein
		LOC_Os01g73670	up		Expressed protein
		LOC_Os01g74020	down		MYB family transcription factor, putative, expressed
		LOC_Os01g74110	up		Metal cation transporter, putative, expressed
		LOC_Os01g74300	up		Metallothionein, putative, expressed
fragment 1 Chr03	1359713-3484027	**LOC_Os03g03300**	**down**	***qDTY3.2***	**Expressed protein**
		LOC_Os03g03490	**up**	***qDTY3.2***	**Expressed protein**
		LOC_Os03g03600	up		Fasciclin-like arabinogalactan protein, putative
		LOC_Os03g03724	up		Expressed protein
		LOC_Os03g03730	down		Regulatory protein, putative, expressed
		LOC_Os03g03750	down		Hypothetical protein
		LOC_Os03g03790	up		AMP-binding domain containing protein, expressed
		LOC_Os03g03880	down		Protein kinase, putative, expressed
		LOC_Os03g04070	up		No apical meristem protein, putative, expressed
		LOC_Os03g04720	down		Retrotransposon protein, putative, unclassified
		LOC_Os03g05049	down		Expressed protein
		LOC_Os03g05100	down		Expressed protein
		LOC_Os03g05130	down		Hypothetical protein
		LOC_Os03g05270	up		RING finger and CHY zinc finger domain-containing protein 1, putative, expressed
		LOC_Os03g05530	up		Nodulin, putative, expressed
		LOC_Os03g05620	up		Inorganic phosphate transporter, putative, expressed

Table 3.2. (Continued)

Introgressed fragment ID	Introgressed fragment position (bp)	DEG's located in the introgressed fragment	IL_drought vs Swarna_drought _flag leaf	*qDTY*s located in/near the introgressed fragment	Functional Annotation
		LOC_Os03g05870	up		Fe-S metabolism associated domain containing protein, expressed
		LOC_Os03g05890	up		Hypothetical protein
		LOC_Os03g05910	up		Expressed protein
		LOC_Os03g05920	up		Expressed protein
		LOC_Os03g06460	up		Type I inositol-1,4,5-trisphosphate 5-phosphatase
		LOC_Os03g06835	up		Expressed protein
		LOC_Os03g06860	up		Transposon protein, putative, unclassified, expressed
fragment 2 Chr03	12154662-13457112	LOC_Os03g21400	up		Cytochrome P450, putative, expressed
		LOC_Os03g21450	down		Bromodomain domain containing protein, expressed
		LOC_Os03g21500	up		Hypothetical protein
		LOC_Os03g21620	down		AGC_AGC_other_RS6K_like.1 - ACG kinases include homologs to PKA, PKG and PKC
		LOC_Os03g21820	up		Expansin precursor, putative, expressed
		LOC_Os03g21900	up		Uroporphyrinogen decarboxylase, putative, expressed
		LOC_Os03g22040	up		Expressed protein
		LOC_Os03g22060	up		Uroporphyrinogen decarboxylase, putative, expressed
		LOC_Os03g22120	down		Sucrose synthase, putative, expressed
		LOC_Os03g22220	down		Retrotransposon protein, putative, unclassified
		LOC_Os03g22230	up		POEI47 - Pollen Ole e I allergen and extensin family protein precursor, expressed
		LOC_Os03g22250	down		POEI48 - Pollen Ole e I allergen and extensin family protein precursor, putative
		LOC_Os03g22370	up		ultraviolet-B-repressible protein, putative, expressed

Table 3.2. (Continued)

Introgressed fragment ID	Introgressed fragment position (bp)	DEG's located in the introgressed fragment	IL_drought vs Swarna_drought _flag leaf	*qDTY*s located in/near the introgressed fragment	Functional Annotation
fragment 1 Chr04	59946-5475158	LOC_Os03g22634	up		Terpene synthase, putative, expressed
		LOC_Os03g22680	down		RING finger and CHY zinc finger domain-containing protein 1, putative, expressed
		LOC_Os04g02120	up		Expressed protein
		LOC_Os04g02450	down		Rust-resistance protein Lr21, putative
		LOC_Os04g02600	up		Retrotransposon protein, putative, LINE subclass
		LOC_Os04g02754	up		Amidase family protein, putative, expressed
		LOC_Os04g02860	up		Disease resistance protein RPM1, putative
		LOC_Os04g02960	up		OsSub32 - Putative Subtilisin homologue
		LOC_Os04g02970	up		Subtilisin-like protease precursor, putative, expressed
		LOC_Os04g03050	up		OsSub34 - Putative Subtilisin homologue, expressed
		LOC_Os04g03120	up		Retrotransposon protein, putative, unclassified
		LOC_Os04g03180	up		Disease resistance protein, putative, expressed
		LOC_Os04g03796	up		OsSub37 - Putative Subtilisin homologue, expressed
		LOC_Os04g03810	up		OsSub38 - Putative Subtilisin homologue, expressed
		LOC_Os04g03850	down		OsSub39 - Putative Subtilisin homologue
		LOC_Os04g03910	up		Conserved hypothetical protein
		LOC_Os04g04040	down		Hypothetical protein
		LOC_Os04g04060	down		Dynamin family protein, putative, expressed
		LOC_Os04g04320	down		Expressed protein
		LOC_Os04g05490	down		Conserved hypothetical protein
		LOC_Os04g05750	up		Hypothetical protein
		LOC_Os04g05770	up		Conserved hypothetical protein

Table 3.2. (Continued)

Introgressed fragment ID	Introgressed fragment position (bp)	DEG's located in the introgressed fragment	IL_drought vs Swarna_drought _flag leaf	*qDTY*s located in/near the introgressed fragment	Functional Annotation
		LOC_Os04g06300	up		Expressed protein
		LOC_Os04g06590	down		Expressed protein
		LOC_Os04g07160	up		Transposon protein, putative, CACTA, En/Spm sub-class
		LOC_Os04g08170	up		CBL-interacting protein kinase, putative
		LOC_Os04g08180	down		Expressed protein
		LOC_Os04g08190	down		Expressed protein
		LOC_Os04g08200	down		Conserved hypothetical protein
		LOC_Os04g08550	up		Oxidoreductase, aldo/keto reductase family protein, putative, expressed
		LOC_Os04g08828	up		Cytochrome P450, putative, expressed
		LOC_Os04g09430	up		Cytochrome P450, putative, expressed
		LOC_Os04g09900	up		Ent-kaurene synthase, chloroplast precursor, putative
		LOC_Os04g09920	up		Cytochrome P450, putative, expressed
		LOC_Os04g10000	up		Sex determination protein tasselseed-2, putative
fragment 2 Chr04	6835634-7304413	LOC_Os04g12390	down		Transposon protein, putative, CACTA, En/Spm sub-class
		LOC_Os04g12540	down		Receptor-like protein kinase, putative, expressed
		LOC_Os04g12580	down		Receptor-like protein kinase, putative
fragment 3 Chr04	9943752-12370219	LOC_Os04g18680	up		Retrotransposon protein, putative, unclassified
		LOC_Os04g18790	down		OsFBX126 - F-box domain containing protein
		LOC_Os04g18800	down		Conserved hypothetical protein
		LOC_Os04g19670	down		Retrotransposon protein, putative, Ty3-gypsy subclass
		LOC_Os04g19740	down		Transketolase, chloroplast precursor, putative
		LOC_Os04g20070	up		Tropinone reductase 2, putative, expressed

Table 3.2. (Continued)

Introgressed fragment ID	Introgressed fragment position (bp)	DEG's located in the introgressed fragment	IL_drought vs Swarna_drought _flag leaf	*qDTY*s located in/near the introgressed fragment	Functional Annotation
		LOC_Os04g20330	up		UDP-glucoronosyl/UDP-glucosyl transferase, putative
		LOC_Os04g20600	down		Hypothetical protein
		LOC_Os04g20749	down		Expressed protein
		LOC_Os04g20960	up		Expressed protein
		LOC_Os04g21150	up		Retrotransposon protein, putative, Ty3-gypsy subclass
		LOC_Os04g21350	up		Flowering promoting factor-like 1, putative, expressed
fragment 1	19351882-20488257	LOC_Os08g31410	up		Sulfate transporter, putative, expressed
Chr08		LOC_Os08g31630	down		Uncharacterized glycosyl hydrolase Rv2006/MT2062, putative, expressed
		LOC_Os08g31670	up		Transporter, putative, expressed
		LOC_Os08g31830	up		UPF0041 domain containing protein, putative, expressed
		LOC_Os08g31850	down		Expressed protein
		LOC_Os08g31910	up		Expressed protein
		LOC_Os08g31980	down		Trehalose-6-phosphate synthase, putative, expressed
		LOC_Os08g32130	up		Heat shock protein DnaJ, putative, expressed
		LOC_Os08g32160	down		Oxidoreductase, 2OG-FeII oxygenase domain c ontaining protein, putative
		LOC_Os08g32300	down		Retrotransposon protein, putative, unclassified
		LOC_Os08g32310	down		Expressed protein
		LOC_Os08g32350	down		Expressed protein
		LOC_Os08g32500	down		Nucleobase-ascorbate transporter, putative, expressed
		LOC_Os08g32540	down		Cyclin, putative, expressed
		LOC_Os08g32550	down		Conserved hypothetical protein

Table 3.2. (Continued)

Introgressed fragment ID	Introgressed fragment position (bp)	DEG's located in the introgressed fragment	IL_drought vs Swarna_drought _flag leaf	*qDTY*s located in/near the introgressed fragment	Functional Annotation
fragment 2 Chr08	23434376-24283101	LOC_Os08g32570	up		Expressed protein
		LOC_Os08g32590	down		Retrotransposon protein, putative, Ty1-copia subclass
		LOC_Os08g33010	down		OsFBDUF45 - F-box and DUF domain containing protein
		LOC_Os08g37115	down		Expressed protein
		LOC_Os08g37300	up		Expressed protein
		LOC_Os08g37390	up		Cyclin, putative, expressed
		LOC_Os08g37470	up		2-aminoethanethiol dioxygenase, putative, expressed
		LOC_Os08g37570	up		Spotted leaf 11, putative, expressed
		LOC_Os08g37690	down		Expressed protein
		LOC_Os08g37940	up		HAD-superfamily hydrolase subfamily IA, variant 3 putative, expressed
		LOC_Os08g37970	up		MYB family transcription factor, putative, expressed
		LOC_Os08g38020	down		bZIP transcription factor domain containing protein
		LOC_Os08g38040	down		Transposon protein, putative, unclassified
		LOC_Os08g38100	up		LTPL131 - Protease inhibitor/seed storage/LTP family protein precursor, putative
		LOC_Os08g38130	down		cytokinin-O-glucosyltransferase 1, putative
		LOC_Os08g38160	up		cytokinin-O-glucosyltransferase, putative
		LOC_Os08g38270	up		Fasciclin domain containing protein, expressed
		LOC_Os08g38320	down		AGC_PVPK_like_kin82y.14 - ACG kinases include homologs to PKA, PKG and PKC, expressed
fragment 3 Chr08	25595968-26038950	LOC_Os08g40590	down		Oxysterol-binding protein, putative, expressed
		LOC_Os08g40615	down		Expressed protein

Table 3.2. (Continued)

Introgressed fragment ID	Introgressed fragment position (bp)	DEG's located in the introgressed fragment	IL_drought vs Swarna_drought _flag leaf	*qDTY*s located in/near the introgressed fragment	Functional Annotation
fragment 1 Chr09	14889045-17924577	LOC_Os08g40680	up		Glycosyl hydrolase, putative, expressed
		LOC_Os08g40700	down		Retrotransposon protein, putative, unclassified, expressed
		LOC_Os08g40820	down		Expressed protein
		LOC_Os08g40850	down		Mitochondrial carrier protein, putative, expressed
		LOC_Os08g41080	down		Expressed protein
		LOC_Os09g25100	up		CAMK_KIN1/SNF1/Nim1_like.35 - CAMK includes calcium/calmodulin depedent protein kinases
		LOC_Os09g25610	up		Class I glutamine amidotransferase, putative, expressed
		LOC_Os09g25690	up		Retrotransposon protein, putative, unclassified
		LOC_Os09g25720	up		Glycine-rich cell wall structural protein 2 precursor, putative, expressed
		LOC_Os09g25740	up		Expressed protein
		LOC_Os09g25770	down		Auxin-induced protein 5NG4, putative, expressed
		LOC_Os09g25945	down		Expressed protein
		LOC_Os09g26000	down		Glutamate receptor, putative
		LOC_Os09g26210	up		ZOS9-12 - C2H2 zinc finger protein, expressed
		LOC_Os09g26240	up		Transposon protein, putative, CACTA, En/Spm sub-class
		LOC_Os09g26260	down		AAA-type ATPase family protein, putative, expressed
		LOC_Os09g26270	up		Hypothetical protein
		LOC_Os09g26370	up		DUF581 domain containing protein, expressed
		LOC_Os09g26880	down		Aldehyde dehydrogenase, putative, expressed
		LOC_Os09g26890	up		Expressed protein
		LOC_Os09g27050	down		HD domain containing protein, putative, expressed
		LOC_Os09g27450	up		Homeobox associated leucine zipper, putative, expressed; Probable transcription factor

Table 3.2. (Continued)

Introgressed fragment ID	Introgressed fragment position (bp)	DEG's located in the introgressed fragment	IL_drought vs Swarna_drought _flag leaf	*qDTY*s located in/near the introgressed fragment	Functional Annotation
		LOC_Os09g27680	down		Expressed protein
		LOC_Os09g27750	down		1-aminocyclopropane-1-carboxylate oxidase 1, putative, expressed
		LOC_Os09g27920	down		Conserved hypothetical protein
		LOC_Os09g27940	up		Aspartic proteinase nepenthesin-1 precursor, putative
		LOC_Os09g27980	up		emp24/gp25L/p24 family protein, putative, expressed
		LOC_Os09g28230	up		Gibberellin receptor GID1L2, putative, expressed
		LOC_Os09g28500	up		EF hand family protein, putative, expressed
		LOC_Os09g28550	up		Hypothetical protein; Negative regulator of brassinosteroid signaling
		LOC_Os09g28640	up		Gibberellin receptor GID1L2, putative, expressed
		LOC_Os09g28650	up		Gibberellin receptor, putative, expressed
		LOC_Os09g28690	up		Gibberellin receptor GID1L2, putative, expressed
		LOC_Os09g28720	up		Alpha/beta hydrolase fold, putative, expressed
		LOC_Os09g29130	up		ZF-HD protein dimerisation region containing protein, expressed; Putative transcription factor
		LOC_Os09g29200	up		Glutathione S-transferase, putative, expressed
		LOC_Os09g29270	down		Expressed protein
fragment 2 Chr09	18307070-20547765	LOC_Os09g30120	up		CSLE1 - cellulose synthase-like family E, expressed
		LOC_Os09g30180	down		OsFBX331 - F-box domain containing protein, expressed
		LOC_Os09g30200	down		ATP binding protein, putative, expressed
		LOC_Os09g30340	up		Photosystem I reaction center subunit, chloroplast precursor, putative, expressed
		LOC_Os09g30360	up		caffeoyl-CoA O-methyltransferase, putative, expressed
		LOC_Os09g30414	up		Aspartic proteinase nepenthesin-2 precursor, putative

Table 3.2. (Continued)

Introgressed fragment ID	Introgressed fragment position (bp)	DEG's located in the introgressed fragment	IL_drought vs Swarna_drought _flag leaf	*qDTY*s located in/near the introgressed fragment	Functional Annotation
		LOC_Os09g30458	down		Subtilisin-like protease, putative, expressed
		LOC_Os09g30510	down		Glucosyl transferase, putative, expressed
		LOC_Os09g30980	down		UDP-glucoronosyl and UDP-glucosyl transferase domain containing protein, expressed
		LOC_Os09g31040	down		EF hand family protein, putative, expressed
		LOC_Os09g31050	down		Cytosolic phospholipase A2 beta, putative, expressed
		LOC_Os09g31478	down		Auxin efflux carrier component, putative, expressed
		LOC_Os09g31490	down		Reductase, putative, expressed
		LOC_Os09g31502	up		Dehydrogenase, putative, expressed
		LOC_Os09g31506	up		Dihydroflavonol-4-reductase, putative, expressed
		LOC_Os09g32010	down		Ternary complex factor MIP1, putative, expressed
		LOC_Os09g32095	down		Expressed protein
		LOC_Os09g32150	down		Expressed protein
		LOC_Os09g32290	up		FAD dependent oxidoreductase domain containing protein, expressed
		LOC_Os09g32310	up		Expressed protein
		LOC_Os09g32320	up		Growth regulator related protein, putative, expressed
		LOC_Os09g32410	up		OsFBX333 - F-box domain containing protein, expressed
		LOC_Os09g32470	up		Membrane protein, putative, expressed
		LOC_Os09g32540	up		Expressed protein
		LOC_Os09g32620	up		Dehydrogenase, putative, expressed
		LOC_Os09g32670	up		UDP-glucuronate 4-epimerase, putative, expressed
		LOC_Os09g33620	up		Leucine Rich Repeat domain containing protein
		LOC_Os09g33740	up		Zinc finger, ZZ type domain containing protein
		LOC_Os09g33780	down		Expressed protein

Table 3.2. (Continued)

Introgressed fragment ID	Introgressed fragment position (bp)	DEG's located in the introgressed fragment	IL_drought vs Swarna_drought _flag leaf	*qDTY*s located in/near the introgressed fragment	Functional Annotation
		LOC_Os09g33850	up		osFTL4 FT-Like4 homologous to Flowering Locus T gene
		LOC_Os09g33876	up		Expressed protein
		LOC_Os09g33920	up		Expressed protein
		LOC_Os09g33930	up		Farnesyltransferase/geranylgeranyltransferase type-1 subunitalpha, putative, expressed
		LOC_Os09g33992	down		Expressed protein
		LOC_Os09g34120	down		Expressed protein
		LOC_Os09g34150	up		NBS-LRR disease resistance protein, putative, expressed
		LOC_Os09g34160	up		Resistance protein, putative, expressed
		LOC_Os09g34190	up		Acyl-coenzyme A thioesterase 10, mitochondrial precursor, putative, expressed
		LOC_Os09g34214	up		UDP-glucoronosyl and UDP-glucosyl transferase domain containing protein, expressed
		LOC_Os09g34250	up		UDP-glucoronosyl and UDP-glucosyl transferase domain containing protein, expressed
		LOC_Os09g34340	down		Expressed protein
		LOC_Os09g34890	up		Expressed protein
		LOC_Os09g34920	up		Glycosyl hydrolase family 29, putative, expressed
		LOC_Os09g34960	down		hydroxymethylglutaryl-CoA synthase, putative, expressed
		LOC_Os09g35010	up		Dehydration-responsive element-binding protein, putative, expressed
		LOC_Os09g35020	up		AP2 domain containing protein, expressed
		LOC_Os09g35580	up		Conserved hypothetical protein
		LOC_Os09g35620	up		Conserved hypothetical protein
fragment 1	14428360-17397576	LOC_Os10g28050	up		Chitinase 2, putative, expressed

Table 3.2. (Continued)

Introgressed fragment ID	Introgressed fragment position (bp)	DEG's located in the introgressed fragment	IL_drought vs Swarna_drought _flag leaf	*qDTY*s located in/near the introgressed fragment	Functional Annotation
		LOC_Os10g28120	down		Glycosyl hydrolase, putative, expressed
		LOC_Os10g28310	down		Retrotransposon protein, putative, unclassified
		LOC_Os10g28560	down		Expressed protein
		LOC_Os10g28590	down		CAF1 family ribonuclease containing protein
		LOC_Os10g28850	down		Retrotransposon protein, putative, unclassified
		LOC_Os10g28870	down		MBTB40 - Bric-a-Brac, Tramtrack
		LOC_Os10g29090	down		Retrotransposon protein, putative, unclassified
		LOC_Os10g29502	up		Expressed protein
		LOC_Os10g29570	down		Late embryogenesis abundant protein D-34, putative
		LOC_Os10g30070	up		Sodium/calcium exchanger protein, putative, expressed
		LOC_Os10g30080	up		Xylosyltransferase, putative, expressed
		LOC_Os10g30090	up		Amino acid permease, putative, expressed
		LOC_Os10g30210	down		Expressed protein
		LOC_Os10g30410	up		Cytochrome P450 71D7, putative, expressed
		LOC_Os10g30880	up		Expressed protein
		LOC_Os10g31780	up		Oxidoreductase, short chain dehydrogenase/reductase family domain containing protein
		LOC_Os10g31940	up		Inosine triphosphate pyrophosphatase, putative, expressed
		LOC_Os10g32470	down		Expressed protein
		LOC_Os10g32520	down		Expressed protein
		LOC_Os10g32600	up		MYB family transcription factor, putative
		LOC_Os10g32710	down		WD domain, G-beta repeat domain containing protein
		LOC_Os10g32740	down		Zinc finger family protein, putative, expressed
		LOC_Os10g32800	down		Hypothetical protein

Table 3.2. (Continued)

Introgressed fragment ID	Introgressed fragment position (bp)	DEG's located in the introgressed fragment	IL_drought vs Swarna_drought _flag leaf	*qDTY*s located in/near the introgressed fragment	Functional Annotation
		LOC_Os10g33104	down		Expressed protein
		LOC_Os10g33130	down		Leucine-rich repeat receptor protein kinase EXS precursor, putative, expressed
		LOC_Os10g33190	up		Expressed protein
fragment 1	20179567-20313437	LOC_Os11g34624	up		TKL_IRAK_DUF26-lc.29 - DUF26 kinases have homology to DUF26 containing loci
Chr11		LOC_Os11g34650	up		Hypothetical protein
fragment 1	20626088-21562147	LOC_Os12g35239	up		Transposon protein, putative, CACTA, En/Spm sub-class
Chr12		LOC_Os12g35460	down		Retrotransposon protein, putative, unclassified, expressed

IL = DTY-IL; Swa = Swarna; D = Drought; C = Control

Table 3.3. Information on introgressed chromosome segments and the differentially expressed genes in flag-leaf in the DTY-IL compared with Swarna under control and reproductive-drought stress conditions and overlapping *qDTY*'s in panicle.

Introgressed fragment ID	Introgressed fragment position (bp)	DEG's located in the introgressed fragment	IL_drought vs Swarna_drought_panicle	*qDTY*s located in/near the introgressed fragment	Functional Annotation
fragment 1 Chr01	22353686-24722142	LOC_Os01g39650	up		Programmed cell death protein 2, putative
		LOC_Os01g39670	down		OsFBD1 - F-box and FBD domain containing protein, expressed
		LOC_Os01g39840	up		Expressed protein
		LOC_Os01g39970	down		Protein kinase domain containing protein, putative, expressed
		LOC_Os01g40120	up		Expressed protein
		LOC_Os01g40550	down		Hsp20/alpha crystallin family protein, putative, expressed
		LOC_Os01g40730	down		Hypothetical protein
		LOC_Os01g40870	up		Aldehyde dehydrogenase, putative, expressed
		LOC_Os01g40940	down		Hypothetical protein
		LOC_Os01g41180	up		THION19 - Plant thionin family protein precursor, putative
		LOC_Os01g41260	up		OsFBD2 - F-box and FBD domain containing protein
		LOC_Os01g41280	up		OsFBD4 - F-box and FBD domain containing protein, expressed
		LOC_Os01g41290	up		OsFBD5 - F-box and FBD domain containing protein, expressed
		LOC_Os01g41310	up		OsFBX18 - F-box domain containing protein, expressed
		LOC_Os01g41360	up		Expressed protein
		LOC_Os01g41370	up		FBD domain containing protein, putative, expressed
		LOC_Os01g41430	up		UDP-glucoronosyl and UDP-glucosyl transferase, putative
		LOC_Os01g41450	down		UDP-glucoronosyl and UDP-glucosyl transferase domain
		LOC_Os01g41565	up		ATP-binding domain-containing protein, putative
		LOC_Os01g41770	down		Leucine rich repeat protein, putative, expressed
		LOC_Os01g41870	up		Protein kinase, putative, expressed

Table 3.3. (Continued)

Introgressed fragment ID	Introgressed fragment position (bp)	DEG's located in the introgressed fragment	IL_drought vs Swarna_drought_panicle	*qDTY*s located in/near the introgressed fragment	Functional Annotation
		LOC_Os01g41910	up		Receptor-like protein kinase 5 precursor, putative
		LOC_Os01g42370	up		Pleiotropic drug resistance protein, putative, expressed; May be general defense protein
		LOC_Os01g42400	up		STE_MEK_ste7_MAP2K.3 - STE kinases include homologs
		LOC_Os01g42780	up		Cysteine proteinase EP-B 2 precursor, putative
fragment 2 Chr01	27047209-27330724	LOC_Os01g47510	up		Retrotransposon protein, putative, unclassified
		LOC_Os01g47610	down		Lipase class 3 family protein, putative, expressed
		LOC_Os01g47710	down		Homeobox domain containing protein, expressed
fragment 3 Chr01	28183638-43104940	LOC_Os01g49120	up		MATE efflux family protein, putative, expressed
		LOC_Os01g49154	down		Expressed protein
		LOC_Os01g49200	up		Microtubule associated protein, putative, expressed
		LOC_Os01g49260	down		Expressed protein
		LOC_Os01g49280	down		Zinc finger family protein, putative, expressed
		LOC_Os01g49614	up		Protein kinase domain containing protein, expressed
		LOC_Os01g49730	up		Expressed protein
		LOC_Os01g50280	down		Expressed protein
		LOC_Os01g50300	down		Hypothetical protein
		LOC_Os01g50730	up		Conserved hypothetical protein
		LOC_Os01g50780	up		Hypothetical protein
		LOC_Os01g50940	up		Helix-loop-helix DNA-binding domain containing protein
		LOC_Os01g51020	up		60S ribosomal protein L28-1, putative, expressed
		LOC_Os01g51410	up		Glycine dehydrogenase, putative, expressed

Table 3.3. (Continued)

Introgressed fragment ID	Introgressed fragment position (bp)	DEG's located in the introgressed fragment	IL_drought vs Swarna_drought_panicle	*qDTY*s located in/near the introgressed fragment	Functional Annotation
		LOC_Os01g51620	up		KRR1 small subunit processome component, putative
		LOC_Os01g52010	up		Alliin lyase precursor, putative, expressed
		LOC_Os01g52060	down		Expressed protein
		LOC_Os01g52260	down		Serine acetyltransferase protein, putative, expressed
		LOC_Os01g52570	up		Lachrymatory factor synthase, putative, expressed
		LOC_Os01g52680	up		OsMADS32 - MADS-box family gene with MIKCc type-box, expressed
		LOC_Os01g52750	up		OsSub3 - Putative Subtilisin homologue, expressed
		LOC_Os01g52760	up		Expressed protein
		LOC_Os01g53030	up		Expressed protein
		LOC_Os01g53180	down		Retrotransposon protein, putative, Ty1-copia subclass
		LOC_Os01g53190	down		Hypothetical protein
		LOC_Os01g53210	down		Metal transporter Nramp3, putative
		LOC_Os01g53230	up		Conserved hypothetical protein
		LOC_Os01g53255	down		Expressed protein
		LOC_Os01g53260	down		OsWRKY23 - Superfamily of TFs having WRKY and ZF domains, expressed
		LOC_Os01g53560	up		Phosphoesterase, putative, expressed
		LOC_Os01g53570	down		Aluminum-activated malate transporter, putative, expressed
		LOC_Os01g53680	up		6-phosphofructokinase, putative, expressed
		LOC_Os01g53800	up		Glutamate carboxypeptidase 2, putative, expressed
		LOC_Os01g54030	down		NADP-dependent malic enzyme, putative, expressed
		LOC_Os01g54090	down		Expressed protein
		LOC_Os01g54300	up		OsMan02 - Endo-Beta-Mannanase
		LOC_Os01g54370	up		Dihydropyrimidinase, putative, expressed

Table 3.3. (Continued)

Introgressed fragment ID	Introgressed fragment position (bp)	DEG's located in the introgressed fragment	IL_drought vs Swarna_drought_panicle	*qDTY*s located in/near the introgressed fragment	Functional Annotation
		LOC_Os01g54520	down		DUF1264 domain containing protein, putative, expressed
		LOC_Os01g54740	up		Transposon protein, putative, unclassified, expressed
		LOC_Os01g54750	up		Conserved hypothetical protein
		LOC_Os01g54980	up		Expressed protein
		LOC_Os01g55510	down		Dynein light chain type 1 domain containing protein, expressed
		LOC_Os01g55160	down		Expressed protein
		LOC_Os01g55750	up		TCP family transcription factor, putative, expressed
		LOC_Os01g55820	down		X8 domain containing protein, expressed
		LOC_Os01g55950	up		Acetamidase, putative, expressed
		LOC_Os01g56010	down		Serpin domain containing protein, putative, expressed
		LOC_Os01g56090	up		Expressed protein
		LOC_Os01g56210	down		Hypothetical protein
		LOC_Os01g56220	down		Expressed protein
		LOC_Os01g56235	up		Expressed protein
		LOC_Os01g56380	down		Decarboxylase, putative, expressed
		LOC_Os01g56610	down		Homocysteine S-methyltransferase protein, putative, expressed
		LOC_Os01g56850	down		Expressed protein
		LOC_Os01g57082	down		Insulin-degrading enzyme, putative
		LOC_Os01g57250	up		Expressed protein
		LOC_Os01g57420	down		Diacylglycerol kinase, putative, expressed
		LOC_Os01g57920	down		OsFBL3 - F-box domain and LRR containing protein
		LOC_Os01g57958	up		Chloroplast 50S ribosomal protein L16, putative, expressed
		LOC_Os01g57962	up		Photosystem I P700 chlorophyll a apoprotein A2, putative
		LOC_Os01g57968	up		Expressed protein

Table 3.3. (Continued)

Introgressed fragment ID	Introgressed fragment position (bp)	DEG's located in the introgressed fragment	IL_drought vs Swarna_drought_panicle	*qDTY*s located in/near the introgressed fragment	Functional Annotation
		LOC_Os01g58038	up		Photosystem II reaction center protein Z, putative
		LOC_Os01g58039	up		Uncharacterized protein ycf70, putative, expressed
		LOC_Os01g58194	down		Protein disulfide isomerase, putative, expressed
		LOC_Os01g58240	up		OsSub6 - Putative Subtilisin homologue, expressed
		LOC_Os01g58330	up		Hypothetical protein
		LOC_Os01g58540	down		Hypothetical protein
		LOC_Os01g59120	up		Cyclin, putative, expressed
		LOC_Os01g59450	down		ZOS1-13 - C2H2 zinc finger protein, expressed
		LOC_Os01g59570	up		Senescence-induced receptor-like serine/threonine-protein kinaseprecursor
		LOC_Os01g60340	down		NTMC2Type1.1 protein, putative
		LOC_Os01g60450	down		Cytochrome P450, putative
		LOC_Os01g60770	up		Expansin precursor, putative, expressed
		LOC_Os01g61070	down		Heavy metal-associated domain containing protein, expressed
		LOC_Os01g61570	up		GDSL-like lipase/acylhydrolase, putative, expressed
		LOC_Os01g61700	down		ATP-dependent Clp protease adaptor protein ClpS
		LOC_Os01g61710	up		Coatomer subunit delta, putative, expressed
		LOC_Os01g61980	down		Expressed protein
		LOC_Os01g62100	down		Retrotransposon protein, putative, unclassified
		LOC_Os01g62190	down		ZOS1-15 - C2H2 zinc finger protein, expressed
		LOC_Os01g62260	down		Thaumatin, putative, expressed
		LOC_Os01g62450	up		Conserved hypothetical protein
		LOC_Os01g62570	up		ATP/GTP/Ca++ binding protein, putative
		LOC_Os01g62610	down		Peptidyl-prolyl cis-trans isomerase, FKBP-type, putative
		LOC_Os01g62740	down		Expressed protein

Table 3.3. (Continued)

Introgressed fragment ID	Introgressed fragment position (bp)	DEG's located in the introgressed fragment	IL_drought vs Swarna_drought_panicle	*qDTY*s located in/near the introgressed fragment	Functional Annotation
		LOC_Os01g62770	down		Expressed protein
		LOC_Os01g62900	down		Amino acid kinase, putative, expressed
		LOC_Os01g62950	down		Ras-related protein, putative, expressed
		LOC_Os01g62980	down		LTPL101 - Protease inhibitor/seed storage/LTP family protein precursor, expressed
		LOC_Os01g63890	down		G10 protein, putative, expressed
		LOC_Os01g64020	up		Transcription factor, putative, expressed
		LOC_Os01g64100	up		Glycosyl hydrolase, putative, expressed
		LOC_Os01g64660	up		Fructose-1,6-bisphosphatase, putative, expressed
		LOC_Os01g64670	down		Soluble inorganic pyrophosphatase, putative, expressed
		LOC_Os01g65120	up		Peptide transporter, putative
		LOC_Os01g65590	up		Galactosyltransferase, putative, expressed
		LOC_Os01g65620	down		Expressed protein
		LOC_Os01g65650	up		Receptor-like protein kinase HAIKU2 precursor, putative
		LOC_Os01g65860	down		ANTH domain containing protein, expressed
		LOC_Os01g65880	up		Nodulin MtN3 family protein, putative, expressed
		LOC_Os01g65950	up		Thioesterase family protein, putative, expressed
		LOC_Os01g65992	down		Expressed protein
		LOC_Os01g66100	up		Gibberellin 20 oxidase 2, putative, expressed
		LOC_Os01g66180	**up**	***qDTY1.1***	**Cytochrome c, putative, expressed**
		LOC_Os01g66440	**up**	***qDTY1.1***	**Hypothetical protein**
		LOC_Os01g66730	**down**	***qDTY1.1***	**Exosome complex exonuclease RRP40, putative, expressed**
		LOC_Os01g66820	**up**	***qDTY1.1***	**Inactive receptor kinase At1g27190 precursor, putative**
		LOC_Os01g66840	**up**	***qDTY1.1***	**Pectinacetylesterase domain containing protein**

Table 3.3. (Continued)

Introgressed fragment ID	Introgressed fragment position (bp)	DEG's located in the introgressed fragment	IL_drought vs Swarna_drought_panicle	*qDTY*s located in/near the introgressed fragment	Functional Annotation
		LOC_Os01g67070	down		Hypothetical protein
		LOC_Os01g67160	down		Cyclin-dependent kinase B1-1, putative, expressed
		LOC_Os01g67314	up		Expressed protein
		LOC_Os01g67810	up		Transposon protein, putative, unclassified, expressed
		LOC_Os01g68290	down		Expressed protein
		LOC_Os01g68670	down		Cysteine proteinase inhibitor precursor, putative
		LOC_Os01g69190	up		Regulatory protein, putative, expressed
		LOC_Os01g70210	up		CRAL/TRIO domain containing protein, expressed
		LOC_Os01g70520	down		Os1bglu5 - beta-glucosidase homologue, similar to G. max isohydroxyurate hydrolase
		LOC_Os01g70560	up		Expressed protein
		LOC_Os01g70660	up		Potassium transporter, putative, expressed
		LOC_Os01g70720	down		Expressed protein
		LOC_Os01g70830	up		Esterase PIR7A, putative, expressed
		LOC_Os01g70840	up		Esterase, putative, expressed
		LOC_Os01g70850	up		Esterase, putative, expressed
		LOC_Os01g71340	up		Glycosyl hydrolases family 17, putative, expressed
		LOC_Os01g71380	up		Glycosyl hydrolases family 17, putative, expressed
		LOC_Os01g71640	down		Conserved hypothetical protein
		LOC_Os01g71720	down		Amino acid permease family protein, putative, expressed
		LOC_Os01g71740	up		Amino acid permease family protein, putative, expressed
		LOC_Os01g71790	up		NAM, putative, expressed
		LOC_Os01g71810	down		Glycosyl hydrolases family 17, putative, expressed
		LOC_Os01g72009	down		Expressed protein
		LOC_Os01g72170	up		Glutathione S-transferase, putative, expressed
		LOC_Os01g72390	down		NBS type disease resistance protein, putative

Table 3.3. (Continued)

Introgressed fragment ID	Introgressed fragment position (bp)	DEG's located in the introgressed fragment	IL_drought vs Swarna_drought_panicle	*qDTY*s located in/near the introgressed fragment	Functional Annotation
		LOC_Os01g72670	down		Expressed protein
		LOC_Os01g72700	up		Expressed protein
		LOC_Os01g73024	up		Expressed protein
		LOC_Os01g73060	down		Expressed protein
		LOC_Os01g73170	up		Peroxidase precursor, putative, expressed
		LOC_Os01g73220	down		Peroxidase precursor, putative, expressed
		LOC_Os01g73250	down		Abscisic stress-ripening, putative, expressed
		LOC_Os01g73630	down		rhoGAP domain containing protein, expressed
		LOC_Os01g73644	up		Expressed protein
		LOC_Os01g73650	up		Hypothetical protein
		LOC_Os01g73656	up		Expressed protein
		LOC_Os01g73670	up		Expressed protein
		LOC_Os01g73780	up		Chloroplast outer envelope 24 kD protein, putative, expressed
		LOC_Os01g73830	up		Expressed protein
		LOC_Os01g74020	down		MYB family transcription factor, putative, expressed
		LOC_Os01g74110	up		Metal cation transporter, putative, expressed
		LOC_Os01g74120	up		Hypothetical protein
		LOC_Os01g74160	up		Carboxyl-terminal peptidase, putative, expressed
		LOC_Os01g74170	up		Expressed protein
		LOC_Os01g74390	down		Transposon protein, putative, unclassified
fragment 1 Chr03	1359713-3484027	**LOC_Os03g03260**	**up**	***qDTY3.2***	**Homeobox domain containing protein, expressed**
		LOC_Os03g03300	**down**	***qDTY3.2***	**Expressed protein**
		LOC_Os03g03320	**up**	***qDTY3.2***	**Expressed protein**

Table 3.3. (Continued)

Introgressed fragment ID	Introgressed fragment position (bp)	DEG's located in the introgressed fragment	IL_drought vs Swarna_drought_panicle	*qDTY*s located in/near the introgressed fragment	Functional Annotation
		LOC_Os03g03510	**down**	***qDTY3.2***	**CAMK_KIN1/SNF1/Nim1_like.15 - CAMK includes calcium/calmodulin dependent protein kinases**
		LOC_Os03g03540	down		No apical meristem protein, putative, expressed
		LOC_Os03g03600	up		Fasciclin-like arabinogalactan protein, putative, expressed
		LOC_Os03g04150	up		Transposon protein, putative, Mutator sub-class
		LOC_Os03g04310	down		BHLH transcription factor, putative, expressed
		LOC_Os03g04580	up		Expressed protein
		LOC_Os03g04650	up		Cytochrome P450 protein, putative, expressed
		LOC_Os03g04780	down		RNA recognition motif containing protein, putative
		LOC_Os03g04900	down		MYB family transcription factor, putative, expressed
		LOC_Os03g05049	down		Expressed protein
		LOC_Os03g05100	down		Expressed protein
		LOC_Os03g05130	down		Hypothetical protein
		LOC_Os03g05530	down		Nodulin, putative, expressed
		LOC_Os03g05610	up		Inorganic phosphate transporter, putative, expressed
		LOC_Os03g05620	up		Inorganic phosphate transporter, putative, expressed
		LOC_Os03g05910	up		Expressed protein
		LOC_Os03g05920	up		Expressed protein
		LOC_Os03g06360	down		Late embryogenesis abundant protein D-34, putative
		LOC_Os03g06460	up		Type I inositol-1,4,5-trisphosphate 5-phosphatase, putative
		LOC_Os03g06580	down		MTN26L2 - MtN26 family protein precursor, expressed
		LOC_Os03g06610	down		Expressed protein
		LOC_Os03g06670	up		Core histone H2A/H2B/H3/H4 domain containing protein
		LOC_Os03g06835	up		Expressed protein
		LOC_Os03g06860	up		Transposon protein, putative, unclassified, expressed

Table 3.3. (Continued)

Introgressed fragment ID	Introgressed fragment position (bp)	DEG's located in the introgressed fragment	IL_drought vs Swarna_drought_panicle	*qDTY*s located in/near the introgressed fragment	Functional Annotation
Chr03		LOC_Os03g21500	up		Hypothetical protein
		LOC_Os03g21650	down		Expressed protein
		LOC_Os03g21730	up		Receptor-like protein kinase precursor, putative, expressed
		LOC_Os03g21780	up		Pentatricopeptide repeat domain containing protein, putative, expressed
		LOC_Os03g21790	down		Cupin domain containing protein, expressed
		LOC_Os03g21820	up		Expansin precursor, putative, expressed
		LOC_Os03g21960	up		Aminotransferase, putative, expressed
		LOC_Os03g22210	up		POEI46 - Pollen Ole e I allergen and extensin family protein
		LOC_Os03g22230	up		POEI47 - Pollen Ole e I allergen and extensin family protein
		LOC_Os03g22250	down		POEI48 - Pollen Ole e I allergen and extensin family protein
		LOC_Os03g22370	up		ultraviolet-B-repressible protein, putative, expressed
		LOC_Os03g22470	up		Desiccation-related protein PCC13-62 precursor, putative,
		LOC_Os03g22490	up		Heavy metal-associated domain containing protein, expressed
		LOC_Os03g22590	down		Nodulin MtN3 family protein, putative, expressed
		LOC_Os03g22620	down		Terpene synthase family, metal binding domain
fragment 1	59946-5475158				
		LOC_Os04g02450	down		Rust-resistance protein Lr21, putative
Chr04		LOC_Os04g02754	up		Amidase family protein, putative, expressed
		LOC_Os04g02860	up		Disease resistance protein RPM1, putative
		LOC_Os04g02960	up		OsSub32 - Putative Subtilisin homologue
		LOC_Os04g02970	up		Subtilisin-like protease precursor, putative, expressed

Table 3.3. (Continued)

Introgressed fragment ID	Introgressed fragment position (bp)	DEG's located in the introgressed fragment	IL_drought vs Swarna_drought_panicle	*qDTY*s located in/near the introgressed fragment	Functional Annotation
		LOC_Os04g03120	up		Retrotransposon protein, putative, unclassified
		LOC_Os04g03180	up		Disease resistance protein, putative, expressed
		LOC_Os04g03796	up		OsSub37 - Putative Subtilisin homologue, expressed
		LOC_Os04g03810	up		OsSub38 - Putative Subtilisin homologue, expressed
		LOC_Os04g03850	down		OsSub39 - Putative Subtilisin homologue
		LOC_Os04g03860	down		Expressed protein
		LOC_Os04g03890	down		Cytochrome P450, putative
		LOC_Os04g03910	up		Conserved hypothetical protein
		LOC_Os04g04040	down		Hypothetical protein
		LOC_Os04g04050	down		Conserved hypothetical protein
		LOC_Os04g04070	down		Hypothetical protein
		LOC_Os04g04390	down		Retrotransposon protein, putative, unclassified, expressed
		LOC_Os04g05470	up		Protein kinase, putative
		LOC_Os04g05650	down		Expressed protein
		LOC_Os04g05750	up		Hypothetical protein
		LOC_Os04g05770	up		Conserved hypothetical protein
		LOC_Os04g06100	up		Transposon protein, putative, CACTA, En/Spm sub-class
		LOC_Os04g06510	up		Conserved hypothetical protein
		LOC_Os04g07450	up		Retrotransposon protein, putative, unclassified
		LOC_Os04g07600	down		AGAP002737-PA, putative
		LOC_Os04g07830	down		Conserved hypothetical protein
		LOC_Os04g07890	down		AGAP002737-PA, putative, expressed
		LOC_Os04g07920	down		Expressed protein
		LOC_Os04g08110	up		Conserved hypothetical protein

Table 3.3. (Continued)

Introgressed fragment ID	Introgressed fragment position (bp)	DEG's located in the introgressed fragment	IL_drought vs Swarna_drought_panicle	*qDTY*s located in/near the introgressed fragment	Functional Annotation
		LOC_Os04g08180	down		Expressed protein
		LOC_Os04g08190	down		Expressed protein
		LOC_Os04g08200	down		Conserved hypothetical protein
		LOC_Os04g08550	up		Oxidoreductase, aldo/keto reductase family protein, putative, expressed
		LOC_Os04g08650	down		Hypothetical protein
		LOC_Os04g08828	up		Cytochrome P450, putative, expressed
		LOC_Os04g08836	up		Cytochrome P450 79A1, putative
		LOC_Os04g09430	up		Cytochrome P450, putative, expressed
		LOC_Os04g09770	up		Ser/Thr protein kinase, putative
fragment 2 Chr04	6835634-7304413	LOC_Os04g12390	down		Transposon protein, putative, CACTA, En/Spm sub-class
		LOC_Os04g12460	down		Leucine Rich Repeat family protein, expressed
		LOC_Os04g12540	down		Receptor-like protein kinase, putative, expressed
		LOC_Os04g12580	down		Receptor-like protein kinase, putative
		LOC_Os04g12669	down		Conserved hypothetical protein
		LOC_Os04g12990	down		OsFBX122 - F-box domain containing protein
		LOC_Os04g13170	up		OsFBD10 - F-box and FBD domain containing protein
fragment 3 Chr04	9943752-12370219	LOC_Os04g18800	down		Conserved hypothetical protein
		LOC_Os04g19540	down		Retrotransposon protein, putative, Ty3-gypsy subclass
		LOC_Os04g19670	down		Retrotransposon protein, putative, Ty3-gypsy subclass
		LOC_Os04g19800	up		F-box domain containing protein, expressed
		LOC_Os04g19810	up		OsFBL12 - F-box domain and LRR containing protein
		LOC_Os04g20210	up		Expressed protein

Table 3.3. (Continued)

Introgressed fragment ID	Introgressed fragment position (bp)	DEG's located in the introgressed fragment	IL_drought vs Swarna_drought_panicle	*qDTY*s located in/near the introgressed fragment	Functional Annotation
fragment 1 Chr08	19351882-20488257	LOC_Os04g20600	down		Hypothetical protein
		LOC_Os04g20749	down		Expressed protein
		LOC_Os04g20880	down		Wax synthase isoform 1, putative, expressed
		LOC_Os04g21710	down		Expressed protein
		LOC_Os08g31340	down		Heavy metal-associated domain containing protein, expressed
		LOC_Os08g31630	down		Uncharacterized glycosyl hydrolase Rv2006/MT2062, putative expressed
		LOC_Os08g31670	up		Transporter, putative, expressed
		LOC_Os08g31814	down		OsAPRL4 adenosine 5'-phosphosulfate reductase OsAPRL4
		LOC_Os08g31830	up		UPF0041 domain containing protein, putative, expressed
		LOC_Os08g31870	up		Cell division cycle protein 48, putative, expressed
		LOC_Os08g31910	up		Expressed protein
		LOC_Os08g31920	up		Retrotransposon protein, putative, unclassified, expressed
		LOC_Os08g32310	down		Expressed protein
		LOC_Os08g32330	down		Expressed protein
		LOC_Os08g32350	down		Expressed protein
		LOC_Os08g32370	down		Mucin-associated surface protein, putative
		LOC_Os08g32390	down		Hypothetical protein
		LOC_Os08g32420	down		Hypothetical protein
		LOC_Os08g32430	up		Hypothetical protein
		LOC_Os08g32540	up		Cyclin, putative, expressed
		LOC_Os08g32560	down		Hypothetical protein
		LOC_Os08g32570	up		Expressed protein

Table 3.3. (Continued)

Introgressed fragment ID	Introgressed fragment position (bp)	DEG's located in the introgressed fragment	IL_drought vs Swarna_drought_panicle	*qDTY*s located in/near the introgressed fragment	Functional Annotation
fragment 2 Chr08	23434376-24283101	LOC_Os08g32910	up		Expressed protein
		LOC_Os08g37130	down		Oxidoreductase, short chain dehydrogenase/reductase family
		LOC_Os08g37930	up		Beta-expansin precursor, putative, expressed
		LOC_Os08g37940	up		HAD-superfamily hydrolase subfamily IA, variant 3, putative,expressed
		LOC_Os08g38040	down		Transposon protein, putative, unclassified
		LOC_Os08g38050	down		Transposon protein, putative, unclassified
		LOC_Os08g38110	up		cytokinin-O-glucosyltransferase 1, putative
		LOC_Os08g38160	up		cytokinin-O-glucosyltransferase, putative
		LOC_Os08g38270	up		Fasciclin domain containing protein, expressed
fragment 3 Chr08	25595968-26038950	LOC_Os08g38340	down		Interferon-related developmental regulator family protein,
		LOC_Os08g40550	down		Retrotransposon protein, putative, unclassified
		LOC_Os08g40555	up		ATPase, E1-E2 type, putative, expressed
		LOC_Os08g40615	down		Expressed protein
		LOC_Os08g40680	up		Glycosyl hydrolase, putative, expressed
		LOC_Os08g40700	down		Retrotransposon protein, putative, unclassified, expressed
		LOC_Os08g40720	up		FAD-binding and arabino-lactone oxidase domain
fragment 1 Chr09	14889045-17924577	LOC_Os09g25430	down		ZOS9-07 - C2H2 zinc finger protein, expressed
		LOC_Os09g25440	up		ZOS9-08 - C2H2 zinc finger protein, expressed
		LOC_Os09g25690	up		Retrotransposon protein, putative, unclassified

Table 3.3. (Continued)

Introgressed fragment ID	Introgressed fragment position (bp)	DEG's located in the introgressed fragment	IL_drought vs Swarna_drought_panicle	*qDTY*s located in/near the introgressed fragment	Functional Annotation
		LOC_Os09g25770	down		Auxin-induced protein 5NG4, putative, expressed
		LOC_Os09g25784	down		Auxin-induced protein 5NG4, putative, expressed
		LOC_Os09g25810	down		Nodulin, putative, expressed
		LOC_Os09g25865	up		Hypothetical protein
		LOC_Os09g25945	down		Expressed protein
		LOC_Os09g25990	down		Glutamate receptor, putative
		LOC_Os09g26270	up		Hypothetical protein
		LOC_Os09g26380	down		Aminotransferase, classes I and II, domain containing protein
		LOC_Os09g26610	down		OsSAUR38 - Auxin-responsive SAUR gene family member
		LOC_Os09g26890	up		Expressed protein
		LOC_Os09g26980	up		Cytochrome P450, putative, expressed
		LOC_Os09g27040	down		GEX1, putative, expressed
		LOC_Os09g27680	down		Expressed protein
		LOC_Os09g27890	up		lysM domain-containing GPI-anchored protein precursor
		LOC_Os09g27920	down		Conserved hypothetical protein
		LOC_Os09g28550	up		Hypothetical protein; Negative regulator of brassinosteroid
		LOC_Os09g28660	down		Gibberellin receptor GID1L2, putative, expressed
		LOC_Os09g29050	down		Mitochondrial carrier protein, putative
		LOC_Os09g29200	up		Glutathione S-transferase, putative, expressed
		LOC_Os09g29239	down		Purine permease, putative, expressed
fragment 2 Chr09	18307070-20547765	LOC_Os09g30120	up		CSLE1 - cellulose synthase-like family E, expressed
		LOC_Os09g30200	down		ATP binding protein, putative, expressed

Table 3.3. (Continued)

Introgressed fragment ID	Introgressed fragment position (bp)	DEG's located in the introgressed fragment	IL_drought vs Swarna_drought_panicle	*qDTY*s located in/near the introgressed fragment	Functional Annotation
		LOC_Os09g30380	up		AP005392-AK108636 - NBS/LRR genes
		LOC_Os09g30411	down		UBX domain-containing protein, putative, expressed
		LOC_Os09g30414	up		Aspartic proteinase nepenthesin-2 precursor, putative
		LOC_Os09g30510	down		Glucosyl transferase, putative, expressed
		LOC_Os09g31040	down		EF hand family protein, putative, expressed
		LOC_Os09g31050	down		Cytosolic phospholipase A2 beta, putative, expressed
		LOC_Os09g31190	down		Slowmo homolog, putative
		LOC_Os09g31420	up		Leucine rich repeat N-terminal domain containing protein
		LOC_Os09g31490	down		Reductase, putative, expressed
		LOC_Os09g31502	up		Dehydrogenase, putative, expressed
		LOC_Os09g32290	up		FAD dependent oxidoreductase domain containing protein
		LOC_Os09g32310	up		Expressed protein
		LOC_Os09g32320	up		Growth regulator related protein, putative, expressed
		LOC_Os09g32470	up		Membrane protein, putative, expressed
		LOC_Os09g32560	up		Conserved hypothetical protein
		LOC_Os09g32620	up		Dehydrogenase, putative, expressed
		LOC_Os09g32964	up		Peroxidase precursor, putative, expressed
		LOC_Os09g33620	up		Leucine Rich Repeat domain containing protein, expressed
		LOC_Os09g33710	up		Os9bglu33 - beta-glucosidase homologue, similar to G. max hydroxyisourate hydrolase
		LOC_Os09g33720	up		Protein transport protein Sec61, putative, expressed
		LOC_Os09g33740	up		Zinc finger, ZZ type domain containing protein, expressed
		LOC_Os09g33820	down		Lecithine cholesterol acyltransferase, putative, expressed
		LOC_Os09g33850	up		osFTL4 FT-Like4 homologous to Flowering Locus T gene

Table 3.3. (Continued)

Introgressed fragment ID	Introgressed fragment position (bp)	DEG's located in the introgressed fragment	IL_drought vs Swarna_drought_panicle	*qDTY*s located in/near the introgressed fragment	Functional Annotation
		LOC_Os09g33930	up		Farnesyltransferase/geranylgeranyltransferase type-1
		LOC_Os09g34150	up		NBS-LRR disease resistance protein, putative, expressed
		LOC_Os09g34160	up		Resistance protein, putative, expressed
		LOC_Os09g34180	up		Formin, putative, expressed
		LOC_Os09g34214	up		UDP-glucoronosyl and UDP-glucosyl transferase domain
		LOC_Os09g34330	up		Helix-loop-helix DNA-binding domain containing protein
		LOC_Os09g34340	down		Expressed protein
		LOC_Os09g34890	up		Expressed protein
		LOC_Os09g34920	up		Glycosyl hydrolase family 29, putative, expressed
		LOC_Os09g35580	up		Conserved hypothetical protein
fragment 1 Chr10	14428360-17397576	LOC_Os10g27480	down		Expressed protein
		LOC_Os10g28060	up		3-ketoacyl-CoA synthase, putative, expressed
		LOC_Os10g28094	up		Retrotransposon protein, putative, unclassified, expressed
		LOC_Os10g28120	down		Glycosyl hydrolase, putative, expressed
		LOC_Os10g28230	up		Core histone H2A/H2B/H3/H4 domain containing protein
		LOC_Os10g28299	up		Expressed protein
		LOC_Os10g28310	down		Retrotransposon protein, putative, unclassified
		LOC_Os10g28370	down		Chlorophyllase-2, chloroplast precursor, putative, expressed
		LOC_Os10g28410	down		GA19388-PA, putative, expressed
		LOC_Os10g28560	down		Expressed protein
		LOC_Os10g28590	down		CAF1 family ribonuclease containing protein
		LOC_Os10g28700	up		Expressed protein

Table 3.3. (Continued)

Introgressed fragment ID	Introgressed fragment position (bp)	DEG's located in the introgressed fragment	IL_drought vs Swarna_drought_panicle	*qDTY*s located in/near the introgressed fragment	Functional Annotation
		LOC_Os10g28970	down		BTB6 - Bric-a-Brac, Tramtrack, Broad Complex BTB domain expressed
		LOC_Os10g29180	up		MBTB47 - Bric-a-Brac, Tramtrack
		LOC_Os10g29260	up		Speckle-type POZ protein, putative
		LOC_Os10g29320	up		Speckle-type POZ protein, putative, expressed
		LOC_Os10g29470	down		Dehydrogenase, putative, expressed
		LOC_Os10g29570	down		Late embryogenesis abundant protein D-34, putative
		LOC_Os10g29610	down		DUF623 domain containing protein
		LOC_Os10g30162	down		Hsp20/alpha crystallin family protein, putative, expressed
		LOC_Os10g30170	down		Hypothetical protein
		LOC_Os10g30270	up		Retrotransposon, putative, centromere-specific
		LOC_Os10g30410	up		Cytochrome P450 71D7, putative, expressed
		LOC_Os10g30690	up		MYB family transcription factor, putative, expressed
		LOC_Os10g30880	up		Expressed protein
		LOC_Os10g31040	up		Citrate transporter protein, putative, expressed
		LOC_Os10g31240	up		Plant protein of unknown function domain containing protein, expressed
		LOC_Os10g31290	up		Expressed protein
		LOC_Os10g31320	down		Retrotransposon protein, putative, unclassified, expressed
		LOC_Os10g31930	up		Shugoshin-1, putative, expressed
		LOC_Os10g32020	down		Expressed protein
		LOC_Os10g32470	down		Expressed protein
		LOC_Os10g32520	down		Expressed protein
		LOC_Os10g32800	down		Hypothetical protein
		LOC_Os10g32810	down		Beta-amylase, putative, expressed

Table 3.3. (Continued)

Introgressed fragment ID	Introgressed fragment position (bp)	DEG's located in the introgressed fragment	IL_drought vs Swarna_drought_panicle	*qDTY*s located in/near the introgressed fragment	Functional Annotation
		LOC_Os10g32900	down		CCT motif family protein, expressed
		LOC_Os10g32930	down		Hypothetical protein
		LOC_Os10g33104	down		Expressed protein
		LOC_Os10g33130	down		Leucine-rich repeat receptor protein kinase EXS precursor
		LOC_Os10g33140	up		hcrVf2 protein, putative, expressed
fragment 1 Chr11	20179567-20313437	LOC_Os11g34624	up		TKL_IRAK_DUF26-lc.29 - DUF26 kinases
		LOC_Os11g34640	up		Hypothetical protein
		LOC_Os11g34650	up		Hypothetical protein
fragment 1 Chr12	20626088-21562147	LOC_Os12g35239	up		Transposon protein, putative, CACTA, En/Spm sub-class
		LOC_Os12g35460	down		Retrotransposon protein, putative, unclassified, expressed

Table 3.4. List of DEGs in the Nipponbare *qDTY1.1* region across the different pairwise comparisons in the flag-leaf transcriptome.

FeatureID	IL_DvsSwa_D	IL_CvsSwa_C	IL_DvsIL_C	Swa_DvsSwa_C	Annotations
LOC_Os01g66120			1.162225454	1.289536342	no apical meristem protein; putative; expressed
LOC_Os01g66130				1.122587114	armadillo/beta-catenin repeat family protein; putative; expressed
LOC_Os01g66150			-1.460295711	-1.447406099	expressed protein
LOC_Os01g66180	1.713188847				cytochrome c; putative; expressed
LOC_Os01g66240	-1.119228147		-1.391530728		mitochondrion protein; putative; expressed
LOC_Os01g66250				-2.192722995	S-locus-like receptor protein kinase, putative, expressed
LOC_Os01g66300			-1.068330222	-1.278646148	KH domain containing protein; putative; expressed
LOC_Os01g66310		1.272913477		1.474187087	expressed protein
LOC_Os01g66350			-2.291888562	-1.900695549	DUF647 domain containing protein; putative; expressed
LOC_Os01g66360				-1.478776473	2-C-methyl-D-erythritol 4-phosphate cytidylyltransferase; putative
LOC_Os01g66379				1.20864579	expressed protein
LOC_Os01g66440	1.5736119		2.262664564	1.750683134	expressed protein
LOC_Os01g66510			-2.260297215	-2.871977577	MLO domain containing protein; putative; expressed
LOC_Os01g66530			-1.826026374	-1.50128164	ARGOS; putative; expressed
LOC_Os01g66544		-1.99824599			expressed protein
LOC_Os01g66590				1.640935597	DUF260 domain containing protein; putative; expressed
LOC_Os01g66690	-1.389770769			1.86340423	ZIP4/SPO22; putative; expressed
LOC_Os01g66720	1.569862518	2.003757375			NADP-dependent oxidoreductase; putative; expressed
LOC_Os01g66760				-1.64289312	inactive receptor kinase At2g26730 precursor; putative; expressed
LOC_Os01g66810	1.457644302	1.861965982			expressed protein
LOC_Os01g66820			-2.645276416	-3.925004367	inactive receptor kinase At1g27190 precursor; putative; expressed
LOC_Os01g66830			1.803094587		pectinacetylesterase domain containing protein; expressed
LOC_Os01g66840				-2.575535053	pectinacetylesterase domain containing protein; expressed
LOC_Os01g66850			-3.127972782	-3.917728521	pectinacetylesterase domain containing protein; expressed
LOC_Os01g66860			-2.782946381	-4.11826861	serine/threonine protein kinase, putative, expressed
LOC_Os01g66890			-1.310662554	-1.173573308	BTBZ1 - Bric-a-Brac; Tramtrack; & Broad Complex BTB domain

Table 3.4. (Continued)

FeatureID	IL_DvsSwa_D	IL_CvsSwa_C	IL_DvsIL_C	Swa_DvsSwa_C	Annotations
LOC_Os01g66920			-1.015000053	-1.184808756	Ser/Thr protein phosphatase family protein; putative; expressed
LOC_Os01g66930			1.559382363	1.839852935	transposon protein, putative, CACTA, En/Spm sub-class, expressed
LOC_Os01g66940			-1.024705886	-1.377150176	kinase; pfkB family; putative; expressed
LOC_Os01g66970			-1.827855171	-2.138689341	zinc finger; C3HC4 type domain containing protein; expressed
LOC_Os01g67040		1.02200738			OsRhmbd5 - Putative Rhomboid homologue; expressed
LOC_Os01g67054			1.032725389		calreticulin precursor protein; putative; expressed
LOC_Os01g67070	-4.166393363	-3.210681953			expressed protein
LOC_Os01g67090			1.601382602	1.447474933	IQ calmodulin-binding motif domain containing protein; expressed

IL = DTY-IL; Swa = Swarna; D = Drought; C = Control

Table 3.5. List of DEGs in the Nipponbare *qDTY1.1* region across the different pairwise comparisons in the panicle transcriptome.

FeatureID	IL_DvsSwa_D	IL_CvsSwa_C	IL_DvsIL_C	Swa_DvsSwa_C	Annotations
LOC_Os01g66120			1.162225454	1.289536342	no apical meristem protein; putative; expressed
LOC_Os01g66180	1.651397374				cytochrome c; putative; expressed
LOC_Os01g66250				2.787226645	S-locus-like receptor protein kinase; putative; expressed
LOC_Os01g66260		-4.201720712		-2.347371308	expressed protein
LOC_Os01g66290			-1.383260346	-1.172799952	OsMADS21 - MADS-box family gene with MIKCc type-box; expressed
LOC_Os01g66330			-1.203148305	-1.405189394	ATP-dependent Clp protease ATP-binding subunit clpX; putative; expressed
LOC_Os01g66440	1.41161385	2.204373723	2.136053912	2.928813785	expressed protein
LOC_Os01g66510				-1.538147186	MLO domain containing protein; putative; expressed
LOC_Os01g66544			1.29087826	2.007647884	expressed protein
LOC_Os01g66590				-1.103930234	DUF260 domain containing protein; putative; expressed
LOC_Os01g66630			1.094188466	1.139370286	S-domain receptor-like protein kinase; putative; expressed
LOC_Os01g66640			2.188934114	1.961539951	S-domain receptor-like protein kinase; putative; expressed
LOC_Os01g66650		1.967995503			expressed protein
LOC_Os01g66660				-1.401590115	expressed protein
LOC_Os01g66670				-1.712322837	expressed protein
LOC_Os01g66700			-2.511980879	-2.826246729	beta-hexosaminidase precursor; putative; expressed
LOC_Os01g66720				-1.234848598	NADP-dependent oxidoreductase; putative; expressed
LOC_Os01g66730	-1.631476401	-1.620420709			exosome complex exonuclease RRP40; putative; expressed
LOC_Os01g66760			1.533858164	1.438689054	inactive receptor kinase At2g26730 precursor; putative; expressed
LOC_Os01g66810			1.175843512		expressed protein
LOC_Os01g66820	2.167177052			-1.675568027	inactive receptor kinase At1g27190 precursor; putative; expressed
LOC_Os01g66840	1.45455861			-1.249373149	pectinacetylesterase domain containing protein; expressed
LOC_Os01g66850			-1.574772675	-3.039235946	pectinacetylesterase domain containing protein; expressed
LOC_Os01g66870				-3.881941481	transposon protein; putative; CACTA; En/Spm sub-class; expressed
LOC_Os01g66910			1.483532047	1.217857549	expressed protein

Table 3.5. (Continued)

FeatureID	IL_DvsSwa_D	IL_CvsSwa_C	IL_DvsIL_C	Swa_DvsSwa_C	Annotations
LOC_Os01g66930			1.449439576	2.91537742	transposon protein, putative, CACTA, En/Spm sub-class, expressed
LOC_Os01g66940				-1.035481468	kinase; pfkB family; putative; expressed
LOC_Os01g66980				-1.023775138	expressed protein
LOC_Os01g66990			1.937747046	2.280755547	expressed protein
LOC_Os01g67030	3.08735683				auxin-responsive protein; putative; expressed
LOC_Os01g67054			1.883172505	1.334225635	calreticulin precursor protein; putative; expressed
LOC_Os01g67070	-2.983690204	-2.182578113			expressed protein
LOC_Os01g67080			1.272428658		expressed protein
LOC_Os01g67090			-2.169426961	-2.690754195	IQ calmodulin-binding motif domain containing protein; expressed

IL = DTY-IL; Swa = Swarna; D = Drought; C = Control

Figure 3.2. Multiple peptide sequence alignment of LOC_Os01g67030 in Nipponbare, MH63v2, N22_v2, and a clone amplified from N22 (N22_Sanger). Nipponbare sequence was obtained from the Rice Genome Annotation Project (RGAP 7), while MH63v2 sequence was obtained from the Rice Information Gateway (RIGW). Predictions in N22v2 were made in FGENESH. Protein alignment was done using Clustal Omega using default parameters with ClustalW output format. Conserved domains search was done through CD-search in NCBI with default settings. The DOMON_DOH and Cyt_b561_FRRS1_like conserved domains were underlined. Note: The Sanger sequencing result of N22 validates the SNPs and Indels in the predicted AA of N22_v2. Nonsynonymous SNPs and a Glycine deletion unique to N22v2 were highlighted (red rectangular box). *, identical residues.

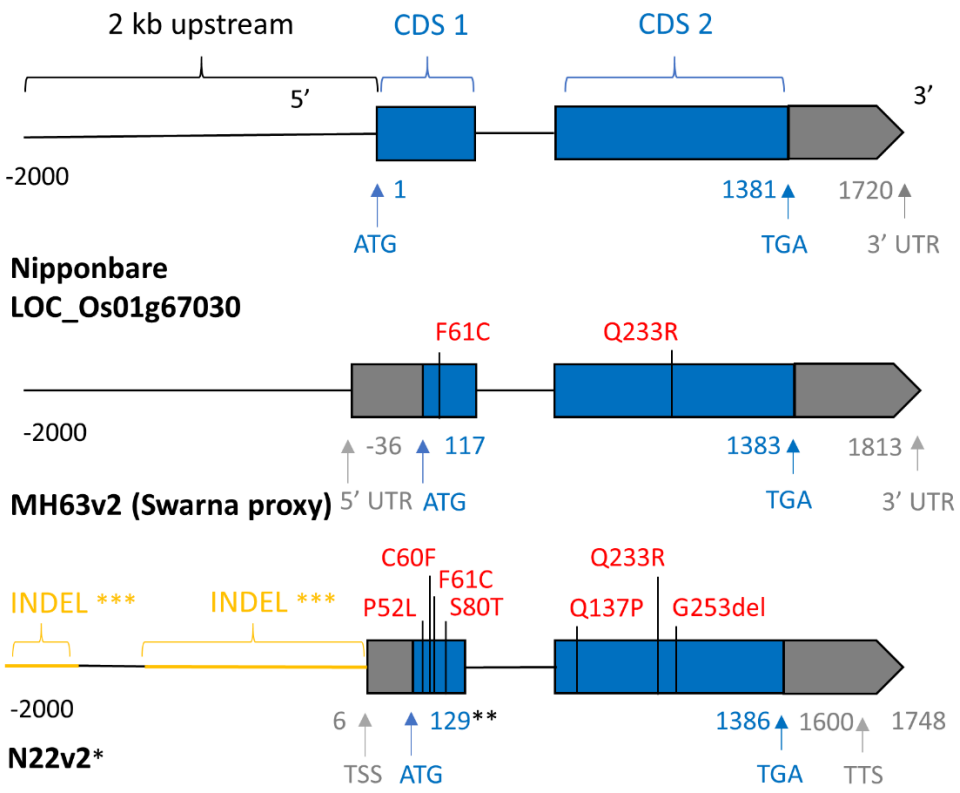

Figure 3.3. Comparison of gene structure including the 2-kb upstream region of AuxRe. The 2-kb upstream and full-length sequence of AuxRe in Nipponbare was used to lift over the corresponding sequences of AuxRe in MH63v2 and N22v2 genomes via blastn. Organization of exons (blue box), introns, and UTRs (gray box) of AuxRe (LOC_Os01g67030) gene in the gene body and the 2-kb upstream sequences of the gene in Nipponbare, MH63v2, and N22v2 representing *Nipponbare*, *Indica*, and *Ausboro* genomes respectively. The alignment of the promoter and the full-length genomic region was done using Blastn. Gene structure annotation was present in Nipponbare (RGAP 7) and MH63v2 (RIGW) while it was predicted in the N22v2 using FGENESH. The SNP's (in color red texts) was determined relative to the Nipponbare sequence. *FGENESH prediction; **Different start codon in FGENESH prediction; ***Alignment result through Blastn in NCBI Blast. CDS = coding sequence; UTR = untranslated region; ATG = start codon; TGA = stop codon; TSS = transcription start site; TTS = transcription termination site.

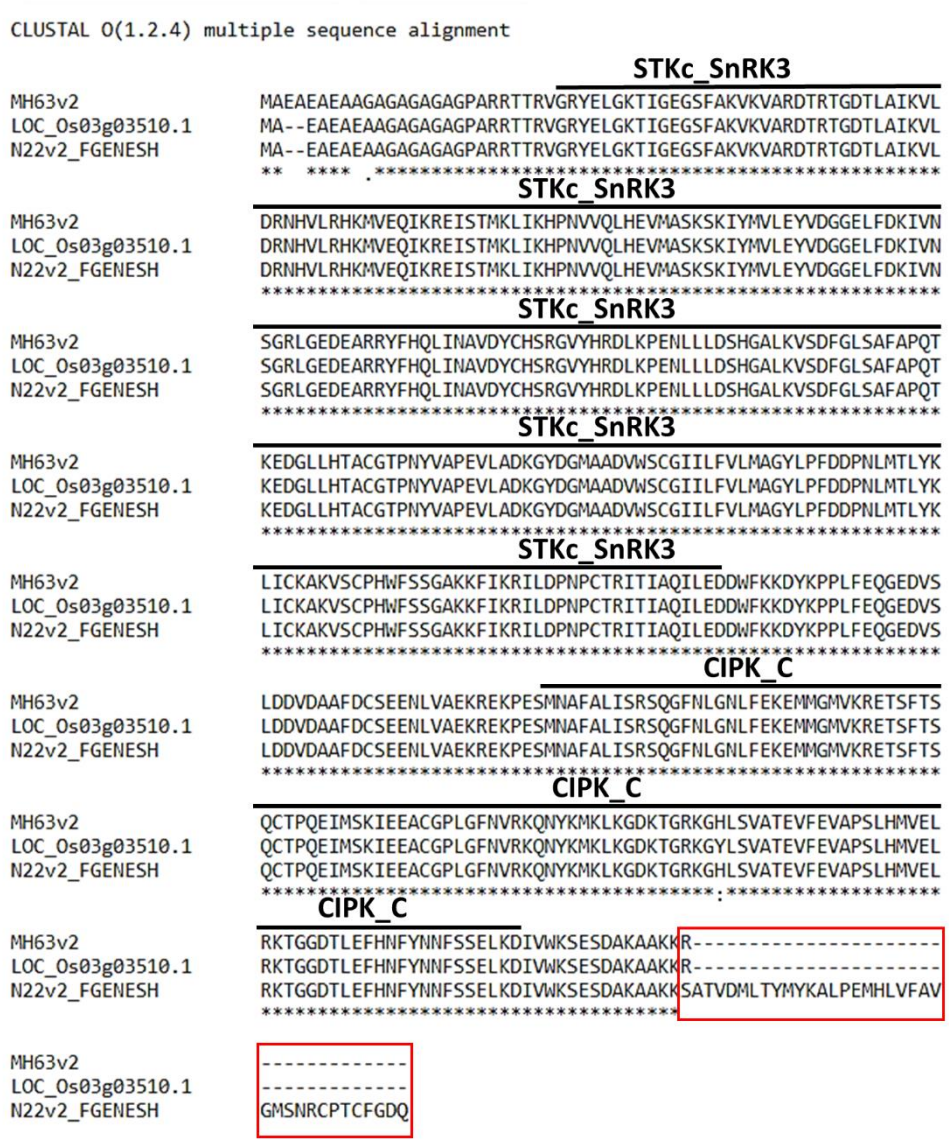

Figure 3.4. Multiple peptide sequence alignment of LOC_Os03g03510 in Nipponbare, MH63, and N22 sequences. Nipponbare sequence was obtained from the Rice Genome Annotation Project (RGAP 7), while MH63v2 sequence was obtained from the Rice Information Gateway (RIGW). Predictions in N22v2 were made in FGENESH. Protein alignment was done using Clustal Omega using default parameters with ClustalW output format. Conserved domains search was done through CD-search in NCBI with default settings. The STKc_SnRK3 and CIPK_C conserved domains were underlined. The extended C-terminal region (red rectangular box) in N22v2 was highlighted. *, identical residues.

Table 3.6. Gene Models and transposable elements in the *qDTY1.1* region in the Nipponbare, N22, and MH63 genomes.

	Nipponbare (NB)	**N22**	**MH63**
Size and position of *qDTY1.1* region			
Size of locus (kb)	480	506	491
Position_Chromosome 1 (bp)	38414421-38895056	38095880-38602311	39675143-40166200
Gene number (incl. TE genes)			
Total number of genes (gff3)	75	72	81
Genes with clear annotation	45	38	42
Unclear gene annotation	21	14	26
Genes with NB equivalent	-	53	60
Genes common in N22 and MH63	-	4	4
Unique genes	6	13	16
Retro-/transposon genes	9	15	12

Unclear annotation = expressed or hypothetical/uncharacterized proteins; unique genes = number of genes that is unique in the *qDTY1.1* region of three genomes without any equivalent; genes common in N22 and MH63 = genes without any NB equivalent but aligns between N22 and MH63.

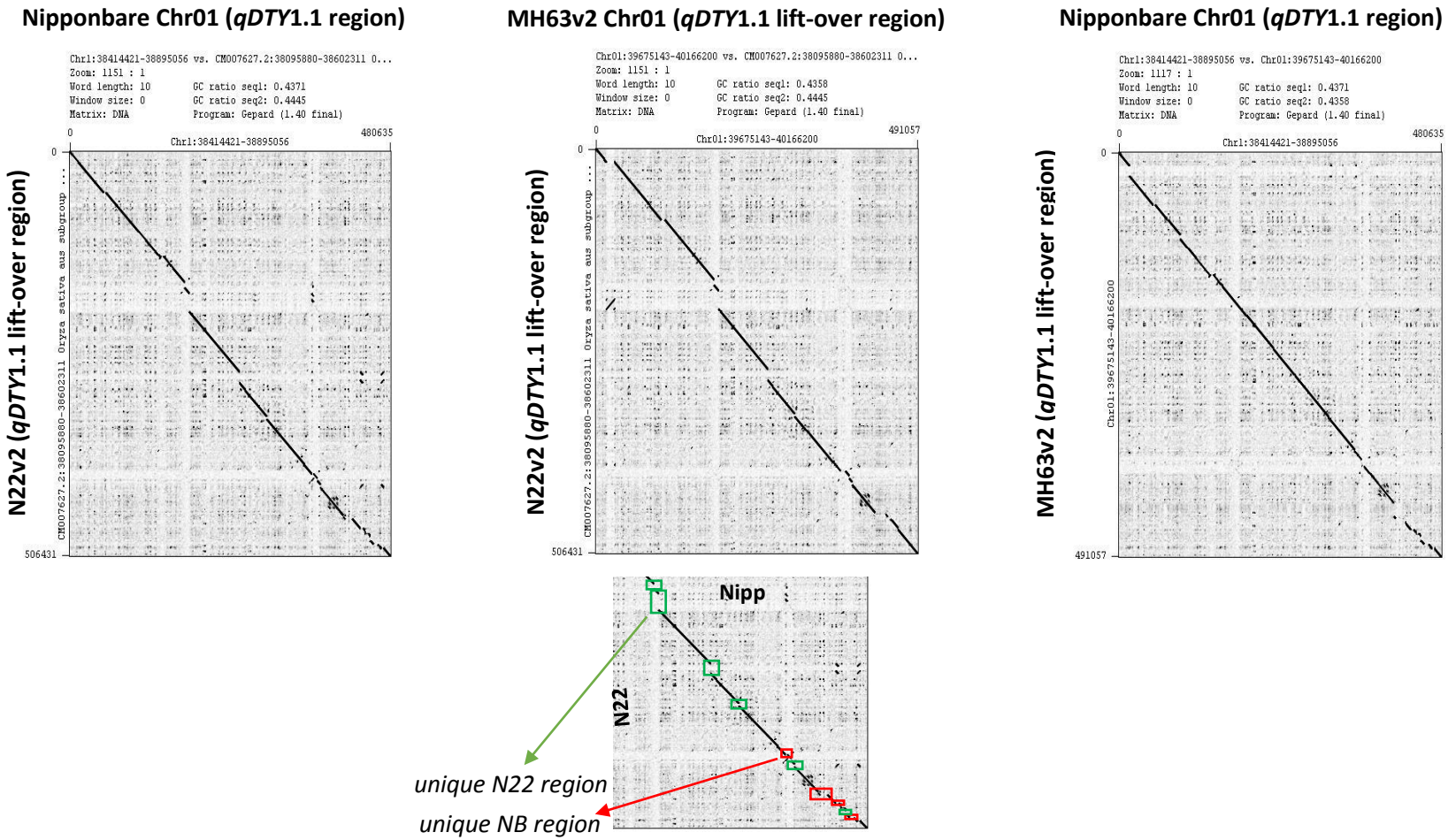

Figure 3.5. The *qDTY1.1* region in the Nipponbare reference and its syntenic region in the MH63 and N22 genome sequences as shown in the pairwise dot plot alignment.

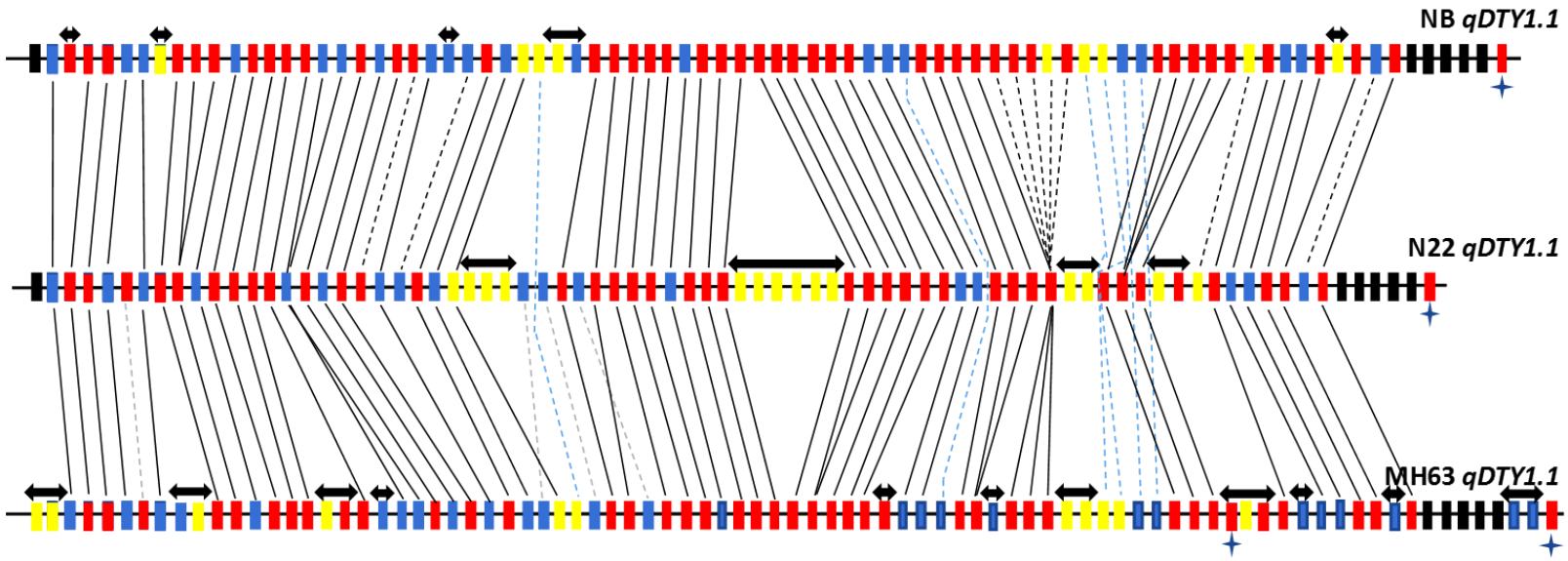

Figure 3.6. Presence-absence variation in the Nipponbare, N22, and MH63 *qDTY1.1* region.

Table 3.7. *qDTY1.1* pan comparison across Nipponbare, N22, and MH63 genome sequences. Gene-by-gene comparison on the *qDTY1.1* locus with few genes included in the fuzzy border (in bold).

unified gene ID	MSU7_qDTY1.1 region	N22RS2_qDTY1.1 region	N22RS2 Locus_ID	MH63RS2_qDTY1.1 region	MH63RS2 Locus_ID
LOC_Os01g66140.1	**LOC_Os01g66140.1**	**LOC_Os01g66140.1_N22**	**01G0124300**	**-**	**-**
LOC_Os01g66150.1	LOC_Os01g66150.1	LOC_Os01g66150.1_N22	01G0425000	LOC_Os01g66150.1_MH63	OsMH_01G0637500
LOC_Os01g66160.1	LOC_Os01g66160.1	-	-	-	-
LOC_Os01g66170.1	LOC_Os01g66170.1	LOC_Os01g66170.1_N22	01G0425100	LOC_Os01g66170.1_MH63	OsMH_01G0637600
LOC_Os01g66180.1	LOC_Os01g66180.1	LOC_Os01g66180.1_N22	01G0597000	LOC_Os01g66180.1_MH63	OsMH_01G0637700
LOC_Os01g66190.1	LOC_Os01g66190.1	LOC_Os01g66190.1_N22	01G0036700	LOC_Os01g66190.1_MH63	OsMH_01G0637800
LOC_Os01g66200.1	LOC_Os01g66200.1	LOC_Os01g66200.1_N22	01G0124500	LOC_Os01g66200.1_MH63	OsMH_01G0638000
LOC_Os01g66210.1	LOC_Os01g66210.1	-	-	-	-
LOC_Os01g66230.1	LOC_Os01g66230.1	LOC_Os01g66230.1_N22	01G0425600	LOC_Os01g66230.1_MH63	OsMH_01G0638300
LOC_Os01g66240.1	LOC_Os01g66240.1	LOC_Os01g66240.1_N22	01G0036800	LOC_Os01g66240.1_MH63	OsMH_01G0638400
LOC_Os01g66250.1	LOC_Os01g66250.1	LOC_Os01g66250.1_N22	01G0036800	LOC_Os01g66250.1_MH63	OsMH_01G0638400
LOC_Os01g66260.1	LOC_Os01g66260.1	LOC_Os01g66260.1_N22	01G0036900	LOC_Os01g66260.1_MH63	OsMH_01G0638500
LOC_Os01g66270.1	LOC_Os01g66270.1	LOC_Os01g66270.1_N22	01G0597100	LOC_Os01g66270.1_MH63	OsMH_01G0638600
LOC_Os01g66280.1	LOC_Os01g66280.1	LOC_Os01g66280.1_N22	01G0425700	LOC_Os01g66280.1_MH63	OsMH_01G0638700
LOC_Os01g66290.1	LOC_Os01g66290.1	LOC_Os01g66290.1_N22	01G0425200	LOC_Os01g66290.1_MH63	OsMH_01G0638800
LOC_Os01g66300.1	LOC_Os01g66300.1	LOC_Os01g66300.1_N22	01G0124600	LOC_Os01g66300.1_MH63	OsMH_01G0639100
LOC_Os01g66310.1	LOC_Os01g66310.1	LOC_Os01g66310.1_N22	01G0425300	LOC_Os01g66310.1_MH63	OsMH_01G0639300
LOC_Os01g66320.1	LOC_Os01g66320.1	LOC_Os01g66320.1_N22	01G0425800	LOC_Os01g66320.1_MH63	OsMH_01G0639400

Table 3.7. (Continued)

unified gene ID	MSU7_qDTY1.1 region	N22RS2_qDTY1.1 region	N22RS2 Locus_ID	MH63RS2_qDTY1.1 region	MH63RS2 Locus_ID
LOC_Os01g66330.1	LOC_Os01g66330.1	LOC_Os01g66330.1_N22	01G0425800	LOC_Os01g66330.1_MH63	OsMH_01G0639500
LOC_Os01g66340.1	LOC_Os01g66340.1	LOC_Os01g66340.1_N22	01G0597200	LOC_Os01g66340.1_MH63	OsMH_01G0639600
LOC_Os01g66350.1	LOC_Os01g66350.1	LOC_Os01g66350.1_N22	01G0425400	LOC_Os01g66350.1_MH63	OsMH_01G0639700
LOC_Os01g66360.1	LOC_Os01g66360.1	LOC_Os01g66360.1_N22	01G0425500	-	-
LOC_Os01g66379.1	LOC_Os01g66379.1	LOC_Os01g66379.1_N22	01G0124700	LOC_Os01g66379.1_MH63	OsMH_01G0639800
LOC_Os01g66400.1	LOC_Os01g66400.1	-	-	-	-
LOC_Os01g66410.1	LOC_Os01g66410.1	LOC_Os01g66410.1_N22	01G0426500	-	-
LOC_Os01g66420.1	LOC_Os01g66420.1	LOC_Os01g66420.1_N22	01G0426600	LOC_Os01g66420.1_MH63	OsMH_01G0639900
LOC_Os01g66440.1	LOC_Os01g66440.1	LOC_Os01g66440.1_N22	01G0425900	LOC_Os01g66440.1_MH63	OsMH_01G0640000
LOC_Os01g66450.1	LOC_Os01g66450.1	-	-	LOC_Os01g66450.1_MH63	OsMH_01G0640200
LOC_Os01g66460.1	LOC_Os01g66460.1	LOC_Os01g66460.1_N22	01G0426000	LOC_Os01g66460.1_MH63	OsMH_01G0640300
LOC_Os01g66470.1	LOC_Os01g66470.1	-	-	-	-
LOC_Os01g66480.1	LOC_Os01g66480.1	-	-	-	-
LOC_Os01g66490.1	LOC_Os01g66490.1	LOC_Os01g66490.1_N22	01G0426800	LOC_Os01g66490.1_MH63	OsMH_01G0640500
LOC_Os01g66500.1	LOC_Os01g66500.1	LOC_Os01g66500.1_N22	01G0124900	LOC_Os01g66500.1_MH63	OsMH_01G0640600
LOC_Os01g66510.1	LOC_Os01g66510.1	LOC_Os01g66510.1_N22	01G0427000	LOC_Os01g66510.1_MH63	OsMH_01G0640800
LOC_Os01g66520.1	LOC_Os01g66520.1	LOC_Os01g66520.1_N22	01G0125000	LOC_Os01g66520.1_MH63	OsMH_01G0640900
LOC_Os01g66530.1	LOC_Os01g66530.1	LOC_Os01g66530.1_N22	01G0037000	LOC_Os01g66530.1_MH63	OsMH_01G0641000

Table 3.7. (Continued)

unified gene ID	MSU7_qDTY1.1 region	N22RS2_qDTY1.1 region	N22RS2 Locus_ID	MH63RS2_qDTY1.1 region	MH63RS2 Locus_ID
LOC_Os01g66560.1	LOC_Os01g66560.1	LOC_Os01g66560.1_N22	01G0427100	LOC_Os01g66560.1_MH63	OsMH_01G0641300
LOC_Os01g66570.1	LOC_Os01g66570.1	LOC_Os01g66570.1_N22	01G0597300	LOC_Os01g66570.1_MH63	OsMH_01G0641400
LOC_Os01g66580.1	LOC_Os01g66580.1	LOC_Os01g66580.1_N22	01G0427300	LOC_Os01g66580.1_MH63	OsMH_01G0641500
LOC_Os01g66590.1	LOC_Os01g66590.1	LOC_Os01g66590.1_N22	01G0125400	LOC_Os01g66590.1_MH63	OsMH_01G0641600
LOC_Os01g66600.1	LOC_Os01g66600.1	LOC_Os01g66600.1_N22	01G0125600	LOC_Os01g66600.1_MH63	OsMH_01G0641700
LOC_Os01g66610.1	LOC_Os01g66610.1	LOC_Os01g66610.1_N22	01G0428700	LOC_Os01g66610.1_MH63	OsMH_01G0641700
LOC_Os01g66620.1	LOC_Os01g66620.1	LOC_Os01g66620.1_N22	01G0037200	LOC_Os01g66620.1_MH63	OsMH_01G0641800
LOC_Os01g66630.1	LOC_Os01g66630.1	LOC_Os01g66630.1_N22	01G0428800	LOC_Os01g66630.1_MH63	OsMH_01G0641900
LOC_Os01g66640.1	LOC_Os01g66640.1	LOC_Os01g66640.1_N22	01G0428400	LOC_Os01g66640.1_MH63	OsMH_01G0642000
LOC_Os01g66650.1	LOC_Os01g66650.1	LOC_Os01g66650.1_N22	01G0428900	LOC_Os01g66650.1_MH63	OsMH_01G0642200
LOC_Os01g66660.1	LOC_Os01g66660.1	LOC_Os01g66660.1_N22	01G0428500	LOC_Os01g66660.1_MH63	OsMH_01G0642300
LOC_Os01g66670.1	LOC_Os01g66670.1	-		LOC_Os01g66670.1_MH63	OsMH_01G0642400
LOC_Os01g66680.1	LOC_Os01g66680.1	LOC_Os01g66680.1_N22	01G0428600	LOC_Os01g66680.1_MH63	OsMH_01G0642500
LOC_Os01g66690.1	LOC_Os01g66690.1	LOC_Os01g66690.1_N22	01G0125500	LOC_Os01g66690.1_MH63	OsMH_01G0718100
LOC_Os01g66700.1	LOC_Os01g66700.1	LOC_Os01g66700.1_N22	01G0125700	LOC_Os01g66700.1_MH63	OsMH_01G0642600
LOC_Os01g66710.1	LOC_Os01g66710.1	LOC_Os01g66710.1_N22	01G0429000	LOC_Os01g66710.1_MH63	OsMH_01G0642800
LOC_Os01g66720.1	LOC_Os01g66720.1	LOC_Os01g66720.1_N22	01G0429000	-	-
LOC_Os01g66730.1	LOC_Os01g66730.1	LOC_Os01g66730.1_N22	01G0429000	-	-
LOC_Os01g66740.1	LOC_Os01g66740.1	LOC_Os01g66740.1_N22	01G0429000	LOC_Os01g66740.1_MH63	OsMH_01G0642900

Table 3.7. (Continued)

unified gene ID	MSU7_qDTY1.1 region	N22RS2_qDTY1.1 region	N22RS2 Locus_ID	MH63RS2_qDTY1.1 region	MH63RS2 Locus_ID
LOC_Os01g66760.1	LOC_Os01g66760.1	LOC_Os01g66760.1_N22	01G0429000	LOC_Os01g66760.1_MH63	OsMH_01G0643000
LOC_Os01g66780.1	LOC_Os01g66780.1	-	-	LOC_Os01g66780.1_MH63	OsMH_01G0643300
LOC_Os01g66790.1	LOC_Os01g66790.1	-	-	LOC_Os01g66790.1_MH63	OsMH_01G0643400 & OsMH_01G0643500
LOC_Os01g66800.1	LOC_Os01g66800.1	-	-	LOC_Os01g66800.1_MH63	OsMH_01G0643600
LOC_Os01g66810.1	LOC_Os01g66810.1	LOC_Os01g66810.1_N22	01G0429300	LOC_Os01g66810.1_MH63	OsMH_01G0643700
LOC_Os01g66820.1	LOC_Os01g66820.1	LOC_Os01g66820.1_N22	01G0429300	LOC_Os01g66820.1_MH63	OsMH_01G0643800
LOC_Os01g66830.1	LOC_Os01g66830.1	LOC_Os01g66830.1_N22	01G0429600	LOC_Os01g66830.1_MH63	OsMH_01G0643900
LOC_Os01g66840.1	LOC_Os01g66840.1	LOC_Os01g66840.1_N22	01G0429600	LOC_Os01g66840.1_MH63	OsMH_01G0643900
LOC_Os01g66850.1	LOC_Os01g66850.1	LOC_Os01g66850.1_N22	01G0429600	LOC_Os01g66850.1_MH63	OsMH_01G0643900
LOC_Os01g66860.2	LOC_Os01g66860.2	LOC_Os01g66860.2_N22	01G0429700	LOC_Os01g66860.2_MH63	OsMH_01G0644000
LOC_Os01g66870.1	LOC_Os01g66870.1	LOC_Os01g66870.1_N22	01G0430200	-	-
LOC_Os01g66890.1	LOC_Os01g66890.1	LOC_Os01g66890.1_N22	01G0429900	LOC_Os01g66890.1_MH63	OsMH_01G0644400
LOC_Os01g66900.1	LOC_Os01g66900.1	LOC_Os01g66900.1_N22	01G0430300	LOC_Os01g66900.1_MH63	OsMH_01G0644600
LOC_Os01g66910.1	LOC_Os01g66910.1	LOC_Os01g66910.1_N22	01G0430300	LOC_Os01g66910.1_MH63	OsMH_01G0644700
LOC_Os01g66920.1	LOC_Os01g66920.1	LOC_Os01g66920.1_N22	01G0430000	LOC_Os01g66920.1_MH63	OsMH_01G0644900
LOC_Os01g66930.2	LOC_Os01g66930.2	-	-	-	-
LOC_Os01g66940.1	LOC_Os01g66940.1	LOC_Os01g66940.1_N22	01G0125800	LOC_Os01g66940.1_MH63	OsMH_01G0645000
LOC_Os01g66950.1	LOC_Os01g66950.1	LOC_Os01g66950.1_N22	01G0430500	-	-

Table 3.7. (Continued)					
unified gene ID	**MSU7_qDTY1.1 region**	**N22RS2_qDTY1.1 region**	**N22RS2 Locus_ID**	**MH63RS2_qDTY1.1 region**	**MH63RS2 Locus_ID**
LOC_Os01g66970.1	**LOC_Os01g66970.1**	**LOC_Os01g66970.1_N22**	**01G0125900**	**LOC_Os01g66970.1_MH63**	**OsMH_01G0645300**
LOC_Os01g66980.1	**LOC_Os01g66980.1**	**LOC_Os01g66980.1_N22**	**01G0430600**	**LOC_Os01g66980.1_MH63**	**OsMH_01G0645400**
LOC_Os01g66990.1	**LOC_Os01g66990.1**	**LOC_Os01g66990.1_N22**	**01G0430600**	**LOC_Os01g66990.1_MH63**	**OsMH_01G0645500**
LOC_Os01g67000.1	**LOC_Os01g67000.1**	**LOC_Os01g67000.1_N22**	**01G0430700**	**LOC_Os01g67000.1_MH63**	**OsMH_01G0645600**
LOC_Os01g67010.1	**LOC_Os01g67010.1**	**LOC_Os01g67010.1_N22**	**01G0430800**	**LOC_Os01g67010.1_MH63**	**OsMH_01G0645700**
LOC_Os01g67030.1	**LOC_Os01g67030.1**	**LOC_Os01g67030.1_N22**	**01G0430800**	**LOC_Os01g67030.1_MH63**	**OsMH_01G0646000**
OsN22RS2_01G0424700		OsN22RS2_01G0424700		OsN22RS2_01G0424700_MH63	
OsN22RS2_01G0426400		OsN22RS2_01G0426400		OsN22RS2_01G0426400_MH63	
OsN22RS2_01G0426700		OsN22RS2_01G0426700		OsN22RS2_01G0426700_MH63	
OsN22RS2_01G0426900		OsN22RS2_01G0426900		OsN22RS2_01G0426900_MH63	
OsN22RS2_01G0430400		**OsN22RS2_01G0430400**		**OsN22RS2_01G0430400_MH63**	
OsN22RS2_01G0426100		OsN22RS2_01G0426100			
OsN22RS2_01G0426200		OsN22RS2_01G0426200			
OsN22RS2_01G0426300		OsN22RS2_01G0426300			

Table 3.7. (Continued)					
unified gene ID	**MSU7_qDTY1.1 region**	**N22RS2_qDTY1.1 region**	**N22RS2 Locus_ID**	**MH63RS2_qDTY1.1 region**	**MH63RS2 Locus_ID**
OsN22RS2_01G0427400		OsN22RS2_01G0427400			
OsN22RS2_01G0427500		OsN22RS2_01G0427500			
OsN22RS2_01G0427600		OsN22RS2_01G0427600			
OsN22RS2_01G0124800		OsN22RS2_01G0124800			
OsN22RS2_01G0598100		OsN22RS2_01G0598100			
OsN22RS2_01G0429500		OsN22RS2_01G0429500			
OsN22RS2_01G0429100		OsN22RS2_01G0429100			
OsN22RS2_01G0429200		OsN22RS2_01G0429200			
OsN22RS2_01G0429800		OsN22RS2_01G0429800			
OsMH_01G0637300				OsMH_01G0637300	
OsMH_01G0637400				OsMH_01G0637400	
OsMH_01G0638100				OsMH_01G0638100	
OsMH_01G0638200				OsMH_01G0638200	
OsMH_01G0638900				OsMH_01G0638900	

Table 3.7. (Continued)					
unified gene ID	**MSU7_qDTY1.1 region**	**N22RS2_qDTY1.1 region**	**N22RS2 Locus_ID**	**MH63RS2_qDTY1.1 region**	**MH63RS2 Locus_ID**
OsMH_01G0639200				OsMH_01G0639200	
OsMH_01G0642100				OsMH_01G0642100	
OsMH_01G0642700				OsMH_01G0642700	
OsMH_01G0643100				OsMH_01G0643100	
OsMH_01G0643200				OsMH_01G0643200	
OsMH_01G0644100				OsMH_01G0644100	
OsMH_01G0644200				OsMH_01G0644200	
OsMH_01G0644300				OsMH_01G0644300	
OsMH_01G0644500				OsMH_01G0644500	
OsMH_01G0645100				OsMH_01G0645100	
OsMH_01G0645800				**OsMH_01G0645800**	
OsMH_01G0645900				**OsMH_01G0645900**	

Table 3.8. List of panicles DEGs in the *qDTY1.1* region across the different pairwise comparisons in the three reference genomes in the panicle transcriptome. NB = Nipponbare; IL = DTY-IL; Swa = Swarna; D = Drought; C = Control.

Locus_ID	IL_DvsSwa_D			IL_CvsSwa_C			IL_DvsIL_C			Swa_DvsSwa_C		
	NB	N22	MH63	NB	N22	MH63	NB	N22	MH63	NB	N22	MH63
LOC_Os01g66120							1.162225			1.289536		
LOC_Os01g66180	1.65139	1.72366	1.64859		1.095015	1.007868						
LOC_Os01g66250										2.787226		
LOC_Os01g66260				-4.20172	-4.15565	-4.13168				-2.34737	-2.31861	-2.03550
LOC_Os01g66290							-1.38326	-1.34366	-1.34174	-1.17279	-1.16424	-1.17377
LOC_Os01g6630							-1.20314		-1.20257	-1.40518		-1.40501
LOC_Os01g66440	1.41161	1.38672	1.23203	2.204373	2.158600	1.480521	2.136053	2.178710	1.776232	2.928813	2.950583	2.024717
LOC_Os01g66510										-1.53814	-1.54618	-1.53102
LOC_Os01g66520											1.050810	
LOC_Os01g66544							1.290878	1.349993	1.333924	2.007647	2.045579	2.077913
LOC_Os01g66590										-1.10393	-1.09514	-1.15828
LOC_Os01g66620			1.83796					-1.15741			-1.80676	-1.90813
LOC_Os01g66630							1.094188			1.139370		
LOC_Os01g66640							2.188934	1.741903	2.123526	1.961539	1.700651	1.765230
LOC_Os01g66650				1.967995		1.895930			-1.24857			
LOC_Os01g66660									-1.04545	-1.40159		-1.24683
LOC_Os01g66670								1.99883		-1.71232		
LOC_Os01g66700							-2.51198	-2.51041	-2.57164	-2.82624	-2.82129	-2.81375
LOC_Os01g66720										-1.23484		

Table 3.8. (Continued)

Locus_ID	IL_DvsSwa_D			IL_CvsSwa_C			IL_DvsIL_C			Swa_DvsSwa_C		
	NB	N22	MH63	NB	N22	MH63	NB	N22	MH63	NB	N22	MH63
LOC_Os01g66730	-1.6314			-1.620420								
LOC_Os01g66760							1.533858		1.424097	1.438689		1.609033
LOC_Os01g66810					1.204591		1.175843					
LOC_Os01g66820	2.16717	1.29276	2.24675		1.204591					-1.675568		-1.77343
LOC_Os01g66840	1.45455									-1.249373		-1.14172
LOC_Os01g66850							-1.57477			-3.039235		-1.14172
OsMH_01G0644100			-3.04926			-3.60959						
LOC_Os01g66870										-3.881941		
OsMH_01G0644300			6.02325			5.449405						
OsN22RS2_01G0429800		7.C211			6.759679							
OsMH_01G0644500									-1.62085			-2.71134
OsN22RS2_01G0430400											-1.83470	
LOC_Os01g66910							1.483532			1.217857		
LOC_Os01g66920						-1.10279						-1.58298
LOC_Os01g66930							1.449439			2.915377		
LOC_Os01g66940										-1.035481	-1.0285	-1.06827
LOC_Os01g66980										-1.02377		-1.02396
LOC_Os01g66990							1.937747		1.967442	2.280755		2.295450
LOC_Os01g67030	3.08735		3.13275									

Table 3.9. List of flag-leaf DEGs in the *qDTY1.1* region across the different pairwise comparisons in the three reference genomes in the panicle transcriptome. NB = Nipponbare; IL = DTY-IL; Swa = Swarna; D = Drought; C = Control.

Locus_ID	IL_DvsSwa_D			IL_CvsSwa_C			IL_DvsIL_C			Swa_DvsSwa_C		
	NB	N22	MH63	NB	N22	MH63	NB	N22	MH63	NB	N22	MH63
LOC_Os01g66120							1.16222			1.289536		
LOC_Os01g66140											1.11940	
LOC_Os01g66150								-1.43628	-1.48466		-1.38219	-1.48816
LOC_Os01g66180	1.71318											
LOC_Os01g66240	-1.1192	-1.14954	-1.12778				-1.39153	-1.30545	-1.32416			
LOC_Os01g66250		-1.14954	-1.12778					-1.30545	-1.32416	2.787226		
LOC_Os01g66260				-4.20172						-2.347371		
LOC_Os01g66290							-1.38326			-1.172799		
LOC_Os01g66300								-1.14630	-1.10058		-1.39951	-1.29447
OsMH_01G0639200						1.75390						1.57680
LOC_Os01g66310					1.29606	1.22878					1.513067	1.41039
LOC_Os01g66330							-1.20314			-1.405189		
LOC_Os01g66350								-2.31617	-2.28270		-1.95550	-1.91020
LOC_Os01g66360											-1.43395	
LOC_Os01g66379											1.277268	1.11457
LOC_Os01g66440	1.57361	1.608323	1.42102	2.204373			2.136053	2.324977	1.628516	2.928813	1.741777	
LOC_Os01g66500					1.15848							
LOC_Os01g66510								-2.33040	-2.26820	-1.538147	-2.94781	-2.84046
LOC_Os01g66530									-1.86078			

Table 3.9. (Continued)

Locus_ID	IL_DvsSwa_D			IL_CvsSwa_C			IL_DvsIL_C			Swa_DvsSwa_C		
	NB	N22	MH63	NB	N22	MH63	NB	N22	MH63	NB	N220	MH63
LOC_Os01g66544					-1.95616	-1.83041	1.29087			2.007647		
LOC_Os01g66590										-1.103930	1.65855	1.56579
LOC_Os01g66600											0.995894	1.01171
LOC_Os01g66610											1.085015	1.01171
LOC_Os01g66630							1.094188			1.139370		
LOC_Os01g66640							2.188934			1.961539		
LOC_Os01g66650				1.967995								
LOC_Os01g66660										-1.401590		
LOC_Os01g66670										-1.712322		
LOC_Os01g66690	-1.3897	-1.40928							1.17104	1.863404	1.855177	1.69685
LOC_Os01g66700							-2.51198			-2.826246		
LOC_Os01g66710		1.361921			1.21924							
LOC_Os01g66720	1.56986				1.21924					-1.234848		
LOC_Os01g66740						1.25238						
LOC_Os01g66760					1.21924		1.533858			1.438689		-1.53316
LOC_Os01g66810	1.45764		1.38319		1.37038	1.83754	1.175843					
LOC_Os01g66820		1.847768			1.37038				-2.56189	-1.675568		-3.76990
LOC_Os01g66840								-2.13579	-2.22112	-1.249373	-3.16414	-3.23998
LOC_Os01g66850							-1.57477	-2.13579	-2.22112	-3.039235	-3.16414	-3.23998

Table 3.9. (Continued)

Locus_ID	IL_DvsSwa_D			IL_CvsSwa_C			IL_DvsIL_C			Swa_DvsSwa_C		
	NB	N22	MH63	NB	N22	MH63	NB	N22	MH63	NB	N220	MH63
LOC_Os01g66860								-3.02806	-2.85218		-4.19545	-4.21573
LOC_Os01g66870										-3.88194		
OsN22RS2_01G0430400								2.303517	2.690708			
LOC_Os01g66890								-1.28806	-1.31802		-1.12223	-1.2149
LOC_Os01g66910							1.483532			1.217857		
LOC_Os01g66920								-1.04037			-1.24391	-1.17049
LOC_Os01g66930							1.449439			2.9153774		
LOC_Os01g66940								-1.00715	-1.03954	-1.03548	-1.35238	-1.39919
LOC_Os01g66970												-1.14614
LOC_Os01g66980										-1.023775		
LOC_Os01g66990							1.937747			2.2807555		

Table 3.10. Unique *cis* regulatory elements in the 2-kb upstream of LOC_Os01g67030 in Nipponbare, MH63, and N22 genomic sequences as extracted in the PLACE database. The common *cis* regulatory elements within the 2-kb upstream region of the three-reference sequence were not included.

Factor or Site Name	Location	Strand	Signal Sequence	Site #	Description
Nipponbare					
BOXIIPCCHS	1265	(+)	ACGTGGC	S000229	Essential for light regulation
LRENPCABE	1265	(+)	ACGTGGCA	S000231	"LRE"; A positive light regulatory element in tobacco (N.t.) CAB (cab-E) gene
ACGTABREMOTIFA2OSEM	1265	(+)	ACGTGKC	S000394	Experimentally determined sequence requirement of ACGT-core of motif A in ABRE
MH63v2					
ARE1	1270	(-)	RGTGACNNNGC	S000022	"ARE (antioxidant response element)" of rat glutathione S-transferase Ya subunit
N22v2					
MYCATERD1	21; 941	(-); (-)	CATGTG	S000413	Necessary for expression of erd1 (early responsive to dehydration) in *Arabidopsis thaliana* (A.t.).
MYCATRD22	21;941	(+); (+)	CACATG	S000174	Binding site for MYC in A.t. dehydration-responsive gene, rd22
E2FCONSENSUS	149; 618; 1864	(+); (-); (-)	WTTSSCSS	S000476	"E2F consensus sequence" of all different E2F-DP-binding motifs
CRTDREHVCBF2	171	(-); (+)	GTCGAC	S000411	Preferred sequence for AP2 transcriptional activator HvCBF2 of barley
MYBPZM	176; 493; 1391; 1875	(+); (-); (+); (+)	CCWACC	S000179	Core of consensus maize P (myb homolog) binding site; W=A/T; 6 bp core
GCCCORE	207	(+)	GCCGCC	S000430	Core of GCC-box found in many pathogen-responsive genes

Table 3.10. (Continued)

Factor or Site Name	Location	Strand	Signal Sequence	Site #	Description
DRECRTCOREAT	210	(+)	RCCGAC	S000418	Core motif of DRE/CRT (dehydration-responsive element/C-repeat) in A.t. and rice
LTRECOREATCOR15	211	(+)	CCGAC	S000153	Core of low temperature responsive element (LTRE) of cor15a gene in A.t.
POLASIG1	337; 437; 949; 1074; 1910	(+); (-); (+); (+); (-)	AATAAA	S000080	"PolyA signal"; poly A signal found in legA gene of pea, rice alpha-amylase
P1BS	384	(-); (+)	GNATATNC	S000459	PHR1-binding sequence found in the upstream regions of phosphate starvation genes
LECPLEACS2	416	(-)	TAAAATAT	S000465	Core element in LeCp (tomato Cys protease) binding *cis* element
HSELIKENTACIDICPR1	664	(-); (+)	CNNGAANNNTTCNNG	S000056	"HSE-like motif" in -56 region of acidic PR1 gene of tobacco (N.t.)
MYB2AT	890; 1265; 1711	(+); (-); (-)	TAACTG	S000177	Involved in regulation of genes that are responsive to water stress in A.t.
XYLAT	925	(-)	ACAAAGAA	S000510	*Cis* element identified among the promoters of the "core xylem gene set"
TATABOXOSPAL	979	(+)	TATTTAA	S000400	Binding site for OsTBP2, found in the promoter of rice pal gene
SEF3MOTIFGM	1010; 1519	(+); (-)	AACCCA	S000115	"SEF3 binding site"; Soybean (G.m.) consensus sequence found in the 5' upstream
MYB1LEPR	1187	(-)	GTTAGTT	S000443	Tomato Pti4(ERF) regulates defense-related gene expression via GCC and non-GCC box
ACGTOSGLUB1	1344	(+)	GTACGTG	S000278	"ACGT motif" found in GluB-1 gene in rice required for endosperm-specific expression
TGTCACACMCUCUMISIN	1534	(-)	TGTCACA	S000422	A novel enhancer element necessary for fruit-specific expression of cucumisin gene
WBOXATNPR1	1699	(+)	TTGAC	S000390	"W-box" found in promoter of A.t. NPR1 gene
GT1CORE	1824	(-)	GGTTAA	S000125	Critical for GT-1 binding to box II of rbcS
BP5OSWX	2023	(-)	CAACGTG	S000436	OsBP-5 (a MYC protein) binding site in Wx promoter;
-300ELEMENT	2028	(+)	TGHAAARK	S000122	Present upstream of the promoter from the B-hordein gene of barley

REFERENCES

Asard, H.; Barbaro, R.; Trost, P., and Bérczi, A. 2013. Cytochromes b561: Ascorbate-mediated trans-membrane electron transport. *Antioxid. Redox Signal. 19*, 1026–1035.

Basu, S., Ramegowda, V., Kumar, A., and Pereira, A. 2016. Plant adaptation to drought stress. *F1000Research, 5*, 1554. doi:10.12688/f1000research.7678.1

Bernier J, Kumar A, Venuprasad R, Spaner D, Verulkar S, Mandal N, Sinha P, Peeraju P, Dongre P, Mahto RN, Atlin G: Characterization of the effect of a QTL for drought resistance in rice, qtl12.1, over a range of environments in the Philippines and eastern India. Euphytica. 2009, 166: 207-217. 10.1007/s10681-008-9826-y.

Cao, Jun, and Tan, Xiaona. 2019. Comprehensive Analysis of the Chitinase Family Genes in Tomato (*Solanum lycopersicum*). *Plants* 8, no. 3: 52. https://doi.org/10.3390/plants8030052

Choudhury, F.K.; Rivero, R.M.; Blumwald, E., and Mittler, R. 2016. Reactive oxygen species, abiotic stress and stress combination. *Plant J. 90*, 856–867.

Collins, N.C., Shirley, N.J., Saeed, M., Pallotta, M. and Gustafson, J.P. 2008. An ALMT1 gene cluster controlling aluminum tolerance at the Alt4 locus of rye (*Secale cereale* L.). *Genetics*, **179**, 669–682.

Conti, L., Price, G., O'Donnell, E., Schwessinger, B., Dominy, P. and Sadanandom, A. 2008. Small ubiquitin-like modifier proteases OVERLY TOLERANT TO SALT1 and -2 regulate salt stress responses in Arabidopsis. *Plant Cell*, **20**, 2894–2908.

Conti, L., Nelis, S., Zhang, C. ***et al.*** 2014. Small Ubiquitin-like Modifier protein SUMO enables plants to control growth independently of the phytohormone gibberellin. *Dev. Cell*, **28**, 102–110.

Gamuyao R, Chin JH, Pariasca-Tanaka J, Pesaresi P, Catausan S, Dalid C, Slamet-Loedin I, Tecson-Mendoza EM, Wissuwa M, Heuer S: The protein kinase Pstol1 from traditional rice confers tolerance of phosphorus deficiency. Nature. 2012, 488: 535-10.1038/nature11346.

Garris AJ, McCouch SR, Kresovich S: Population structure and its effect on haplotype diversity and linkage disequilibrium surrounding the xa5 locus of rice (Oryza sativa L.). Genetics. 2003, 165: 759-769.

Garris, A., Tai,T., Coburn, J., Kresovich, S., and McCouch, S. 2005. Genetic Structure and Diversity in *Oryza sativa* L. GENETICS **169:** 1631-1638. 10.1534/genetics.104.035642.

Gorantla, M., Babu, P., Lachagari, V. R., Reddy, A., Wusirika, R., Bennetzen, J. L., and Reddy, A. R. 2006. Identification of stress-responsive genes in an indica rice (Oryza sativa L.) using ESTs generated from drought-stressed seedlings. *Journal of Experimental Botany*, *58*(2), 253–265. doi: 10.1093/jxb/erl213

Hattori Y, Nagai K, Furukawa S, Song XJ, Kawano R, Sakakibara H, Wu J, Matsumoto T, Yoshimura A, Kitano H, Matsuoka M, Mori H, Ashikari M: The ethylene response factors SNORKEL1 and SNORKEL2 allow rice to adapt to deep water. Nature. 2009, 460: 1026-1030. 10.1038/nature08258.

Hirabak, E.M.; Chan, C.W.; Gribskov, M.; Harper, J.F.; Choi, J.H.; Halford, N.; Kudla, J.; Luan, S.; Nimmo, H.G., and Sussman, M.R. 2003. The Arabidopsis CDPK-SnRK Superfamily of Protein Kinases. *Plant Physiol. 132*, 666–680.

Ismail, A.M., Heuer, S., Thomson, M.J. and Wissuwa, M. 2007. Genetic and genomic approaches to develop rice germplasm for problem soils. *Plant Mol. Biol*. **65**, 547–570

Jena, K.K. and Mackill, D.J. .2008. Molecular markers and their use in marker-assisted selection in rice. *Crop Sci*. **48**, 1266–1276

Kurepa, J., Walker, J. M., Smalle, J., Gosink, M. M., Davis, S. J., Durham, T. L., et al. 2003. The small ubiquitn-like modifier (SUMO) protein modification system in Arabidopsis. *J. Biol. Chem.* 278, 6862–6872.

Krumsiek J, Arnold R, Rattei T. 2007. Gepard: A rapid and sensitive tool for creating dotplots on genome scale. Bioinformatics, 23(8): 1026-8.

Lawlor, D.W., and Paul, M.J. 2014. Source/sink interactions underpin crop yield: The case for trehalose 6-phosphate/SnRK1 in improvement of wheat. *Front. Plant Sci. 5*, 418.

Lenka, S. K., Katiyar, A., Chinnusamy, V., and Bansal, K. C. 2011. Comparative analysis of drought-responsive transcriptome in Indica rice genotypes with contrasting drought tolerance. *Plant Biotechnology Journal*,*9*(3), 315-327. doi:10.1111/j.1467-7652.2010.00560.x

Lyer, L.M.; Anantharaman, V., and Aravind, L. 2007. The DOMON domains are involved in heme and sugar recognition. *Bioinformatics*, *23*, 2660–2664.

Magalhaes, J.V., Liu, J., Guimarães, C.T., Lana, U.G.P., Alves, V.M.C., Wang, Y.-H., Schaffert, R.E., Hoekenga, O.A., Piñeros, M.A., Shaff, J.E., Klein, P.E., Carneiro, N.P., Coelho, C.M., Trick, H.N. and Kochian, L.V. 2007. A gene in the multidrug and toxic compound extrusion (MATE) family confers aluminum tolerance in sorghum. *Nat. Genet*. **39**, 1156–1161.

Misson, J., Raghothama, K.G., Jain, A., Jouhet, J., Block, M.A., Bligny, R., Ortet, P., Creff, A., Somerville, S., Rolland, N., Doumas, P., Nacry, P., Herrerra-Estrella, L., Nussaume, L. and Thibaud, M.C. 2005. A genome-wide transcriptional analysis using *Arabidopsis thaliana* Affymetrix gene chips determined plant responses to phosphate deprivation. *Proc. Natl. Acad. Sci. USA*, **102**, 11 934–11 939.

Mittler, R. 2017. ROS Are Good. *Trends Plant. Sci*. *22*, 11–19.

Morales, K.Y.; Singh, N.; Perez, F.A.; Ignacio, J.C.; Thapa, R.; Arbelaez, J.D.; Tabien, R.E.; Famoso, A.; Wang, D.R.; Septiningsih, E.M.; et al. 2020. An improved 7K SNP array, the C7AIR, provides a wealth of validated SNP markers for rice breeding and genetics studies. *PLoS ONE, 15*, e0232479.

Morrell, R., and Sadanandom, A. 2019. Dealing With Stress: A Review of Plant SUMO Proteases. *Front. Plant Sci.* 10:1122.

Nanasato, Y.; Akashi, K., and Yokota, A. 2005. Co-expression of Cytochrome b561 and Ascorbate Oxidase in Leaves of Wild Watermelon under Drought and High Light Conditions. *Plant Cell Physiol*.1515–1524.

Novatchkova, M., Budhiraja, R., Coupland, G., Eisenhaber, F. and Bachmair, A. 2004. SUMO conjugation in plants. *Planta*, **220**, 1–8.

Oszvald, M.; Primavesi, L.F.; Griffiths, C.A.; Cohn, J.; Basu, S.S.; Nuccio, M.L., and Paul, M.J. 2018. Trehalose 6-Phosphate Regulates Photosynthesis and Assimilate Partitioning in Reproductive Tissue. *Plant Physiol*. *176*, 2623-2638.

Pan, J., Li, Z., Wang, Q., Garrell, A. K., Liu, M., Guan, Y., and Liu, W. 2018. Comparative proteomic investigation of drought responses in foxtail millet. *BMC Plant Biology*, *18*(1). doi: 10.1186/s12870-018-1533-9

Reddy, C. S., Babu, A. P., Swamy, B. P., Kaladhar, K., and Sarla, N. 2009. ISSR markers based on GA and AG repeats reveal genetic relationship among rice varieties tolerant to drought, flood, or salinity. *Journal of Zhejiang University SCIENCE B,10*(2), 133-141. doi:10.1631/jzus.b0820183

Ren, Z.H., Gao, J.P., Li, L.G., Cai, X.L., Huang, W., Chao, D.Y., Zhu, M.Z., Wang, Z.Y., Luan, S. and Lin, H.X. 2005. A rice quantitative trait locus for salt tolerance encodes a sodium transporter. *Nat. Genet*. **37**, 1141–1146.

Sánchez-Barrena, M.J.; Fujii, H.; Angulo, I.; Martínez-Ripoll, M.; Zhu, J., and Albert, A. 2007. The Structure of the C-Terminal Domain of the Protein Kinase AtSOS2 Bound to the Calcium Sensor AtSOS3. *Mol. Cell*, *26*, 427–435.

Sandhu, N., Singh, A., Dixit, S., Cruz, M. S., Maturan, P., Jain, R., and Kumar, A. 2014. Identification and mapping of stable QTL with main and epistasis effect on rice grain yield under upland drought stress. *BMC Genetics,15*(1), 63.

Schatz, M.C., Maron, L.G., Stein, J.C. *et al.* 2014. Whole genome *de novo* assemblies of three divergent strains of rice, *Oryza sativa*, document novel gene space of *aus* and *indica*. *Genome Biol* **15,** 506, 10.1186/s13059-014-0506-z.

Septiningsih, E.M., Pamplona, A.M., Sanchez, D.L., Neeraja, C.N., Vergara, G.V., Heuer, S., Ismail, A.M. and Mackill, D.J. 2008. Development of submergence tolerant rice cultivars: the *Sub1* locus and beyond. *Ann. Bot*, **103**, 151–160.

Srivastava, A.K., Zhang, C., Yates, G., Bailey, M., Brown, A. and Sadanandom, A. 2016. SUMO is a critical regulator of salt stress responses in rice. *Plant Physiol.* **170**, 2378–2391.

Srivastava, A. K., Zhang, C., Caine, R. S., Gray, J., and Sadanandom, A. 2017. Rice SUMO protease Overly Tolerant to Salt 1 targets the transcription factor, OsbZIP23 to promote drought tolerance in rice. *Plant J.* 92, 1031–1043.

Takano-Kai N, Jiang H, Kubo T, Sweeney M, Matsumoto T, Kanamori H, Padhukasahasram B, Bustamante C, Yoshimura A, Doi K, McCouch S: Global dissemination of a single mutation conferring white pericarp in rice. PLoS Genet. 2007, 3: e133-10.1371/journal.pgen.0030133.

Uga, Y.; Sugimoto, K.; Ogawa, S.; Rane, J.; Ishitani, M.; Hara, N.; Kitomi, Y.; Inukai, Y.; Ono, K. and Kanno, N.2013. Control of root system architecture by DEEPER ROOTING 1 increases rice yield under drought conditions. *Nat. Genet. 5*,1097–1102.

Verelst, W., and Asard, H. 2003. A phylogenetic study of cytochrome b561 proteins. *Genome Biol. 4*, 6.

Vikram, P.; Swamy, B.P.; Dixit, S.; Ahmed, H.; Cruz, M.T.; Singh, A., and Kumar, A. 2011. QDTY1.1, a major QTL for rice grain yield under reproductive-stage drought stress with a consistent effect in multiple elite genetic backgrounds. *Bmc Genet. 12*, 89.

Vikram, P., Swamy, B. P., Dixit, S., Singh, R., Singh, B. P., Miro, B., Kohli, A., Kumar, A. 2015. Drought susceptibility of modern rice varieties: an effect of linkage of drought tolerance with undesirable traits. *Scientific Reports,5*(1). doi:10.1038/srep14799

Wang, Y.; Yan, H.; Qiu, Z.; Hu, B.; Zeng, B.; Zhong, C., and Fan, C. 2019. Comprehensive Analysis of SnRK Gene Family and their Responses to Salt Stress in Eucalyptus grandis. *Int. J. Mol. Sci. 20*, 2786.

Xu K, Xu X, Fukao T, Canlas P, Maghirang-Rodriguez R, Heuer S, Ismail AM, Bailey-Serres J, Ronald PC, Mackill DJ: Sub1A is an ethylene-response-factor-like gene that confers submergence tolerance to rice. Nature. 2006, 442: 705-708. 10.1038/nature04920.

Yao, W., Li, G., Zhao, H., Wang, G., Lian, X., & Xie, W. (2015). Exploring the rice dispensable genome using a metagenome-like assembly strategy. *Genome Biology, 16*(1). doi:10.1186/s13059-015-0757-3

Yi, K., Wu, Z., Zhou, J., Du, L., Guo, L., Wu, Y. and Wu, P. 2005. OsPTF1, a novel transcription factor involved in tolerance to phosphate starvation in rice. *Plant Physiol*. **138**, 2087–2096.

Zhao KY, Wright M, Kimball J, Eizenga G, McClung A, Kovach M, Tyagi W, Ali ML, Tung CW, Reynolds A, Bustamante CD, McCouch SR. 2010. Genomic diversity and introgression in O. sativa reveal the impact of domestication and breeding on the rice genome. Plos One, 5: e10780-10.1371/journal.pone.0010780.

Ziska, L. H., Manalo, P. A., and Ordonez, R. A. 1996. Intraspecific variation in the response of rice (Oryza sativaL.) to increased CO2and temperature: growth and yield response of 17 cultivars. *Journal of Experimental Botany*,*47*(9), 1353-1359. doi:10.1093/jxb/47.9.1353

CHAPTER 4

CONCLUSIONS

Rice is an important staple crop in many developing countries, especially in Asia, and a primary energy source for over half of the world's population. Approximately 42 million hectares of rice are subject to occasional or frequent drought stress in Asia, resulting in significant yield loss. Reduction in rice grain yield by drought stress occurs during reproductive development, especially at the flowering stage, that even mild drought stress can result in severe grain yield loss. Thus, it is crucial to provide more staple rice to keep global food security and meet a growing world population's food needs. Understanding the molecular mechanisms underlying drought tolerance at the reproductive stage is needed to be a part of a holistic and successful, knowledge-based crop improvement strategy. This research evaluated rice genome-wide transcriptional changes under moderate reproductive-stage drought stress using a drought-tolerant introgression line (DTY-IL) and its recurrent parent, Swarna and identified novel genes and pathways that could be used for genetic improvement of rice.

This study provided novel insights into global transcriptional responses in rice under moderate reproductive-stage drought stress in a DTY-dependent manner and highlighted associated physiological mechanisms that allow DTY-IL to better cope with reproductive-stage drought stress. We focused on reproductive-stage drought tolerance, which from an applied perspective is arguably the most impactful trait in adapting rice to changing climates in both source and sink tissues that drive yield under drought. Through this, we support that the maintenance of intricate source-sink relationships during grain filling under drought is a key driver of drought-tolerant-yield. We also compared the differential expression responses between a drought-susceptible mega variety and its derived drought-tolerant introgression line to demonstrate that the introgression modulates the genome level segments' differences. Through this, the results of gene network analysis can be brought into context with known quantitative trait loci QTL for drought-tolerant-yield.

In DTY-IL flag-leaves, structural and metabolic integrity associated with cell wall re-organization and active ROS metabolism prevented leaf rolling and allowed for maintenance of cellular growth and homeostasis under reproductive-stage drought stress, which supported

sustained rates of photosynthetic activity and consequently provisioning of energy and carbon to developing sinks. In the developing panicles close to anthesis, sustained energy and carbon allocation enabled the minimizing of damage to reproductive structures due to reproductive-stage drought stress through protective mechanisms, including ROS homeostasis, post-transcriptional modifications, detoxification, and secondary metabolite production; ultimately, this results in improved fertility and yield under moderate reproductive-stage drought stress (Figure S21). We overlayed the differential expression data with the introgressed fragments' variant data to prioritized candidate genes in *qDTY1.1* and *qDTY3.2* for drought-tolerant-yield using the most appropriate reference genomes for each analysis. Through these, three candidate genes were proposed and prioritized based on differential expression and non-synonymous variation and discussed in the context of their predicted function and the observed changes in genome-wide expression. One is a member of a well-characterized family of protein kinases (with a Sucrose non-fermenting 1 related kinase (SnRK) domain and a CBL-interacting serine/threonine-protein kinase (CIPK3) domain), previously implicated in source-sink regulation and abiotic stress tolerance. The other is an auxin-responsive protein-containing two less characterized conserved domains with predicted function in redox homeostasis. Another candidate was protease protein unique in the MH63 genome and could potentially act as a negative regulator of drought.

While our results confirmed and supported previous findings regarding mechanisms underlying drought responses, they further suggested specific mechanisms relating to metabolic signaling and reactive oxygen species homeostasis to contribute to drought-tolerant yield.

Though our study was confined to a single time point at the maximum booting stage after two weeks of moderate reproductive-stage drought stress, our study suggested that the drought-tolerant yield-controlled mechanism improved yield under drought by acting at both source and sink tissues. Time-course experiments on the developmental and different levels of drought could be done in the future to capture fully the transcriptional changes and identify common and unique pathways and genes that are affected. Physiological, biochemical, and agronomic characterizations and transgenic approaches are also needed to validate and elaborate the drought tolerance mechanisms and the identified candidate genes in the Nipponbare, MH63, and N22 genome.